R-7313-4
CR-102408

F-1 ENGINE OPERATION IN THE S-IC-5 STAGE OF THE SATURN V AS-505 FLIGHT

Rocketdyne
North American Rockwell

6633 Canoga Avenue,
Canoga Park, California 91304

SP-7597[illegible]

Rocketdyne
North American Rockwell

6633 Canoga Avenue,
Canoga Park, California 91304

R-7313-4

F-1 ENGINE OPERATION IN THE S-IC-5 STAGE OF THE SATURN V AS-505 FLIGHT

Contract NAS8-18734

PREPARED BY

Rocketdyne Engineering
Canoga Park, California

APPROVED BY

D. E. Aldrich
F-1 Project Manager

NO. OF PAGES 188 & xiv **REVISIONS** DATE 18 July 1969

DATE	REV. BY	PAGES AFFECTED	REMARKS

FORM R18-G REV. 5-69

FOREWORD

This report was prepared under Contract NAS8-18734 in compliance with Task A1-4-3 of R-6531-5 F-1 Production Support Plan.

ABSTRACT

This report presents the flight performance analysis of the five F-1 engines used in the S-IC-5 stage of Apollo/Saturn, Vehicle 505.

CONTENTS

ILLUSTRATIONS

TABLES

INTRODUCTION

The Apollo/Saturn Vehicle 505 was successfully launched at 12:49:00 AM (EDT) on 18 May 1969, from Pad B of Launch Complex 39 at Kennedy Space Center (KSC), Florida. This was the third manned flight of a Saturn V vehicle, and the fifth flight test of the F-1 engine system. The purpose of this flight was to develop lunar landing mission techniques consisting of CSM/LM operations in lunar orbit, including lunar module systems performance during simulated descent and ascent and rendezvous techniques between the command module and lunar module. Additional information describing gravitational concentrations on the lunar surface and further detailed information on the proposed landing site were obtained.

The primary S-IC-5 stage objectives were:

1. To launch and to provide the boost trajectory required for the remaining stages to insert the manned Apollo 10 spacecraft into an earth orbit.
2. To evaluate the launch vehicle longitudinal oscillation characteristics.
3. To verify that the POGO solution configuration LOX prevalve accumulators suppress low-frequency longitudinal oscillations (POGO effect).
4. To evaluate thermal environment, structural loads, and dynamic characteristics during flight.
5. To verify the altitude shutdown characteristics of the F-1 engines utilizing the hydraulic orifice configuration incorporated by ECP-F1-444.

The purpose of this report is to present the results of the flight test data evaluation covering operation of the five F-1 engines installed in the S-IC-5 stage of the AS-505 vehicle. The report includes the performance

evaluation of the engines during start, mainstage, and shutdown, as well as trajectory performance of the S-IC-5 stage relative to F-1 engine performance. The engine configuration, and prelaunch history are also presented. The engines installed in the S-IC-5 stage are listed below by engine serial number and stage position.

F2035	Stage Position 1 (Outboard)
F2041	Stage Position 2 (Outboard)
F2040	Stage Position 3 (Outboard)
F2042	Stage Position 4 (Outboard)
F2034	Stage Position 5 (Inboard)

SUMMARY

Liftoff of Saturn V, Vehicle AS-505 occurred at 12:49:00 PM (EDT) on 18 May 1969. F-1 engine operation throughout the AS-505 flight was normal and no anomalies were identified. Engine operation and thrust buildup characteristics during start were normal. The desired 1-2-2 stagger in engine starting was achieved. Engine operation during flight was normal providing steady-state performance that resulted in a satisfactory trajectory. Engine 1 (F2035) indicated a lower than expected thrust (21 kilopounds) at the standard 35-second data slice, although the thrust level was close to predicted at liftoff and inboard engine shutdown. Performance analyses have disclosed no evidence of a hardware failure associated with engine F2035 thrust versus time characteristics.

Inboard engine cutoff (IECO) was initiated by the stage timer and occurred at 135.2-seconds range time. Outboard engine cutoff (OECO) occurred at 161.6-seconds range time and was initiated by the LOX tank low-level sensor, as planned, and was 1.4 seconds later than predicted.

Approximately half of the outboard engine cutoff deviation can be attributed to the fact that the predicted trajectory parameters used as a comparison base do not include the revised F-1 engine TAG values. One significant effect of these revised TAG values was to increase the predicted outboard engine cutoff time by 0.7 second.

Stage performance parameters, actual and predicted, as established by NASA, and average engine performance, as established by Rocketdyne, are listed in Table 1.

TABLE 1

STAGE AND ENGINE PERFORMANCE

Parameter	Actual	Predicted*	Deviation, percent
Range Time, seconds			
Inboard Engine Cutoff	135.2	135.3	-0.07
Outboard Engine Cutoff	161.6	160.20	+0.87
Altitude at Outboard Engine Cutoff, kilometers	65.3	65.8	-0.76
Surface Range at Outboard Engine Cutoff, kilometers	93.4	91.3	+2.30
Space Fixed Velocity at Outboard Engine Cutoff, meters/second	2752	2741	+0.40
Average Engine Sea-Level Thrust, kilopounds	1511	1510	+0.06
Average Engine Specific Impulse at Sea-Level Rated Thrust and Mixture Ratio, seconds	264.3	264.3	0.0
Average Engine Mixture Ratio at Sea-Level Rated Thrust	2.272	2.272	0.0

Engine operating durations for the AS-505 flight as determined from thrust OK pressure switch pickup to dropout were as follows:

Engine Position	Serial Number	Operating Time (+0.10 second), seconds
1	F2035	163.65
2	F2041	163.40
3	F2040	163.65
4	F2042	163.40
5	F2034	137.39

*Predicted values do not include the revised F-1 engine TAG values which lowered predicted engine thrust an average of 9 kilopounds per engine

Engine shutdown characteristics were normal. The maximum thrust decay rate above 40 percent thrust averaged 450 kilopounds per 0.075 second, which is slightly greater than the predicted population nominal of 448 kilopounds per 0.075 second based on ground test data. The average thrust decay rate for AS-504, which was the first flight with ECP F1-444 orificing, was 436 kilopounds per 0.075 second. The average of both flights is 443 kilopounds per 0.075 second, which agrees well with the population nominal of 448 kilopounds per 0.075 second determined from ground test data.

Heat exchanger performance and operation were as predicted. The revised model specification values of LOX and helium flowrate (ECP F1-601) were not exceeded.

Dynamic analyses of acceleration and pressure flight data resulted in the conclusion that POGO did not occur during S-IC stage operation. These data indicate structural and liquid column frequencies, but there is no indication of coupling of the vehicle structure, the propellant suction system, and the engine system. The POGO suppression system appears to have performed as predicted, with the outboard engine LOX suction system first mode frequency maintained at approximately 2 Hz throughout the flight.

Rocketdyne supplies 175 flight instrumentation transducers on the S-IC stage, of which 159 were active for the AS-505 flight. Valid data were received for all recorded parameters; however, partial loss of data was experienced on one parameter, and two parameters yielded questionable data.

Thermal analysis of flight data indicated that all mechanical, structural, and electrical components were adequately protected under the thermal insulation. No components exceeded allowable values. The thermal environment for both the AS-505 and AS-504 flights were approximately the same during most of the flight.

Prelaunch operations and related problems, engine configuration, and engine test history are reported in the appendixes.

ENGINE TRANSIENT ANALYSIS

The F-1 engine thrust chamber pressure buildup transients are presented in Fig. 1. The desired 1-2-2 engine staggered start was attained. The actual time period between engine pairs attaining 100-psig chamber pressure was approximately 50 milliseconds for the first pair and 5 milliseconds for the second pair.

As shown in Fig. 1, the four outboard engines (F2035, F2041, F2040, and F2042) experience a plateau and/or decay in thrust chamber pressure buildup at about 80 percent of their mainstage values. This discontinuity is a normal occurrence when an F-1 engine is tested in a stage position that incorporates the POGO solution configuration oxidizer prevalves, as do the outboard engines, and does not result in any problems.

The engine predicted start times and the actual start times are presented in Table 2. The difference between predicted and actual times from engine control valve open signal to 100-psig chamber pressure attained as corrected to standard turbopump inlet pressure conditions for engine positions 1 through 5 respectively were: 11, 17, 46, 12, and 56 milliseconds.

The time from engine control valve open signal to two of three thrust OK pressure switches actuated, which is used as an approximation of 1370 kilopounds thrust attained, as corrected to standard turbopump inlet conditions, ranged from 4.240 to 4.587 seconds for all engines. These values are well within the model specification maximum value of 5.5 seconds. The actual start times attained are presented in Table 2.

Thrust increase values attained during F-1 engine start did not differ significantly from those values recorded during Rocketdyne acceptance testing, and were within model specification limits. Model specification limits, Rocketdyne acceptance test demonstrated values, and the values attained during start on Vehicle AS-505 are shown in Table 3. When comparing the

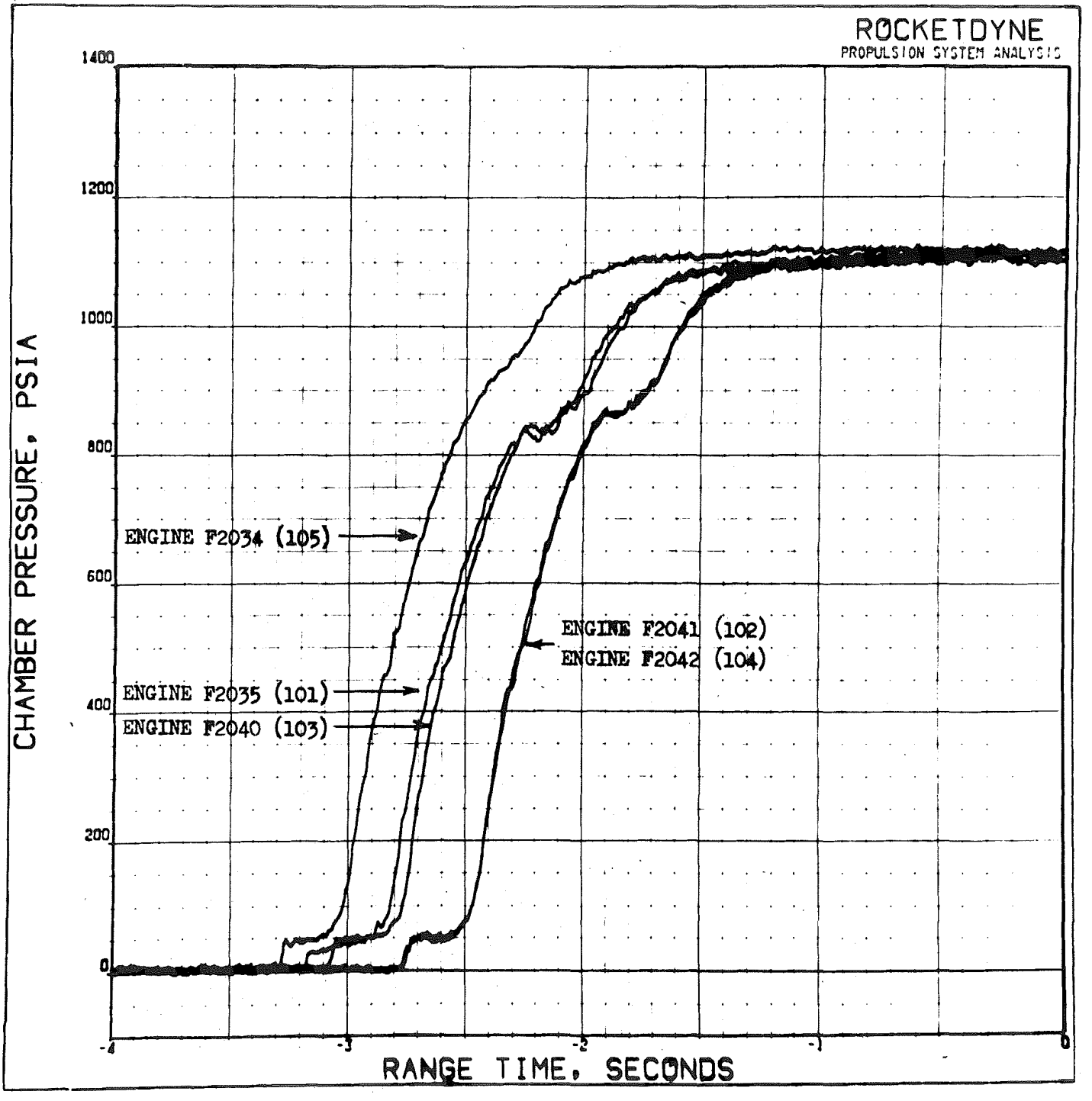

Figure 1. AS-505 F-1 Engine Thrust Chamber Pressure Buildup

TABLE 2

AS-505 F-1 ENGINE START TIMES

Engine		Time From Engine Control Valve Actuation Signal to:						Time Engine Reaches 90 Percent of Rated Thrust (1370 K-lb) Relative to Liftoff, seconds
		Hypergol Switch Dropout, seconds		100-psig Chamber Pressure Attained, seconds		Two to Three Thrust OK Switches Actuated (Thrust OK), seconds		
Position	Serial Number	Predicted	Actual	Predicted	Actual	Predicted	Actual	
1	F2035	3.028	3.021	3.442	3.453	4.131	4.351	T-1.814
2	F2041	3.221	3.237	3.659	3.659	4.320	4.509	T-1.568
3	F2040	3.279	3.195	3.712	3.676	4.480	4.587	T-1.835
4	F2042	3.226	3.245	3.650	3.662	4.354	4.507	T-1.540
5	F2034	3.021	3.092	3.434	3.490	4.128	4.240	T-2.189

NOTES:

1. Actual values corrected to standard prestart turbopump inlet pressures of 80-psia LOX and 45-psia fuel.
2. Vehicle start thrust values are calculated from thrust chamber pressure.

TABLE 3

AS-505 F-1 ENGINE THRUST INCREASE

Engine Position		1	2	3	4	5
Engine Serial Number		F2035	F2041	F2040	F2042	F2034
Thrust Increase Time From 40 to 90 Percent Thrust, seconds	Model Specification	Minimum 0.40				
	Acceptance	0.58	0.61	0.60	0.58	0.60
	Vehicle Start	0.73	0.67	0.75	0.71	0.61
Maximum Thrust Increase for 0.010-Second Interval Between 6 and 65 Percent Thrust, kilopounds	Model Specification	Maximum 200				
	Acceptance	43	58	51	54	49
	Vehicle Start	44	39	40	49	48
Maximum Thrust Increase for 0.010-Second Interval Between 65 Percent and Full Thrust, kilopounds	Model Specification	Maximum 100				
	Acceptance	22	22	22	21	20
	Vehicle Start	26	20	21	20	20

NOTES:

1. Vehicle start thrust values are calculated from thrust chamber pressure.
2. Model specification limits apply to acceptance values only.
3. The difference between acceptance and vehicle start thrust increase time on engine positions 1 through 4 is caused primarily by the effect of the LOX prevalve accumulator.

vehicle start thrust increase values with those attained during acceptance testing, consideration should be given to the fact that acceptance values are obtained using a measured thrust, while launch values are calculated from thrust chamber pressure.

The model specification requires that the time interval between 40 and 90 percent of rated thrust shall not be less than 0.40 second. The time interval attained during Rocketdyne acceptance testing ranged from 0.58 to 0.61 second, and during vehicle start from 0.61 to 0.75 second. The difference from acceptance to vehicle start is attributed to the effect of the LOX prevalve accumulator on the outboard engines.

The maximum thrust increase for any 0.010-second interval between 6 and 65 percent of rated thrust is required by model specification not to exceed 200 kilopounds. Rocketdyne acceptance values ranged from 43 to 58 kilopounds, and vehicle start values ranged from 39 to 49 kilopounds for the noted time and thrust intervals.

The increase in engine thrust for any 0.010-second interval above 65 percent of rated thrust is required by the model specification not to exceed 100 kilopounds. Engine acceptance test values ranged from 20 to 22 kilopounds, and during vehicle start from 20 to 22 kilopounds.

F-1 engine valve opening times attained during the vehicle start transient were as expected. Table 4 compares valve switch times obtained during Rocketdyne acceptance tests, MTF stage static test, and AS-505 start. The AS-505 valve opening times were obtained from the Digital Events Evaluator records. The differences in valve times between acceptance test and stage static tests are due to the post-acceptance test orifice changes of ECP F1-444.

TABLE 4

S-IC-5, AS-505 F-1 ENGINE PROPELLANT VALVE OPERATING TIMES

(Tabulated Values in Milliseconds)

Engine Serial No.	F2035			F2041			F2040			F2042			F2034		
Engine Position	1			2			3			4			5		
Test Location	EFL	MTF	AS-505	EFL	MTF	AS-505	EFL	MTF	AS-505	EFL	MTF	AS-505	EFL	MTF	AS-505
No. 1 MOV Opening	333	316	316	359	328	336	346	324	330	326	312	316	333	320	332
No. 2 MOV Opening	339	316	322	365	324	334	326	332	338	366	336	338	339	324	330
GGBV Opening	230	164	166	201	156	164	233	168	172	221	164	171	198	168	178
No. 1 MFV Opening	556	583	592	596	636	630	564	620	624	576	608	614	576	620	628
No. 2 MFV Opening	583	600	614	557	611	622	551	620	624	570	584	590	564	612	624
No. 1 MOV Closing	358	300	343	384	320	343	345	276	254	358	304	342	365	304	340
No. 2 MOV Closing	390	324	324	307	312	325	403	336	344	410	324	325	403	332	345
GGBV Closing	120	84	137	118	84	137	116	80	137	122	84	136	119	84	131
No. 1 MFV Closing	807	976	913	819	996	1000	723	896	915	717	872	915	781	952	1047
No. 2 MFV Closing	781	952	998	832	1024	1001	813	952	1000	800	996	1000	845	1008	1002

NOTES:

1. All times are switch time.
2. EFL times are averages of performance demonstration tests.
3. MTF times are stage static test values.
4. Differences in valve closing times between acceptance tests and stage-states tests are due to the post acceptance test orifice changes of ECP F1-444.

Prestart redlines and engine prestart limits were not exceeded. The prestart redline and limit parameters, the applicable limit, and the recorded values attained over the time interval immediately prior to engine start (T-10 to T-7 seconds) are noted in Table 5.

Shutdown characteristics of the F-1 engines were as expected. Table 5 presents the Rocketdyne acceptance test values adjusted to acceptance test conditions, and the actual flight values. The Rocketdyne acceptance test values shown in Table 6 are the population nominal values applicable to the hydraulic system orifice changes per ECP F1-444 incorporated subsequent to acceptance testing. When comparing actual flight, adjusted flight, and acceptance values, it should be noted that all flight thrust values are calculated from thrust chamber pressure, while acceptance values are obtained from recorded thrust. Chamber pressure decays adjusted to the time of cutoff signal for all five engines are shown in Fig. 2. The chamber pressure of engine F2035 (position 1) appears to experience a change in thrust decay slope about 0.120 second after cutoff signal. This is attributed to a transducer characteristic and is not typical of a true thrust chamber pressure decay. This causes no problems except when computing thrust decay rate per 0.075 second with the Rocketdyne computer program. To avoid any errors introduced by this change in slope, a manual reduction rather than the computer reduction was used to compute thrust decay rate for this engine.

The model specification requires that the decrease in engine thrust for any 0.075-second time interval during acceptance test engine shutdown shall not exceed 750 kilopounds. The maximum thrust decrease during any 0.075-second time interval attained during flight shutdown ranged from 442 to 454 kilopounds, while the flight values adjusted to acceptance conditions ranged from 422 to 450 kilopounds.

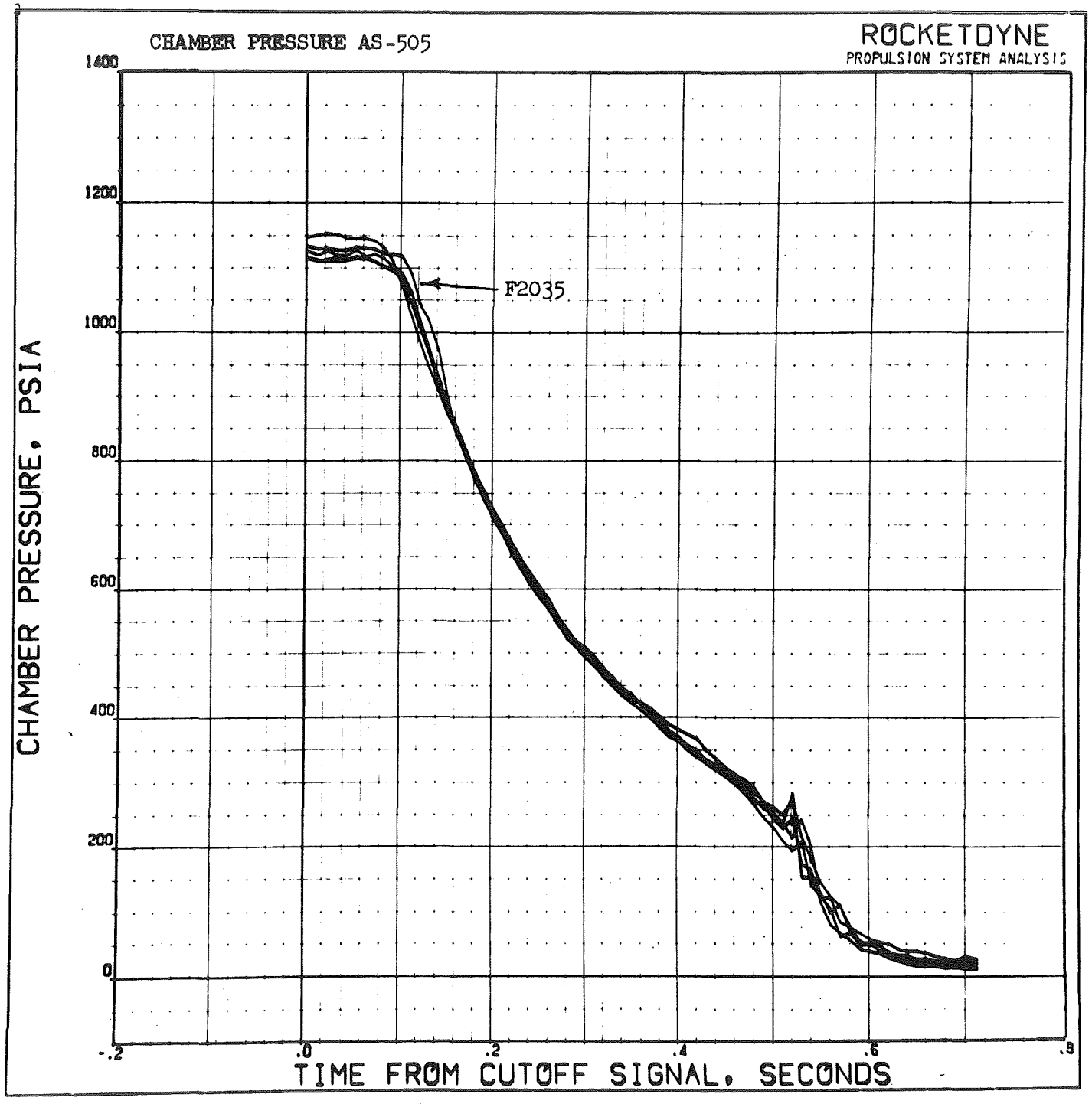

Figure 2. F-1 Engine Thrust Chamber Pressure Shutdown Decay Adjusted to Time of Cutoff Signal

TABLE 5

AS-505 F-1 ENGINE PRESTART LIMIT VALUES

Parameter	Prestart Limit		Recorded Value at T-10 Seconds				
	Minimum	Maximum	F2035	F2041	F2040	F2042	F2034
Hydraulic Supply Temperature, F	60	130	← 72 →				
Hydraulic Supply Pressure, psia	1415	1615	1494	1472	1445	1465	1471
Fuel Inlet Pressure No. 1, psia	43.3	DNA		45.8	45.8	46.3	47.5
Fuel Inlet Pressure No. 2, psia	43.3	DNA	Not Recorded				
LOX Suction Line Pressure, psia	74.9	DNA		80.2	79.8	80.6	82.3
LOX Suction Line Temperature, F	DNA	-275	-287	-290	-284	-289	-287
Turbopump LOX Seal Purge Pressure, psia	75	115	← 101 →				
Engine Environmental Temperature, F	0	130	46	40	48	52	61
Turbopump LOX Seal Cavity Pressure	No liquid leakage		Visual observation verified no liquid leakage				
Turbopump LOX Bearing Temperature, F	0	200	101	118	123	125	119

TABLE 6

AS-505 F-1 ENGINE SHUTDOWN CHARACTERISTICS

Engine Position		1	2	3	4	5
Engine Serial Number		F2035	F2041	F2040	F2042	F2034
Time From Cutoff Signal to 10-Percent Thrust, seconds	Model Specification (1)	Minimum 0.35			Maximum 0.75	
	Acceptance (4)	←		0.53		→
	Adjusted Flight (2)	0.55	0.53	0.54	0.55	0.54
	Actual Flight (3)	0.57	0.56	0.56	0.58	0.56
Maximum Thrust Decreased For 0.075-Second Interval, kilopounds	Model Specification (1)			Maximum 750		
	Acceptance (4)	←		448		→
	Adjusted Flight (2)	443	451	450	452	422(5)
	Actual Flight (3)	450	454	454	452	442(5)
Cutoff Impulse, k-lb Second	Model Specification (1)	Minimum 300			Maximum 600	
	Acceptance (4)	←		464		→
	Adjusted Flight (2)	477	472	470	487	463
	Actual Flight (3)	626	612	610	620	621

NOTES:

1. Model specification limits apply to acceptance values only.
2. Adjusted flight values are flight data reduced to acceptance conditions of performance level and ambient pressure.
3. Actual flight shutdown thrust values are calculated from thrust chamber pressure.
4. Acceptance values are population nominal values because of hydraulic system orifice changes per ECP F1-444 subsequent to acceptance testing.
5. Engine 1 thrust decrease per 0.075 second was manually reduced because of erroneous transducer data which caused the Rocketdyne computer program to give invalid thrust decay rates.

The average thrust decay rate per 0.075 second for AS-505 with ECP F1-444 orificeing is 450 kilopounds for the actual flight shutdown. The average thrust decay rate for AS-504, which was the first flight with ECP F1-444 orificing, was 436 kilopounds per 0.075 second. The average of both flights is 443 kilopounds per 0.075 second, which agrees well with the population nominal of 448 kilopounds per 0.075 second determined from ground test data.

The acceptance test time from the engine cutoff signal to the attainment of 10 percent of rated thrust is required by the model specification to be within the range of 0.35 to 0.75 second. The flight shutdown times when adjusted to acceptance conditions ranged from 0.53 to 0.55 second, which compare favorably to the population nominal of 0.53 second. The actual flight shutdown values attained range from 0.56 to 0.58 second.

Flight cutoff impulse, when reduced to Rocketdyne acceptance test conditions, ranged from 463 to 487 K-lb-sec, which compares favorably with the population nominal value of 464 K-lb-sec. The model specification requires the demonstrated acceptance test cutoff impulse to be within the range of 300 to 600 K-lb-sec at acceptance site conditions. The actual flight cutoff impulse, for which no model specification requirement exists, ranged from 610 to 626 K-lb-sec.

Valve operating times during the shutdown transient were as expected. Table 4 compares valve switch closing times obtained during acceptance test, MTF stage test, and flight. A maximum uncertainty of 0.083 second is associated with the flight valve closing times.

After inboard engine shutdown, the engine position 5 LOX suction line pressure (D131) decayed from approximately 105 to 60 psia in 20 seconds (2.3 psi/sec). As shown in Fig. 3, a similar decay was experienced during the AS-503 and AS-504 flight after inboard engine shutdown. The LOX suction line pressure decay of previous flights was attributed to either a minor leak in the stage or engine downstream of the LOX prevalve, or to

a phenomenon which is not completely understood. The similar decay noted on AS-505 indicates the strong possibility that this is a natural phenomenon which, at this time, is not understood and should probably be expected to occur during future flights. A similar LOX suction line pressure decay (0.5 psi/sec) was also noted during AS-501 flight. During the AS-502 flight, the time between inboard engine and outboard engine shutdown was only 3.5 seconds, which precluded the possibility of accurately defining any pressure transients.

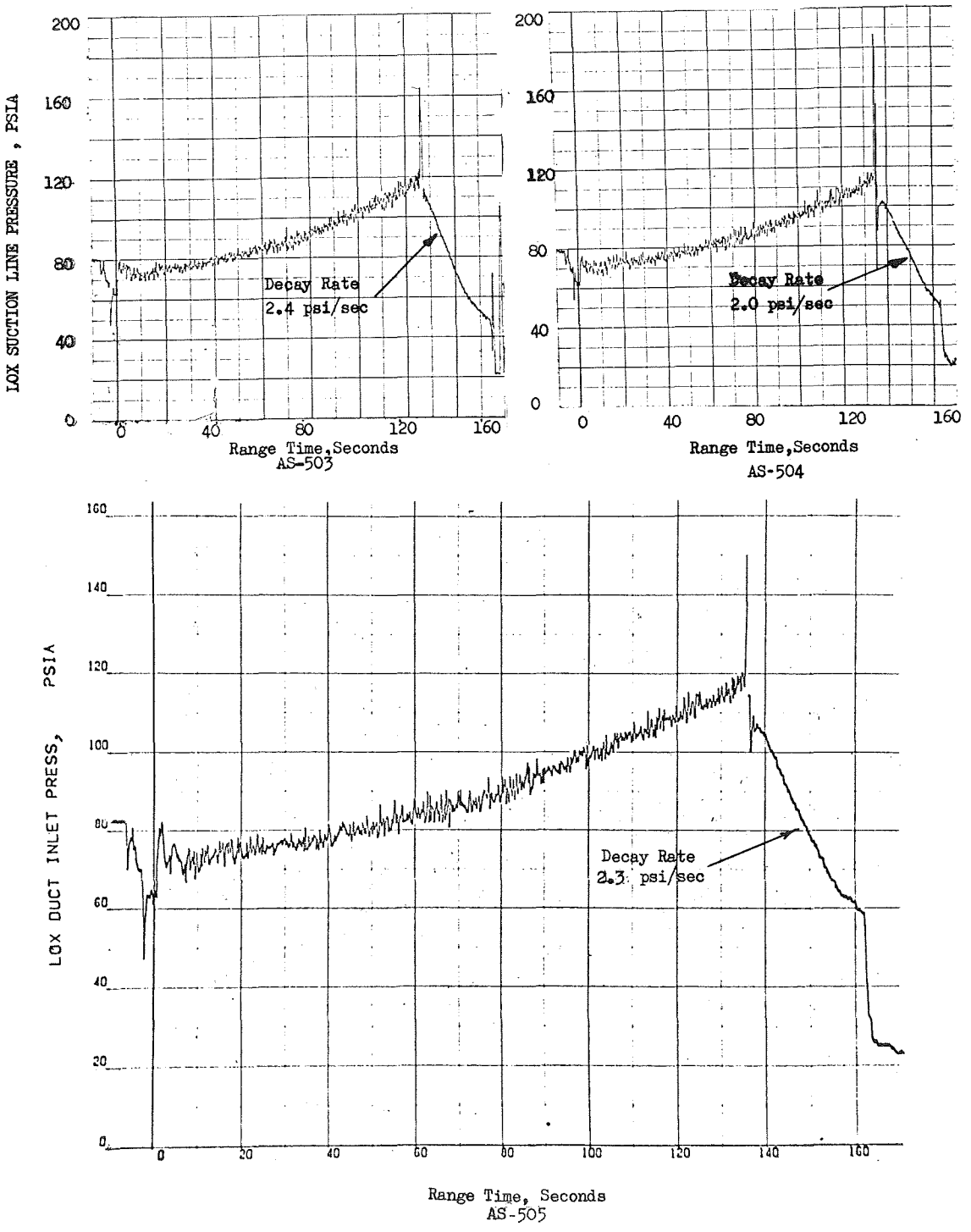

Figure 3. LOX Pressure Versus Range Time

TURBOPUMP FUNCTIONAL PARAMETER ANALYSIS

Turbopump bearing temperatures during flight were nominal. The LOX bearing temperatures (C006) ranged from 100 to 117 F at start, and were stabilized at approximately 114 to 124 F after T+90 seconds (Fig. 4 to 8).

Turbopump bearing jet pressures (D0013) were normal throughout flight. At T+90 seconds, the noted pressures on the five engines ranged from approximately 397 to 454 psia. The individual engines did not differ significantly from the values recorded during stage static testing, and all values were within the safe operating range of 200 to 540 psig (Fig. 9 to 13).

Turbopump LOX seal purge systems performed as expected. The average engine purge flowrate was calculated to be approximately 0.014 lb/sec, which is well below the maximum allowable average flowrate of 0.029 lb/sec. The purge flowrate was calculated from purge sphere pressure decay, with the assumption that calorimeter system purge total flowrate was 0.024 lb/sec.

Turbopump LOX seal cavity pressures were approximately ambient prior to engine start. At vehicle liftoff, all cavity pressures were 1.0 psig or less. The LOX seal cavity pressures reached a maximum pressure for engines 1 through 5 respectively of: 5.8, 4.0, 3.9, 6.1, and 7.2 psig (Fig. 14 to 18). These maximum values were attained in the last 40 seconds of flight operation, and are considered nominal based on the pressures experienced during stage static test and analysis of previous flight data. The stage static test mainstage operation redline is 12 psig, which would be equivlent to approximately 20 psig at the end-of-flight condition. LOX seal cavity pressures attained during ground testing because of the increased expansion of the nominal primary and intermediate seal leakage at altitude, and the attainment of choked flow in the LOX seal cavity drain system.

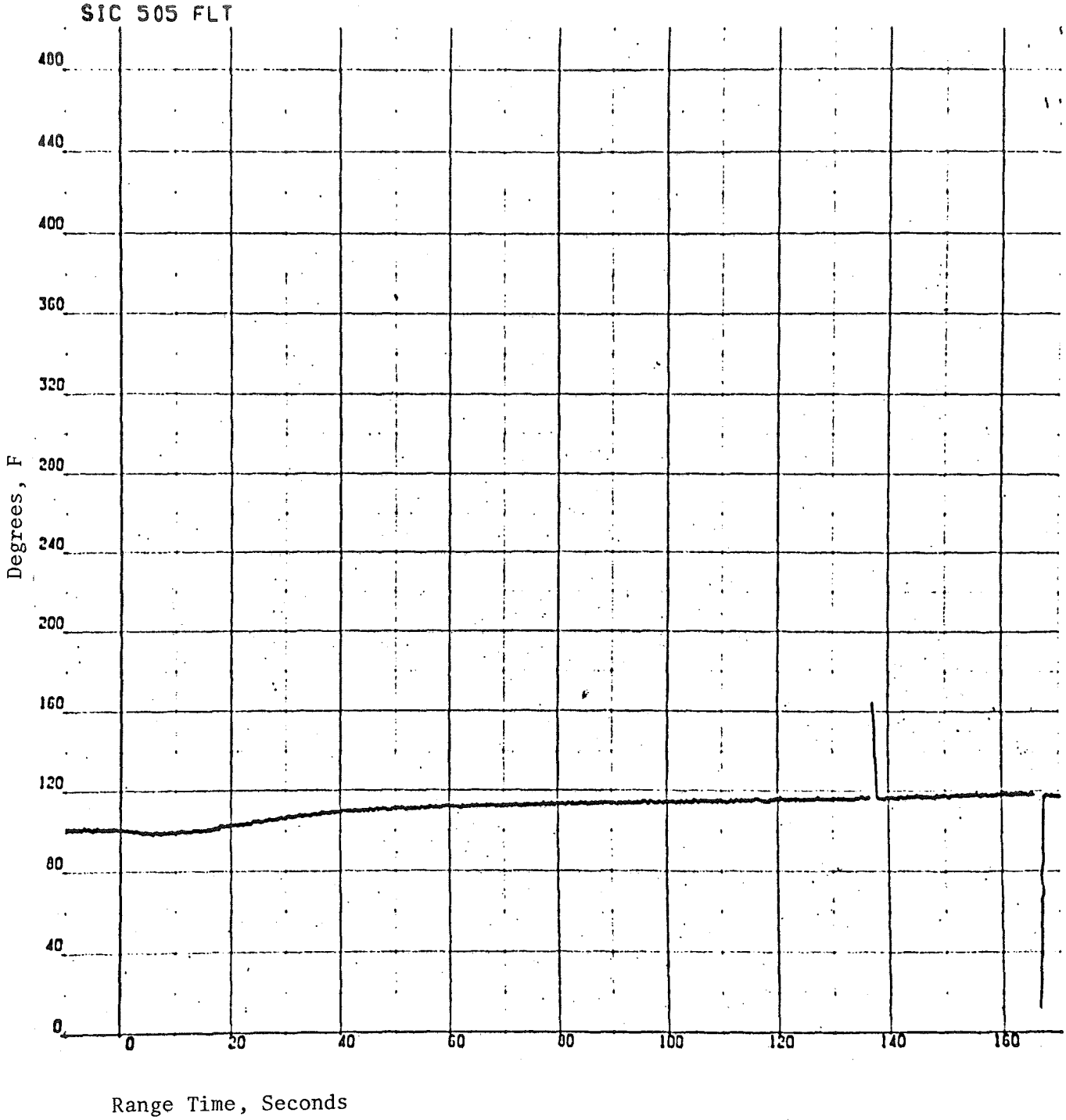

Figure 4. Turbopump LOX Bearing Temperature, Engine Position 1, F2035

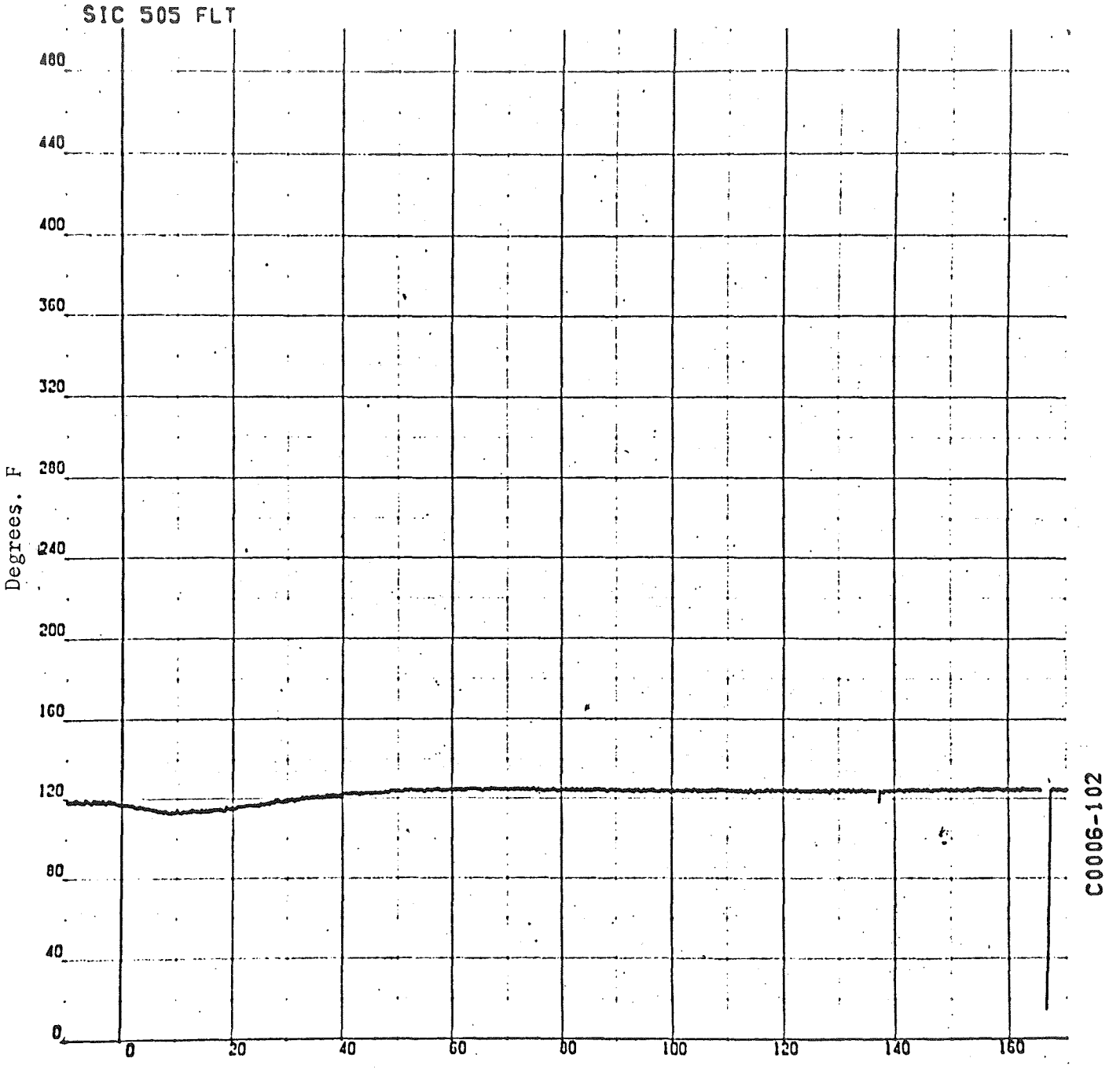

Range Time, Seconds

Figure 5. Turbopump LOX Bearing Temperature, Engine Position 2, F2041

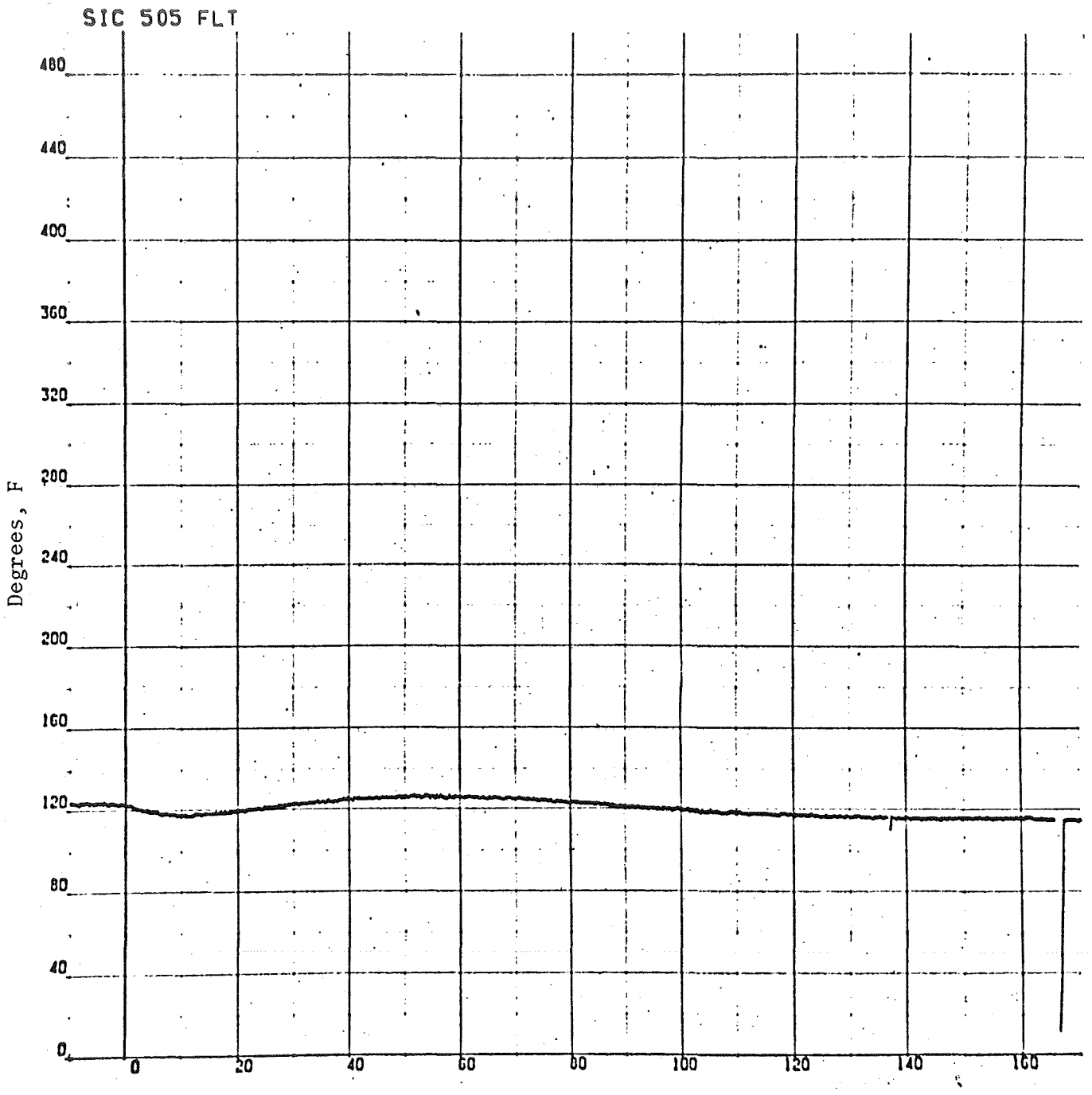

Figure 6. Turbopump LOX Bearing Temperature, Engine Position 3, F2040

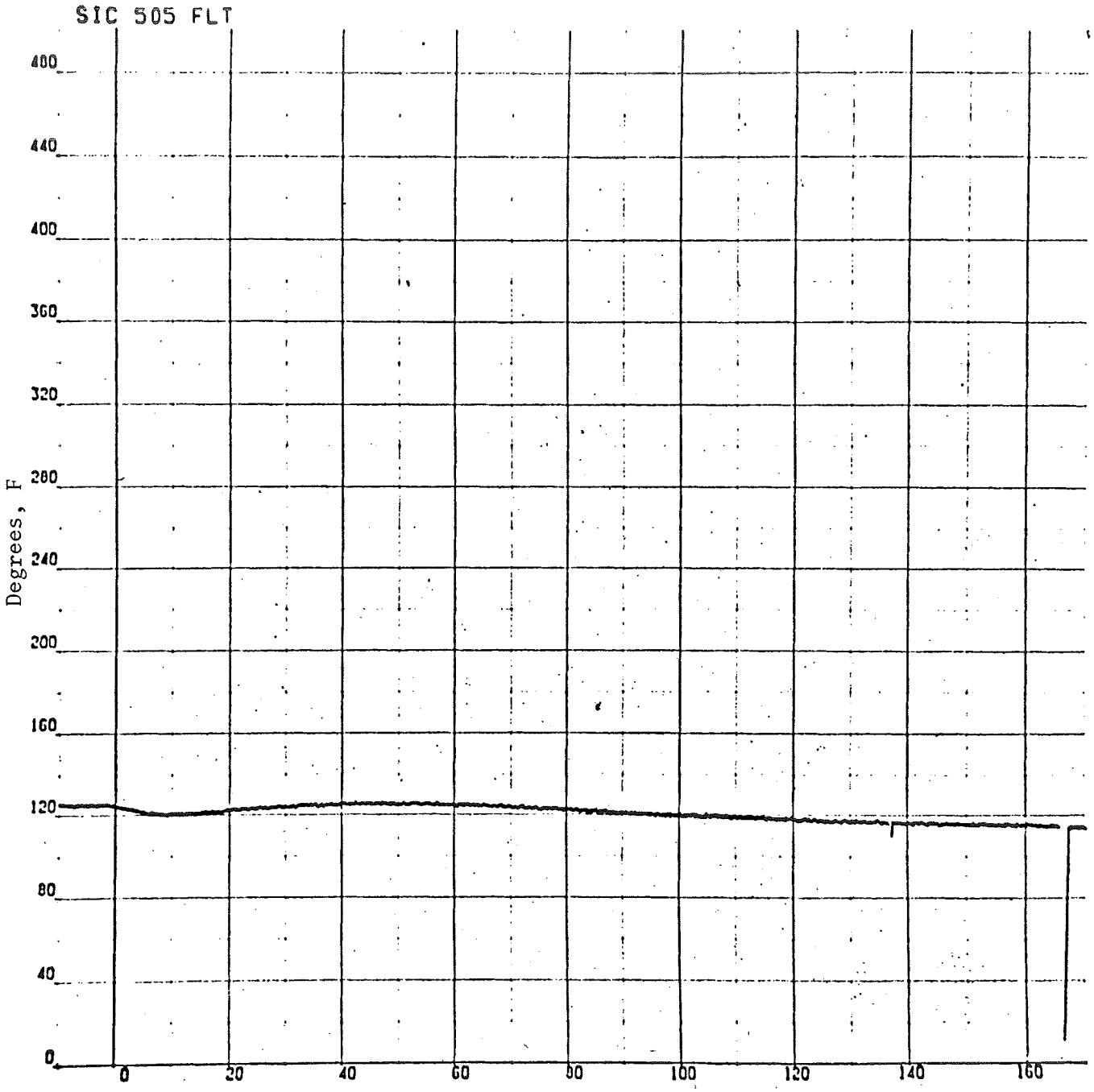

Figure 7. Turbopump LOX Bearing Temperature, Engine Position 4, F2042

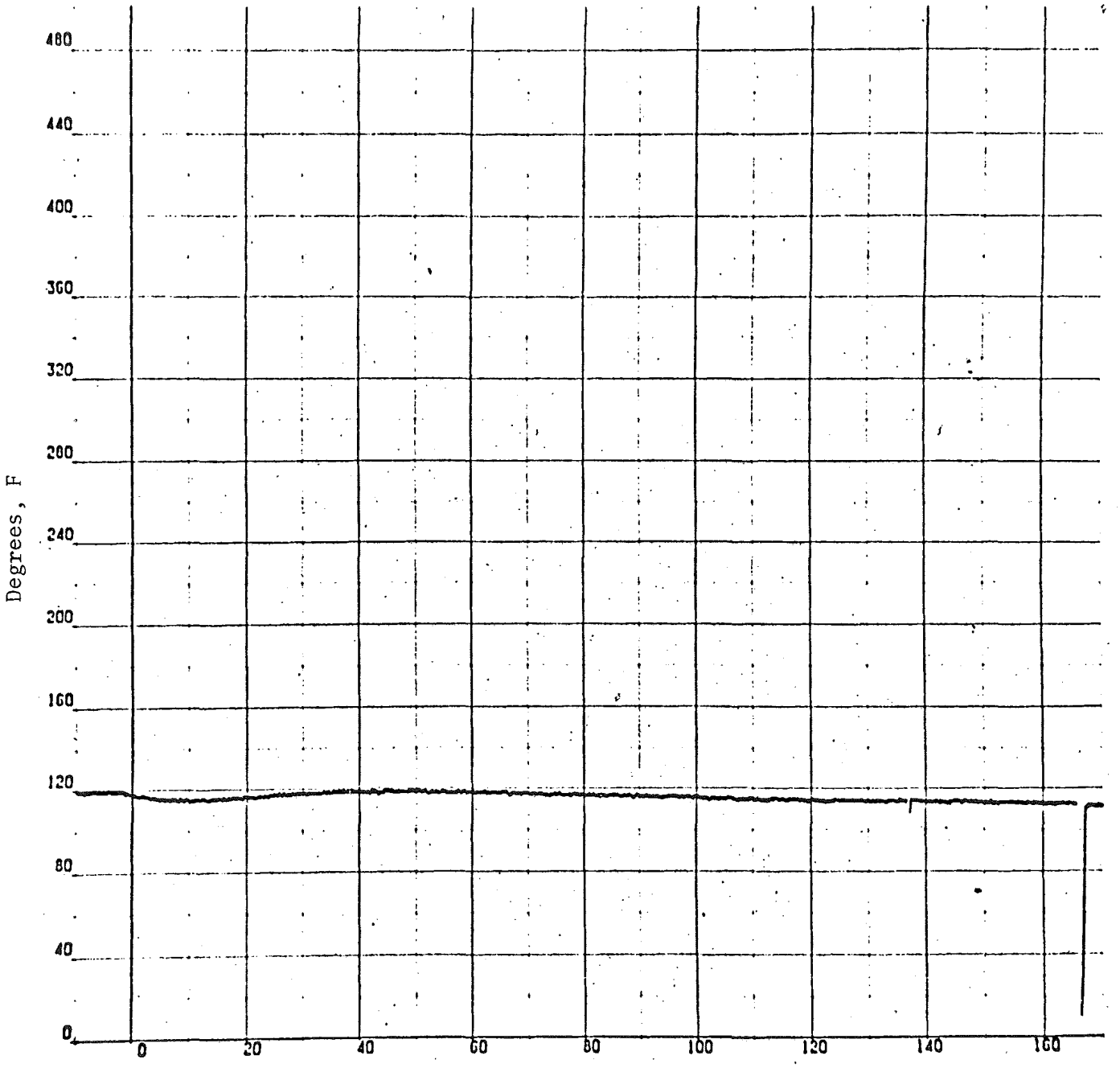

Figure 8. Turbopump LOX Bearing Temperature, Engine Position 5, F2034

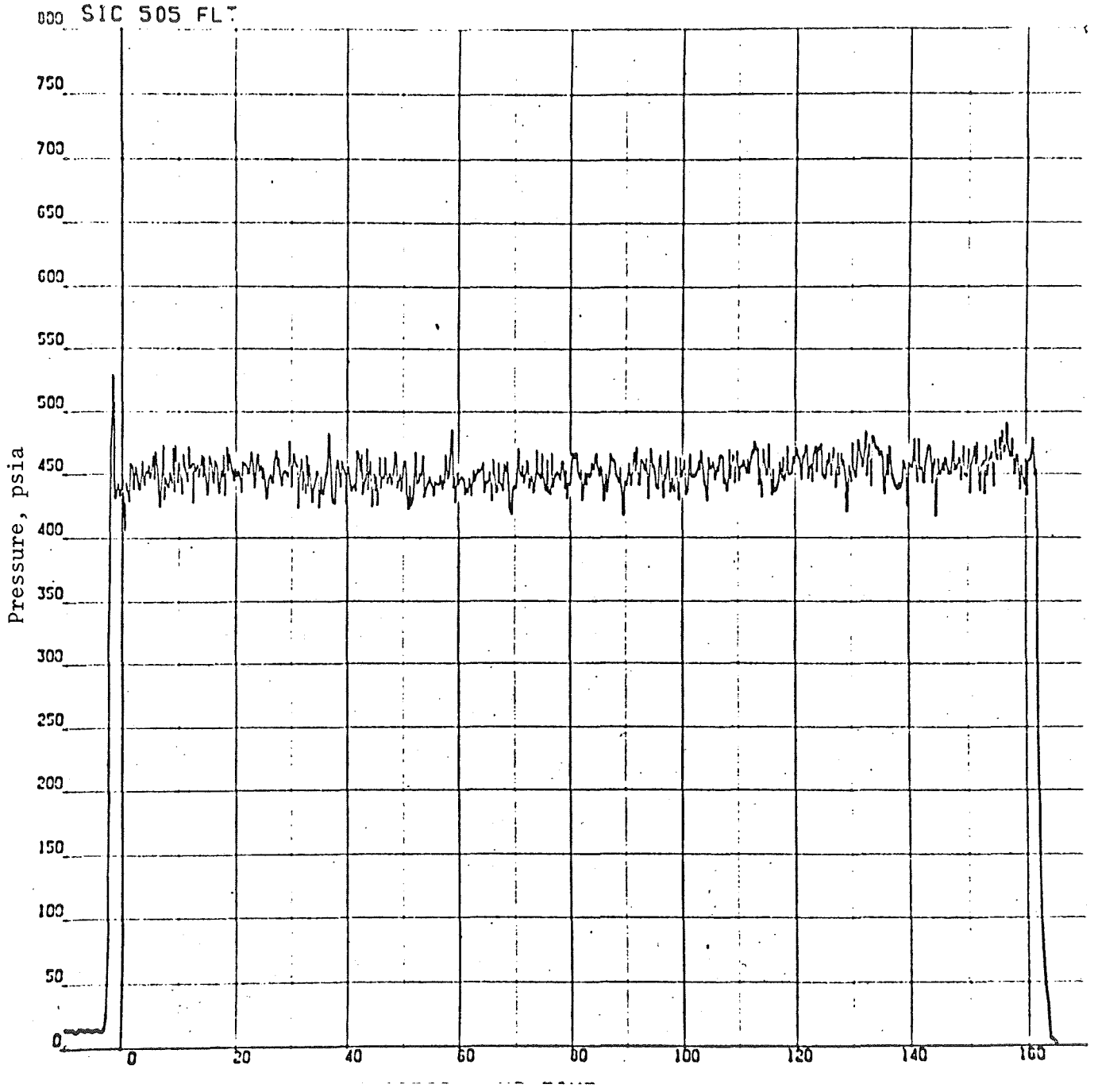

Figure 9. Turbopump LOX Bearing Jet Pressure, Engine Position 1, F2035

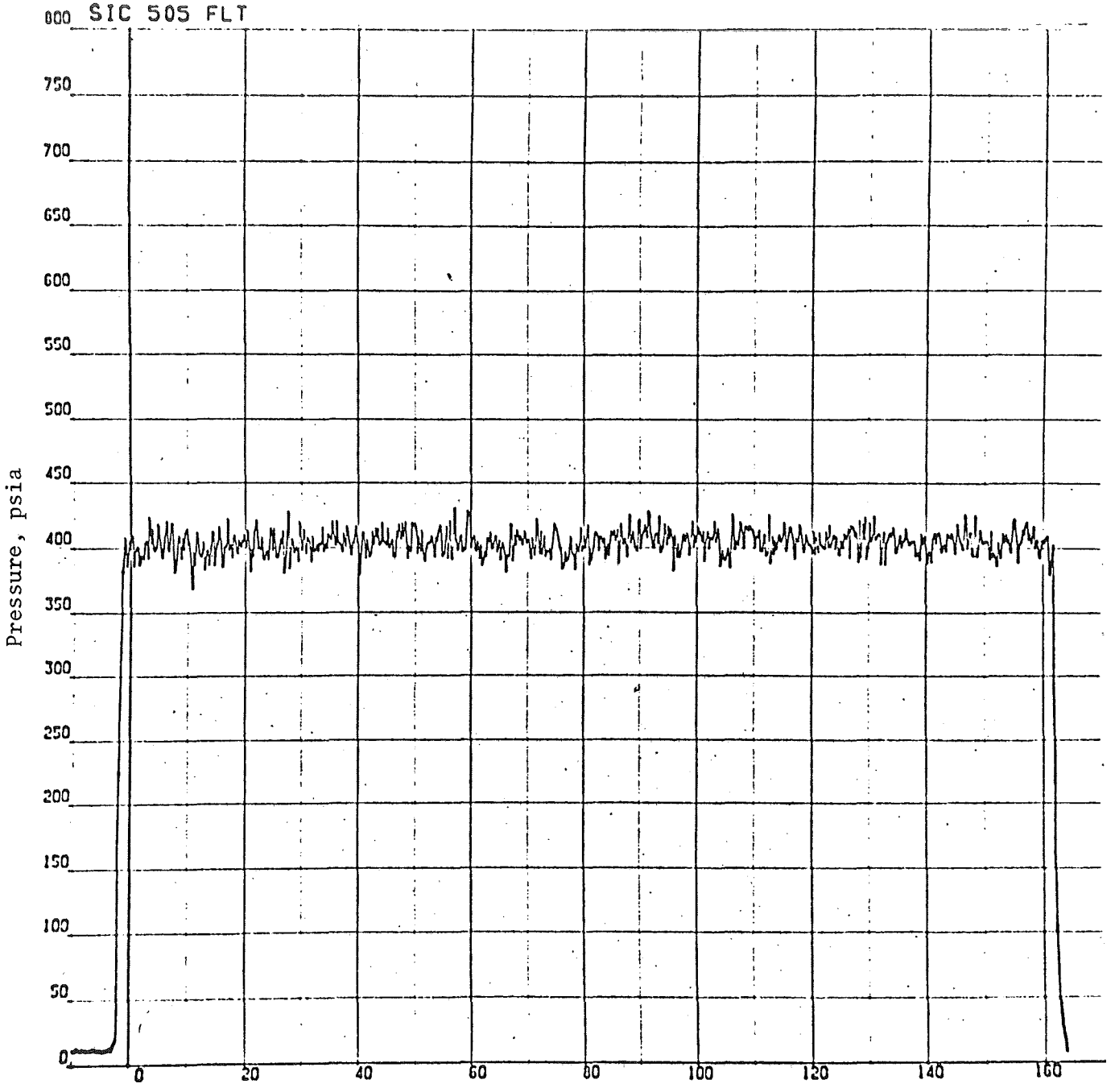

Figure 10. Turbopump LOX Bearing Jet Pressure, Engine Position 2, F2041

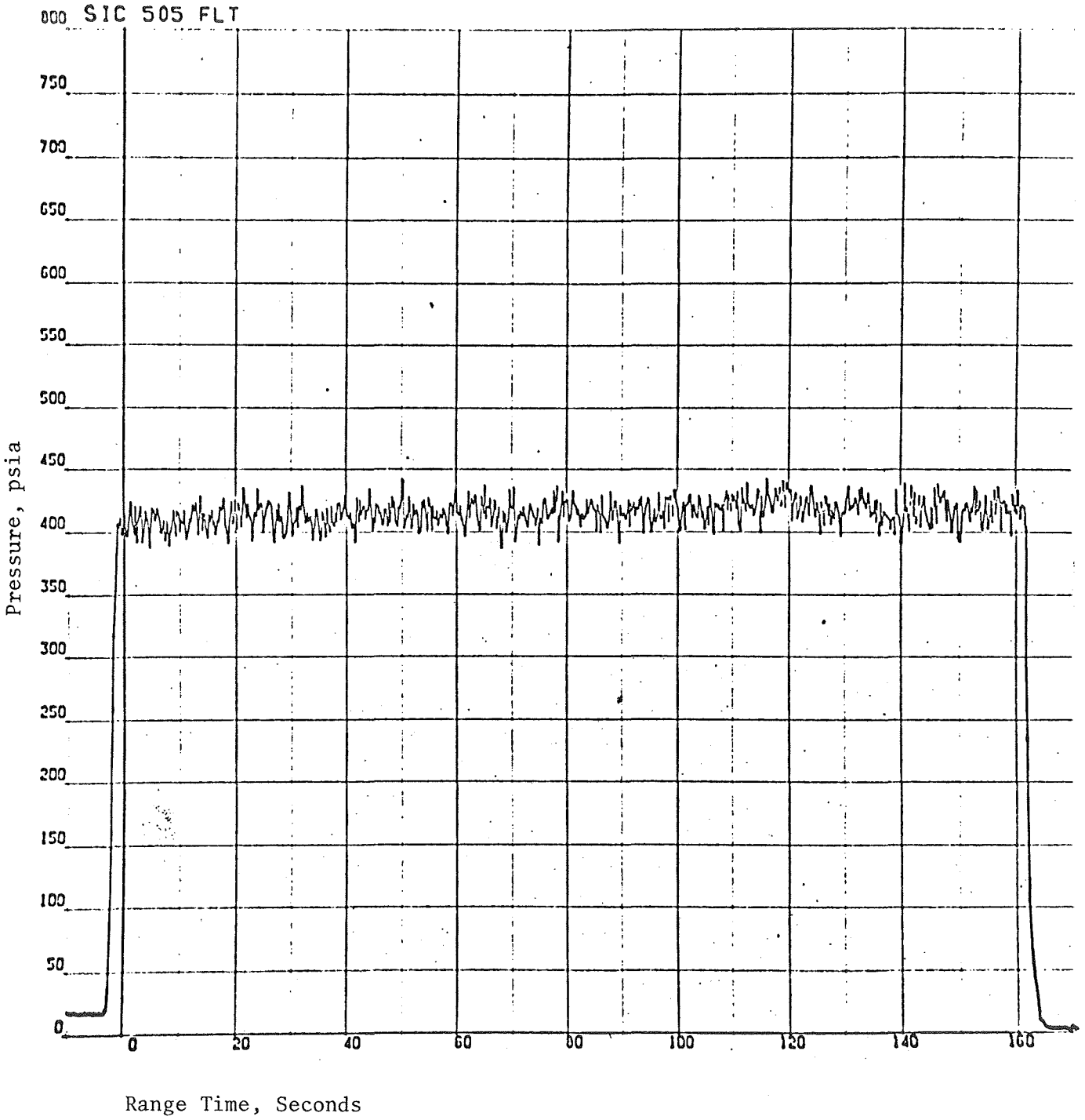

Figure 11. Turbopump LOX Bearing Jet Pressure, Engine Position 3, F2040

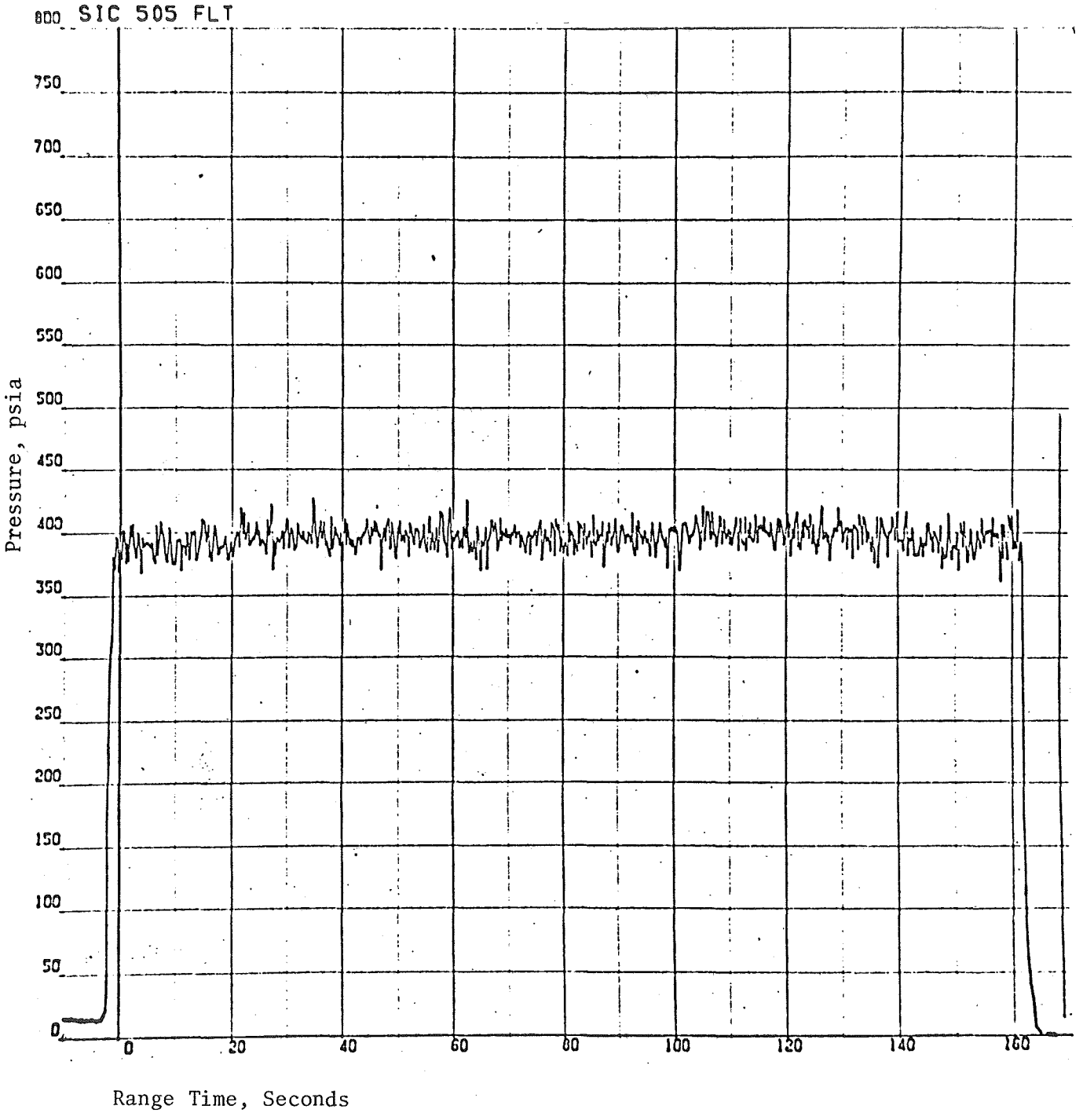

Figure 12. Turbopump LOX Bearing Jet Pressure, Engine Position 4, F2042

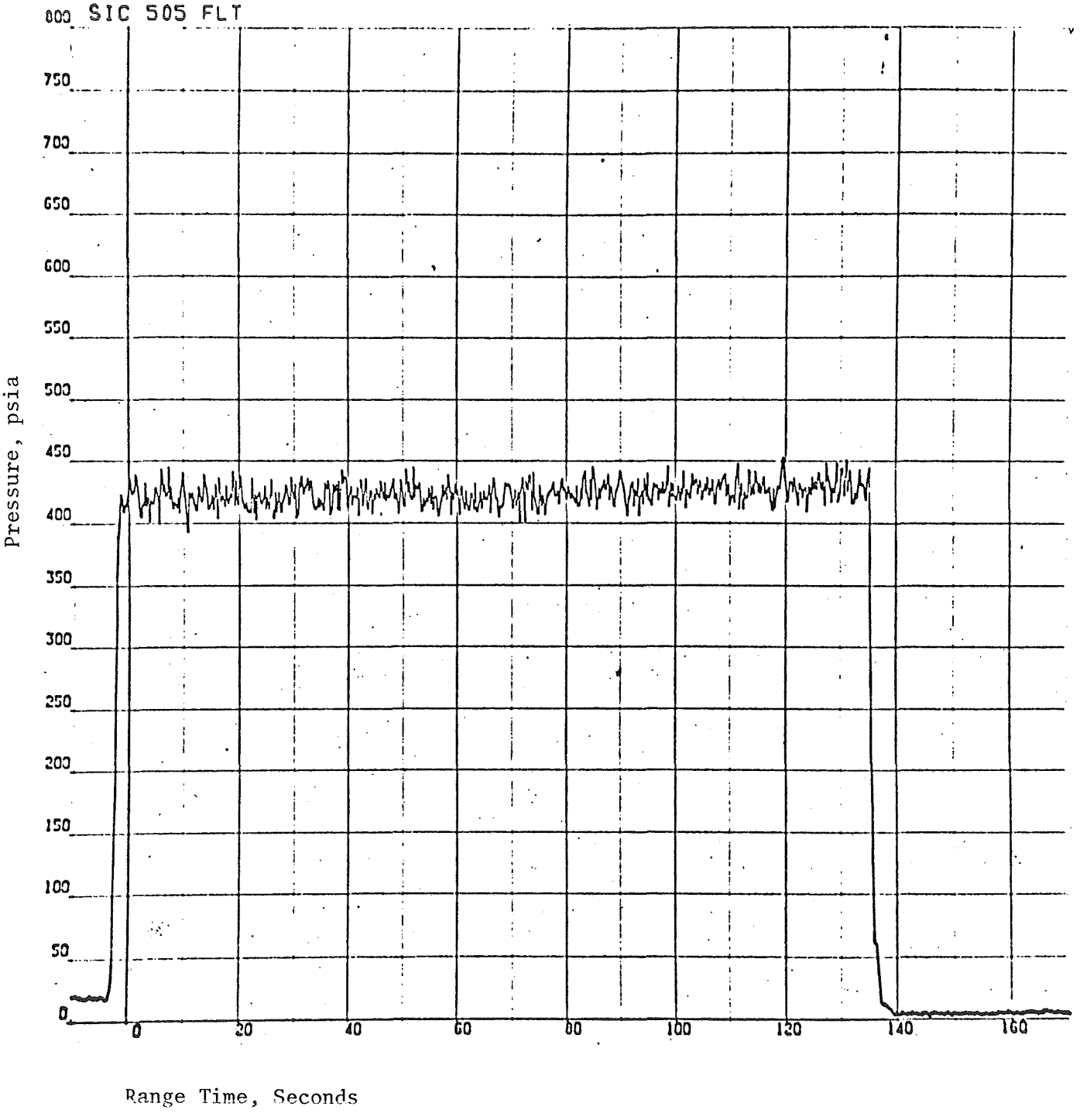

Figure 13. Turbopump LOX Bearing Jet Pressure, Engine Position 5, F2034

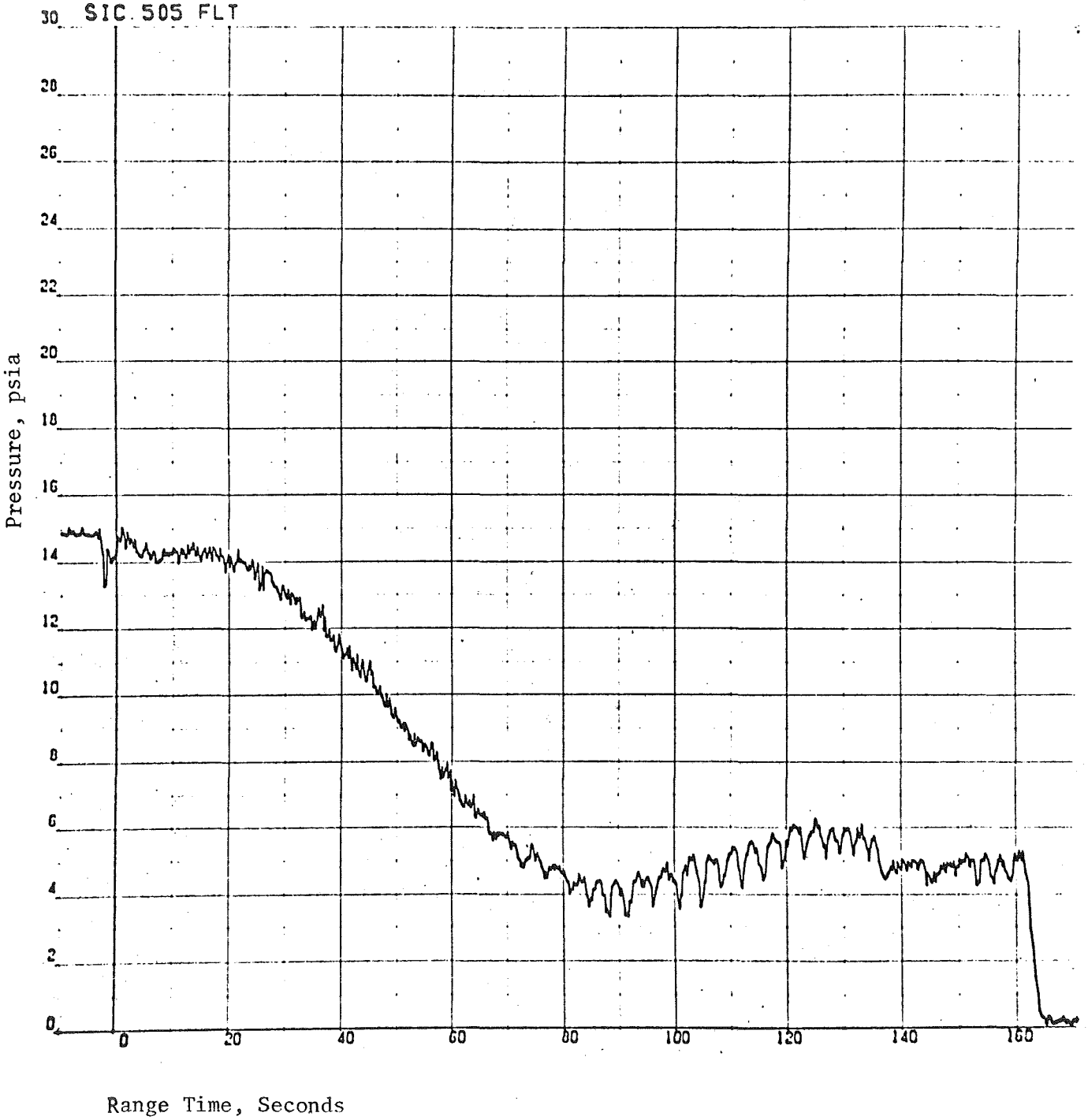

Figure 14. Turbopump LOX Seal Cavity Pressure, Engine Position 1, F2035

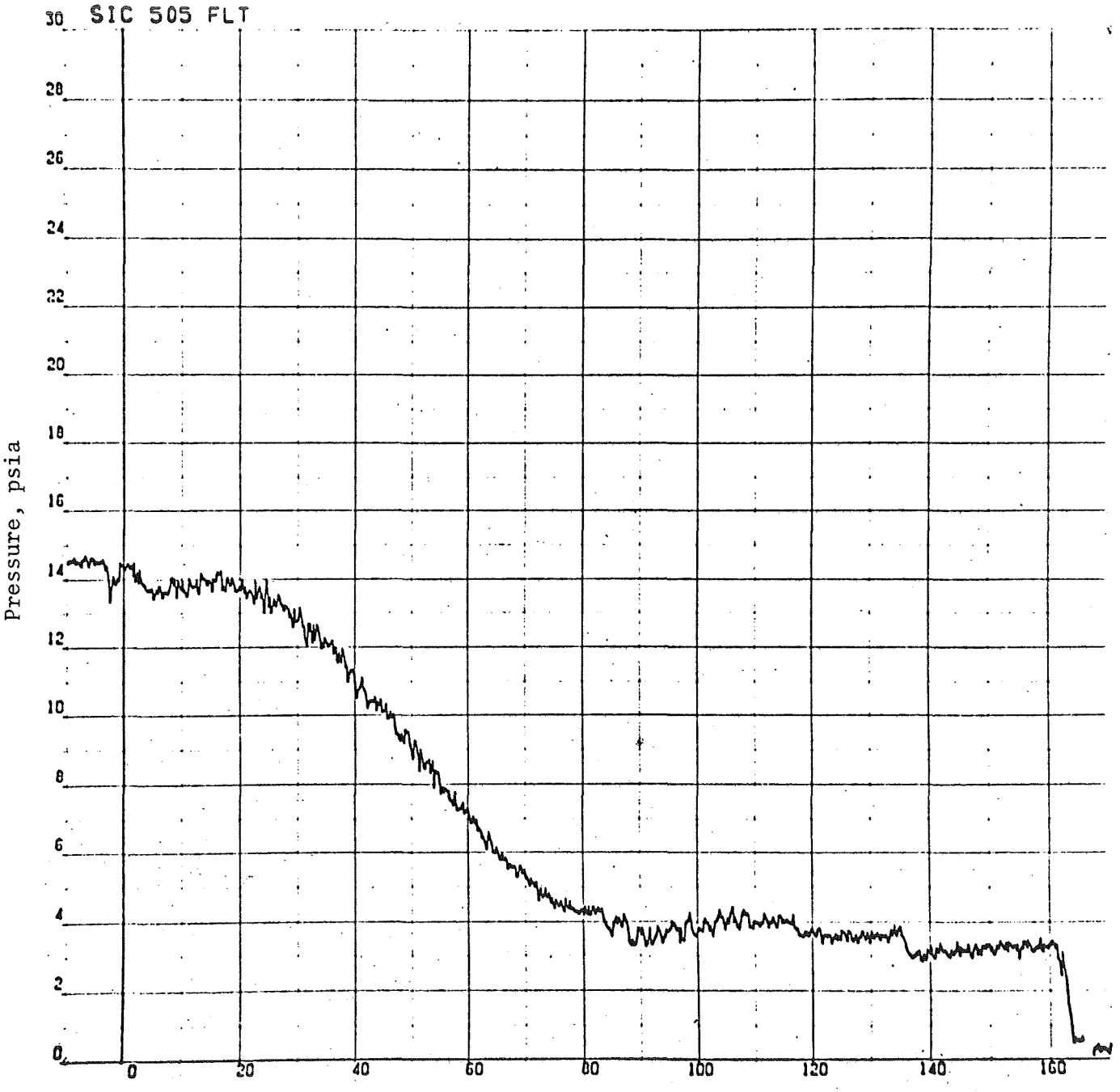

Figure 15. Turbopump LOX Seal Cavity Pressure, Engine Position 2, F2041

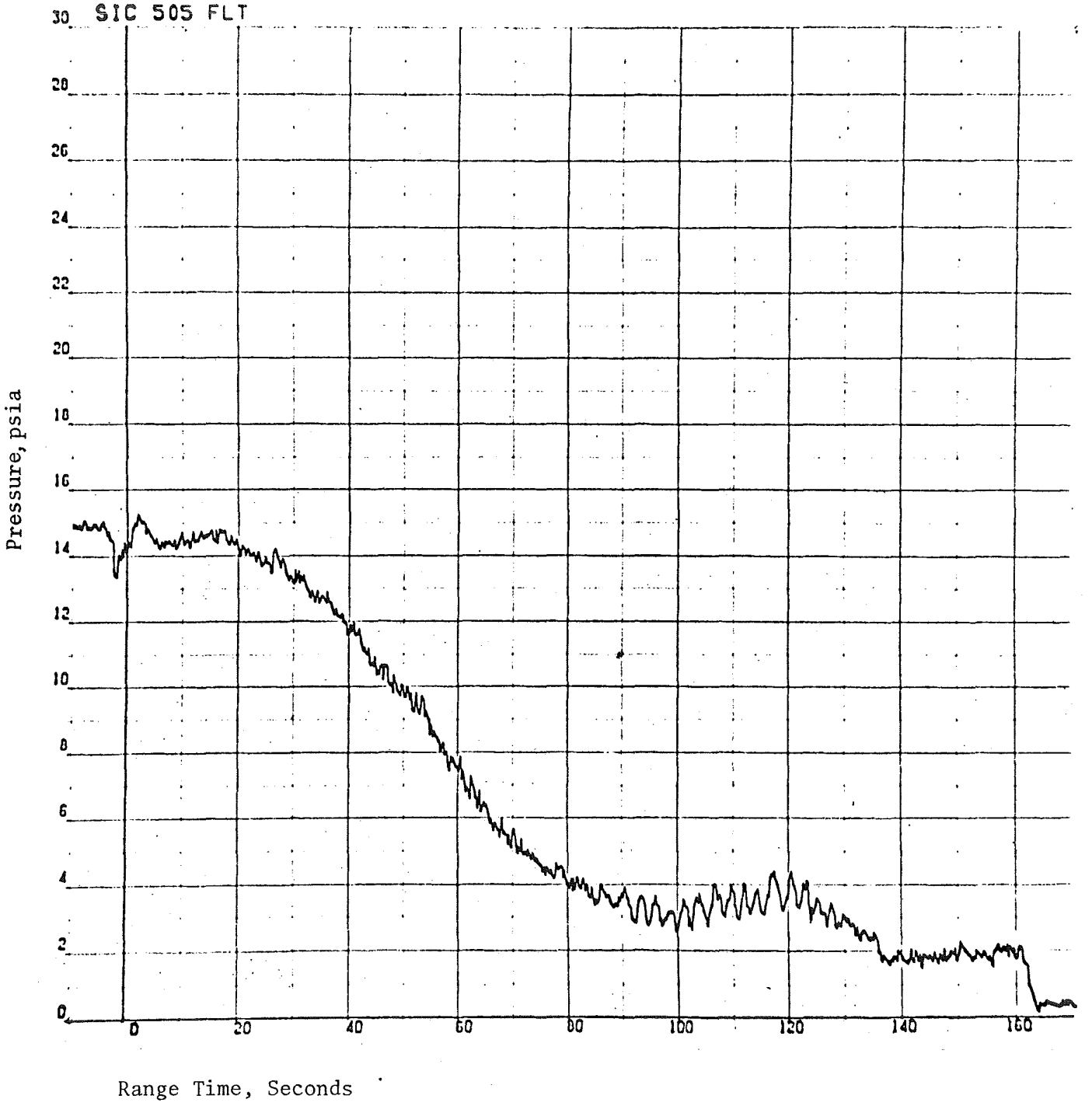

Figure 16. Turbopump LOX Seal Cavity Pressure, Engine Position 3, F2040

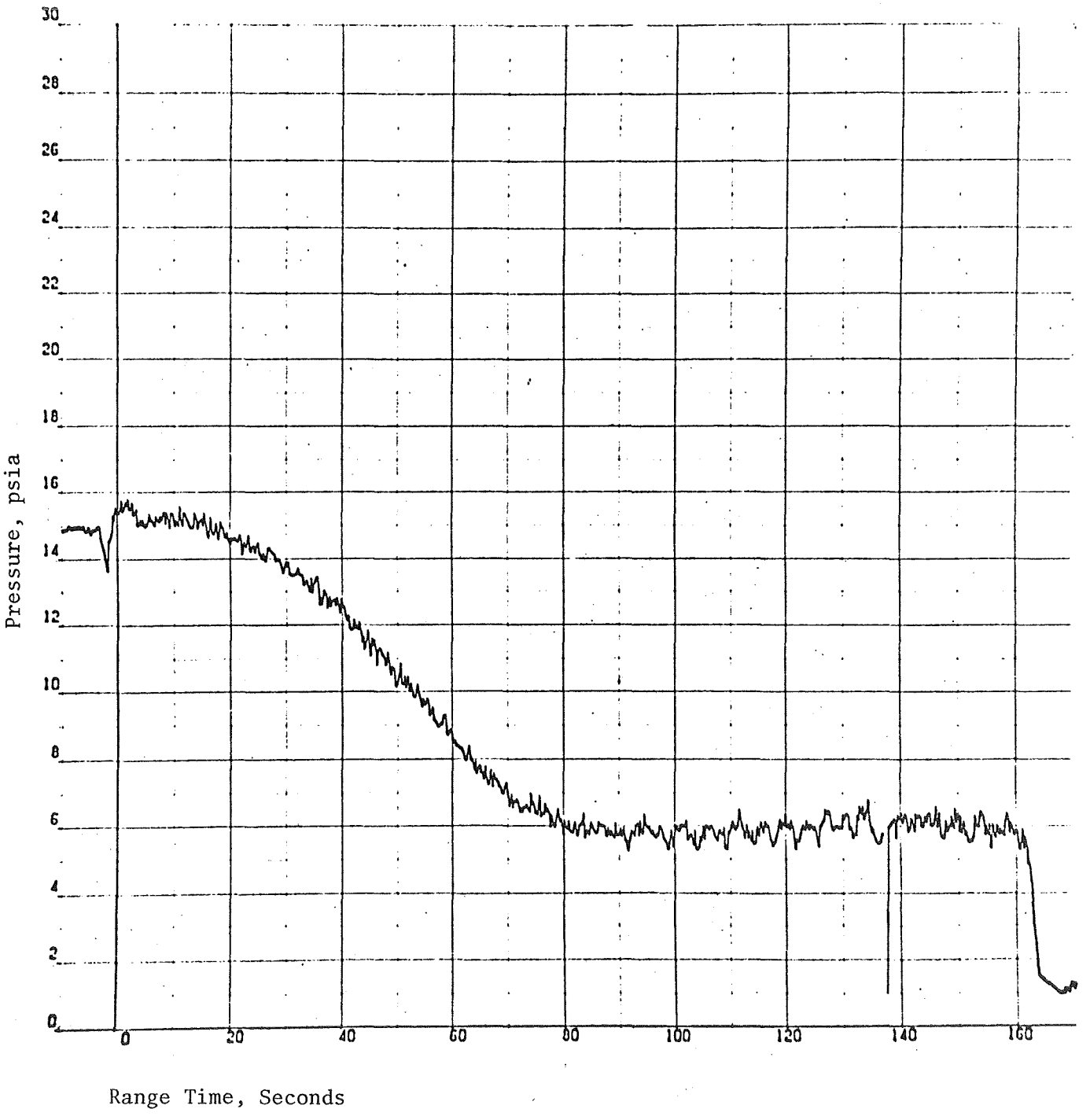

Figure 17. Turbopump LOX Seal Cavity Pressure, Engine Position 4, F2042

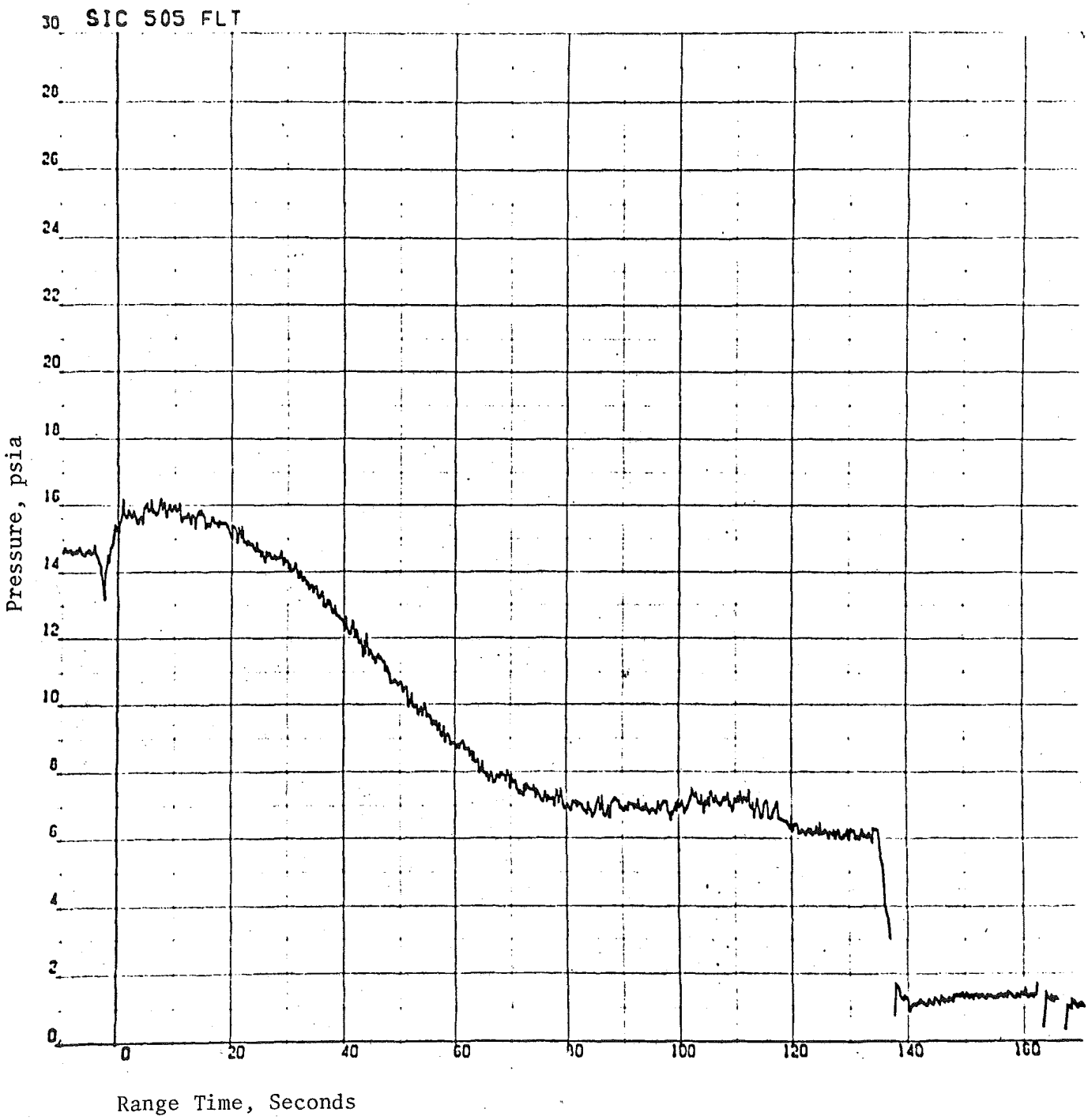

Figure 18. Turbopump LOX Seal Cavity Pressure, Engine Position 5, F2034

ENGINE STEADY-STATE PERFORMANCE ANALYSIS

The steady-state operation of all five F-1 engines was satisfactory. The measured engine performance parameters indicate thrust levels to average 1 kilopound per engine higher than predicted values. The inboard engine (position 5) cutoff was initiated as programmed at 135.2-seconds range time. The four outboard engines were cut off 26.4 seconds later by the LOX tank low-level sensor at 161.6 seconds.

F-1 engine steady-state performance was simulated and analyzed utilizing the FLT F1 MOD 3 data reduction program and the linear influence coefficients flight reconstruction program. Average F-1 engine thrust level for the S-IC-5 stage was 0.07 percent higher than predicted. Predicted and actual performance values of selected parameters are presented in Table 7, and reconstructed parameters are presented in Fig. 19 through 59.

F-1 ENGINE SEA-LEVEL PERFORMANCE AT 35-SECONDS RANGE TIME

Selected data obtained from the FLT F1 digital reduction program versus predicted values are presented in Table 7 at a slice time of 35 seconds after stage test start and 35 seconds after liftoff for flight data. These data are reduced to standard sea-level conditions of turbopump inlet pressures, propellant temperatures, and ambient pressure; also, performance corrections were made for the effect of vehicle acceleration on engine propellant heads. The data are averaged over a 3-second time interval. Data processing and reduction techniques employed are presented in Appendix E.

Rocketdyne-predicted performance values presented in Table 7 were generated using data from Rocketdyne engine acceptance tests and from stage static test data.

The engine thrust levels are automatically calculated from the flight data in the FLT F1 program by matching the chamber pressure and turbopump speed

TABLE 7

S-IC-5 F-1 ENGINE STEADY-STATE FLIGHT PERFORMANCE*

(35 Seconds After Liftoff, Reduced to Sea Level and Standard Turbopump Inlet Conditions)

Engine Position		1	2	3	4	5	
Engine Serial		F2035	F2041	F2040	F2042	F2034	Average
Thrust, kilopounds	Flight	1486	1520	1527	1503	1517	1511
	Predicted	1507	1517	1515	1504	1507	1510
	Flight Minus Predicted	-21	3	12	-1	10	1
Engine Mixture Mixture	Flight	2.271	2.268	2.267	2.273	2.283	2.272
	Predicted	2.273	2.267	2.266	2.273	2.279	2.272
	Flight Minus Predicted	-0.002	0.001	0.001	0.0	0.004	0.0
Specific Impulse, seconds	Flight	263.4	265.4	265.0	263.6	264.3	264.3
	Predicted	263.9	265.4	264.7	263.6	264.0	264.3
	Flight Minus Predicted	-0.5	0.0	0.3	0.0	0.3	0.0
Thrust Chamber Pressure, psia	Flight	1099	1120	1127	1113	1117	1115
	Predicted	1113	1119	1120	1114	1111	1115
	Flight Minus Predicted	-14	1	7	-1	6	0
Turbopump Speed, rpm	Flight	5394	5474	5494	5434	5471	5453
	Predicted	5444	5468	5466	5438	5446	5452
	Flight Minus Predicted	-50	6	28	-4	25	1
Turbine Manifold Temperature, F	Flight	1485	1516	1510	1481	1521	1503
	Predicted	1537	1504	1491	1513	1500	1509
	Flight Minus Predicted	-52	12	19	-32	21	-6

*Flight values are reduced on the FLT F1 MOD 3 data reduction program using EFL acceptance test hardware characteristics with flight thrust chamber pressure, turbopump speed, and inlet condition measurements only. Predicted values are Rocketdyne TAG values reduced on FLT F1 MOD 3 Data Reduction Program.

measurements to the predicted steady-state values for each engine. The best estimate of flight thrust is obtained by averaging the thrust calculated from the flight telemetry value of thrust chamber pressure with the thrust calculated from the handcounted flight turbopump speed. The resulting engine performance values are then reduced to standard sea-level conditions. Comparison of flight and predicted thrust values from Table 7 indicates that the average engine flight value of thrust reduced to sea-level standard conditions was high by 1 kilopound (0.07 percent). Although engine 2035 (position 1) was 21 kilopounds low at the 35 second slice point, engine performance increased subsequently during the flight. Analysis is continuing on this observation, and current information is presented in the Flight Performance Reconstruction section of this report.

Table 7 presents engine mixture ratio and specific impulse values based on Rocketdyne predicted performance data adjusted to correspond to the flight thrust levels. The methods used to calculate the mixture ratio and specific impulse in Table 7 employ Rocketdyne acceptance data for both predicted and flight values so that the differences shown are due only to changes in thrust level and round-off effects. The values of mixture ratio and specific impulse presented in Table 7 are generally considered the best estimates. However, a comparison of measured and calculated propellant flowrates presented in Tables 7a and 7b indicates that during the AS-505 flight, the engine 1 calculated value for fuel flowrate is low compared to the measured value by 1.2 percent. By assuming constant engine specific impulse, a lower engine LOX flowrate was calculated. The lower LOX weight flow is supported by the liquid level measurements presented in Table 7b in that it would decrease the observed difference. Based on these observations, the engine mixture ratio during flight may have been lower than predicted by approximately 1.7 percent.

"Flight" values as presented in Table 7 are used as performance base values at 35-seconds range time for the flight performance reconstruction program flight simulation and analysis.

TABLE 7a

DIFFERENCE BETWEEN MEASURED AND PREDICTED FUEL FLOWRATES AS-502 THROUGH AS-505 FLIGHTS

(Individual Engines)

Vehicle	Position	Engine	Measured Minus Calculated Engine fuel flowrate, lb/
502	1	4017	- 35
	2	4018	- 31
	3	4019	- 27
	4	4021	- 14
	5	4020	- 37
503	1	4024	- 5
	2	4022	- 5
	3	4025	1
	4	4026	21
	5	4027	9
504	1	5029	11
	2	5032	- 15
	3	5031	- 6
	4	5033	- 17
	5	5030	10
505	1	5035	21
	2	5041	- 2
	3	5040	- 2
	4	5042	2
	5	5034	3

TABLE 7b

COMPARISON OF TOTAL VEHICLE PROPELLANT FLOWRATES
AS-501 THROUGH AS-505 FLIGHTS

Total Fuel Flowrate at 35 to 38 seconds in lb/sec

	501	502	503	504	505
From Interval Gages	8771	8788	8837	8712	8795
From Flowmeters	--	8650	8846	8723	8798
From Prediction	8763	8794	8825	8740	8776
Δ Flows					
Flowmeter, Gages	--	-138	9	9	3
Flowmeter, Prediction	--	-144	21	- 17	22

Total LOX Flowrate at 35 to 38 seconds in lb/sec

From Interval Gages	20167	20257	20136	30151	20238
From Prediction	20182	20338	20200	20121	20366
Δ Flow					
Gage, Prediction	- 15	- 81	- 64	30	- 128

TABLE 8

F-1 ENGINE PERFORMANCE AFFECTING COMPONENT CHANGES SUBSEQUENT TO ROCKETDYNE ACCEPTANCE TESTING

Engine Position	1	2	3	4	5
Engine Serial Number	2035	2041	2040	2042	2034
No. 1 Main Fuel Valve		X	X	X	
No. 2 Main Fuel Valve		X	X	X	
Heat Exchanger					X
No. 1 Fuel High-Pressure Duct				X	

Steady-state engine thrust at sea-level inlet conditions and 35 seconds after start for F-1 engines on the first four flight vehicles indicates an average thrust bias per stage of 9 kilopounds per engine exists such that the flight thrust reduced to sea-level inlet conditions is lower than the TAG values. The TAG values for S-IC-5 were lowered by 9 kilopounds as a result of this observation.

FLIGHT PERFORMANCE RECONSTRUCTION AND ANALYSIS

F-1 performance values throughout the flight were reduced to standard sea-level conditions using the linear influence coefficients flight reconstruction program. Engine position 1 (F2035) displayed performance characteristics that are different from that of the other four engines. A detailed analysis of engine 1 performance was made to determine (1) if the engine performance variation could be associated with a particular component characteristic or combination of characteristics, and (2) if these characteristics were indicative of a component malfunction. The results of this analysis indicate that engine 1 performance characteristics are probably caused by a variation of turbine efficiency and turbine nozzle area with time that is not the same as that for the other four engines on the S-IC stage for AS-505.

The following differences in performance parameters of engine F2035 (position 1) have been observed:

1. A sea level thrust at 35 seconds range time 21 kilopounds lower than predicted
2. A 20 kilopounds decrease in sea level thrust from 10 seconds to 35 seconds range time, followed by a 30 kilopounds increase from 35 seconds to 153 seconds

The performance of engine F2035 (position 1) is compared with the performance of the other engines in Fig. 18a and 18b showing turbopump speed and thrust chamber pressure for the entire flight. Telemetry data indicates

that the thrust as computed from pump speed and chamber pressure decreased approximately 1.4 percent during the first 35 seconds and subsequently recovered over the following 100 seconds of operation. A large number of hardware variations, external condition variations, and failure modes which could have caused the observed performance variation were analyzed. Table 8a presents a summary of the parameter variations investigated.

The independent parameter variations which correlate best with the observed performance are turbine efficiency and turbine nozzle area. Figure 18C shows the turbine nozzle area change which is expected and that calculated from telemetry data by the Matrix Match program. The expected variations presented are an average and some variation resulting from manifold temperature and hardware differences is not unusual. Figure 18d shows the turbine efficiency variation which was required along with the above nozzle area change to match the telemetry turbopump speed and turbine exit pressures as shown in Fig. 18e and 18f. Figures 18g through 18m show the correlation between the parameter variations observed and those calculated with the Matrix Match program by allowing turbine nozzle area and efficiency to vary as indicated by Fig. 18c and 18d. This performance difference appears to have originated in the hot gas part of the gas generator-turbine system. The particular thrust climbout of engine position 1 is represented well by a simultaneous change in turbine nozzle throat area and turbine efficiency.

Performance data of previous R&D and production engines are presently being compiled and analyzed relative to the thrust climbout investigation on engine F2035. Several engines have already been identified with thrust climbout characteristics similar to that of F2035 (engine position 1).

The turbine characteristics and the resulting engine performance variation experienced on engine F2035 are within the range of test experience and, although analysis effort will continue, no evidence exists of an engine hardware failure.

Figure 19 presents S-IC-5 flight turbopump speeds reduced to sea-level standard inlet conditions as a ratio to engine base values at 35-seconds range time (Table 7).

TABLE 8a

AS-505 FLIGHT

ENGINE POSITION 1, F2035

PARAMETERS INVESTIGATED BY RECONSTRUCTION ANALYSIS

		Quality of Match
1.	Turbine Nozzle Area and Efficiency	Excellent
2.	GG LOX and Fuel Resistance	Good
3.	LOX Pump Inlet Pressure	Good
4.	Helium Injection	Good
5.	LOX Pump Head and Efficiency	Fair
6.	Fuel Pump Head and Efficiency	Fair
7.	GG LOX System Resistance	Fair
8.	GG Fuel System Resistance	Fair
9.	LOX Pump Inlet Temperature	Fair
10.	Fuel Pump Inlet Pressure	Poor
11.	LOX Pump Head	Poor
12.	Fuel Pump Head	Poor
13.	Turbine Nozzle Area	Poor
14.	Turbine Nozzle Area and Fuel Pump Head	Poor
15.	Fuel Density and Fuel Temperature	Poor
16.	GG Combustor Body Resistance	Poor
17.	Main LOX System Resistance	Poor
18.	Main Fuel System Resistance	Poor
19.	Turbine Exhaust System Resistance	Poor
20.	GG Fuel and Turbine Exhaust System Resistance	Poor
21.	Fuel Density	Poor
22.	Main LOX System Leak	Poor
23.	Main Fuel System Leak	Poor
24.	GG Fuel System Leak	Poor
25.	GG LOX System Leak	Poor
26.	Hot Gas System Leak	Poor

NOTE: Categories of Match Quality

Excellent Good Fair Poor

The reconstructed flight thrust chamber pressures at sea-level standard inlet conditions are shown in Fig. 20 as a ratio to average base value. Thrust chamber pressure measurements on all engines exhibited prestart zero shift biases. The biases were removed by including a correction for the zero shift biases as noted in Appendix E. Both Fig. 19 and 20 show the different pump speed and chamber pressure variation for engine 1 as compared to the other engines.

Engine external conditions as presented in Fig. 21 through 28 are based on telemetered flight measurements. The atmospheric pressure for flight (Fig. 21) is calculated from vehicle altitude as determined from mass point trajectory data and the ARDC standard atmosphere. Telemetered propellant inlet conditions as presented by Fig. 22 through 27 are used for the flight reconstruction. Liquid oxygen pump inlet pressure for outboard engines as presented by Fig. 22 is calculated by averaging the telemetry data from the four outboard engine LOX suction line pressures, correcting for a pressure drop downstream of the measurement, adding the effect of vehicle longitudinal acceleration on the fluid downstream of the measurement, and adding a calculated dynamic head. The inboard engine LOX suction line pressure is treated separately because the line configuration telemetry measurement point location is different from those of the outboard engines. Inboard engine LOX pump inlet pressure is also presented in Fig. 22. Liquid oxygen temperature presented in Fig. 23 is the average of the five telemetered LOX suction line temperatures.

The fuel pump inlet pressure presented in Fig. 24 is the average of five telemetered measurements located one each on the No. 1 fuel inlets of each of the five engines. Fuel pump inlet temperature is presented by Fig. 25, which is the average of five measurements, one per engine. The fuel sample density utilized within this analysis was 50.3 lb/cu ft at a temperature of 60 F.

Fuel and oxidizer pump inlet conditions were used to determine the respective pump NPSH for the engines as presented by Fig. 26 and 27. Both fuel and oxidizer NPSH are shown to be well above the respective required minimum of 80 and 65 feet throughout the mission.

The vehicle acceleration curve (Fig. 28) is obtained from the observed mass point trajectory profile and is used with acceleration influence coefficients to give the effect of vehicle acceleration on the propellant column heights within the engine. Vehicle acceleration effects on the liquids in the low-pressure lines above the pump inlets are included in the pump inlet pressures.

The simulated trend multiplier variation (Fig. 29), considered to be primarily due to coking in the turbine inlet nozzles was included in the flight reconstruction to represent the performance change with time that is observed during engine tests. The effect of the turbine nozzle area reduction is a gradual decrease in engine performance level along with an increase in pressures upstream of the turbine nozzles with time. The magnitude of the simulated nozzle area reduction effect on S-IC-5 stage engine performance is -12 kilopounds thrust per engine over the flight interval from 35 seconds to engine shutdown.

The average engine thrust trend during acceptance testing of the S-1C-5 engines was approximately -20 kilopounds over the interval from 35 seconds to 150 seconds. The reconstruction analysis turbopump speed trend as presented in Fig. 19 indicates the AS-505 flight speed trend to be equivalent to approximately -7 kilopounds thrust from 35 seconds to engine shutdown; however, this analysis includes simulation of a variation in trend multiplier as a function of operating time which, as previously noted, is equivalent to an additional -12 kilopounds of thrust. The reconstruction analysis therefore indicates a thrust trend of approximately -19 kilopounds for the average of engines 2, 3, and 4. Use of the FLT F1 reduction program, which does not utilize a simulated turbine nozzle area variation, indicates a thrust trend of approximately -21 kilopounds for these engines over the same flight interval.

The linear influence coefficients flight reconstruction program is employed to reconstruct individual engine performance parameters. These performance parameters plotted versus time, as presented in Fig. 30 through 59, include flight "telemetry" data, "fitted" data, and "reconstructed" data. The telemetry data are the as-measured flight values with instrumentation biases

removed, as noted in Appendix E. The fitted values are determined by a least-squares mathematical fit of telemetry data over the 5.0-second time interval centered at the particular time presented. The reconstructed values are predicted steady-state values of the applicable program from base values, pump inlet conditions, atmosphere conditions, vehicle acceleration, engine trend characteristics, and F-1 engine influence coefficients. The difference between fitted and reconstructed values represents the deviation between flight and predicted parameter performance.

Reconstructed engine thrust values correlate well with the S-IC-5 stage thrust calculated from the vehicle velocity profile. Figure 30 presents average engine thrust as calculated from vehicle trajectory parameters superimposed upon individual and average engine thrust values as reconstructed from engine base values to the experienced flight conditions.

Figures 31 through 36 present thrust chamber pressure performance. Test data include corrections for prestart zero shifts in both telemetry and fitted values. A comparison of the average reconstructed and average fitted flight chamber pressures is presented in Fig. 36.

Turbopump speed performance is presented by Fig. 37 through 42. Figure 42 presents a comparison of the five engine averages of fitted and reconstructed turbopump speed. Turbine manifold temperatures for the S-1C-5 stage engines are presented in Fig. 43 through 47. Telemetry and fitted data include zero shifts, as indicated in Appendix E. The turbine manifold temperature average is not available because of the engine position 2 measurement shift at 115 seconds range time (Fig. 44). This shift is attributed to the measurement system, as the other measured engine parameters do not show a corresponding shift.

Fuel and oxidizer pump discharge pressures during flight are presented in Fig. 48 through 59. Telemetry data for turbopump discharge pressures are static pressures as measured. Fitted and reconstructed values include the dynamic head, and are presented as total pressure. Flight fuel and ozidizer pump performance correlates well with predictions. The apparent dip in engine 2 fuel discharge pressure is not reflected in other performance parameters and is therefore attributed to the instrumentation system.

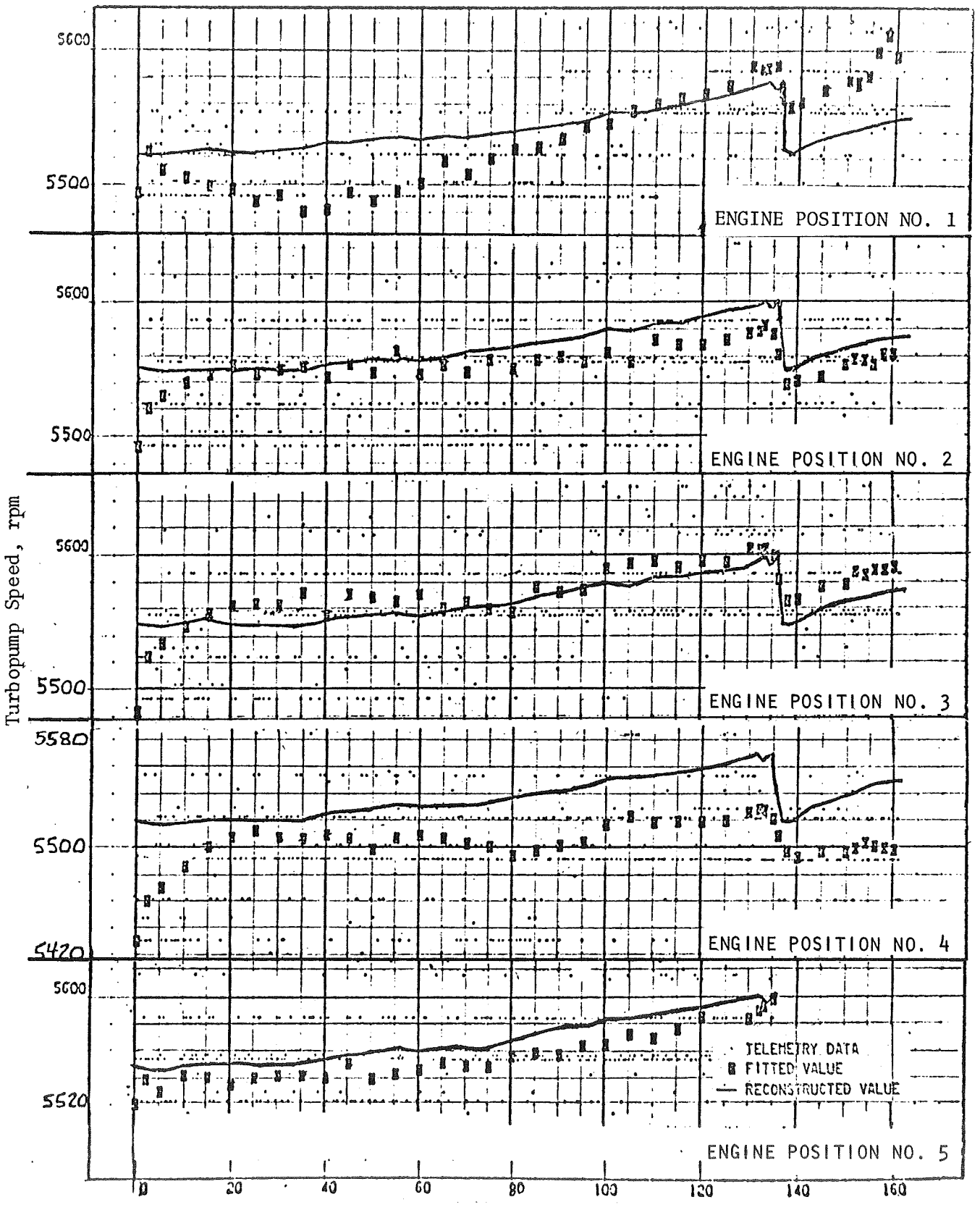

Figure 18a. AS-505 Flight Performance Reconstruction

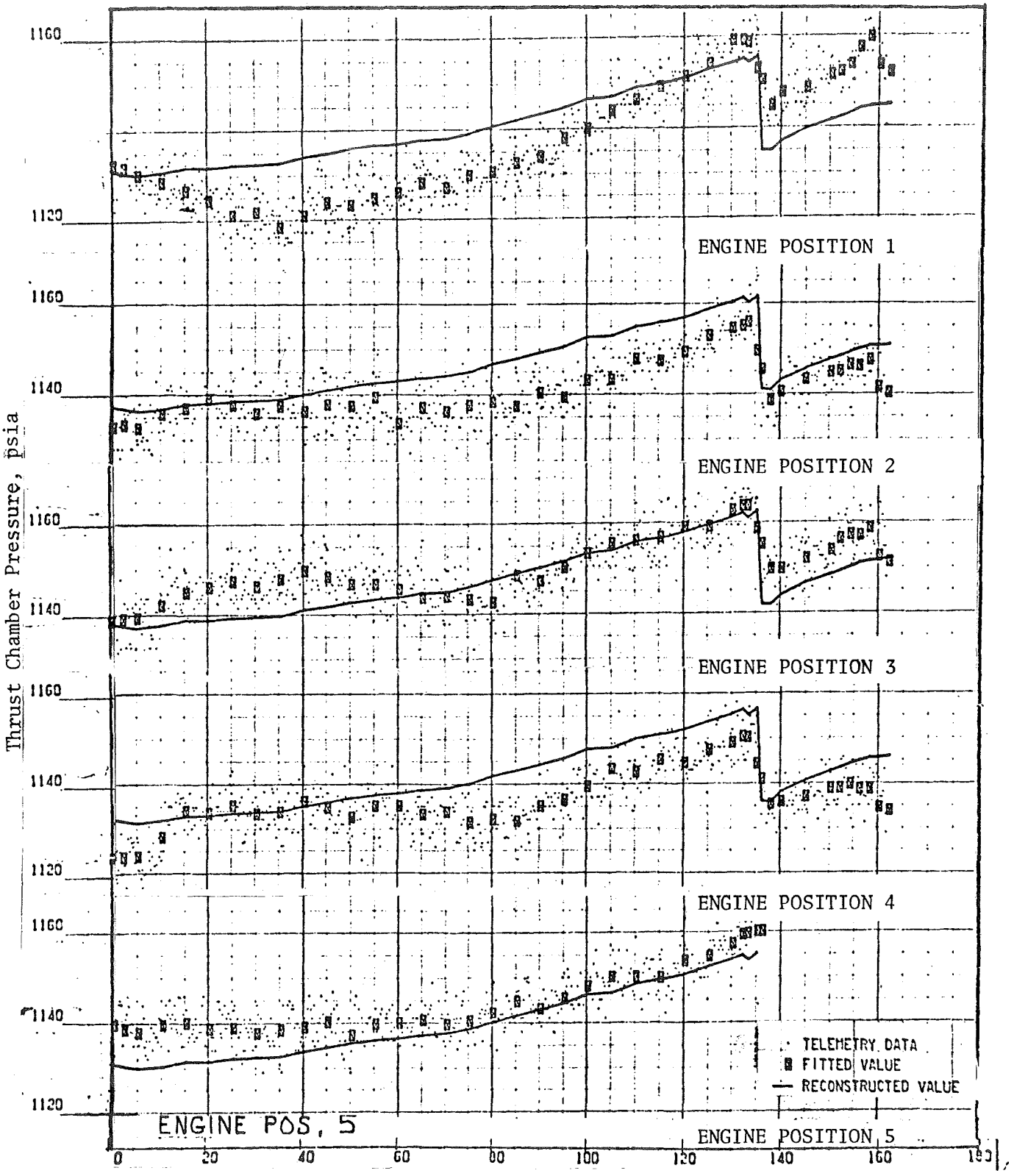

Figure 18b. AS-505 Flight Performance Reconstruction

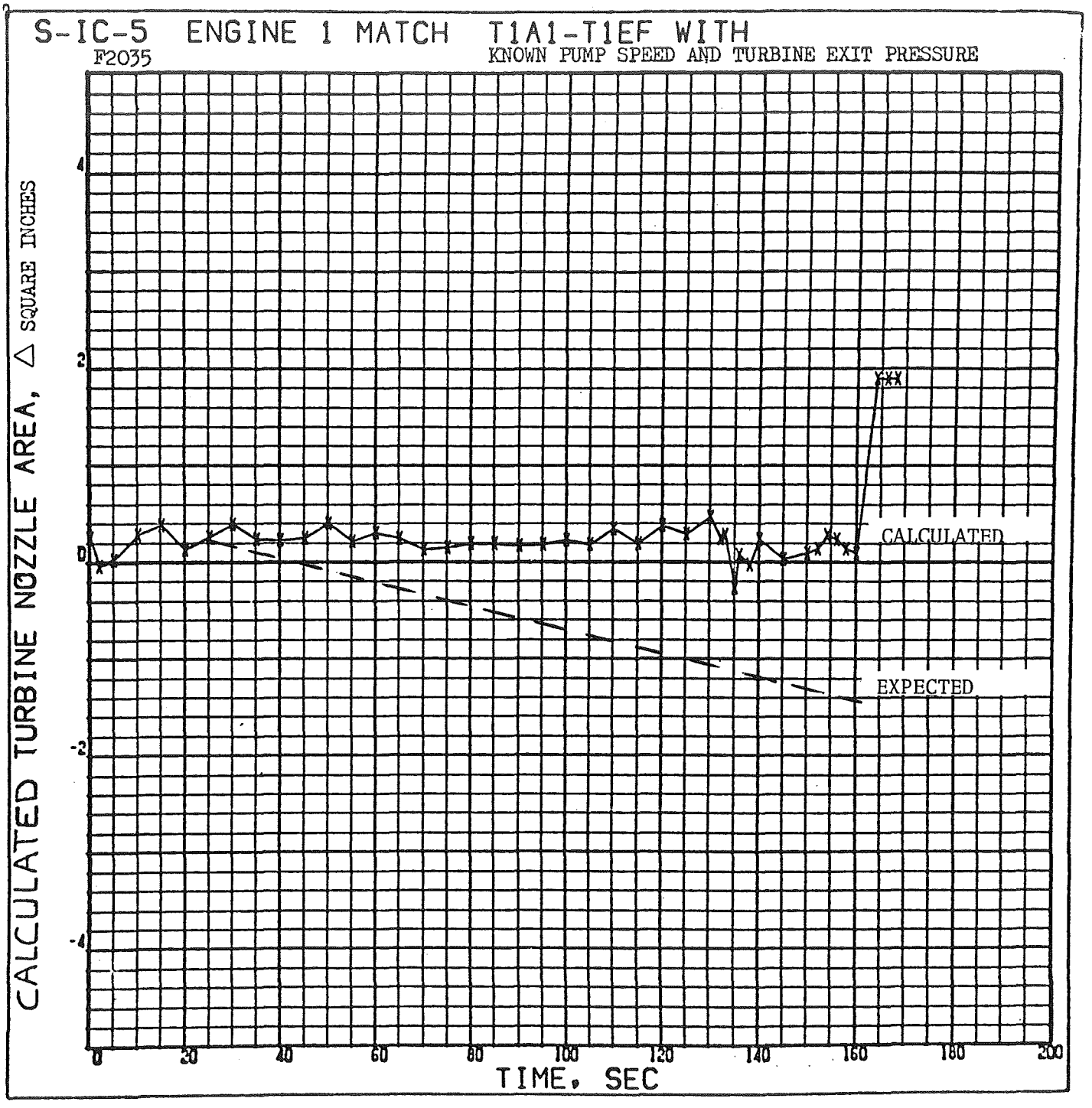

Figure 18c. Calculated Turbine Nozzle Area Change to Match Observed Pump Speed and Turbine Exit Pressure

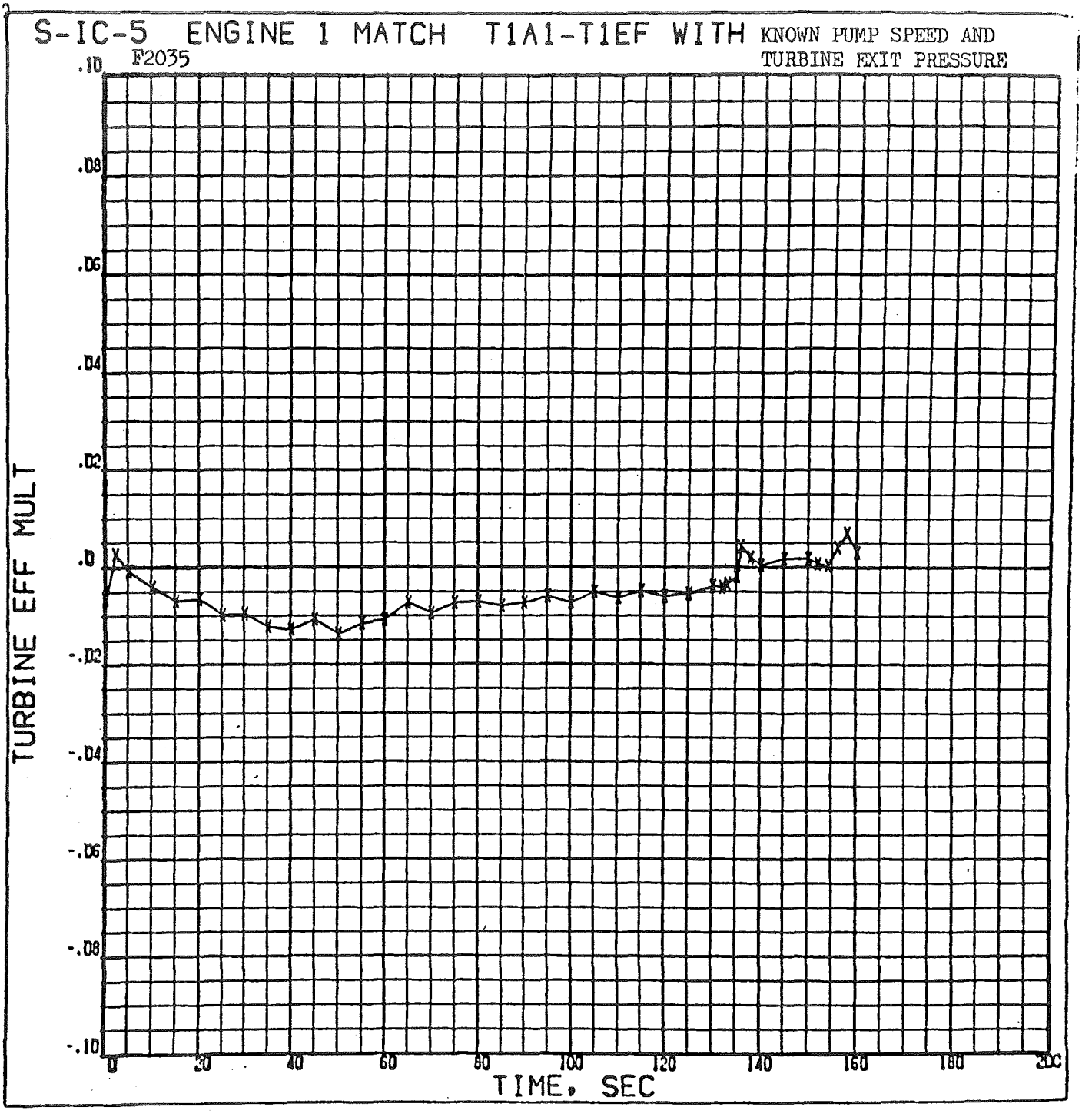

Figure 18d. Calculated Turbine Efficiency Change Required to Match Observed Pump Speed and Turbine Exit Pressure

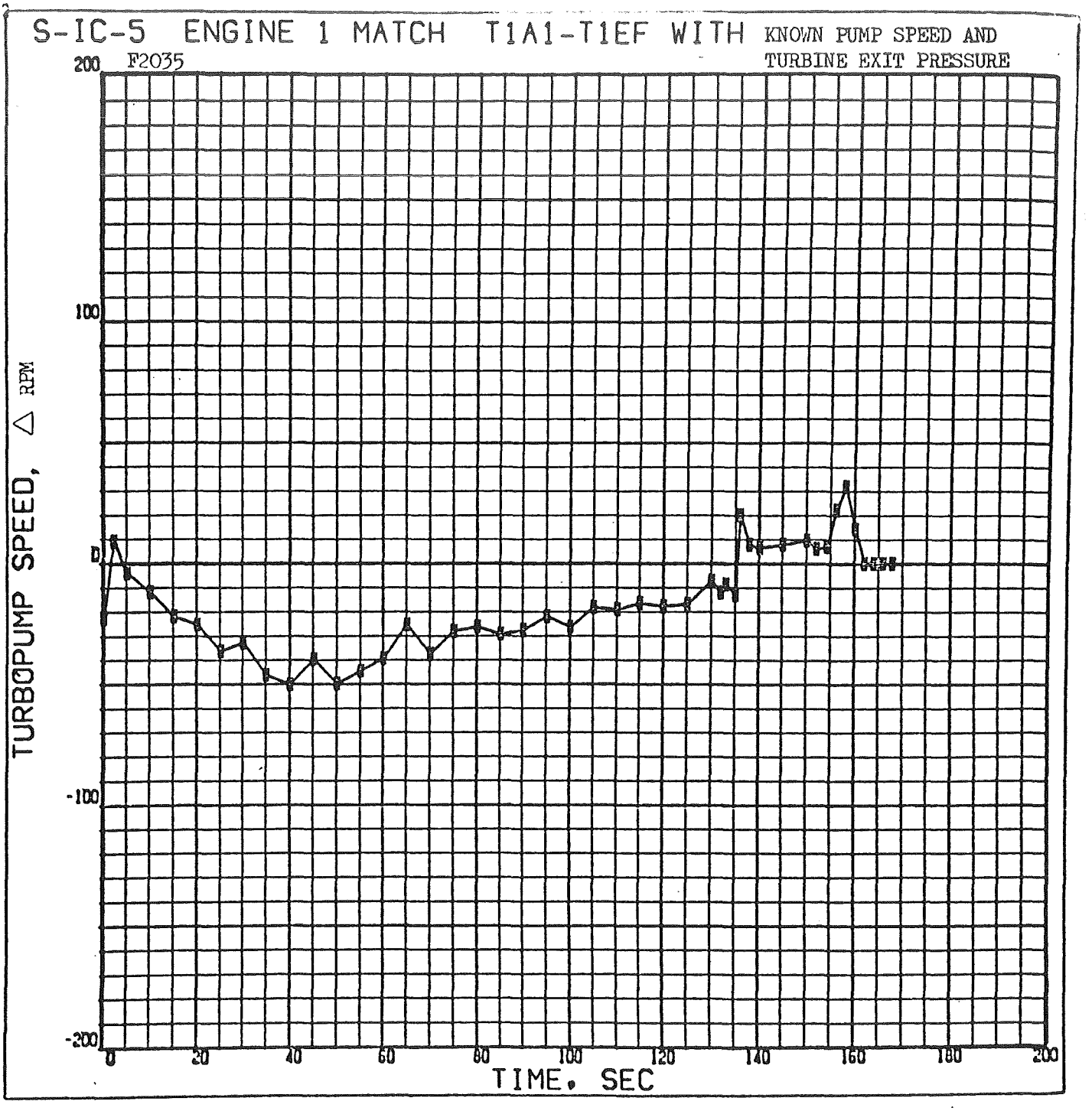

Figure 18e. Observed Turbopump Speed Change

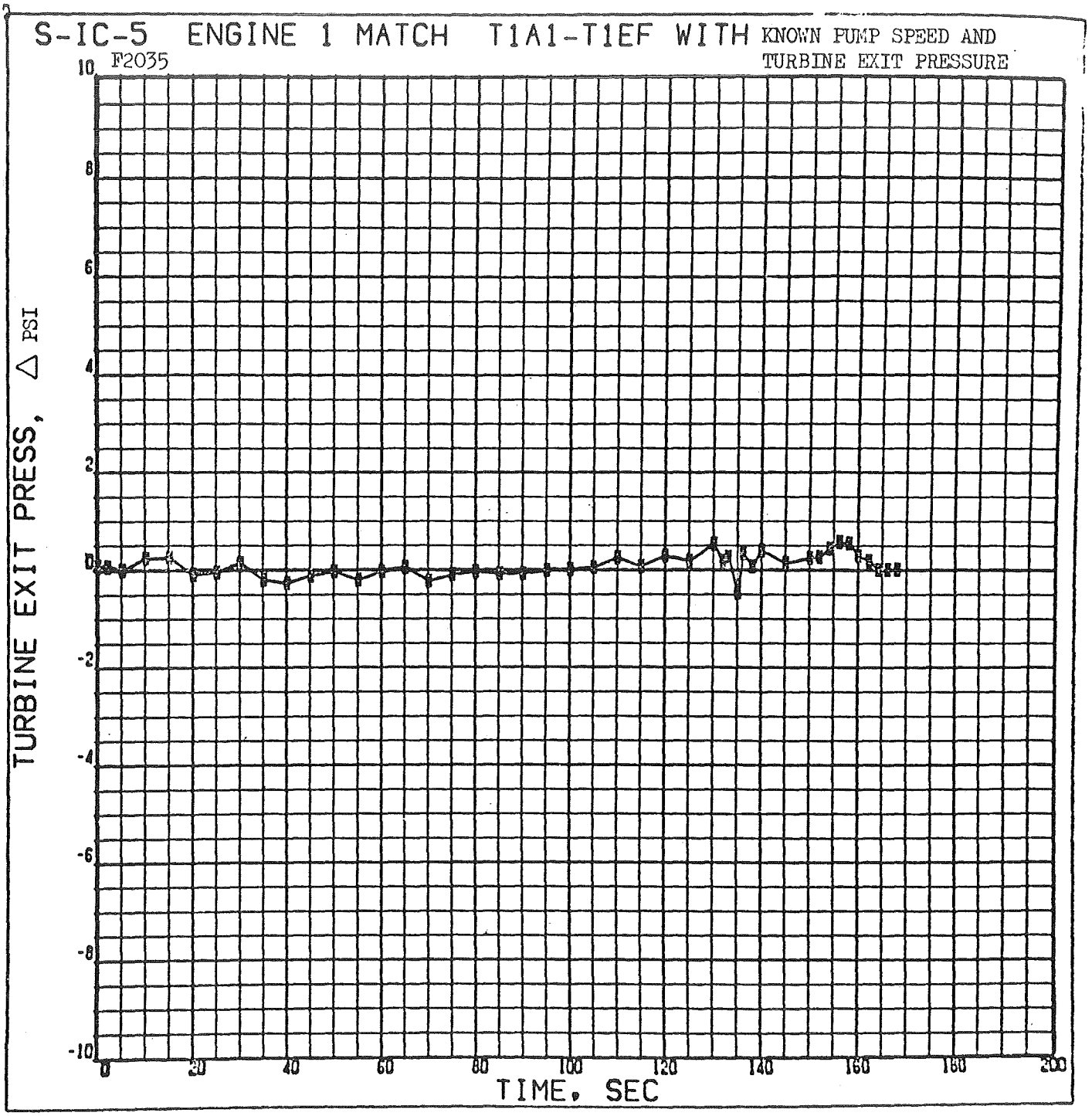

Figure 18f. Observed Turbine Exit Pressure

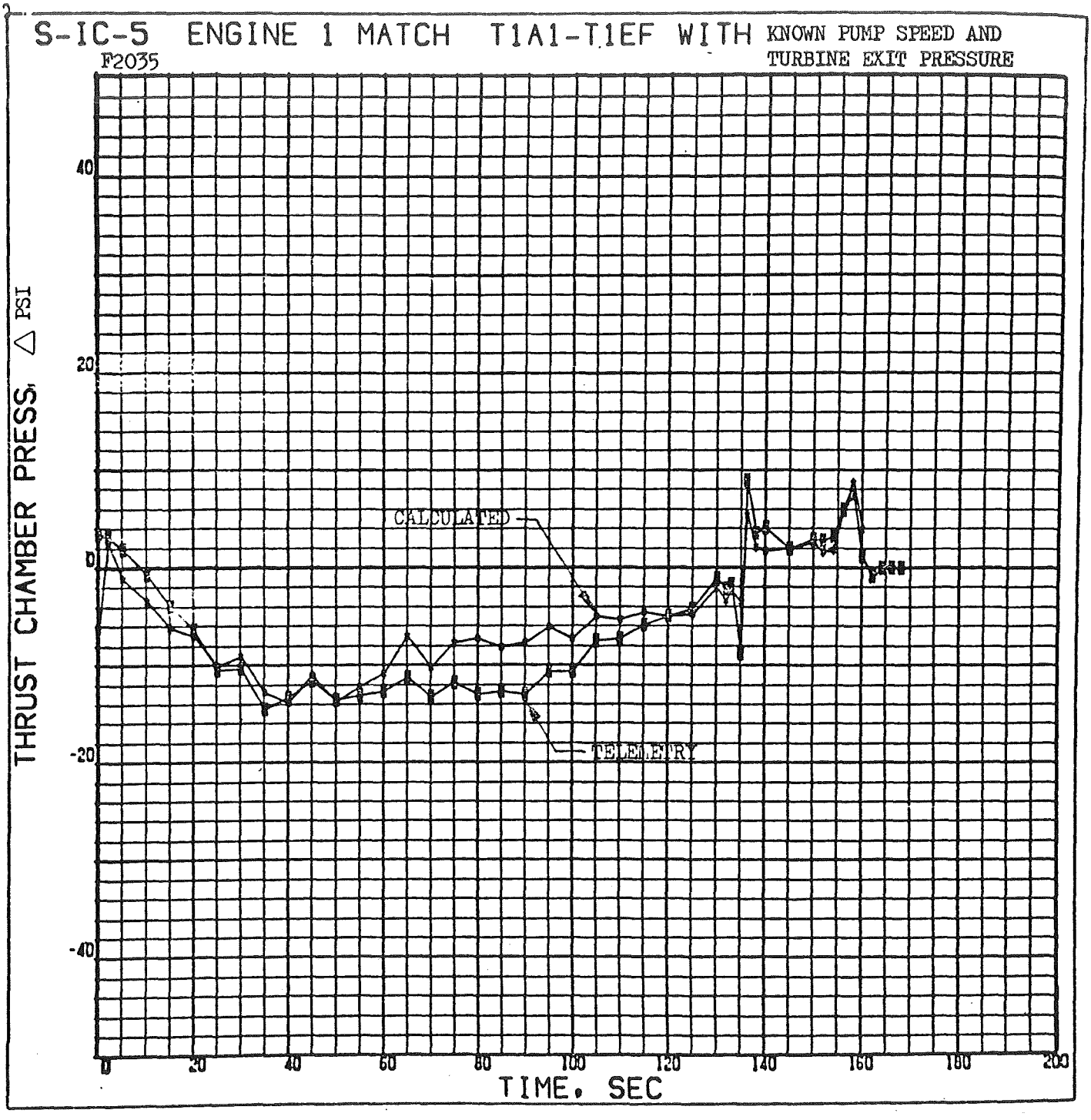

Figure 18g. Match of Observed Thrust Chamber Pressure With an Assumed Change in Turbine Efficiency and Nozzle Area

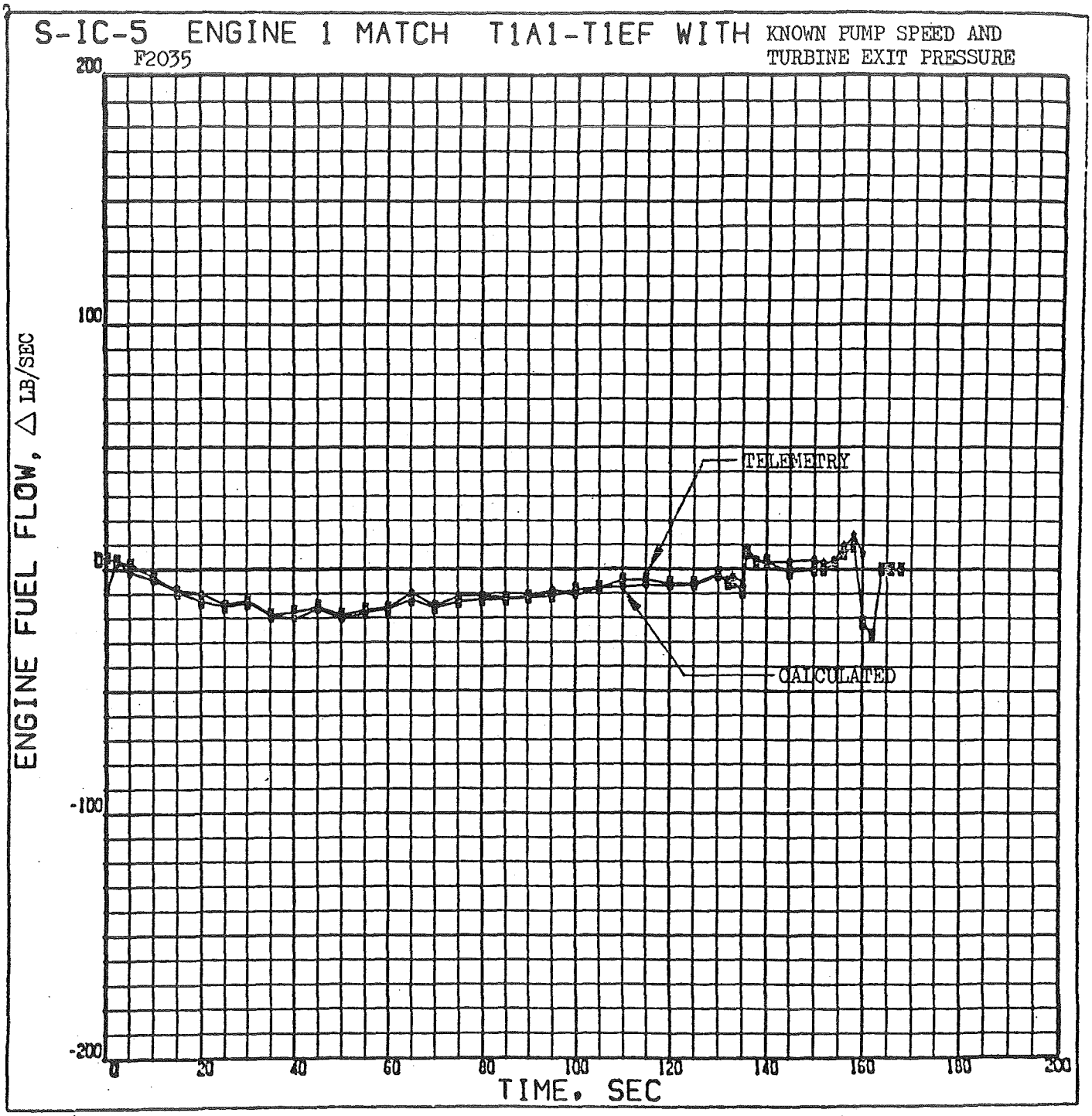

Figure 18h. Match of Observed Engine Fuel Flow With an Assumed Change in Turbine Efficiency and Nozzle Area

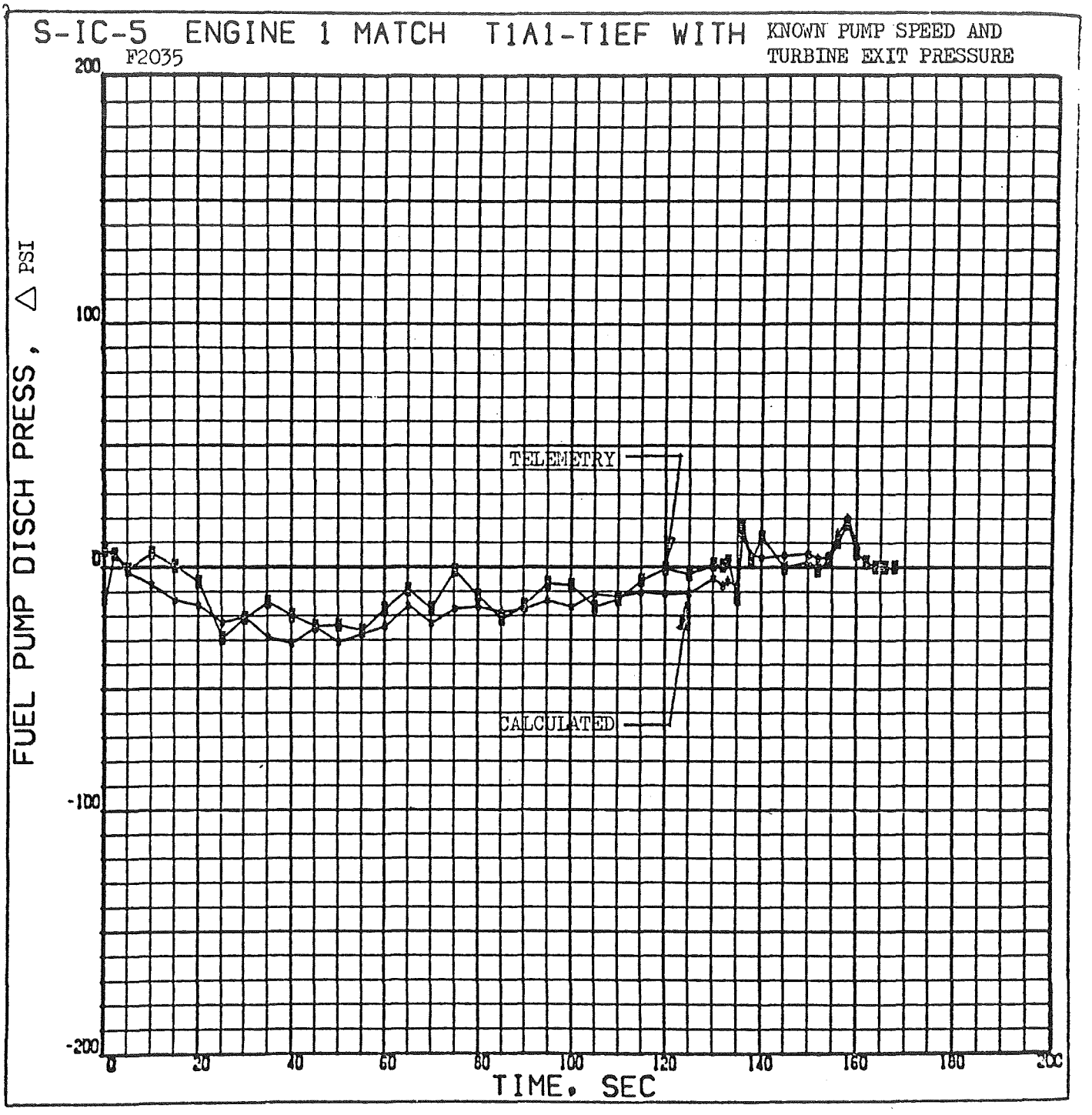

Figure 18i. Match of Observed Fuel Pump Discharge Pressure With an Assumed Change in Turbine Efficiency and Nozzle Area

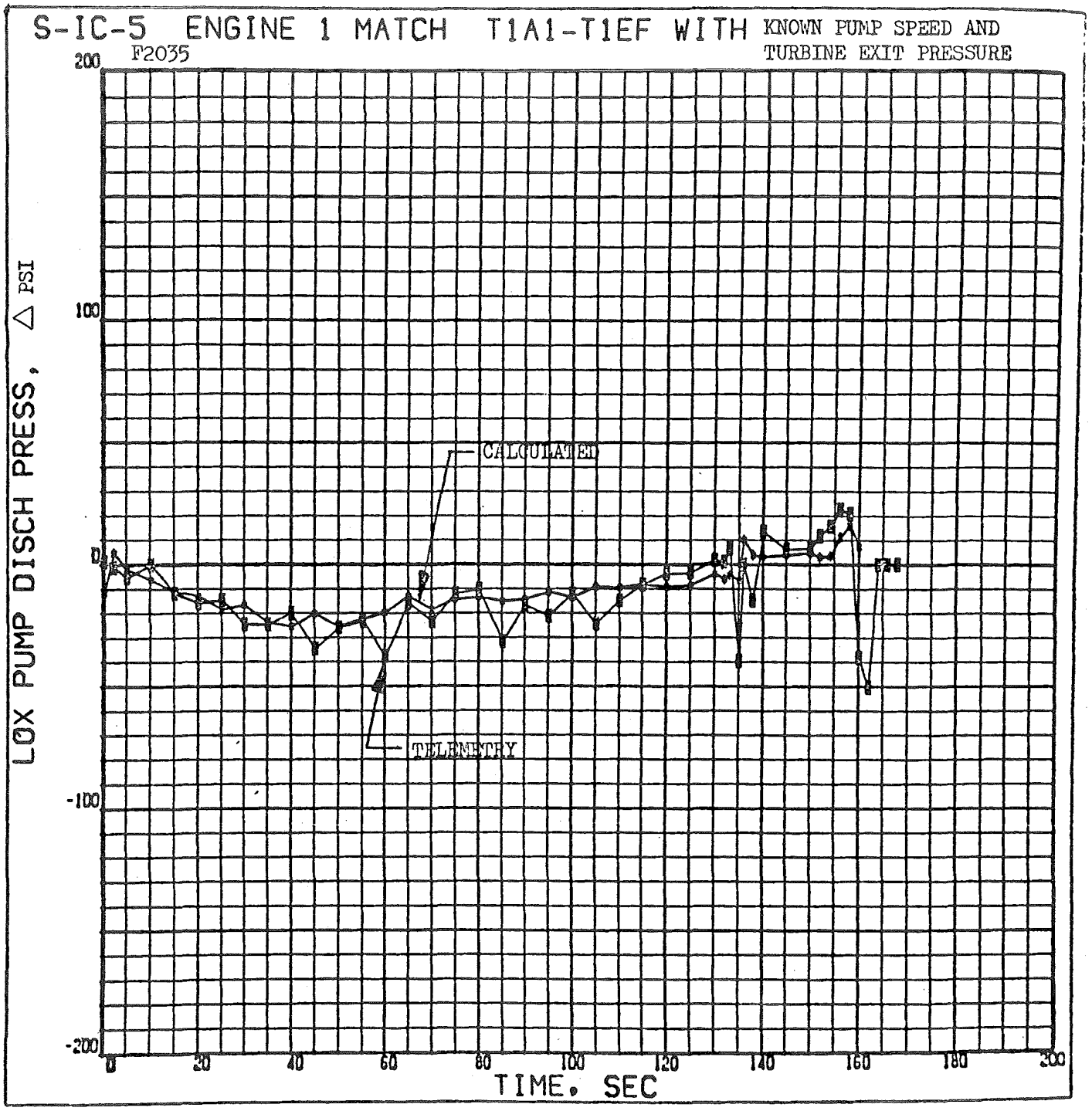

Figure 18j. Match of Observed LOX Pump Discharge Pressure With an Assumed Change in Turbine Efficiency and Nozzle Area

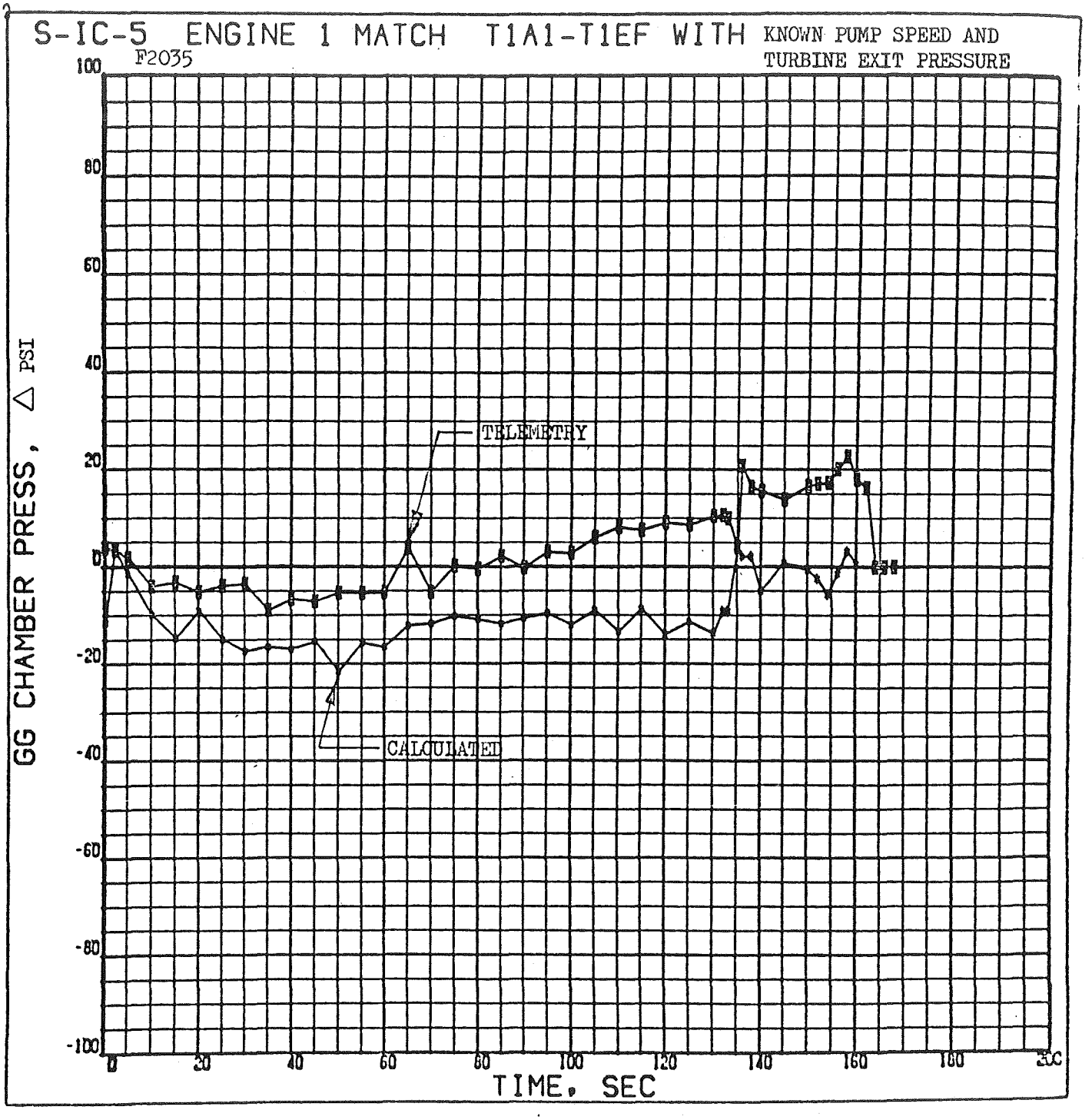

Figure 18k. Match of Observed Gas Generator Chamber Pressure With an Assumed Change in Turbine Efficiency and Nozzle Area

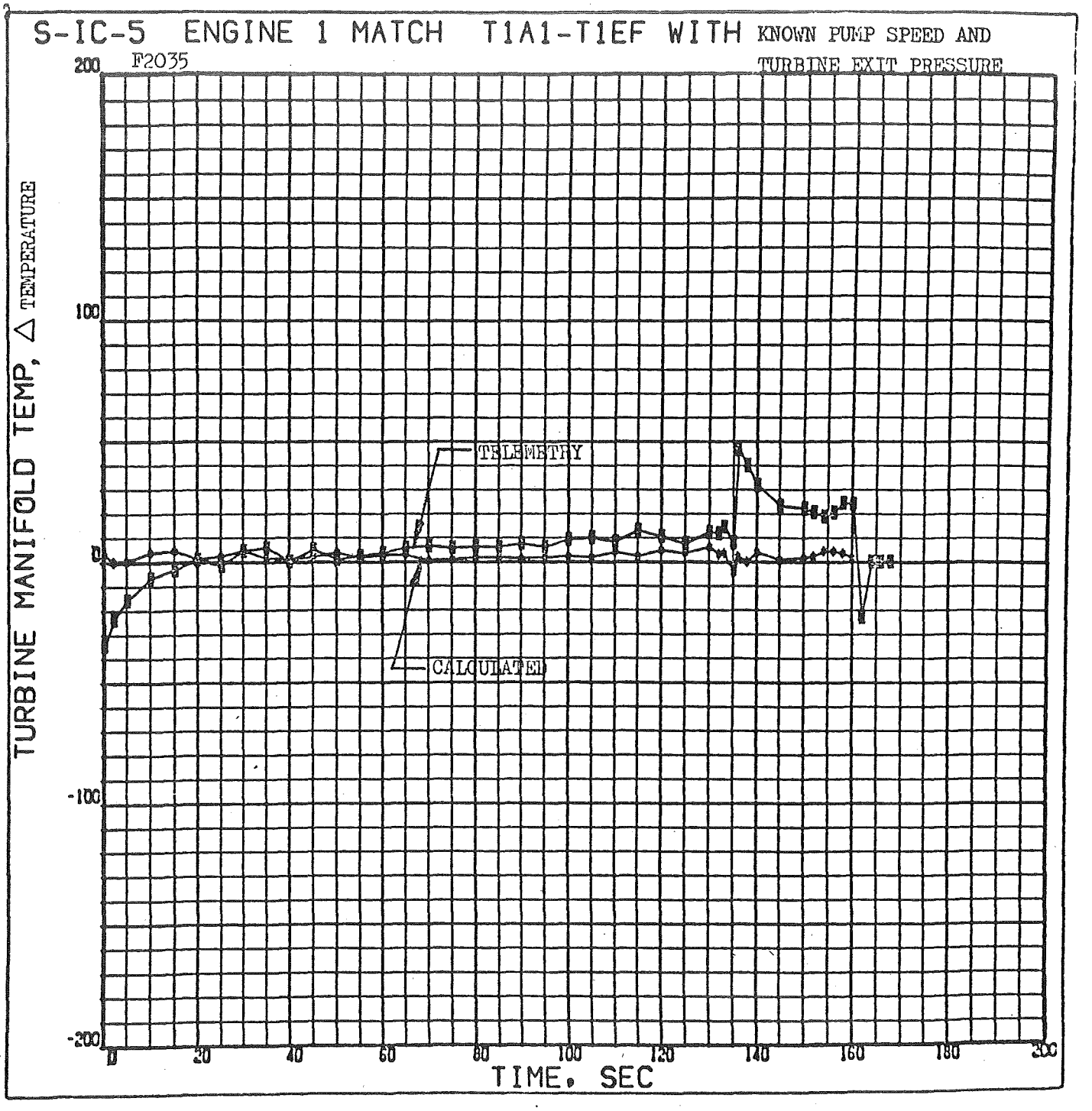

Figure 181. Match of Observed Turbine Manifold Temperature Change With an Assumed Change in Turbine Efficiency And Nozzle Area

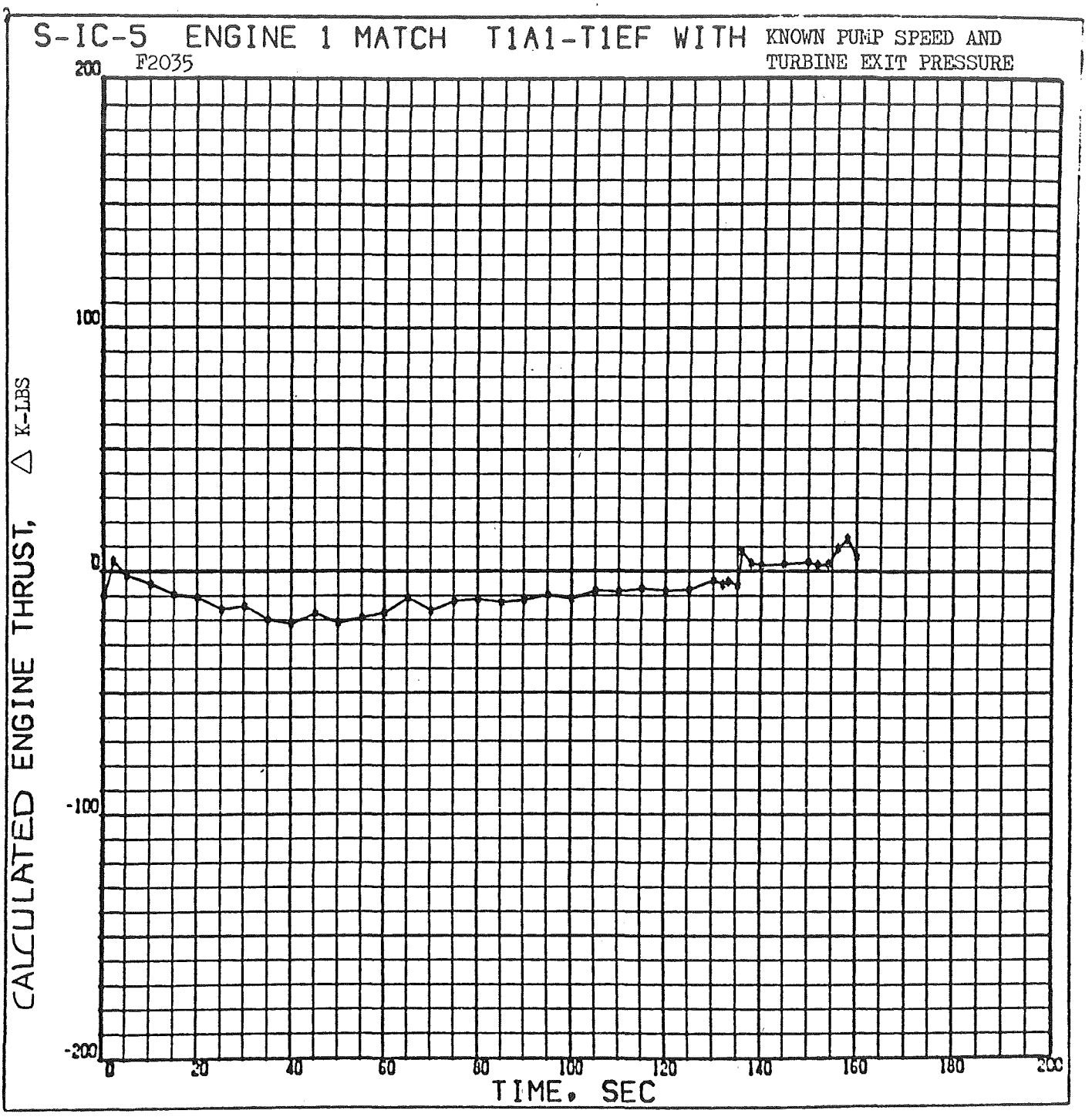

Figure 18m. Calculated Engine Thrust Change Required to Match Observed Pump Speed and Turbine Exit Pressure

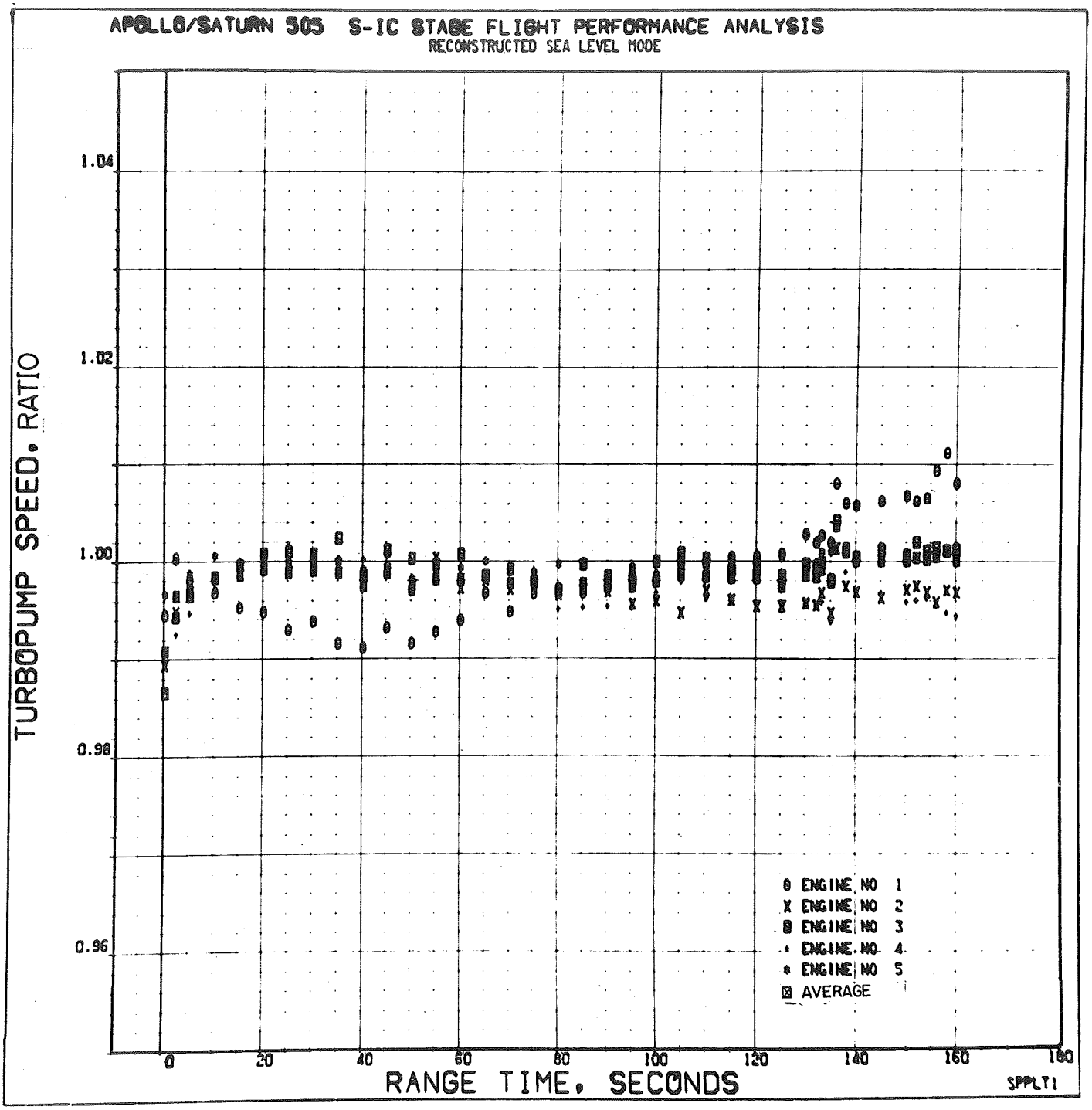

Figure 19. Sea-Level Turbopump Speed as a Ratio of Base Value

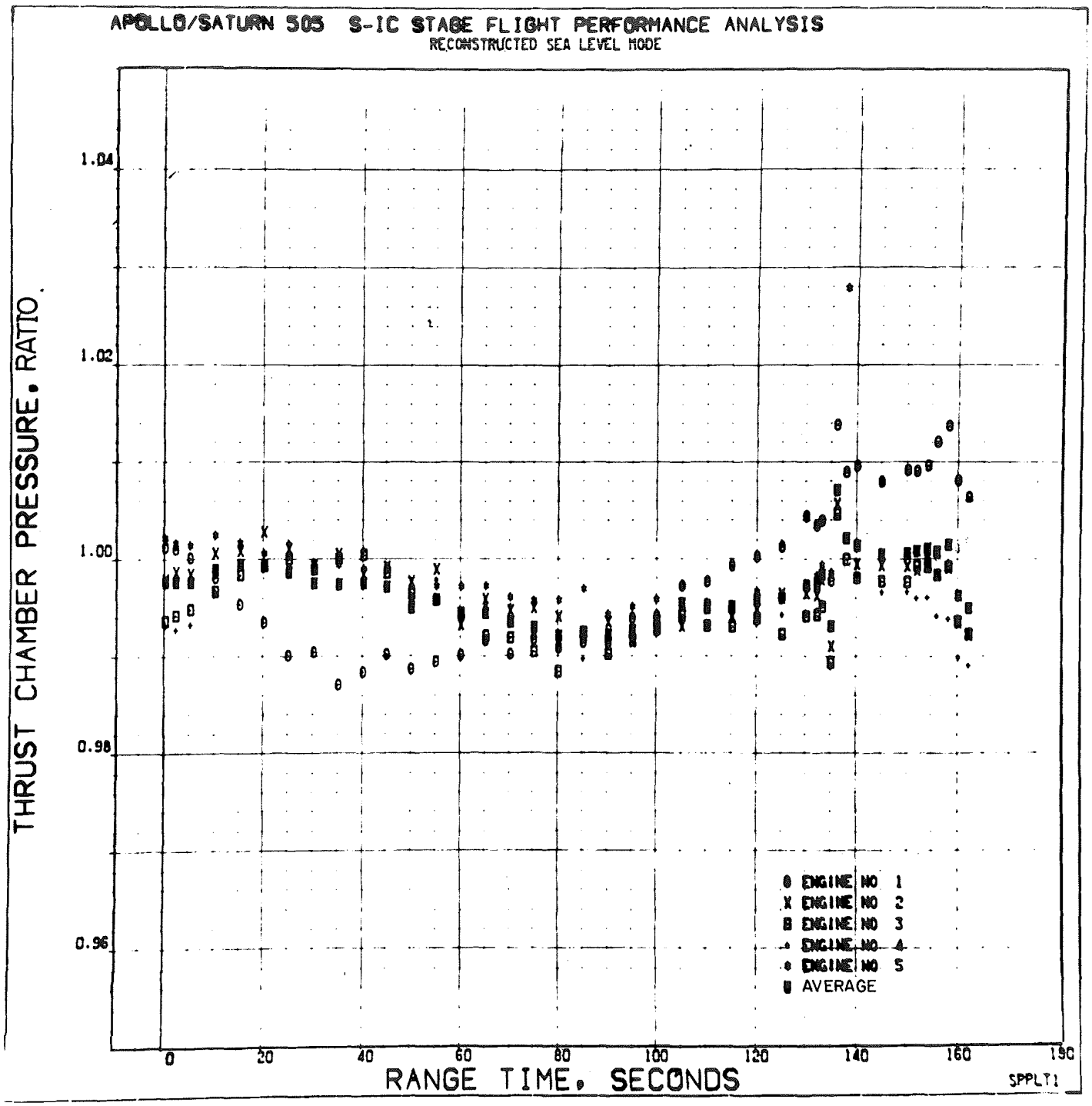

Figure 20. Sea-Level Thrust Chamber Pressure as a Ratio of Base Value

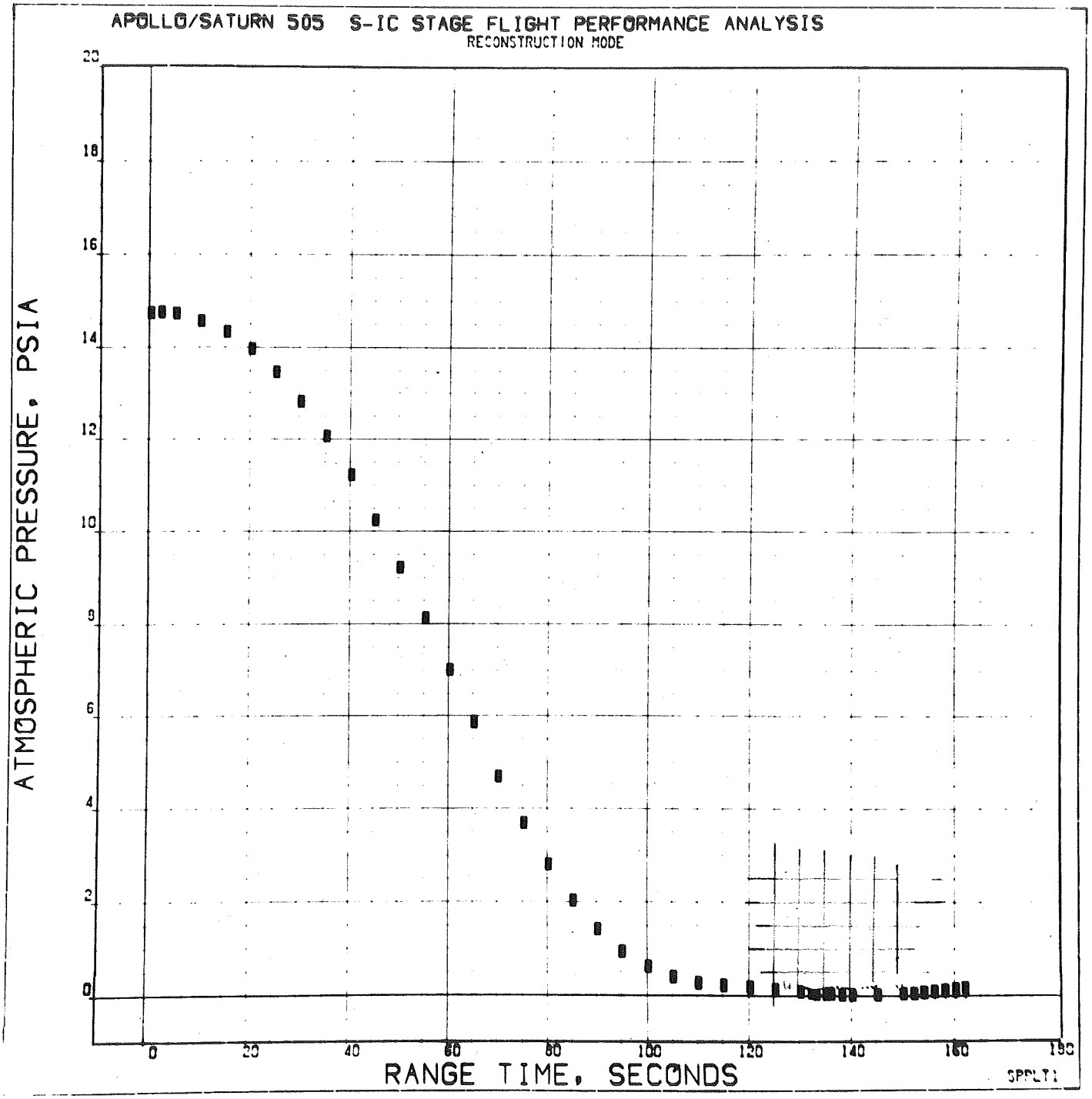

Figure 21. Atmospheric Pressure, All Engines

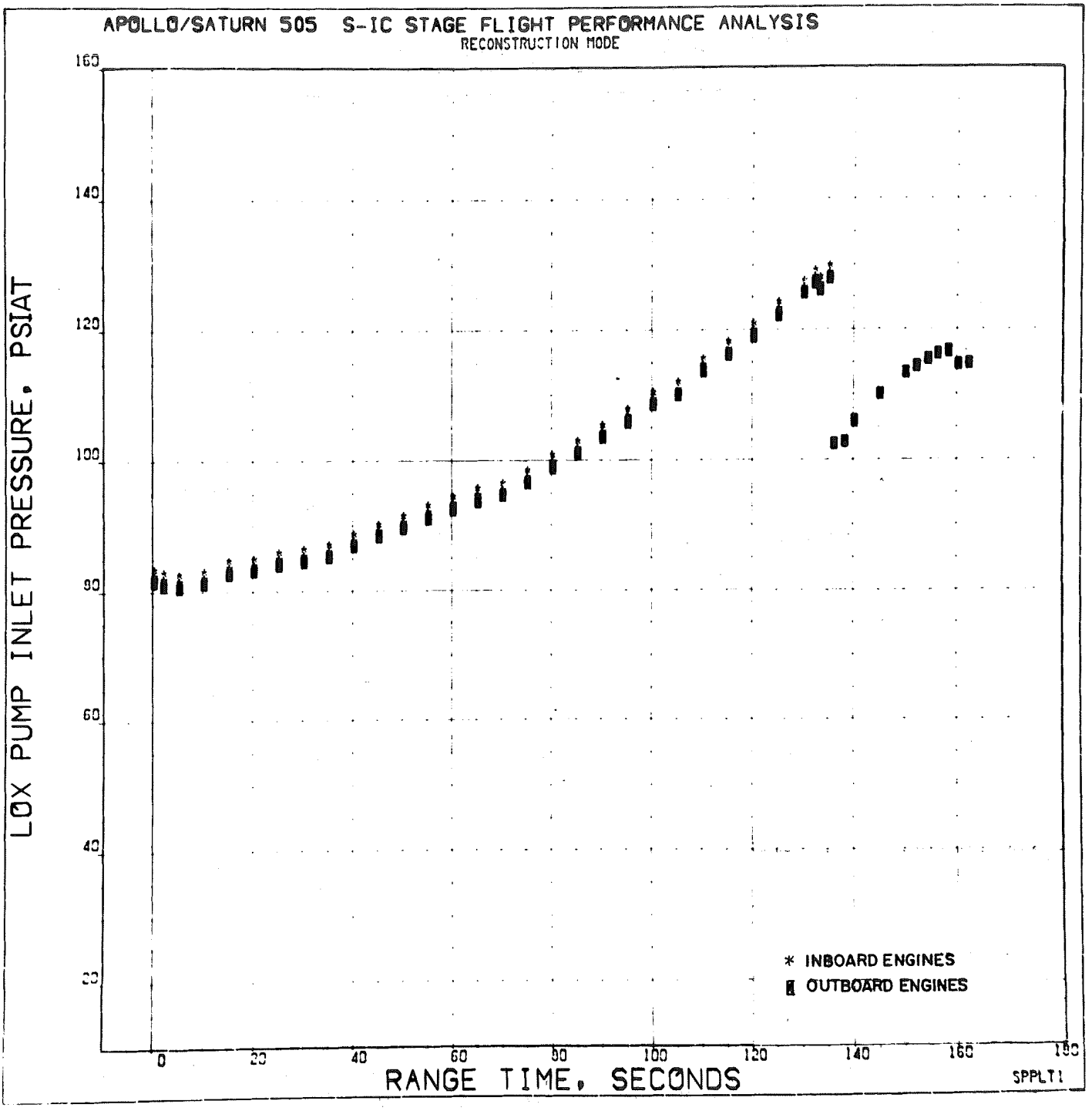

Figure 22. Turbopump LOX Pump Inlet Pressure

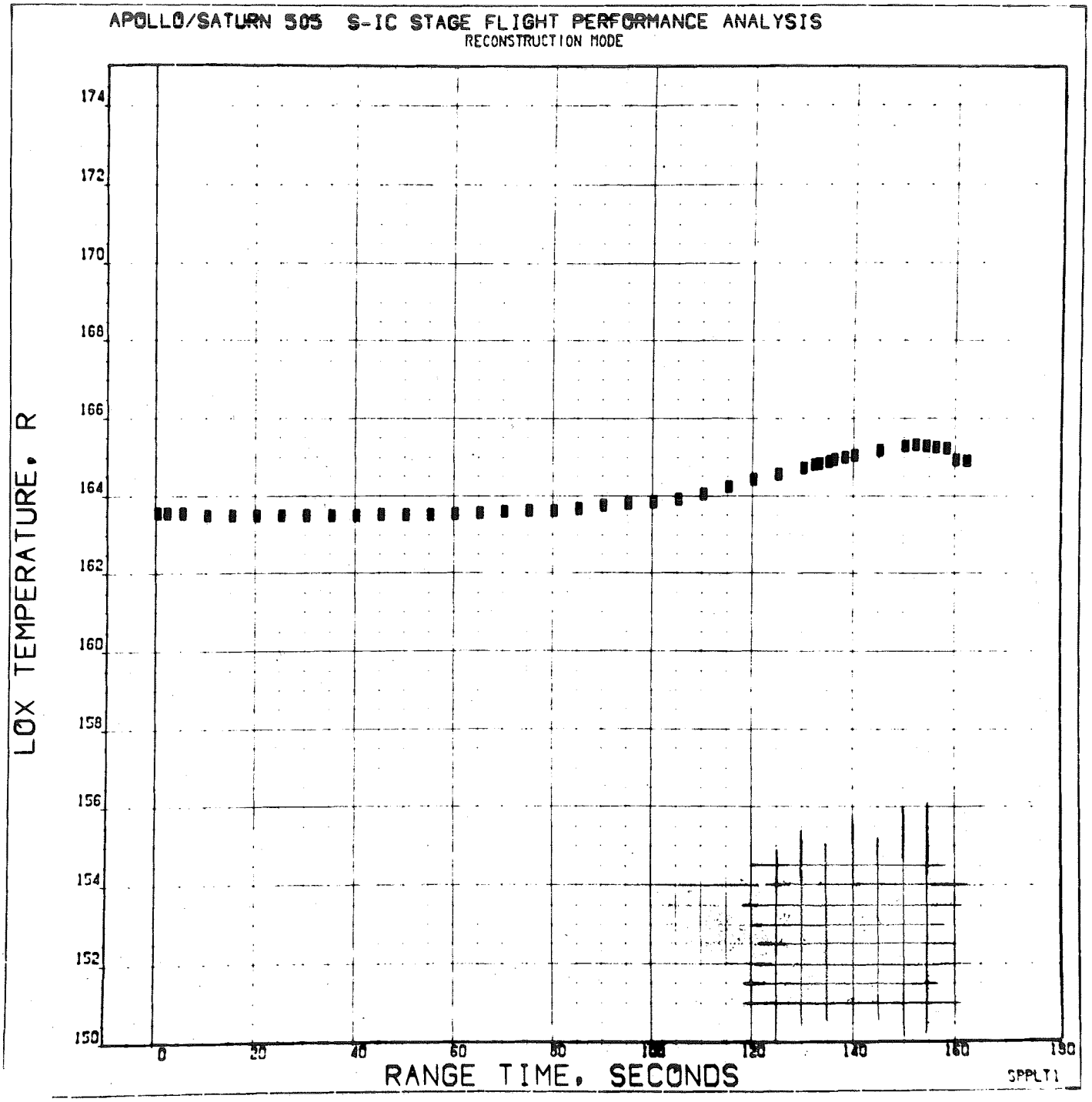

Figure 23. Average LOX Suction Line Temperature

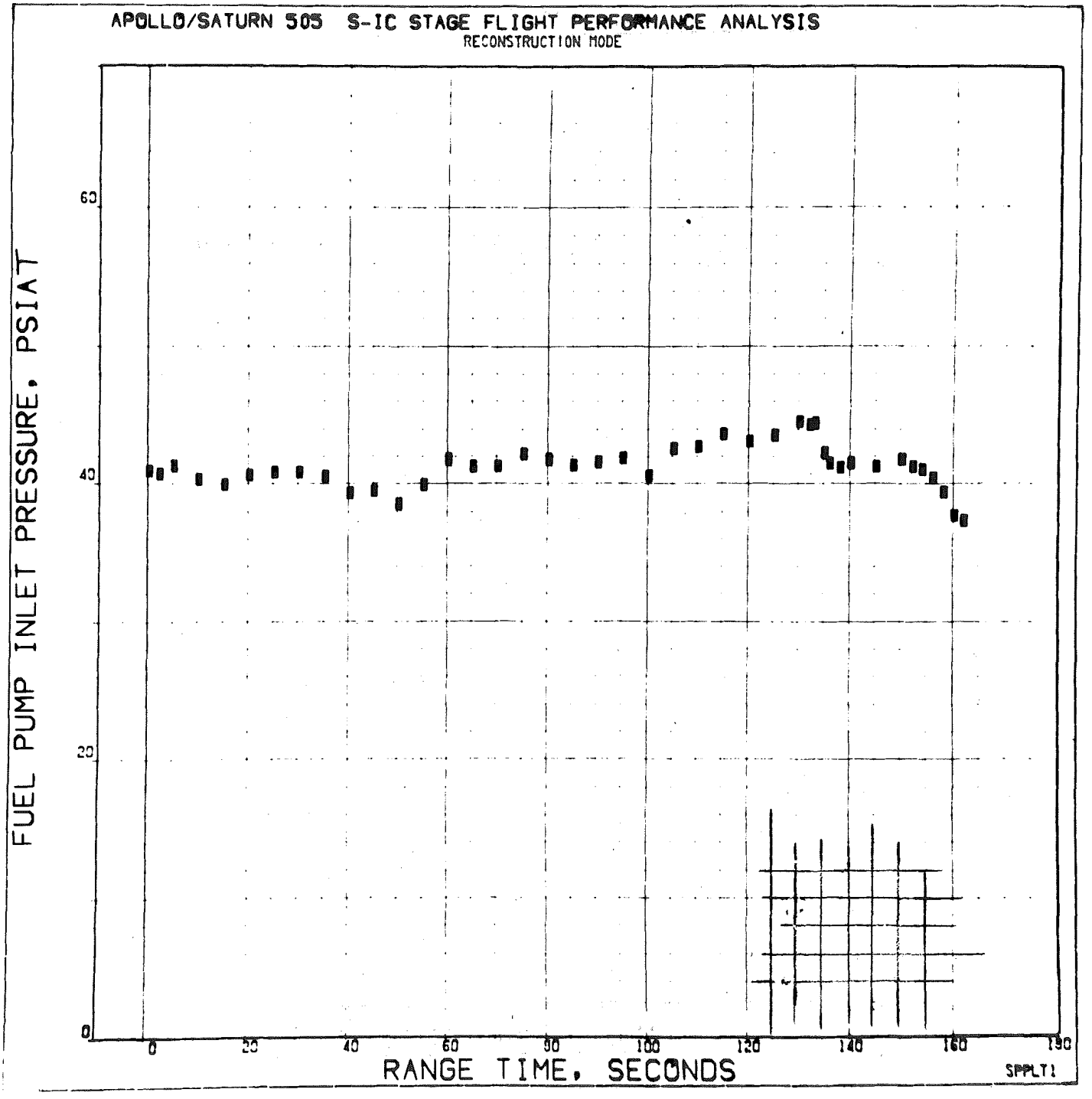

Figure 24. Average Turbopump Fuel Pump Inlet Pressure

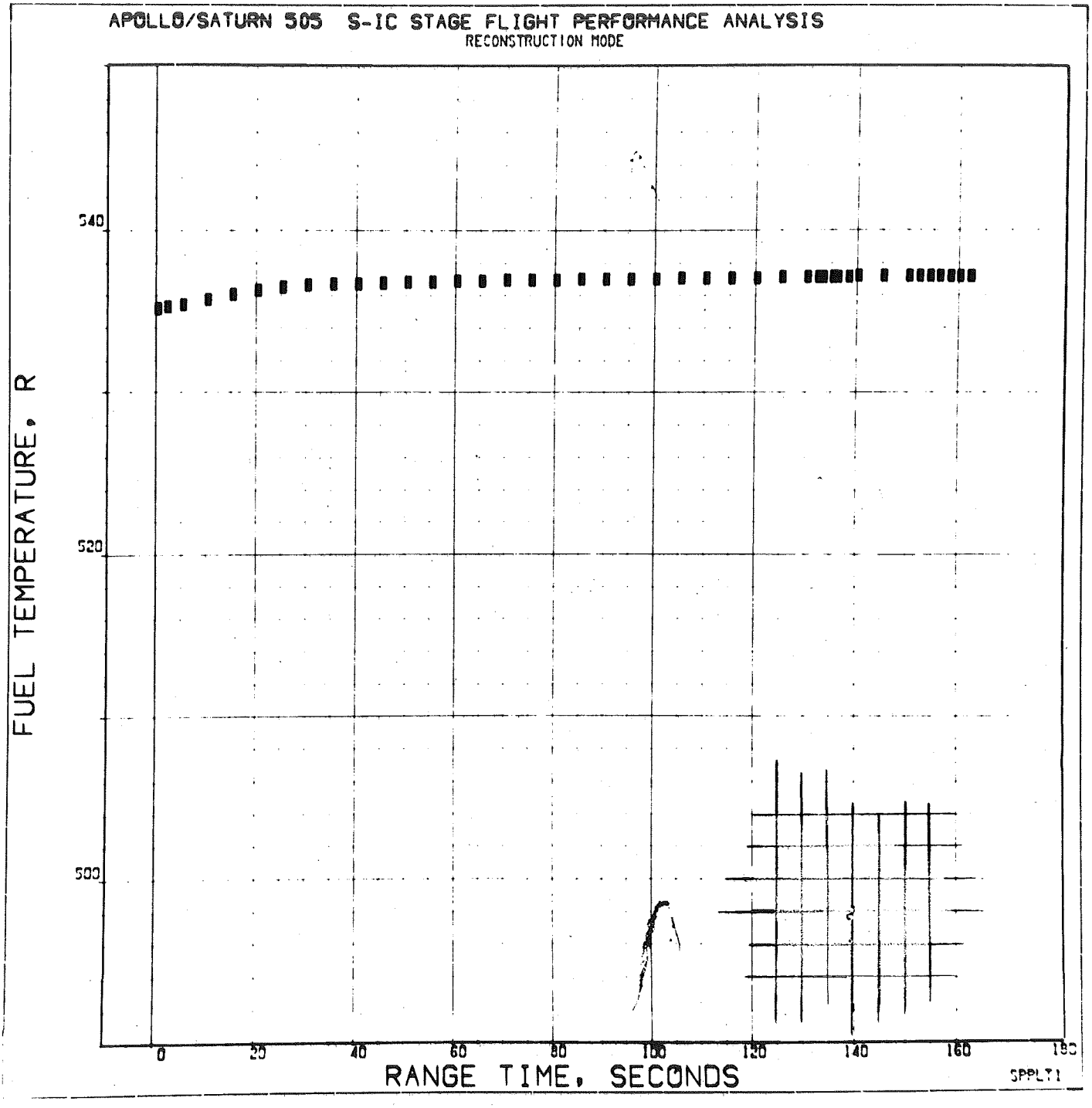

Figure 25. Average Turbopump Fuel Inlet Temperature

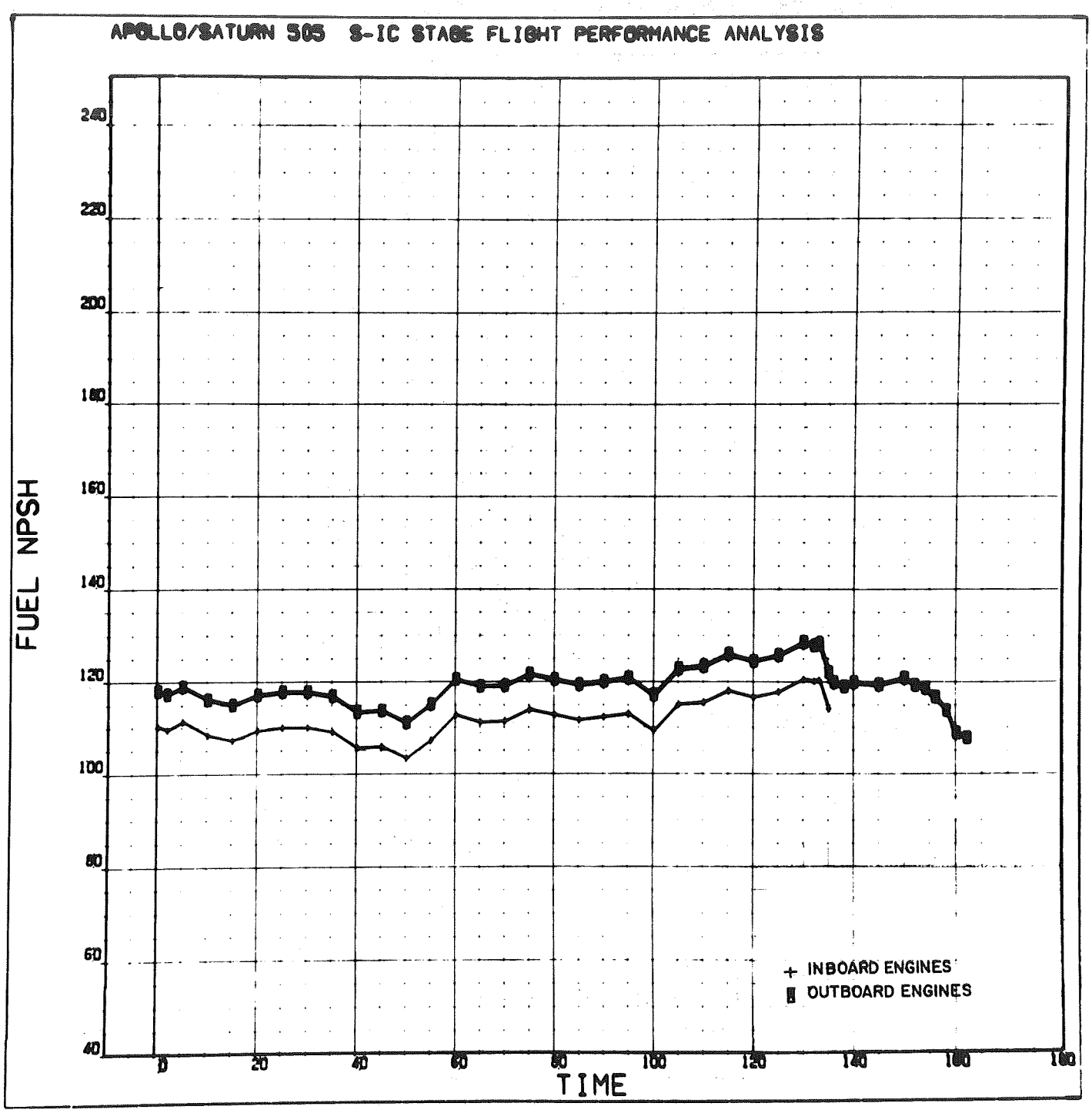

Figure 26. Average Turbopump Fuel Net Positive Suction Head

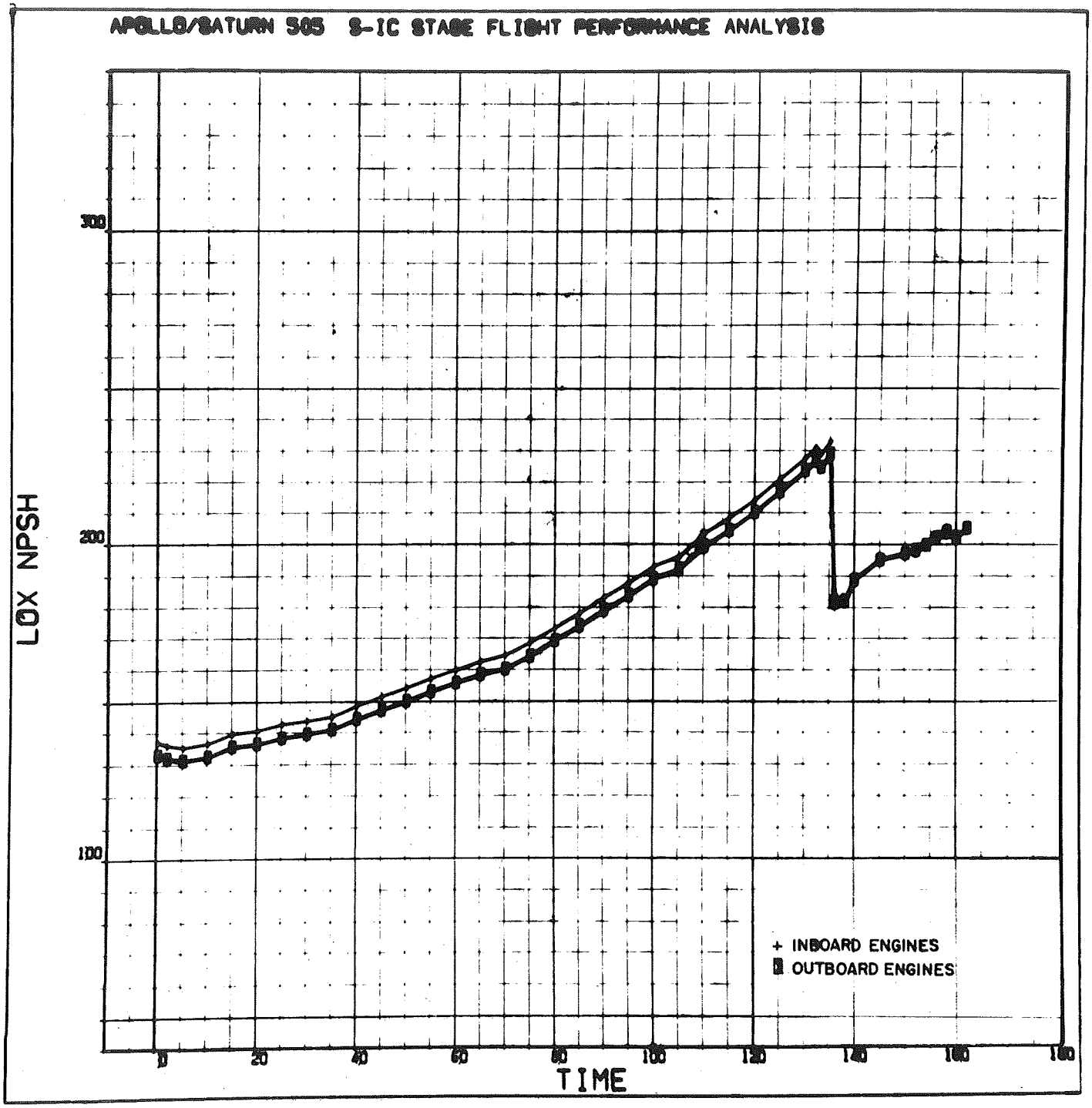

Figure 27. Typical Outboard Engine Turbopump LOX Net Positive Suction Head

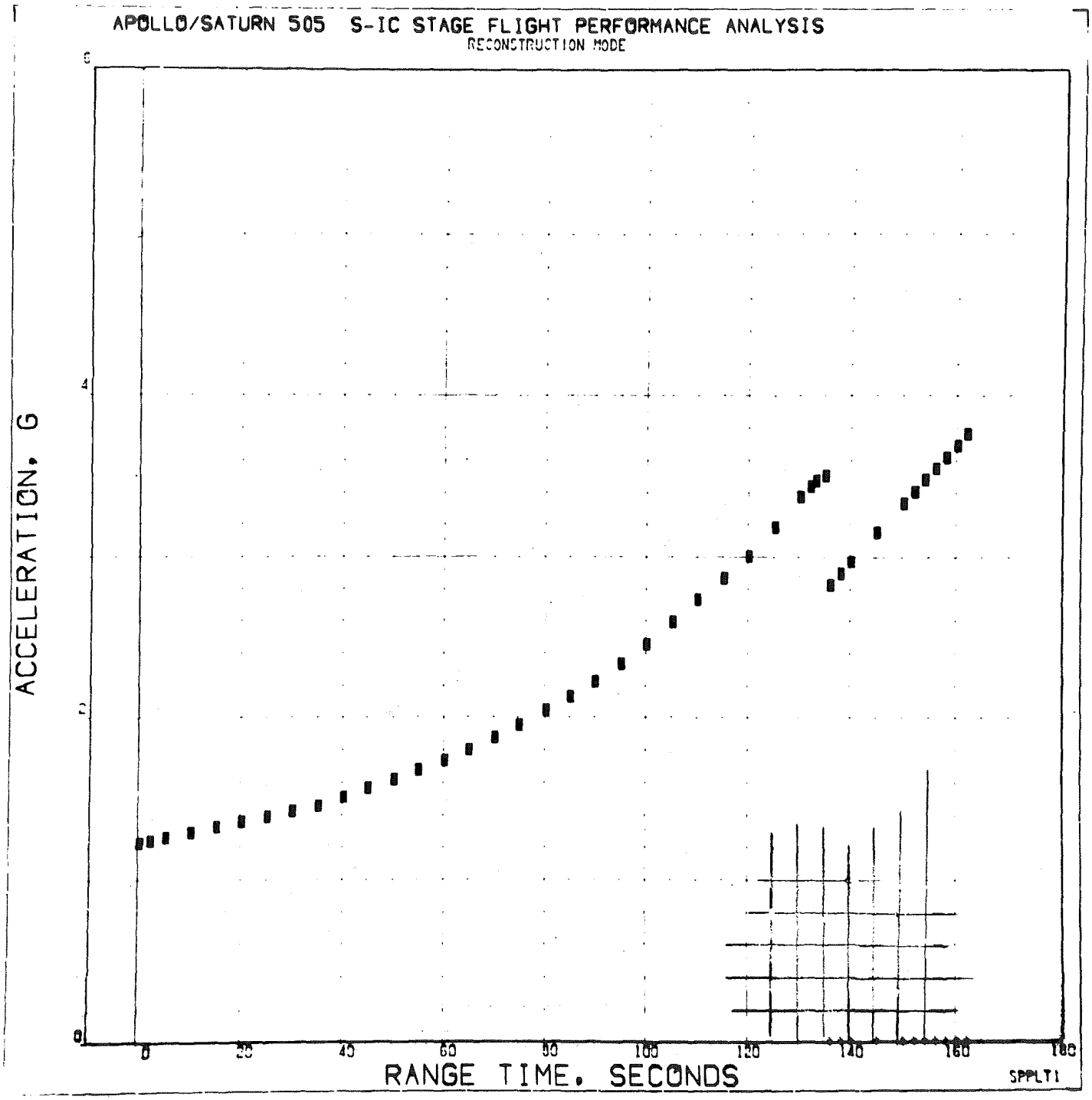

Figure 28. Vehicle Acceleration

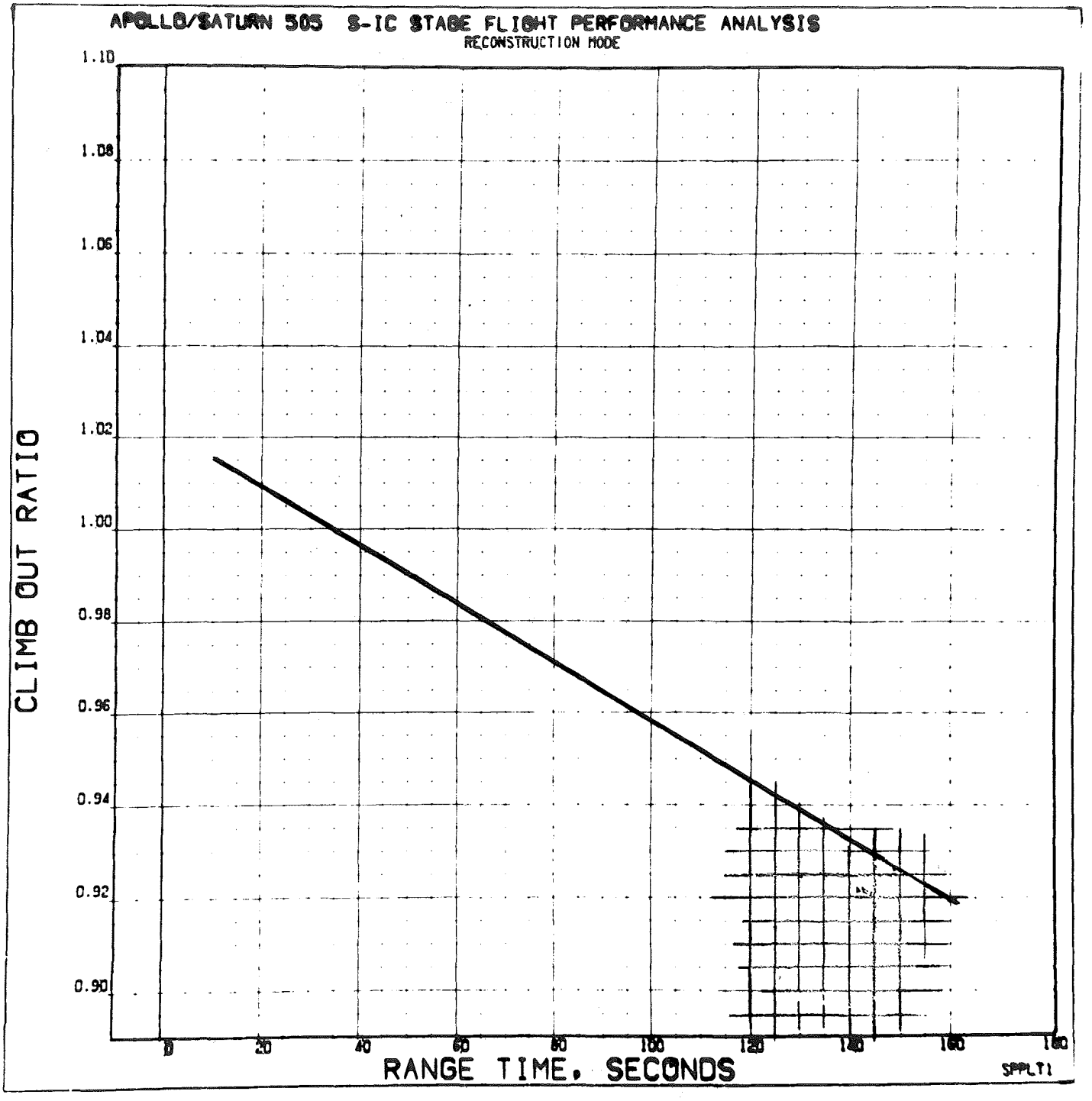

Figure 29. Climbout Ratio

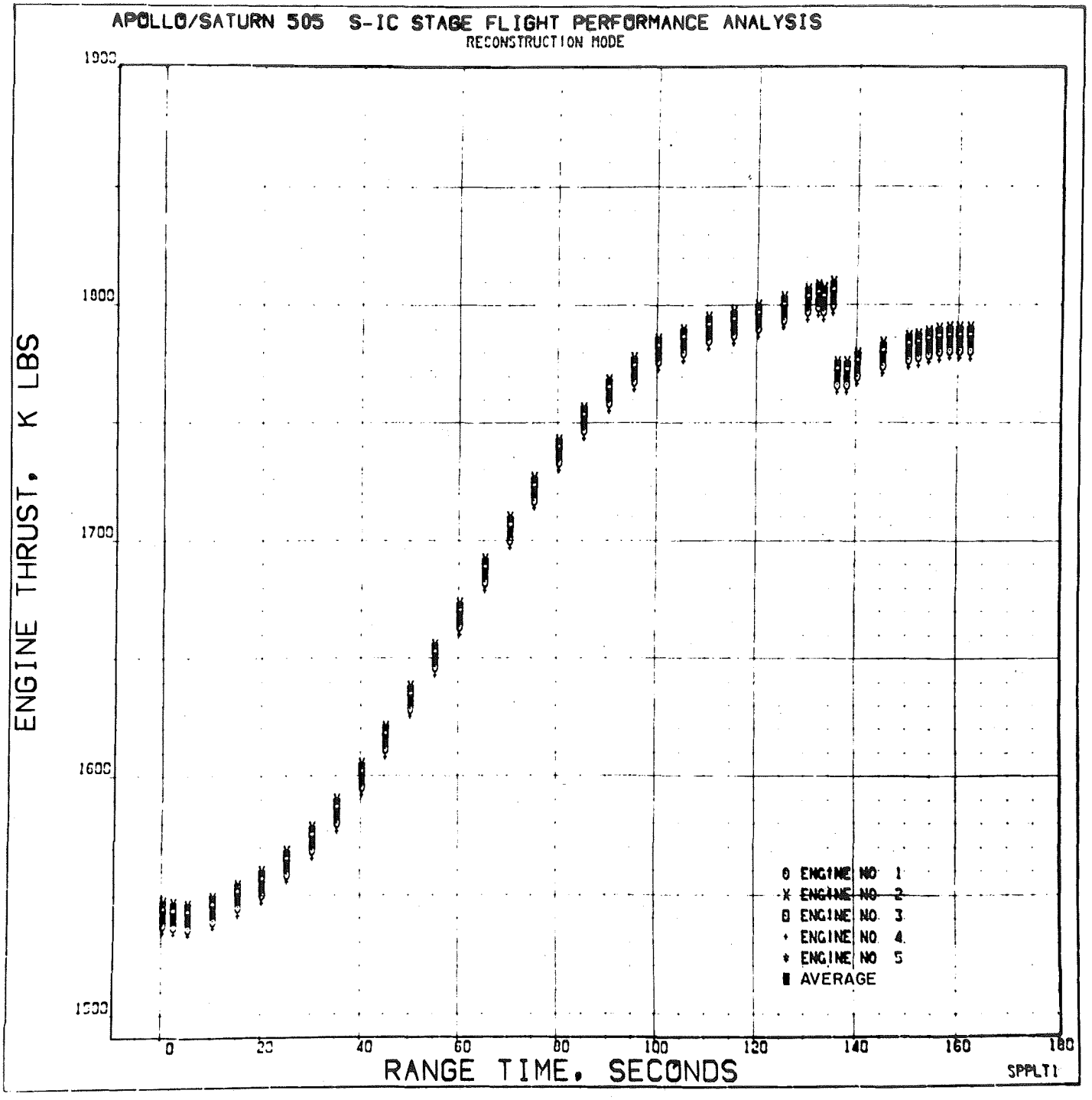

Figure 30. Reconstructed and Velocity Profile Individual and Average Engine Thrust

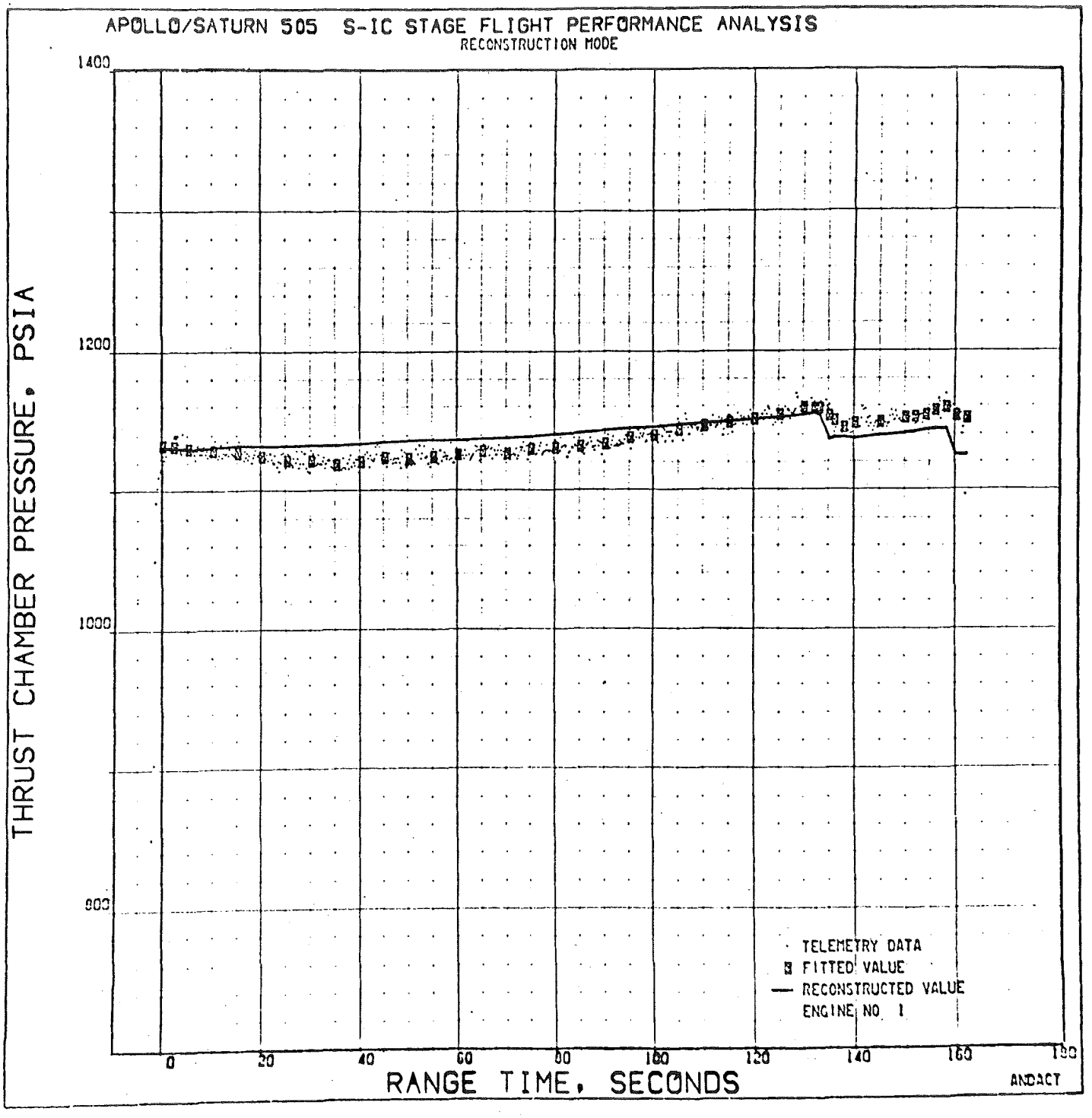

Figure 31. Thrust Chamber Pressure, Engine Position 1, F2035

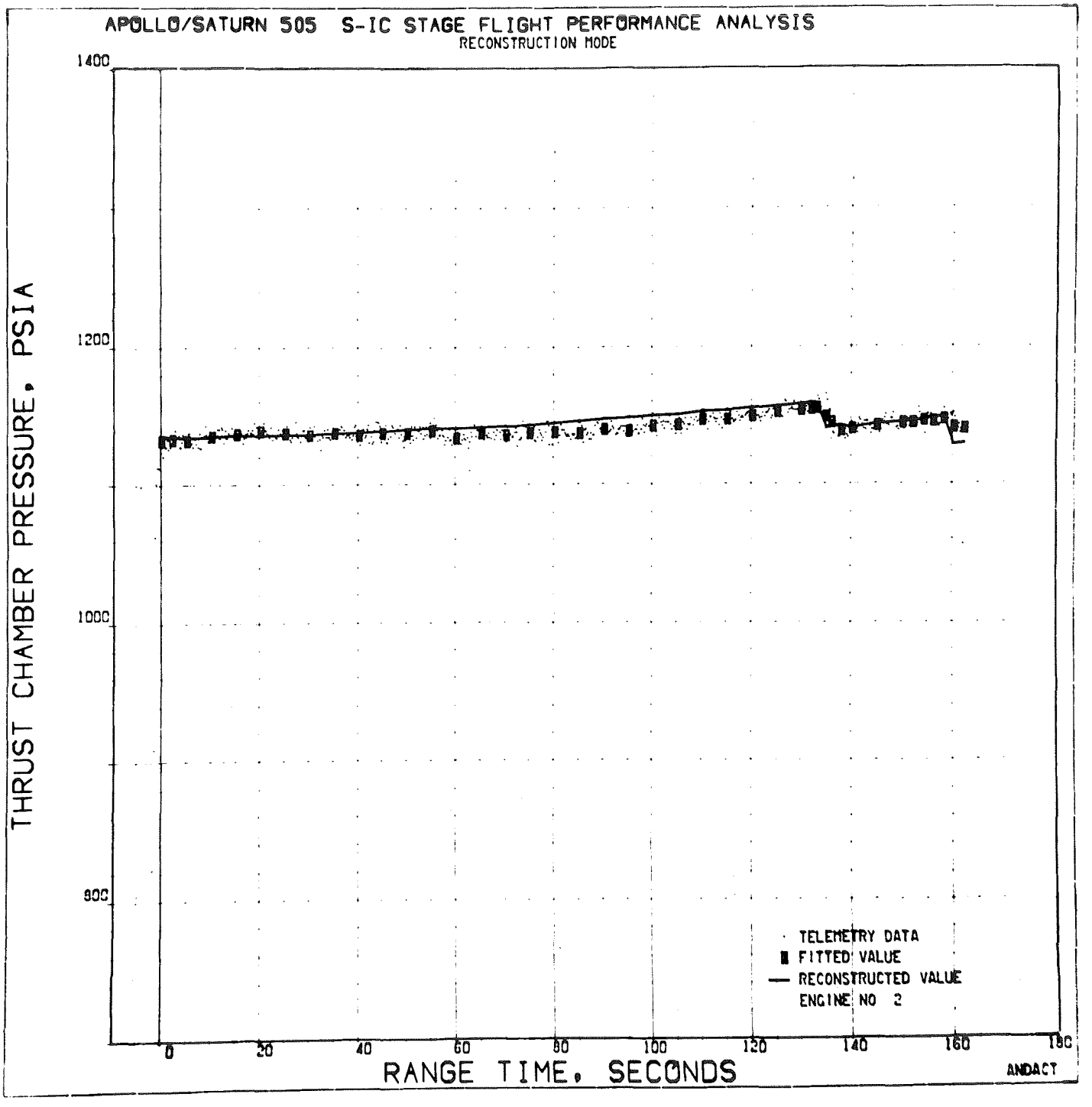

Figure 32. Thrust Chamber Pressure, Engine Position 2, F2041

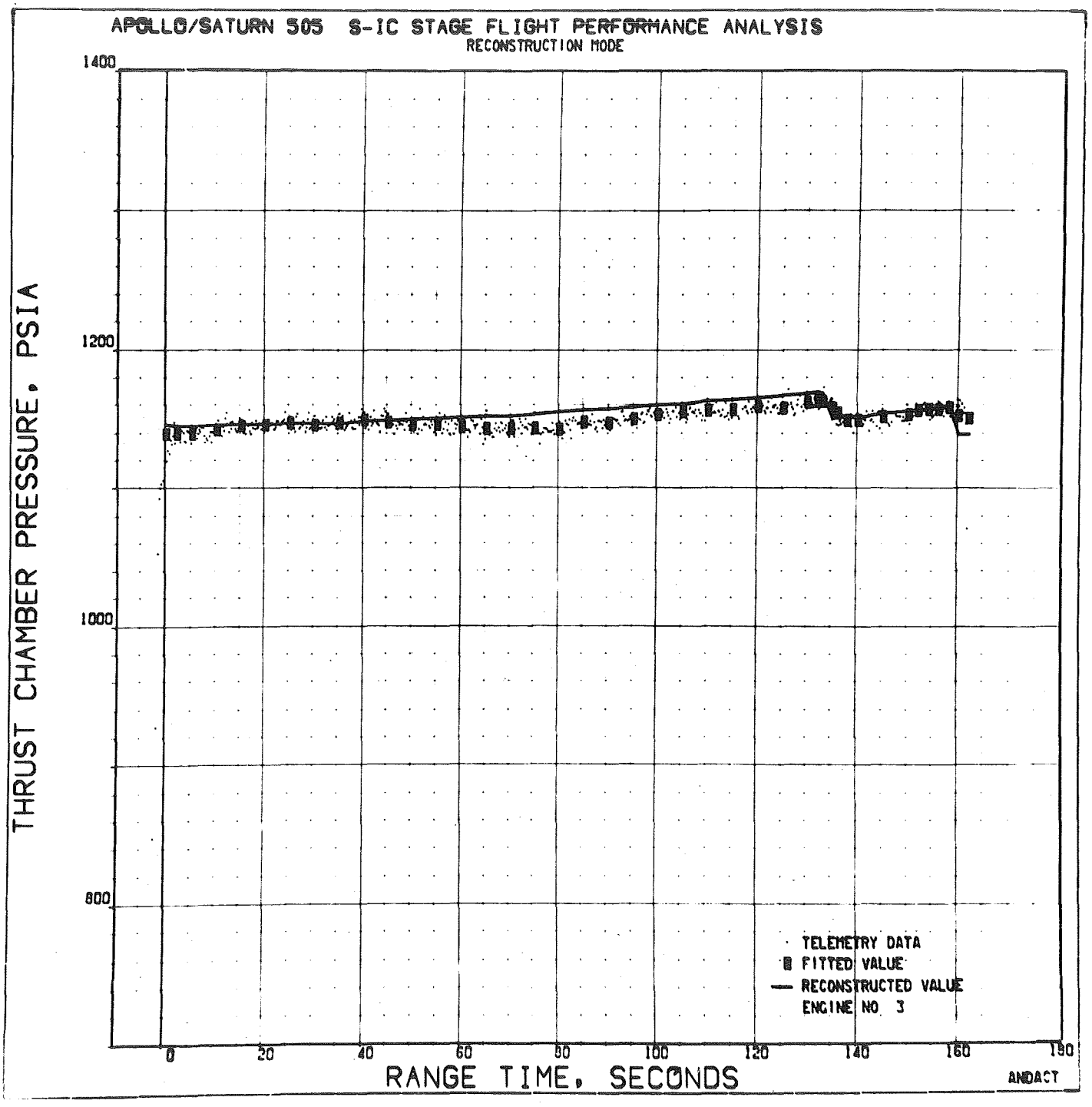

Figure 33. Thrust Chamber Pressure, Engine Position 3, F2040

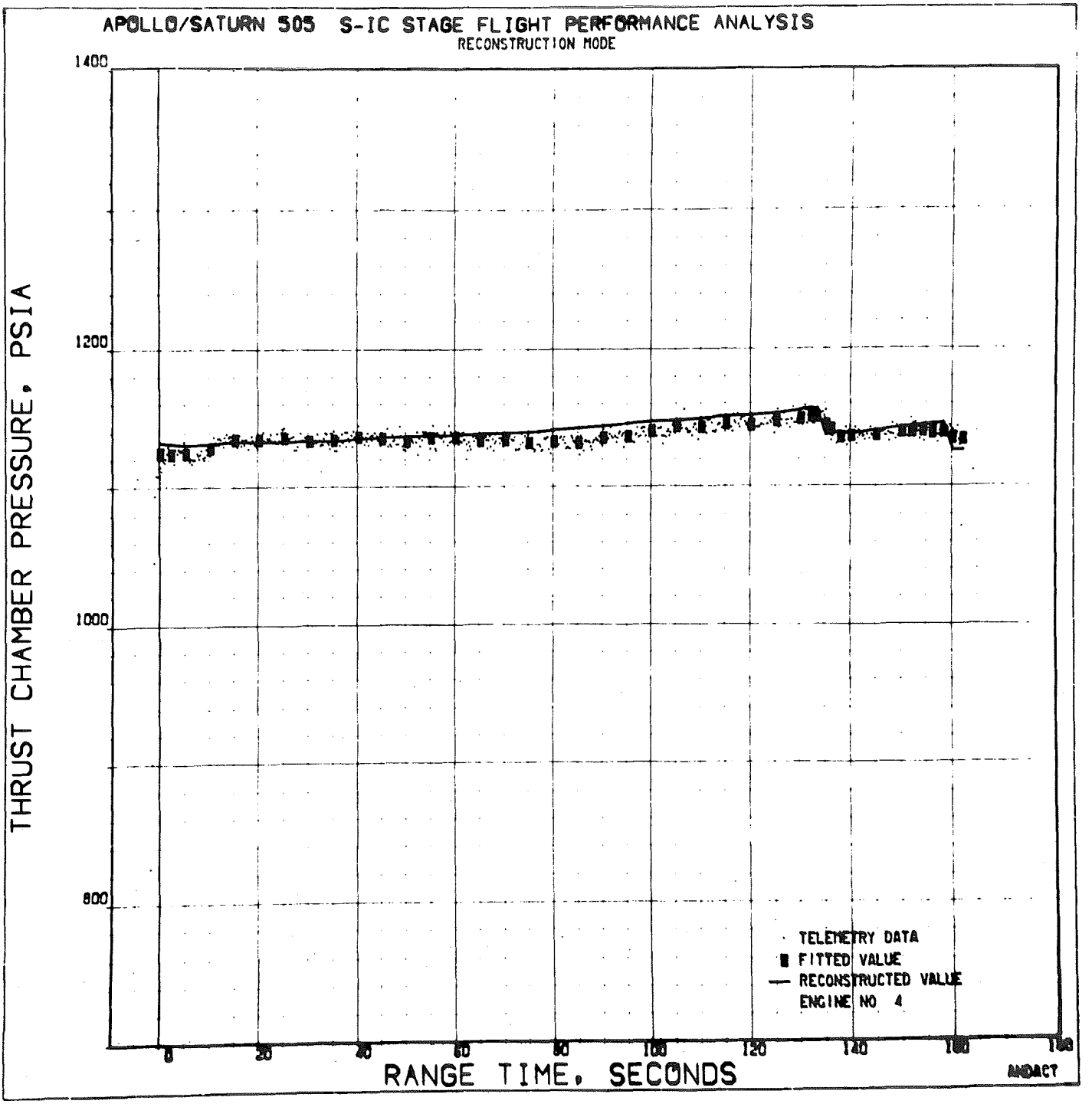

Figure 34. Thrust Chamber Pressure, Engine Position 4, F2042

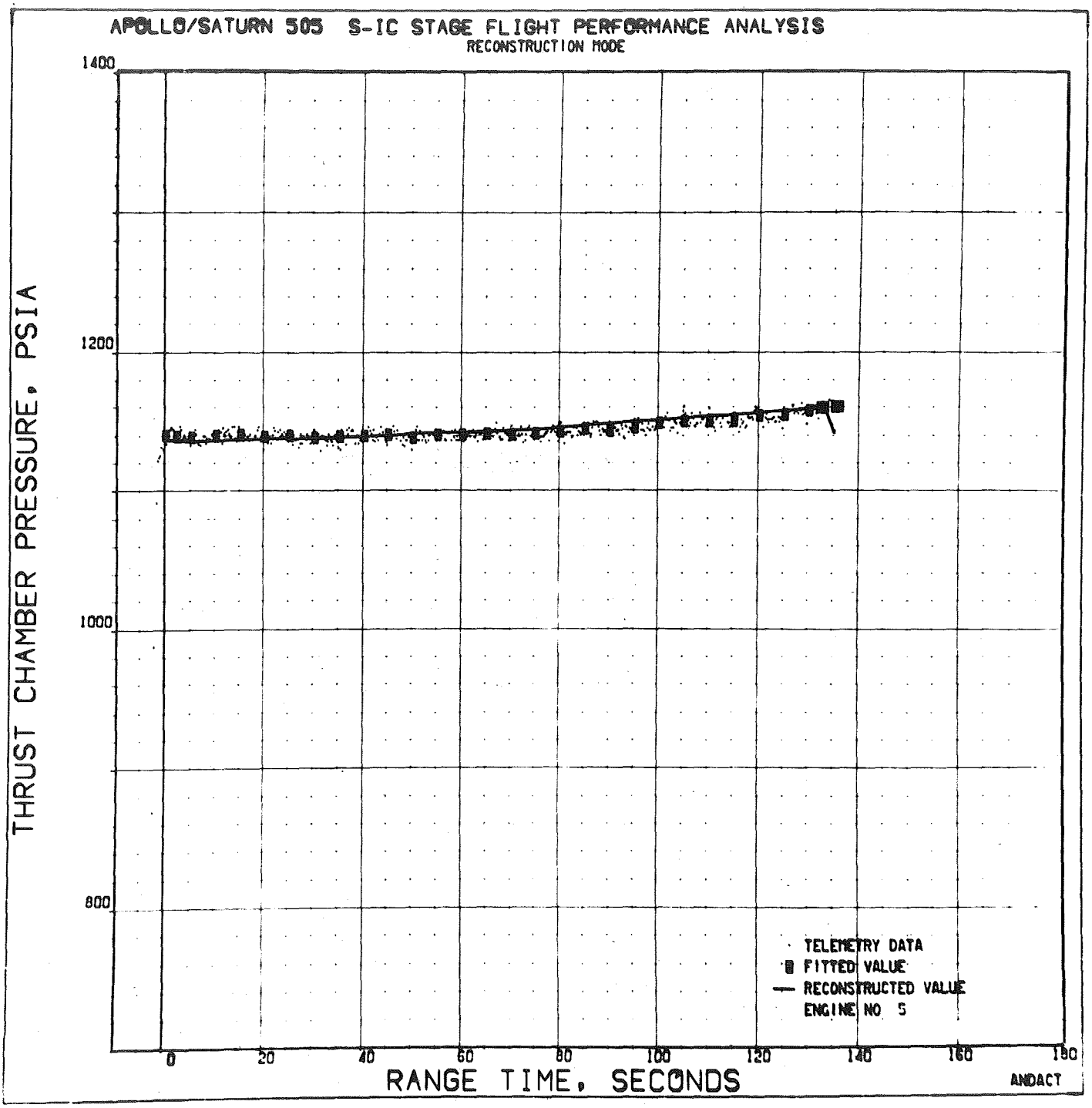

Figure 35. Thrust Chamber Pressure, Engine Position 5, F2034

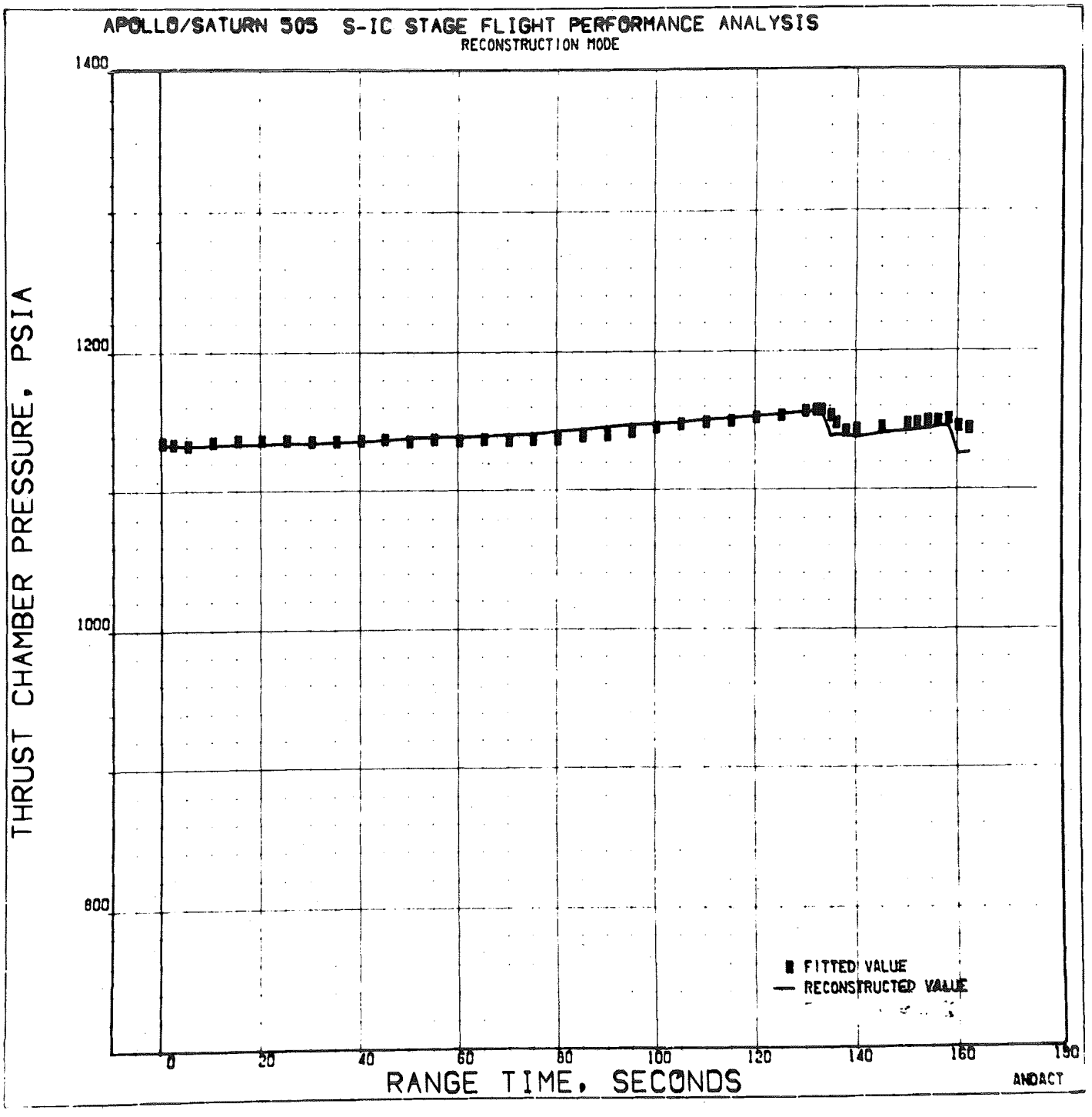

Figure 36. Average Thrust Chamber Pressure

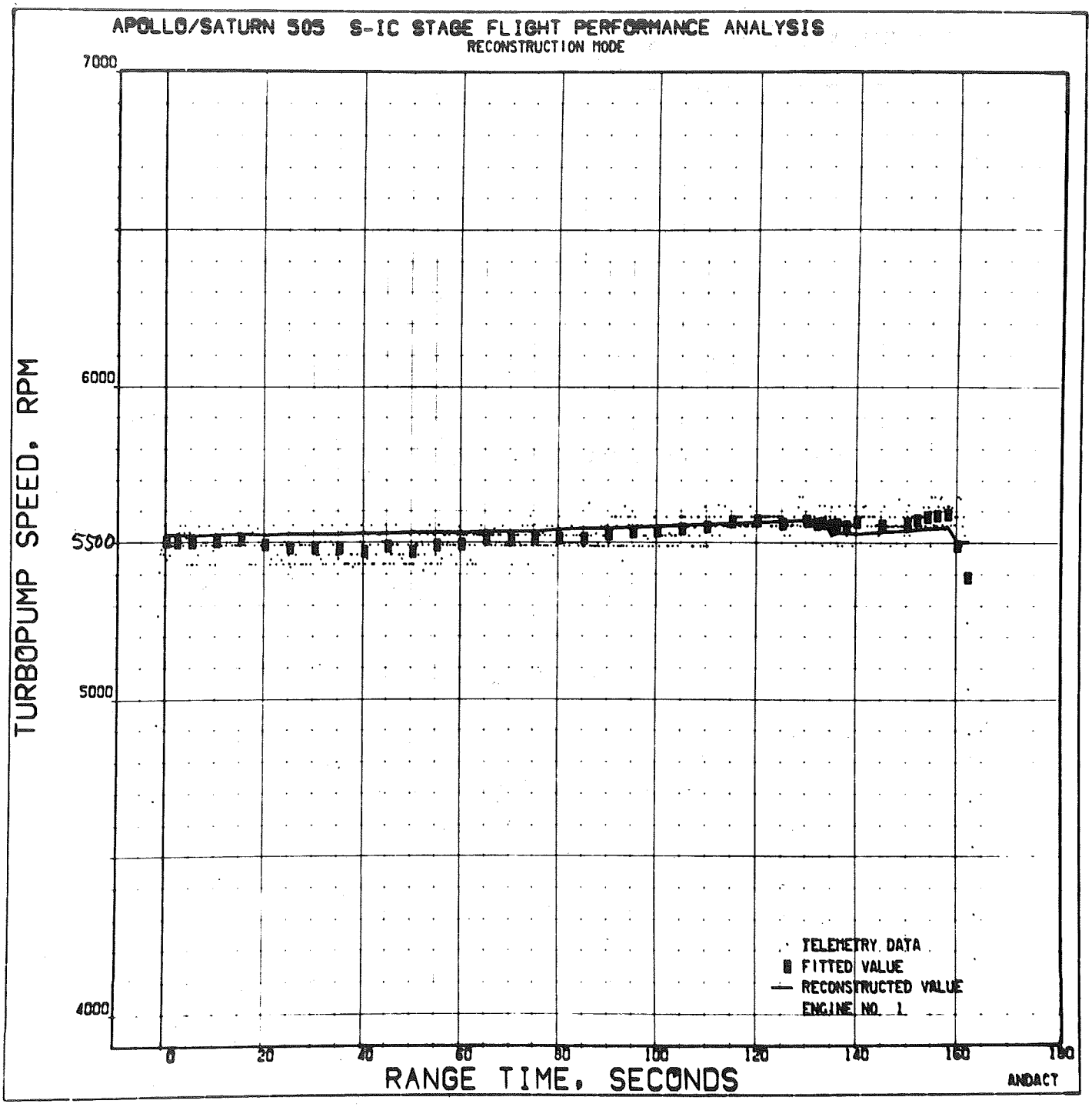

Figure 37. Turbopump Speed, Engine Position 1, F2035

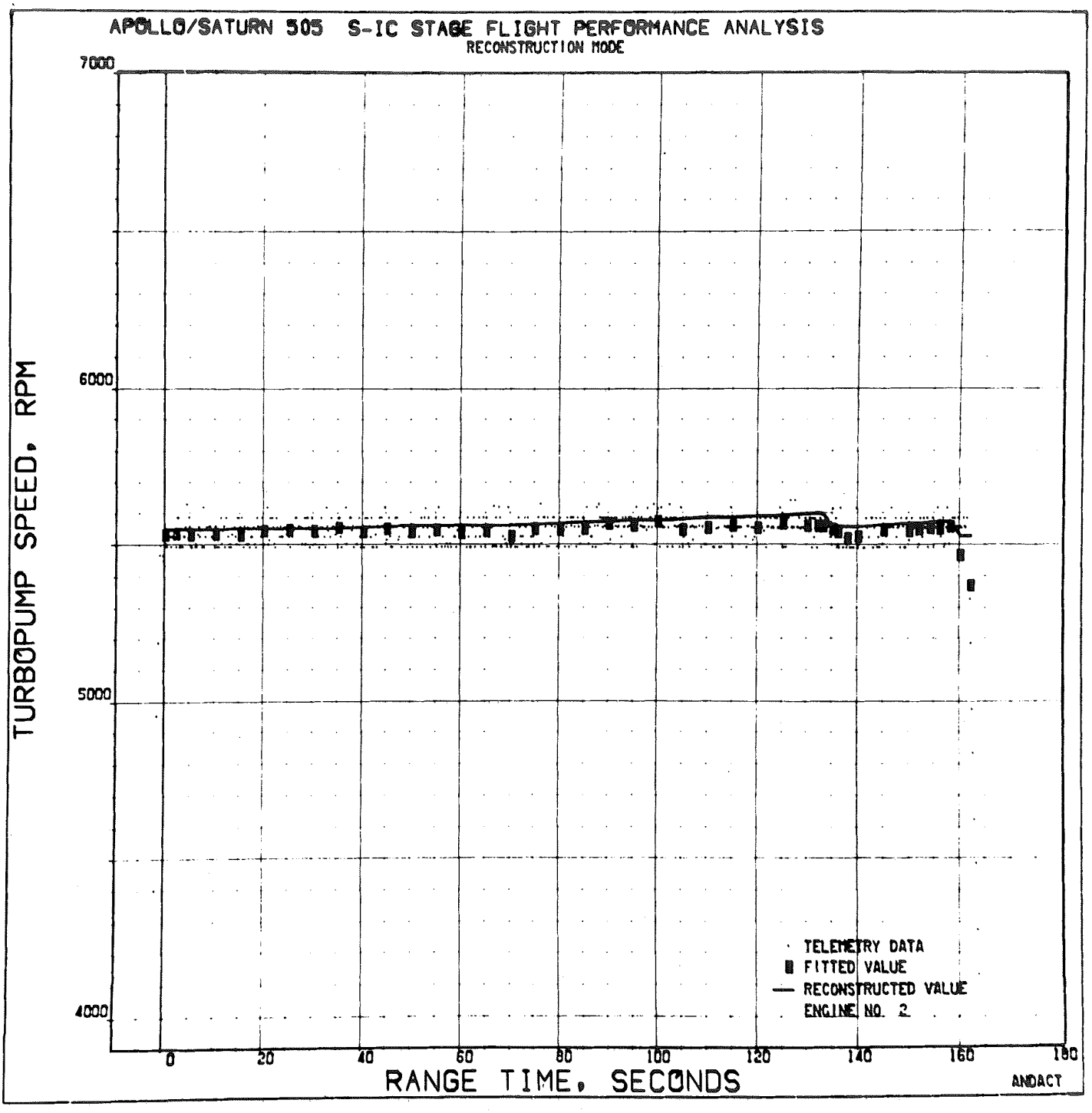

Figure 38. Turbopump Speed, Engine Position 2, F2041

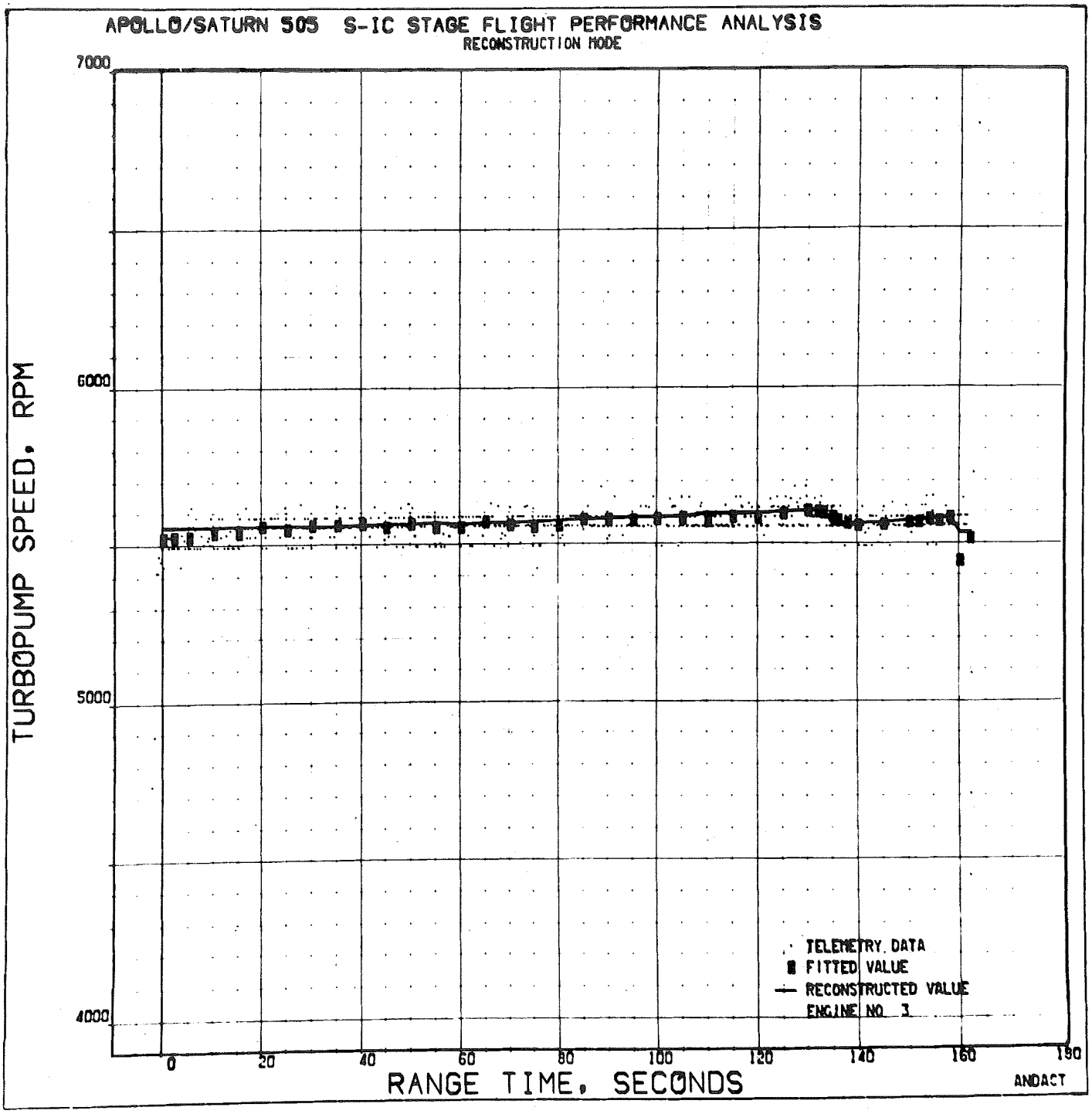

Figure 39. Turbopump Speed, Engine Position 3, F2040

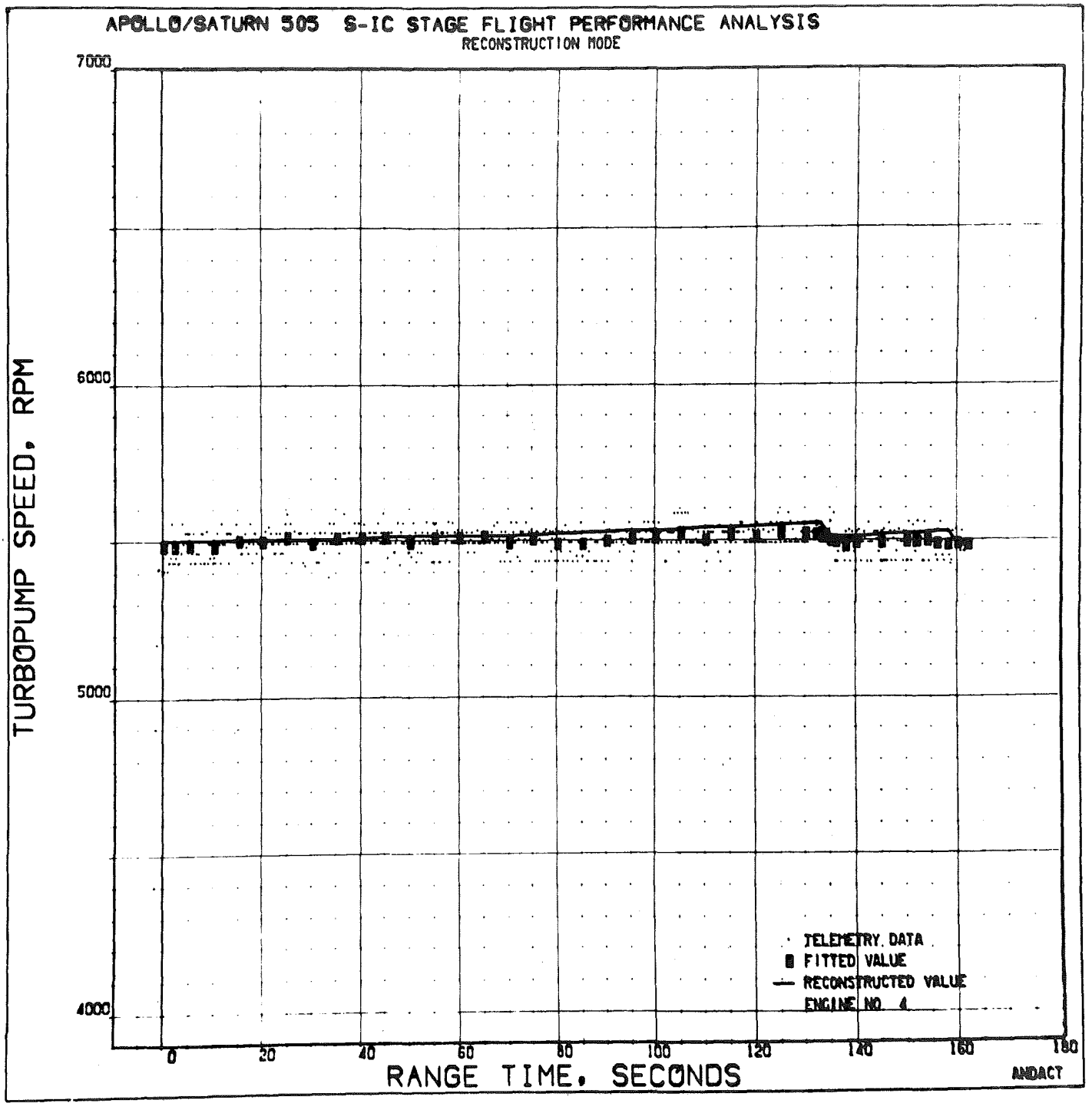

Figure 40. Turbopump Speed, Engine Position 4, F2042

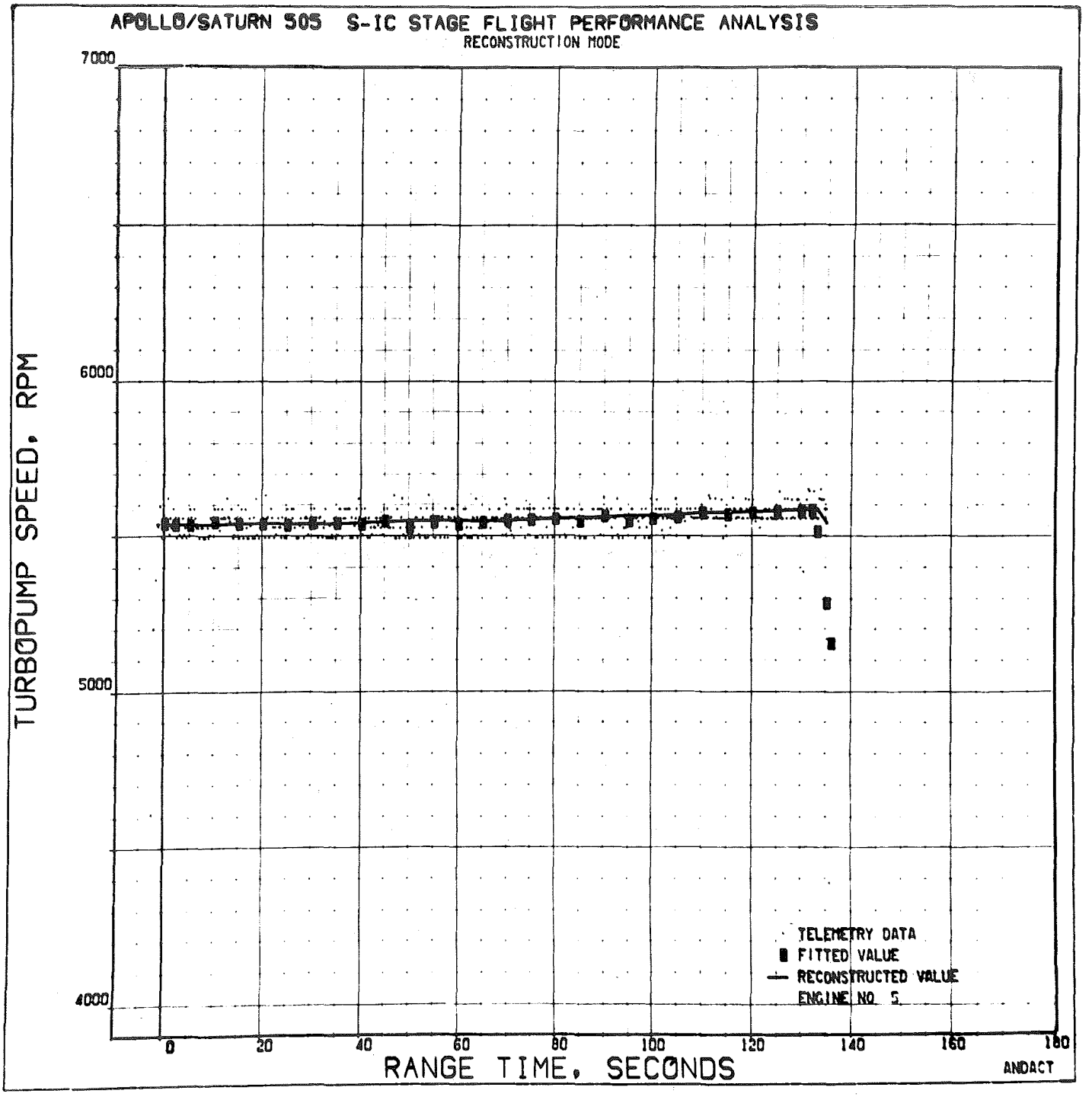

Figure 41. Turbopump Speed, Engine Position 5, F2034

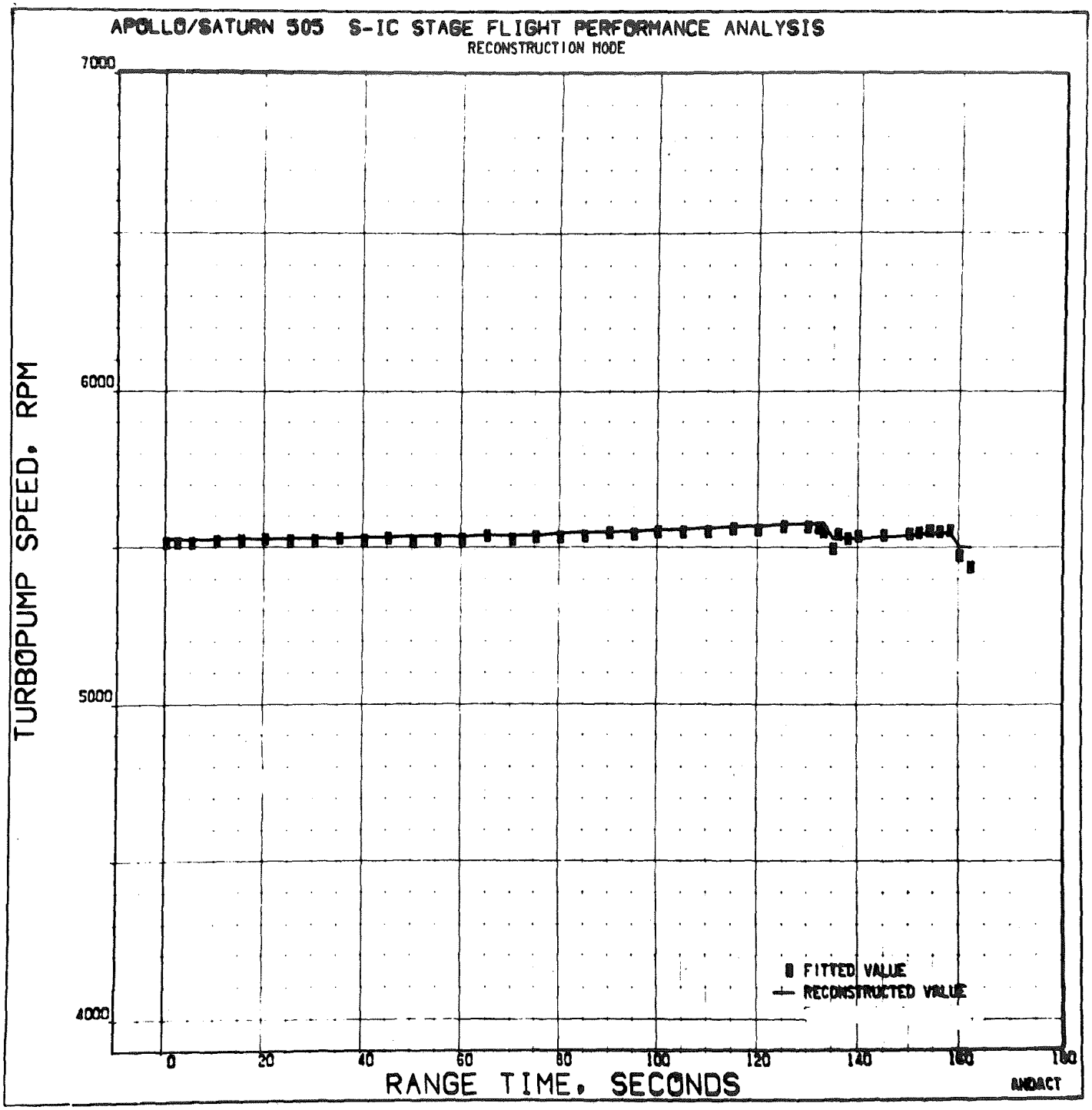

Figure 42. Average Turbopump Speed

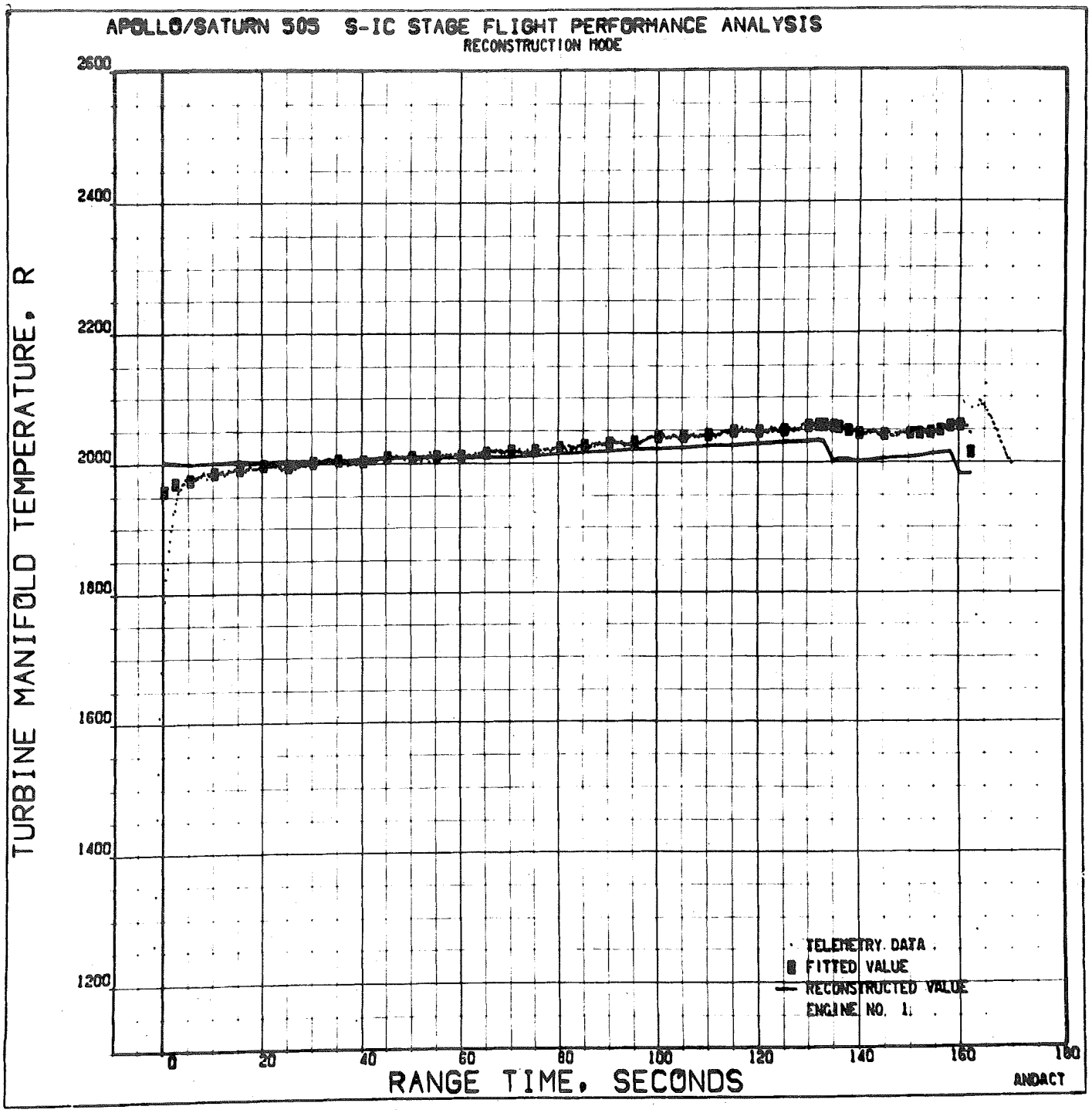

Figure 43. Turbine Manifold Temperature, Engine Position 1, F2035

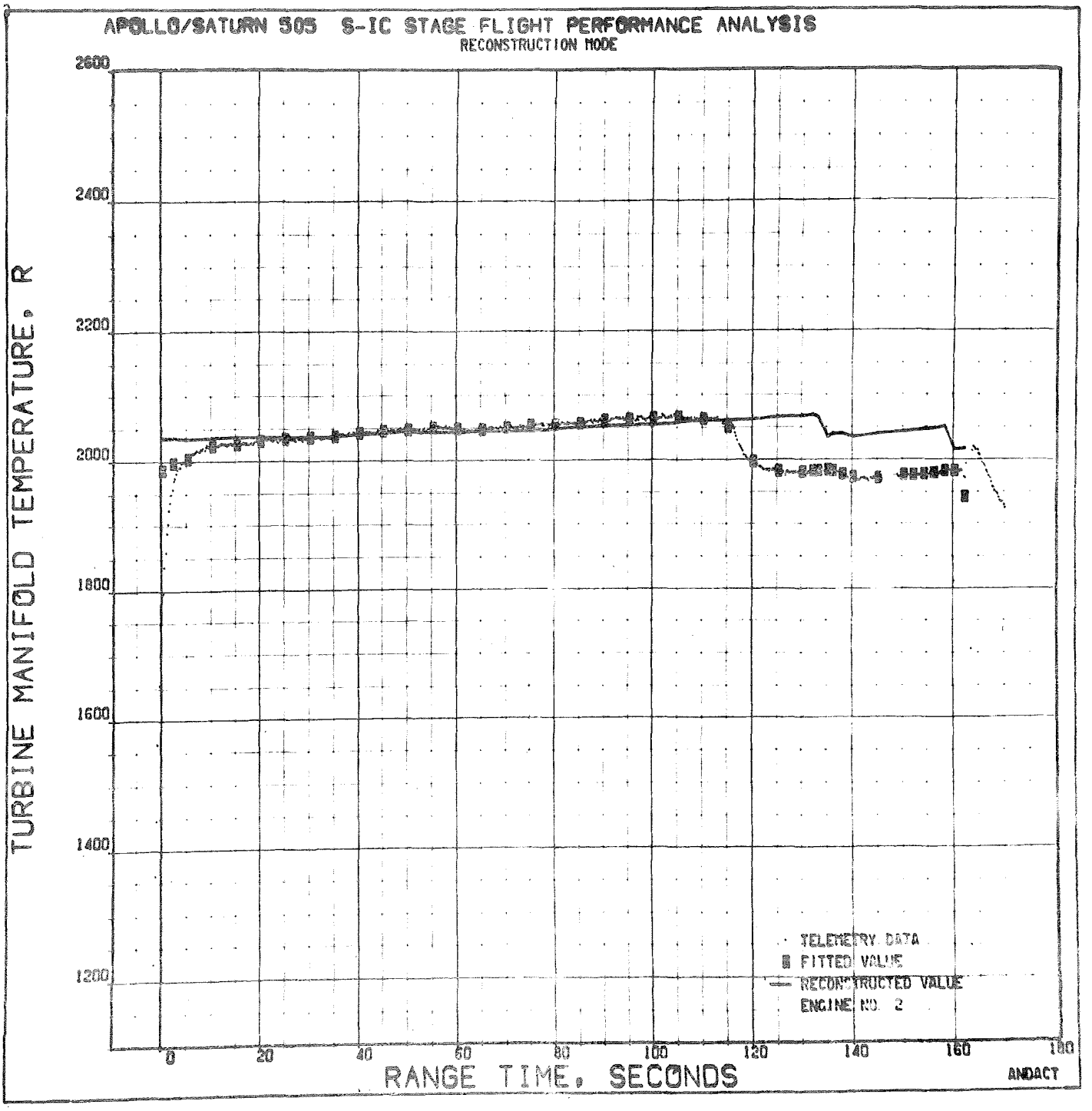

Figure 44. Turbine Manifold Temperature, Engine Position 2, F2041

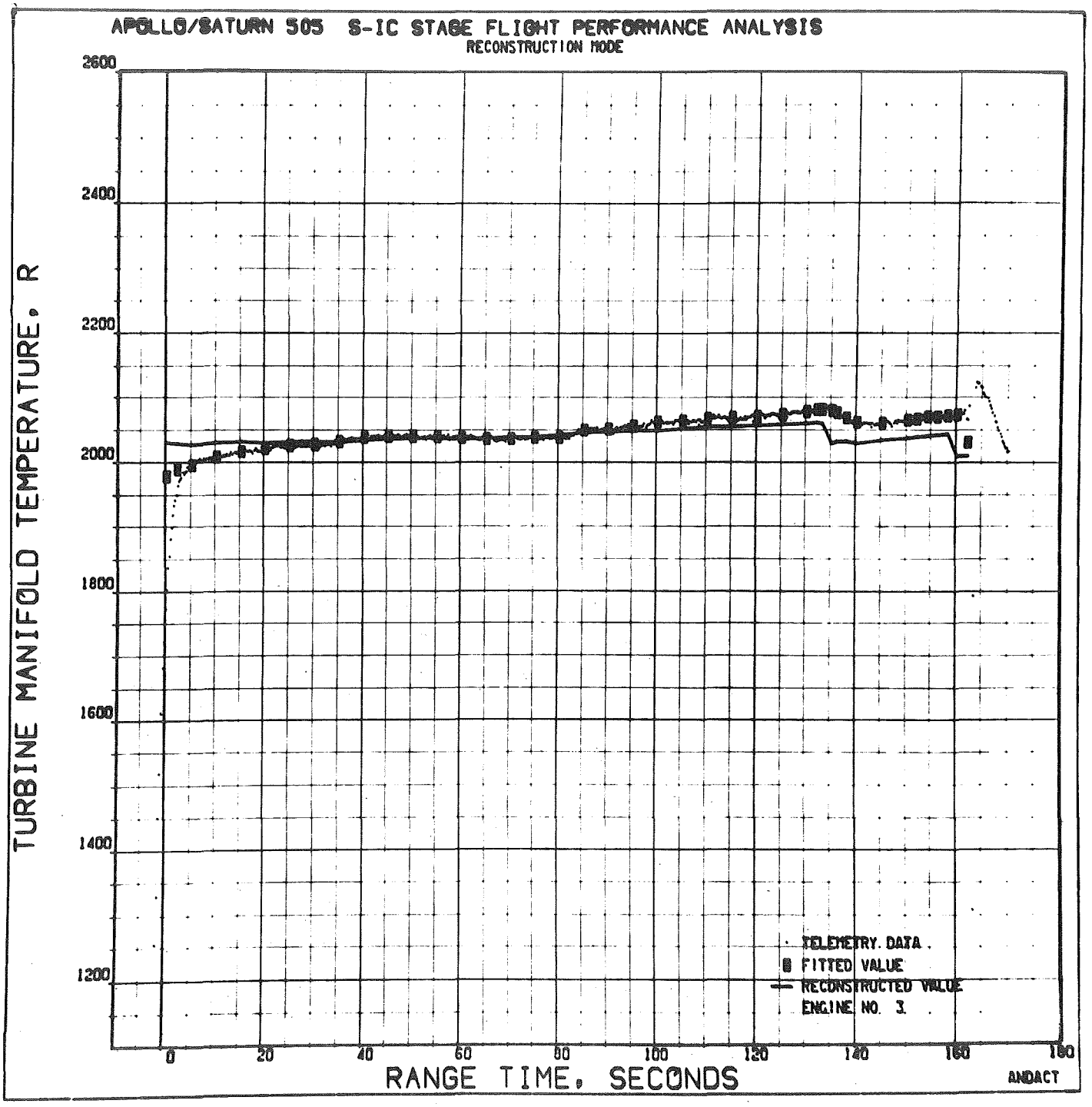

Figure 45. Turbine Manifold Temperature, Engine Position 3, F2040

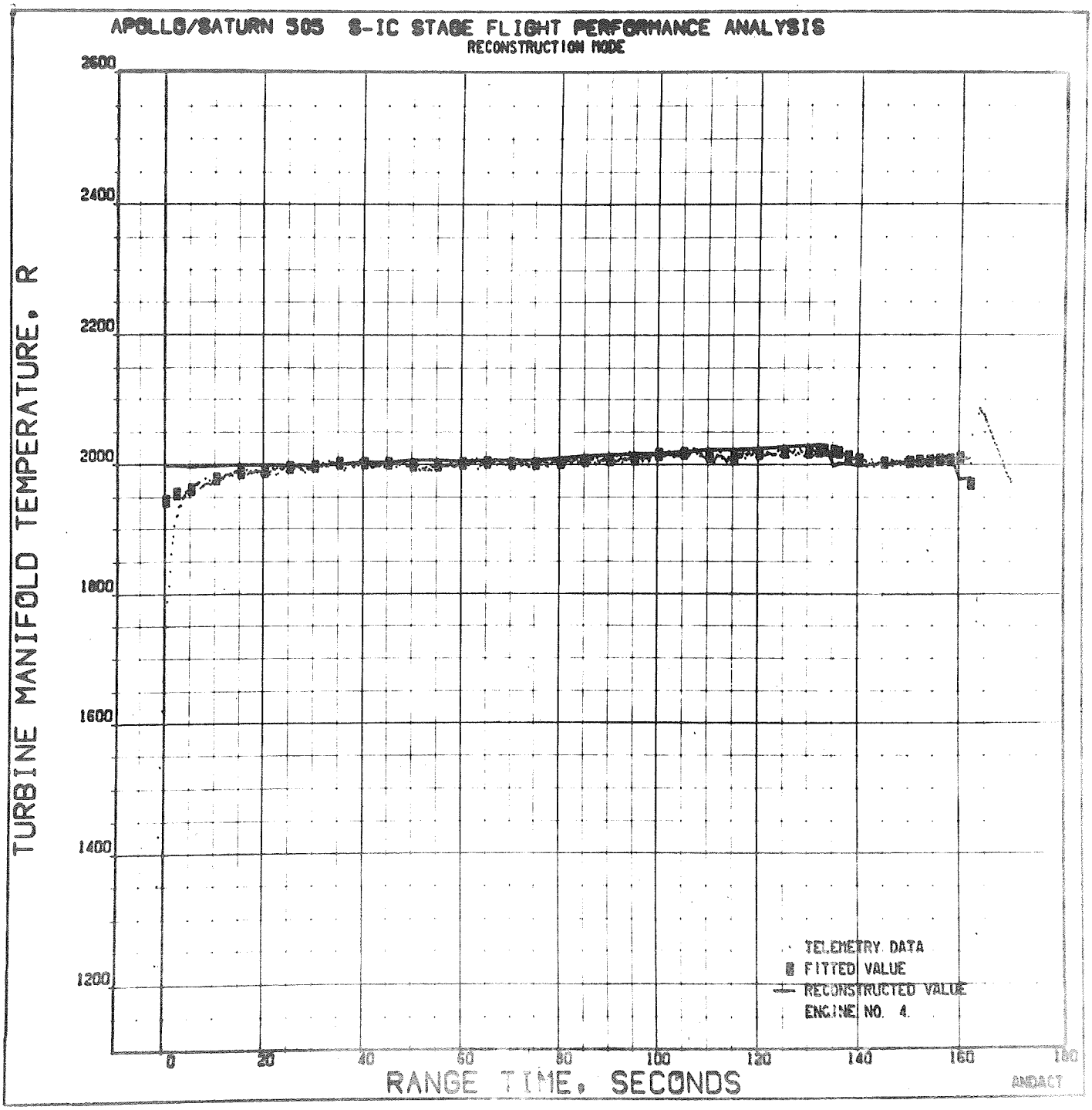

Figure 46. Turbine Manifold Temperature, Engine Position 4, F2042

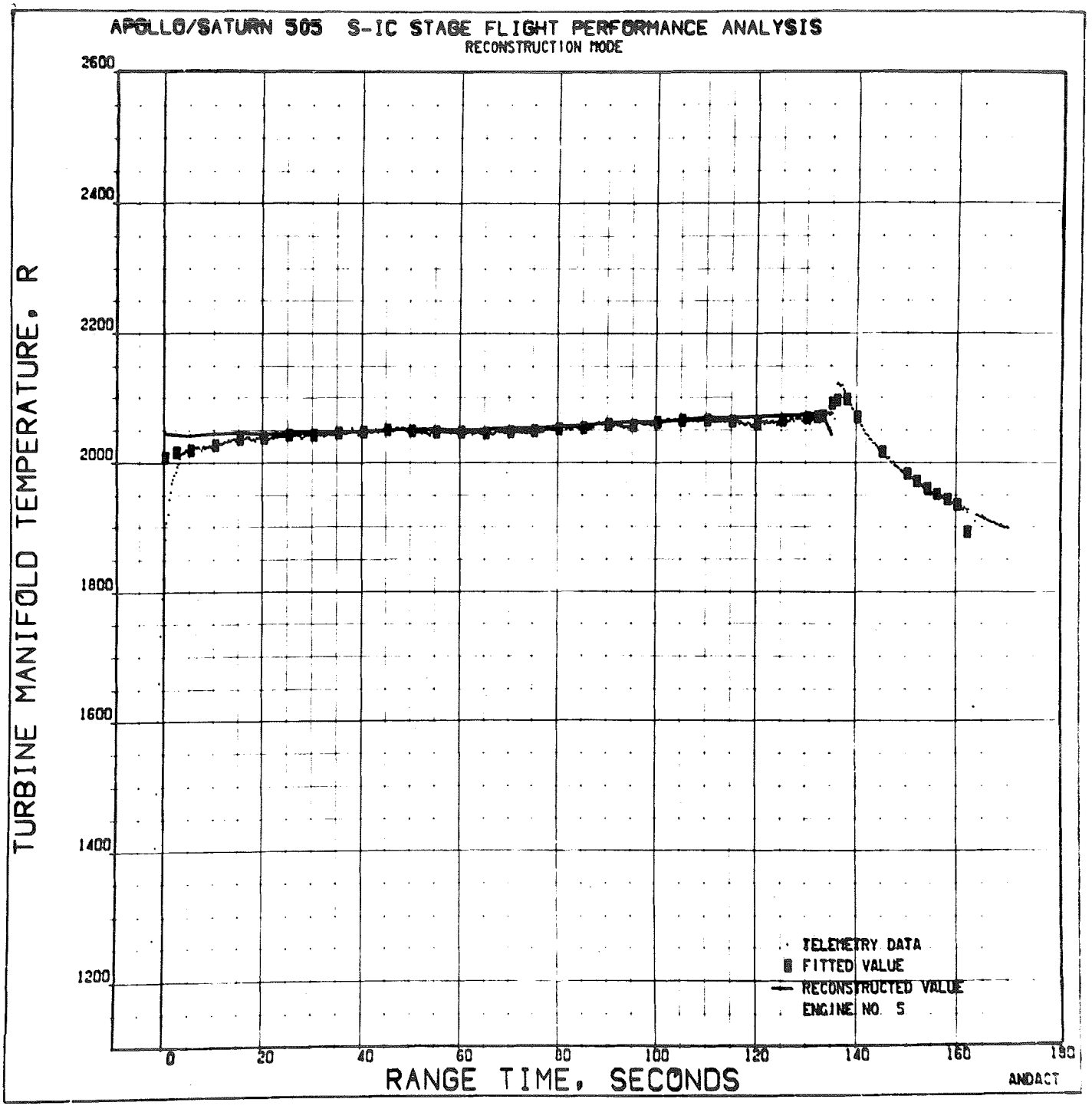

Figure 47. Turbine Manifold Temperature, Engine Position 5, F2034

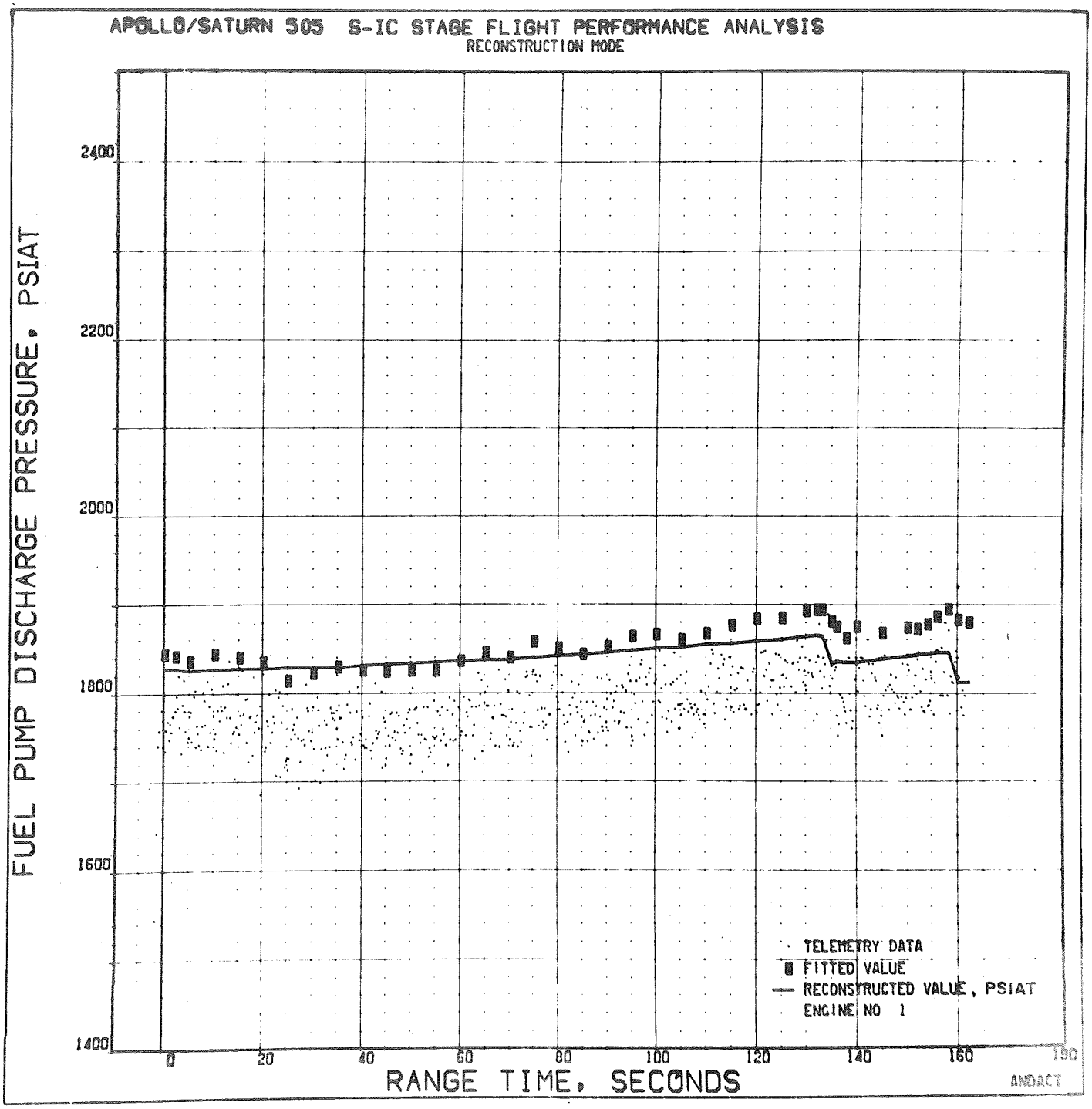

Figure 48. Fuel Pump Discharge Pressure, Engine Position 1, F2035

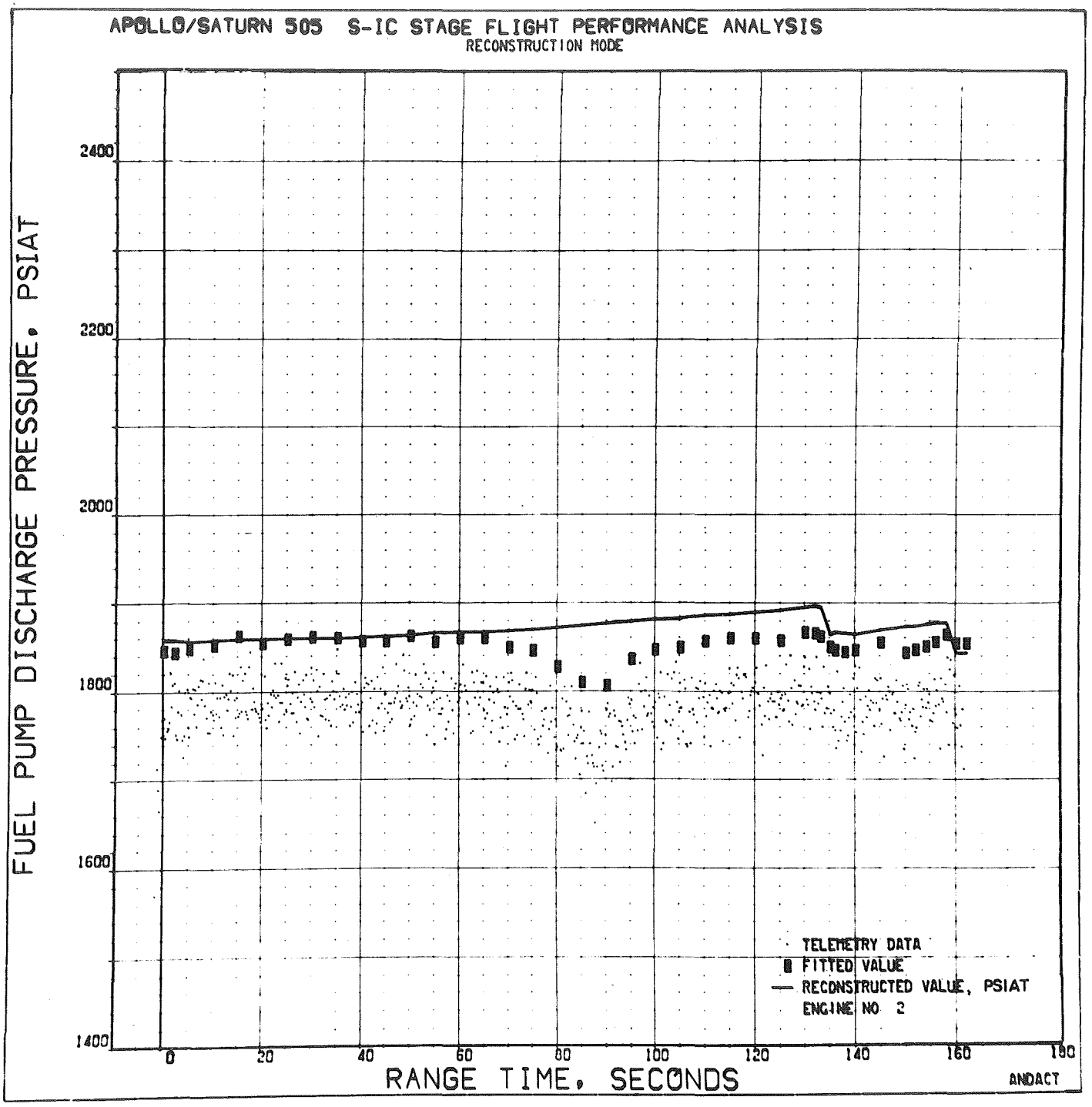

Figure 49. Fuel Pump Discharge Pressure, Engine Position 2, F2041

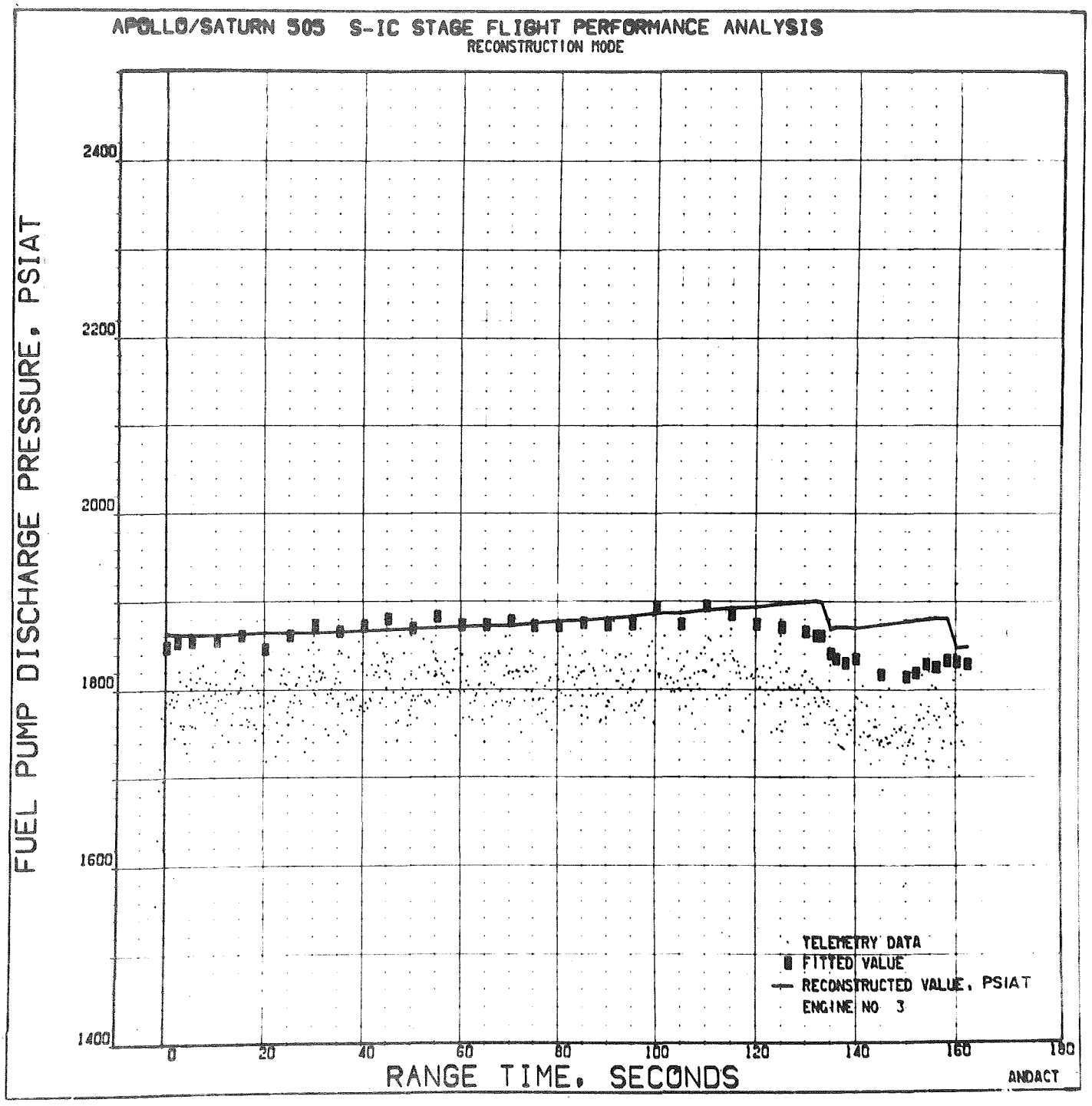

Figure 50. Fuel Pump Discharge Pressure, Engine Position 3, F2040

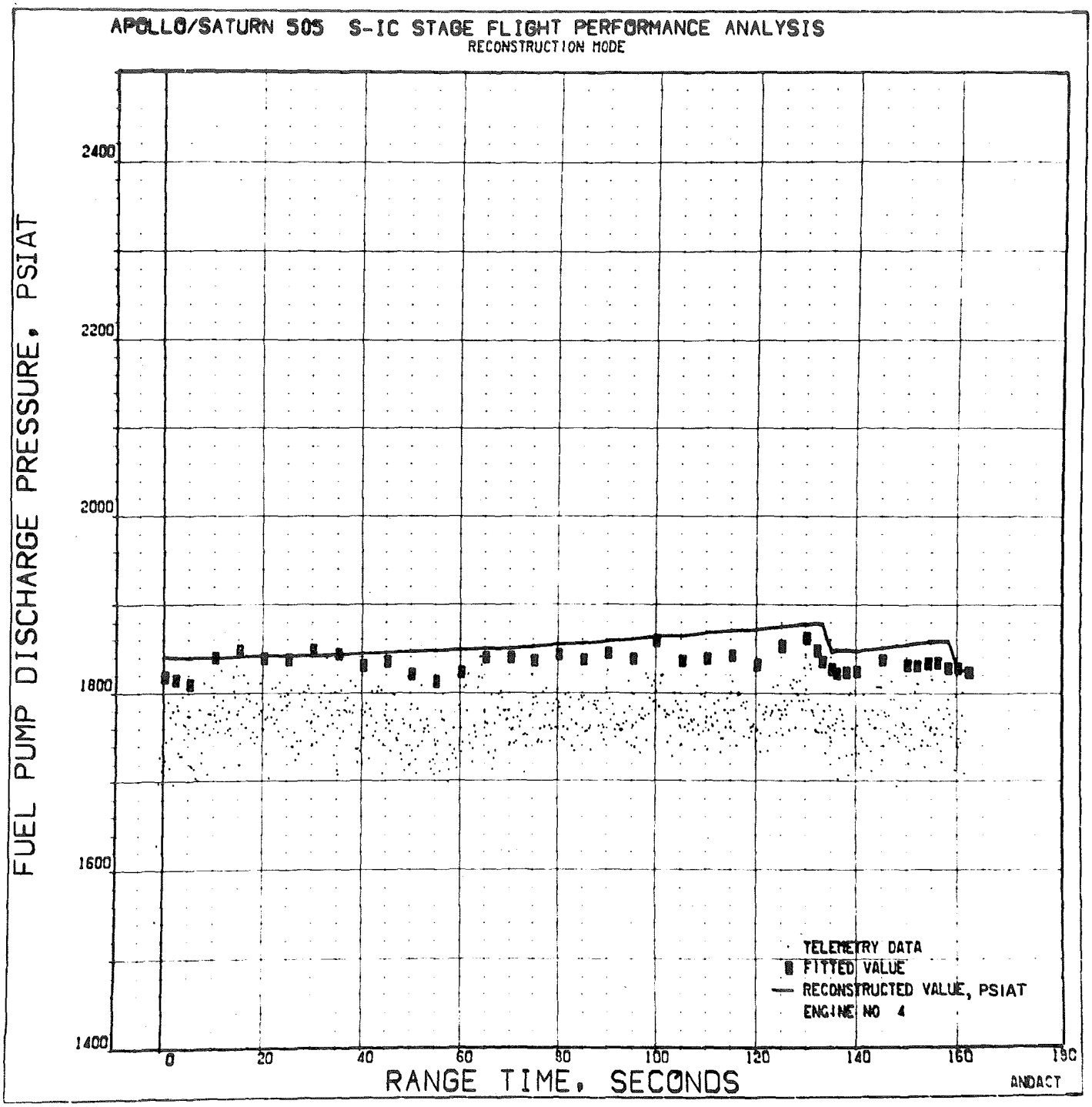

Figure 51. Fuel Pump Discharge Pressure, Engine Position 4, F2042

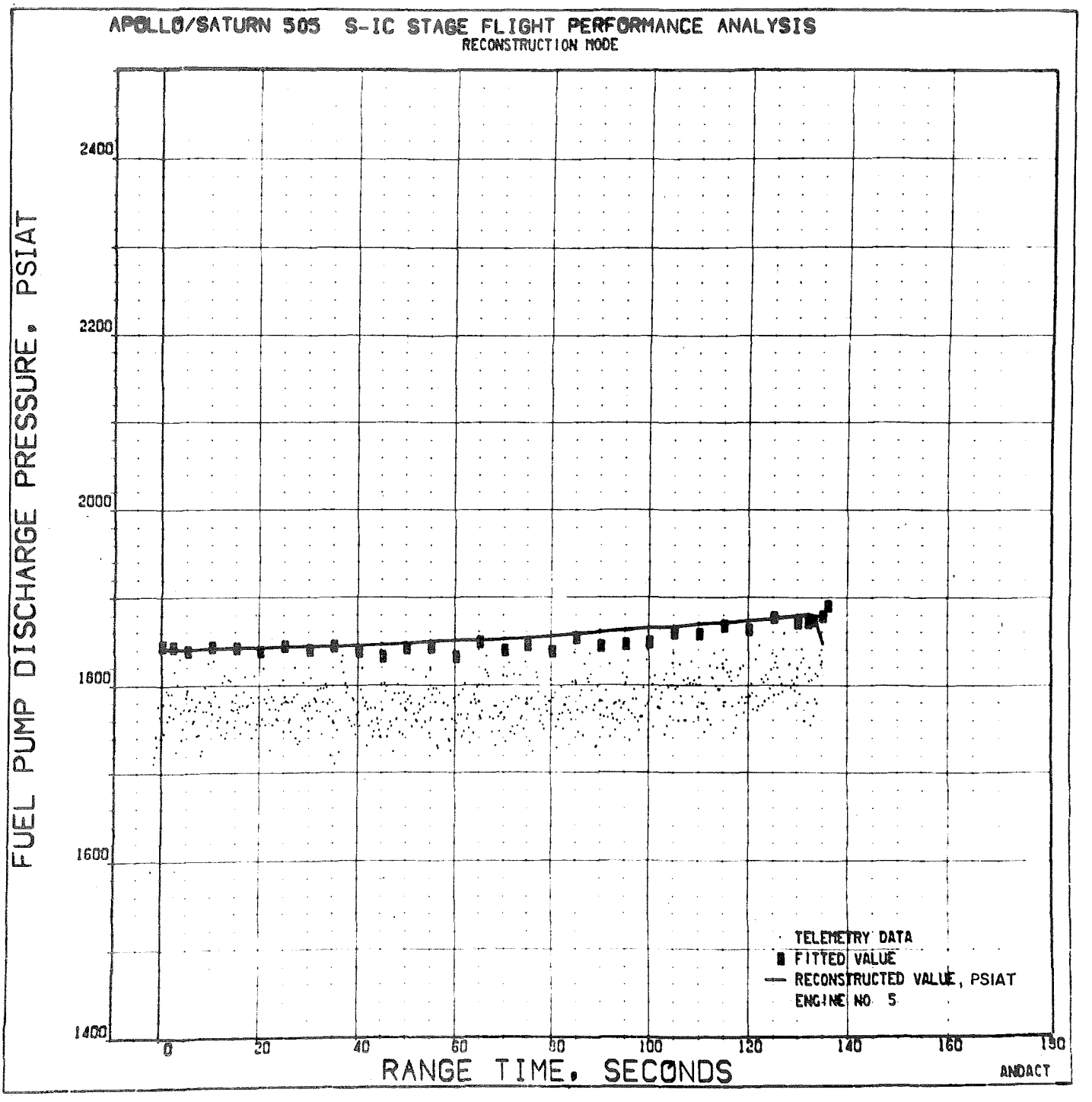

Figure 52. Fuel Pump Discharge Pressure, Engine Position 5, F2034

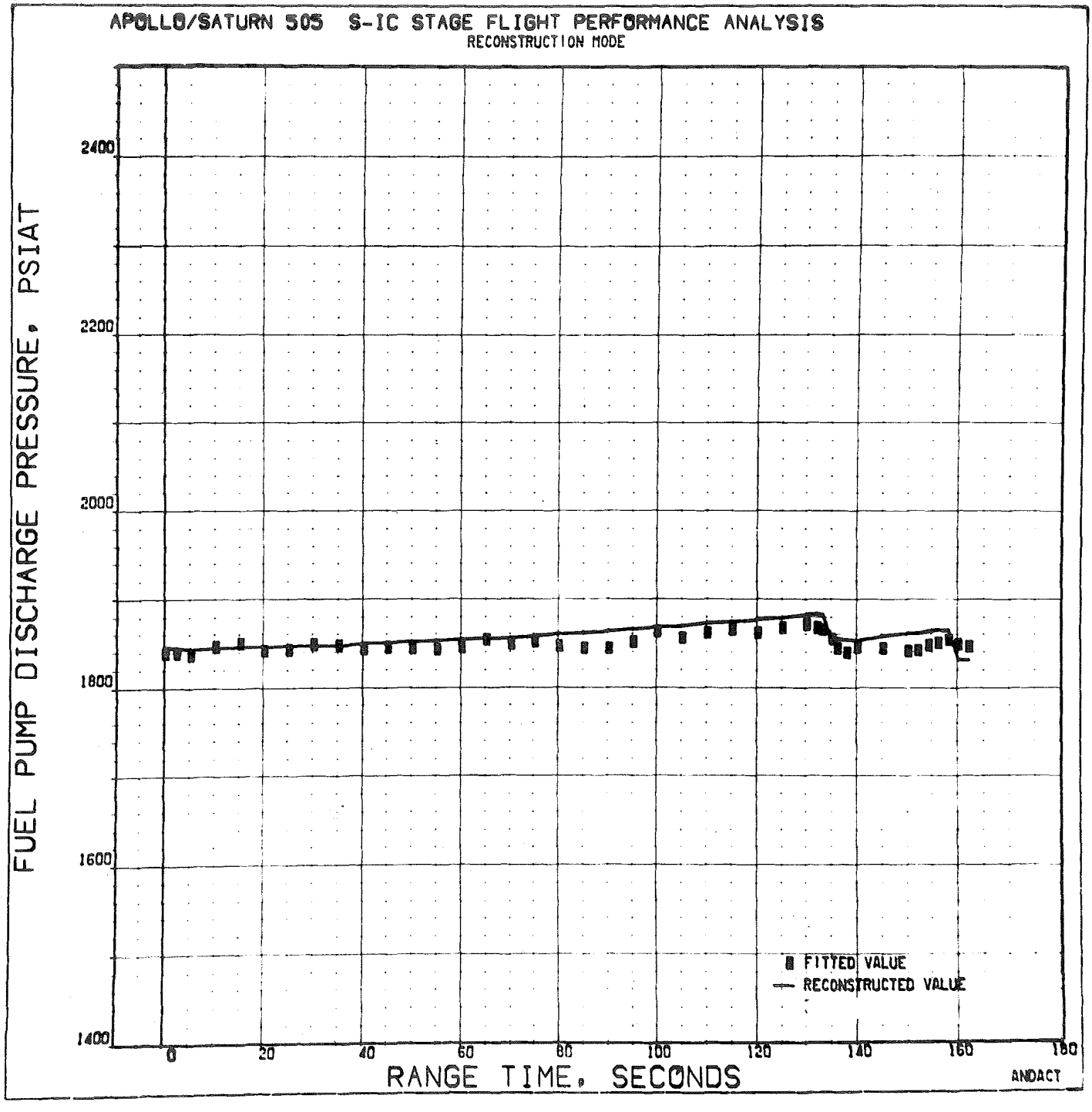

Figure 53. Average Fuel Pump Discharge Total Pressure

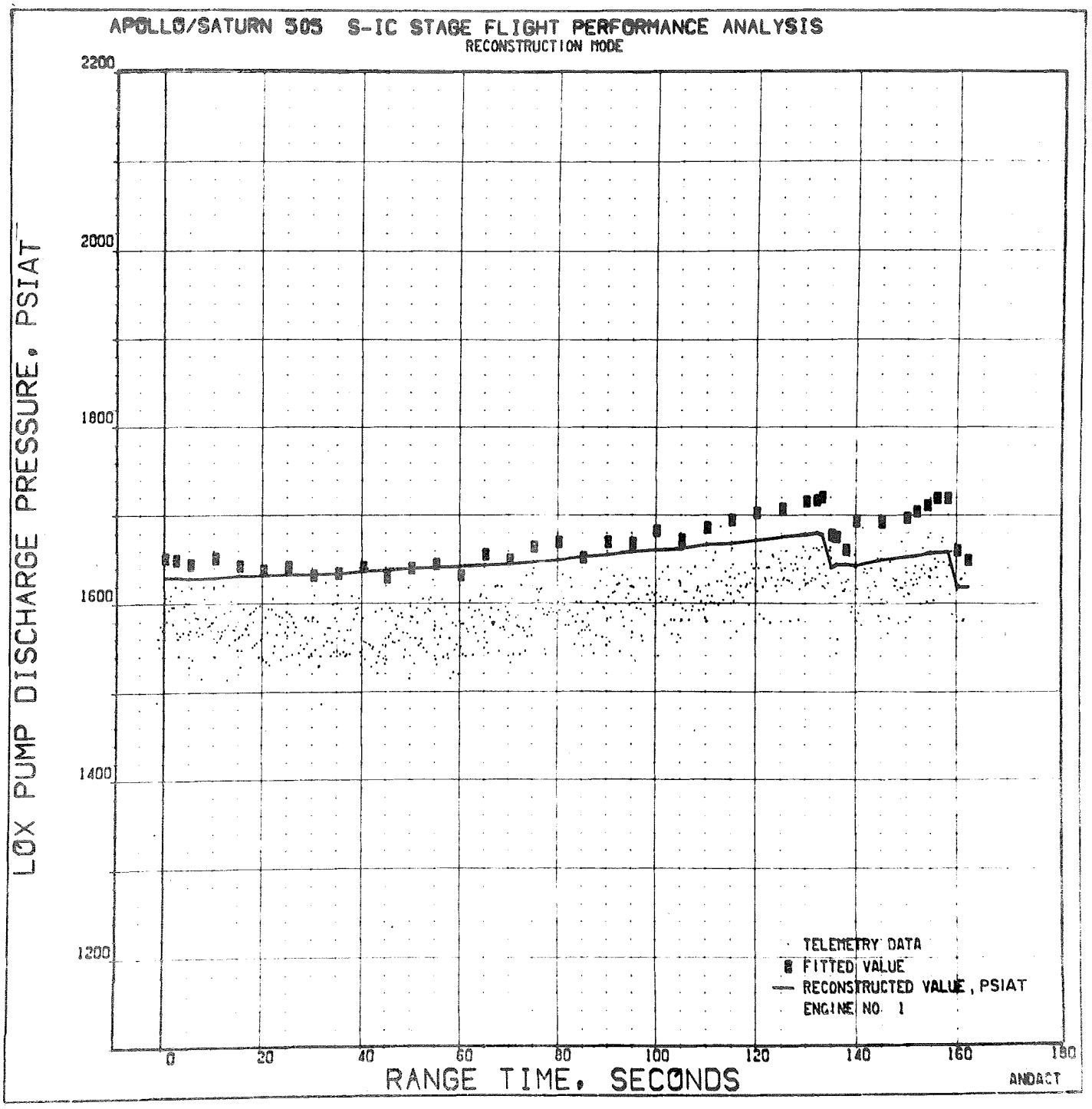

Figure 54. LOX Pump Discharge Pressure, Engine Position 1, F2035

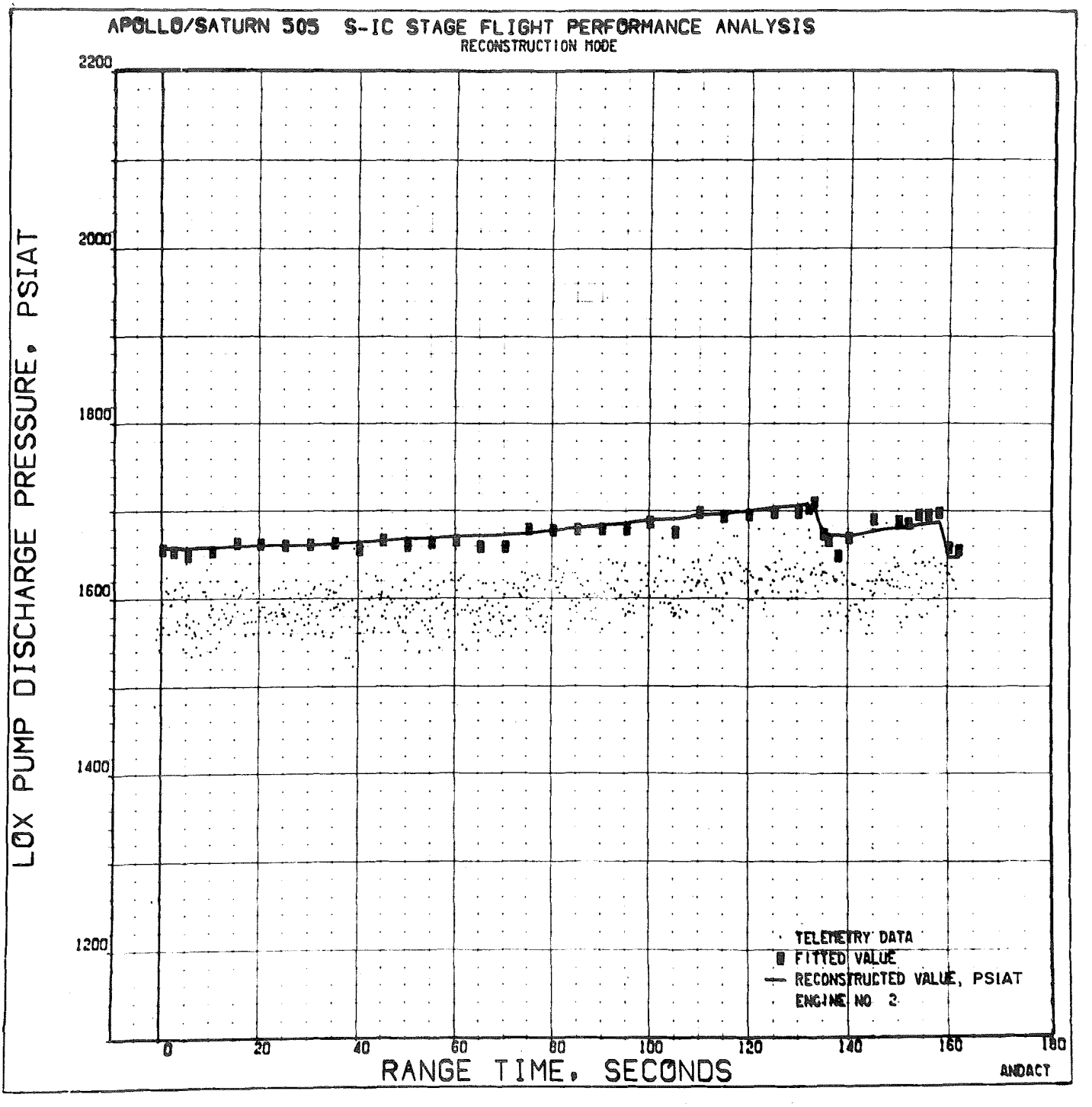

Figure 55. LOX Pump Discharge Pressure, Engine Position 2, F2041

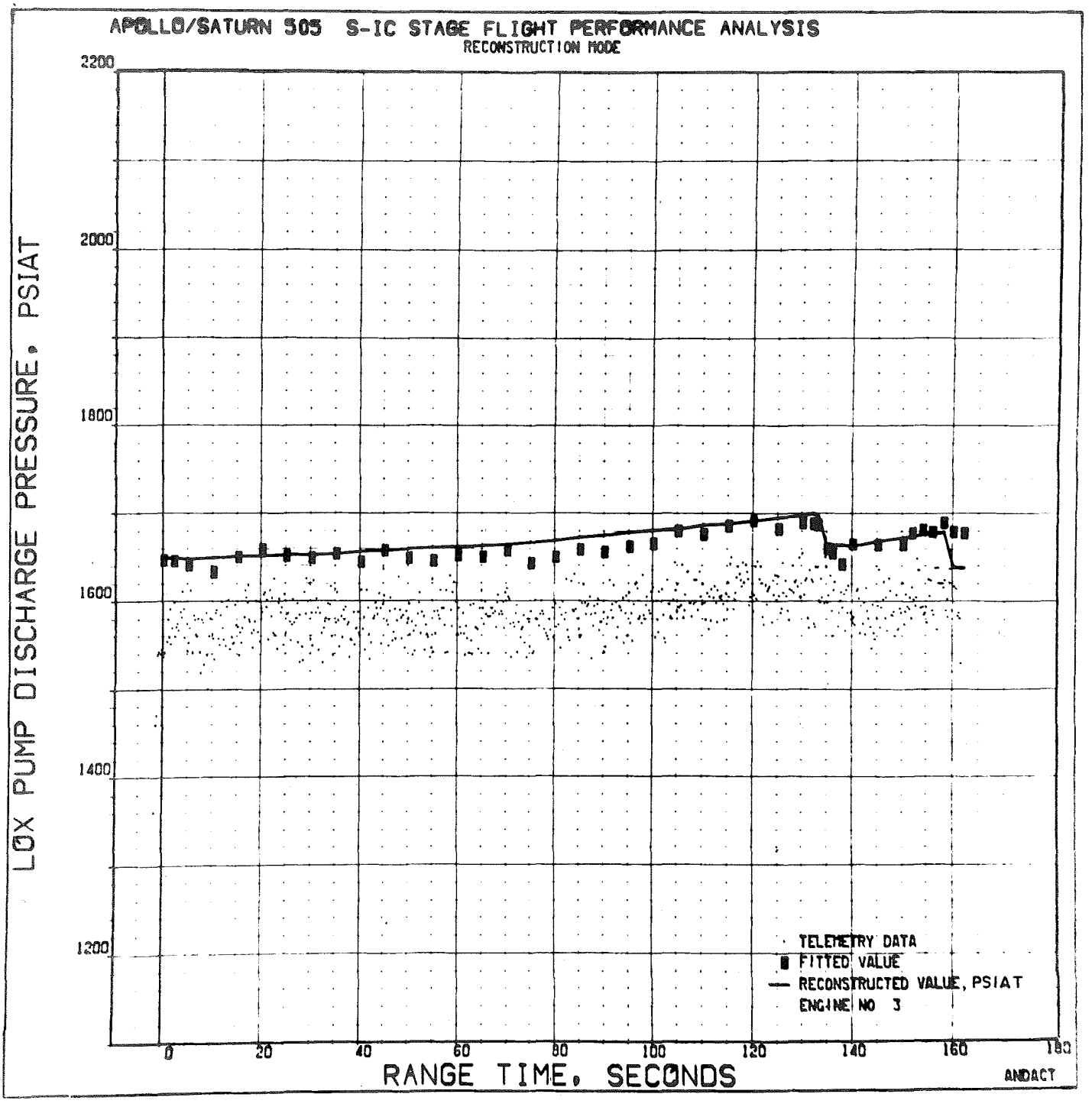

Figure 56. LOX Pump Discharge Pressure, Engine Position 3, F2040

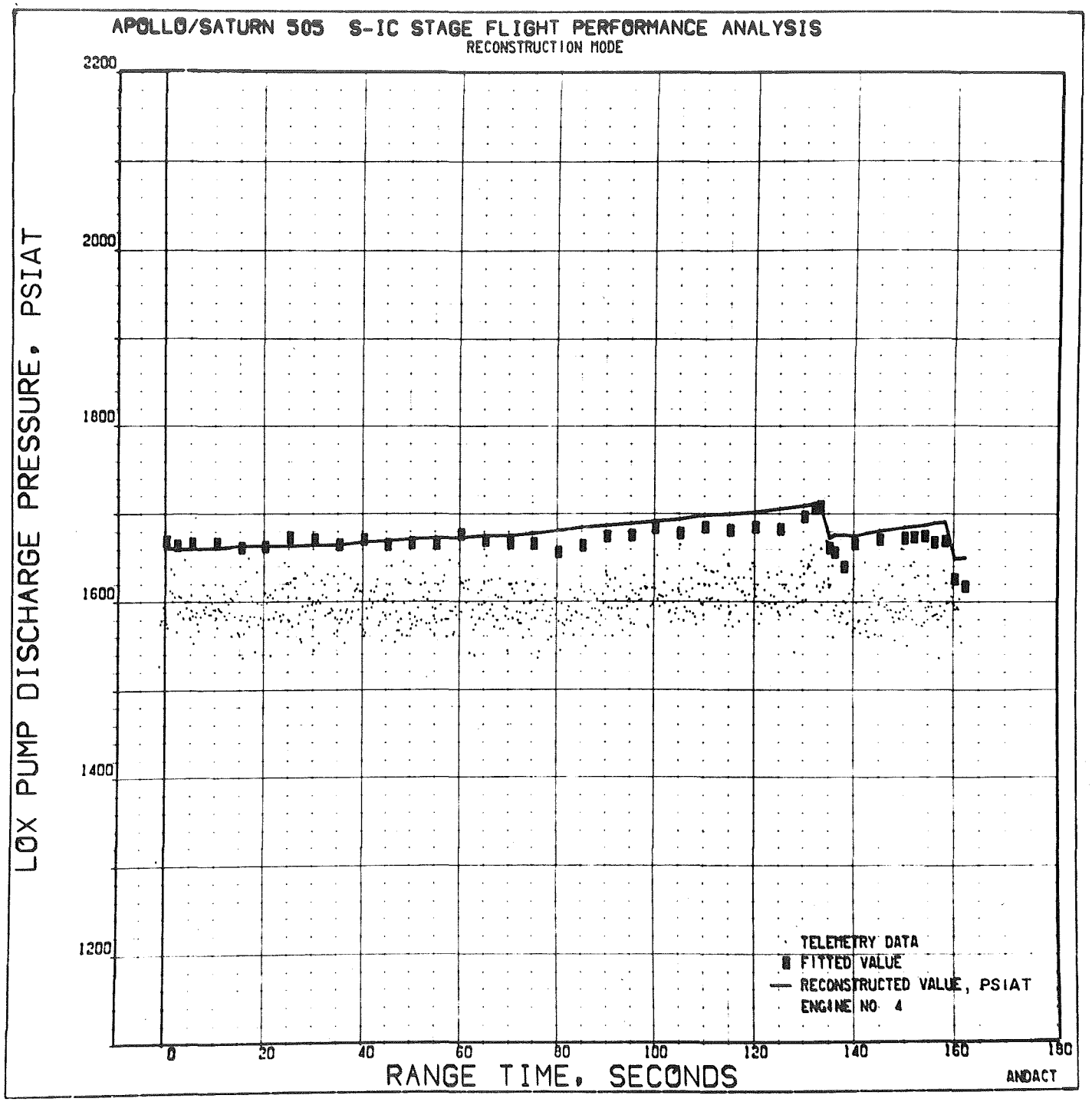

Figure 57. LOX Pump Discharge Pressure, Engine Position 4, F2042

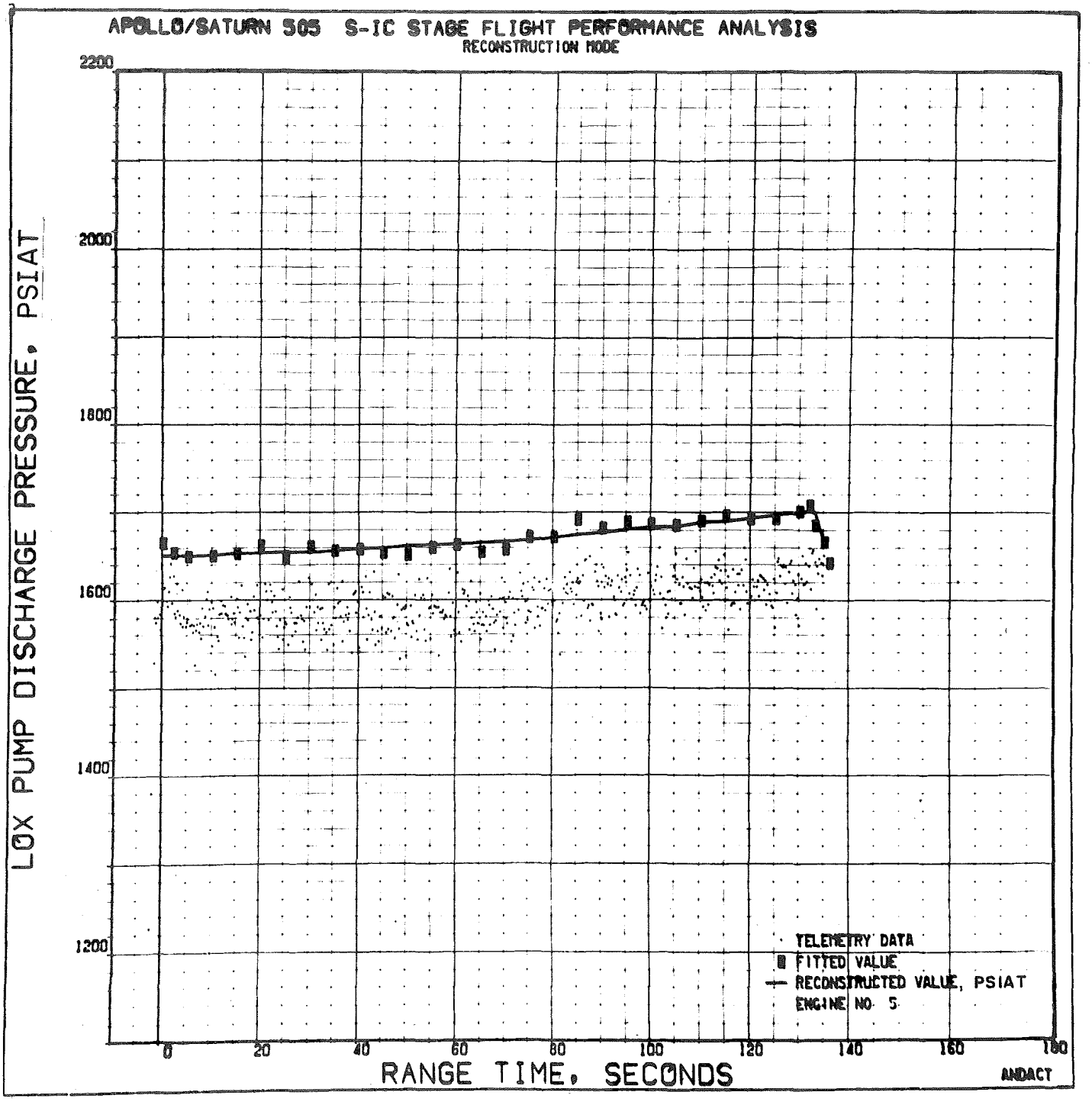

Figure 58. LOX Pump Discharge Pressure, Engine Position 5, F2034

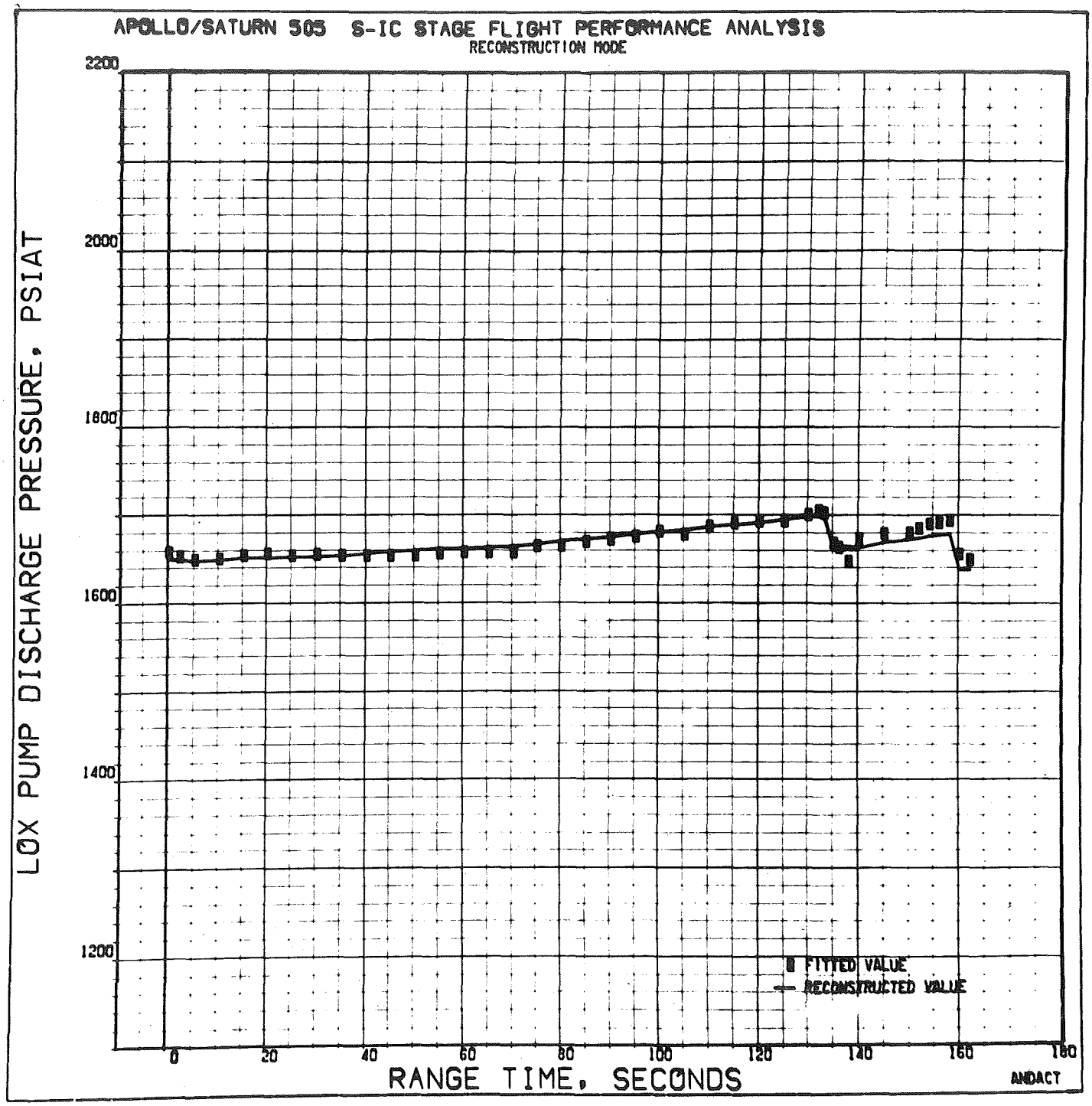

Figure 59. Average LOX Pump Discharge Total Pressure

TRAJECTORY RECONSTRUCTION ANALYSIS

An alternate method used to determine average engine performance considers the vehicle trajectory profile and averaged telemetered inlet condition histories. Engine performance is simulated by a nonlinear engine model representing the average F-1 engine installed in the S-IC-5 stage. The performance of this average engine is constrained to reproduce the vehicle profile.

Average F-1 engine mainstage operating characteristics are reconstructed using measured fuel and LOX pump inlet pressures, LOX temperature, a constant fuel temperature and density of 76.2 F and 49.93 lb/cu ft, respectively, a linearized esitmate of turbine nozzle area variation, vehicle acceleration, and ambient pressure as previously presented in Fig. 30 through 59.

Data provided to the model to provide a description of the vehicle are as follows:

1. Stage geometry, tank, and ducting configuration
2. Vehicle payload, structural, and hardware weights
3. Stage LOX tank pressurant flowrates
4. Stage fuel propellant lubricating flowrates
5. Vehicle loaded propellant weights
6. Aerodynamic characteristics (forebody and base drag coefficients)
7. Flight trajectory characteristics (perturbations in engine gimbaling angles were assumed to have a negligible effect on the trajectory)
   a. Observed mass point velocity profile
   b. Radar and guidance vehicle pitch program
   c. Vehicle angle of attack
   d. Vehicle azimuthal track

Stage performance during the flight was determined by numerical integration of the equations of motion using the previously listed vehicle data and the engine performance provided by the power balance model to determine the resulting average engine performance required to match the velocity profile. Turbine efficiency was used as the parameter to alter the engine power level.

Figure 60 presents the average engine thrust deviation from the predicted values of Table 7 required to simulate AS-505 trajectory profile during the S-IC-5 stage steady-state operation. These thrust increments also contain any errors in vehicle drag characteristics as well as any errors in the velocity profile. The latter effect is more prevalent during the first few seconds of flight immediately following liftoff as a result of curve-fitting a slow rate of change in vehicle position. During the 134.6 seconds of steady-state operation, the five-engine average thrust appeared to decrease uniformly being 0.10 percent (1.5 kilopounds) lower than predicted at 35 seconds and 0.66 percent (10 kilopounds) lower than predicted at 134.6 seconds (IECO).

The LOX and fuel residuals at IECO that resulted from the simulation were 472,332 and 167,912 pounds, respectively. The actual residuals as determined from the flight are not currently available, consequently no comparison is presented.

The total drag used in the calculation of AS-505 (and AS-504) was derived in a different manner than prior S-IC flights. For the S-IC stages of vehicles AS-501, AS-502, and AS-503, the total axial force coefficient composed of forebody and base drag coefficients as a function of Mach number was used. As a result of aerodynamic analysis by MSFC, base drag is now best defined by a relationship with altitude, rather than by Mach number.

Thus, the drag characteristics for AS-505 and subsequent vehicles are represented by forebody drag (Fig. 61) and base drag (Fig. 62), the sum

of these two drag coefficients being the total axial force coefficient. Figure 63, AS-505 total vehicle drag, presents the result of the newly defined total axial force coefficient. Vehicle angle of attack is shown in Fig. 64.

Figures 65 and 66 present the flight simulated reconstruction of thrust chamber injector-end pressure and turbopump speed, respectively. Program simulated chamber pressure had a +0.09 psi bias and turbopump speed a +37.3 rpm bias above their respective acceptance test values.

Figures 67 through 78 present additional significant S-IC-5 stage and vehicle trajectory performance parameters generated by the nonlinear flight simulation program.

Table 9 gives a comparison of simulated and actual trajectory parameters, at 134.60 seconds, inboard engine cutoff time. Because the trajectory solution requires a path-oriented analysis, a satisfactory end-point correlation indicates the acceptability of the performance analysis throughout the entire flight simulation.

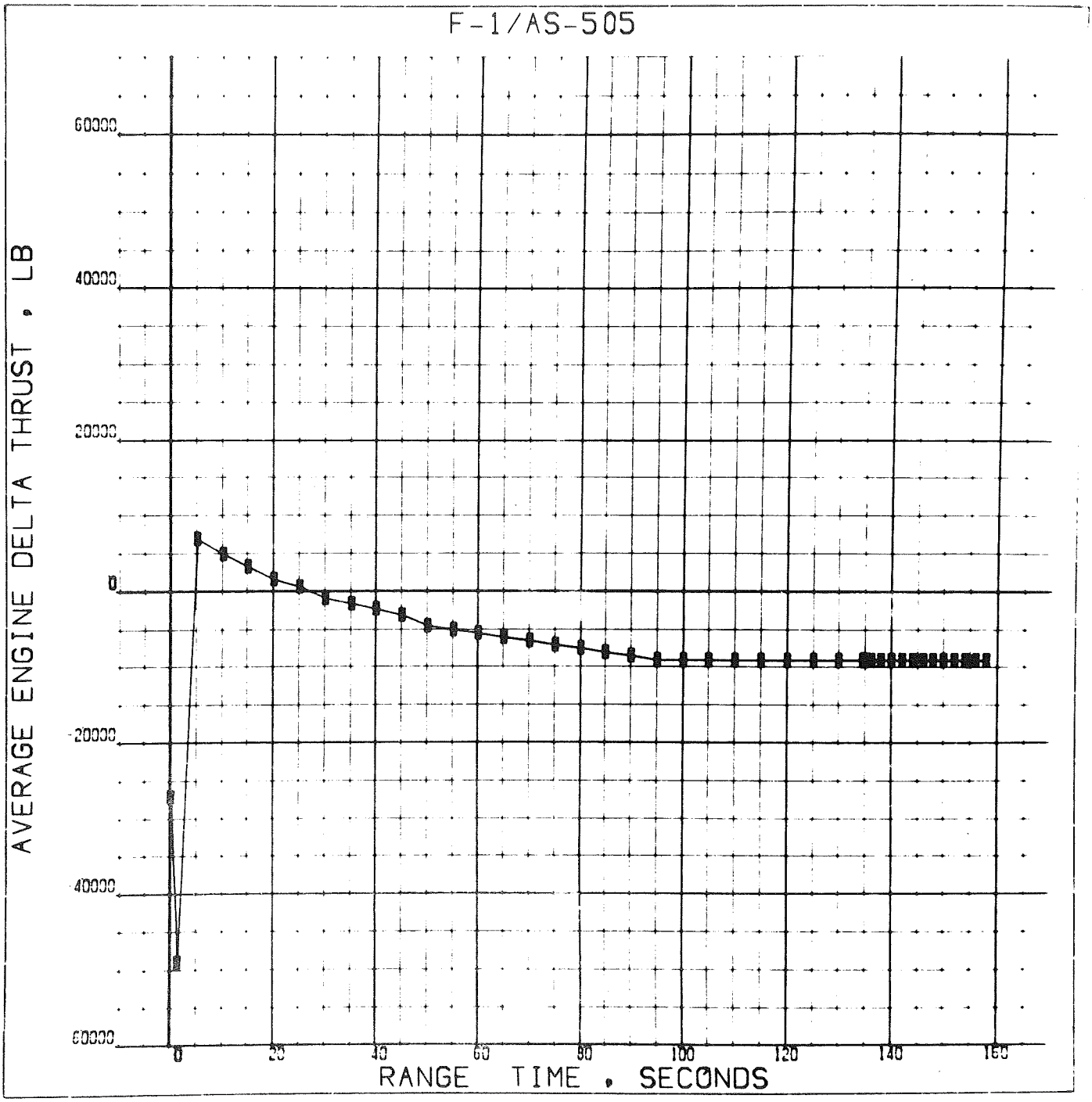

Figure 60. S-IC Stage Average Engine Thrust Deviation From Predicted to Match Trajectory Profile

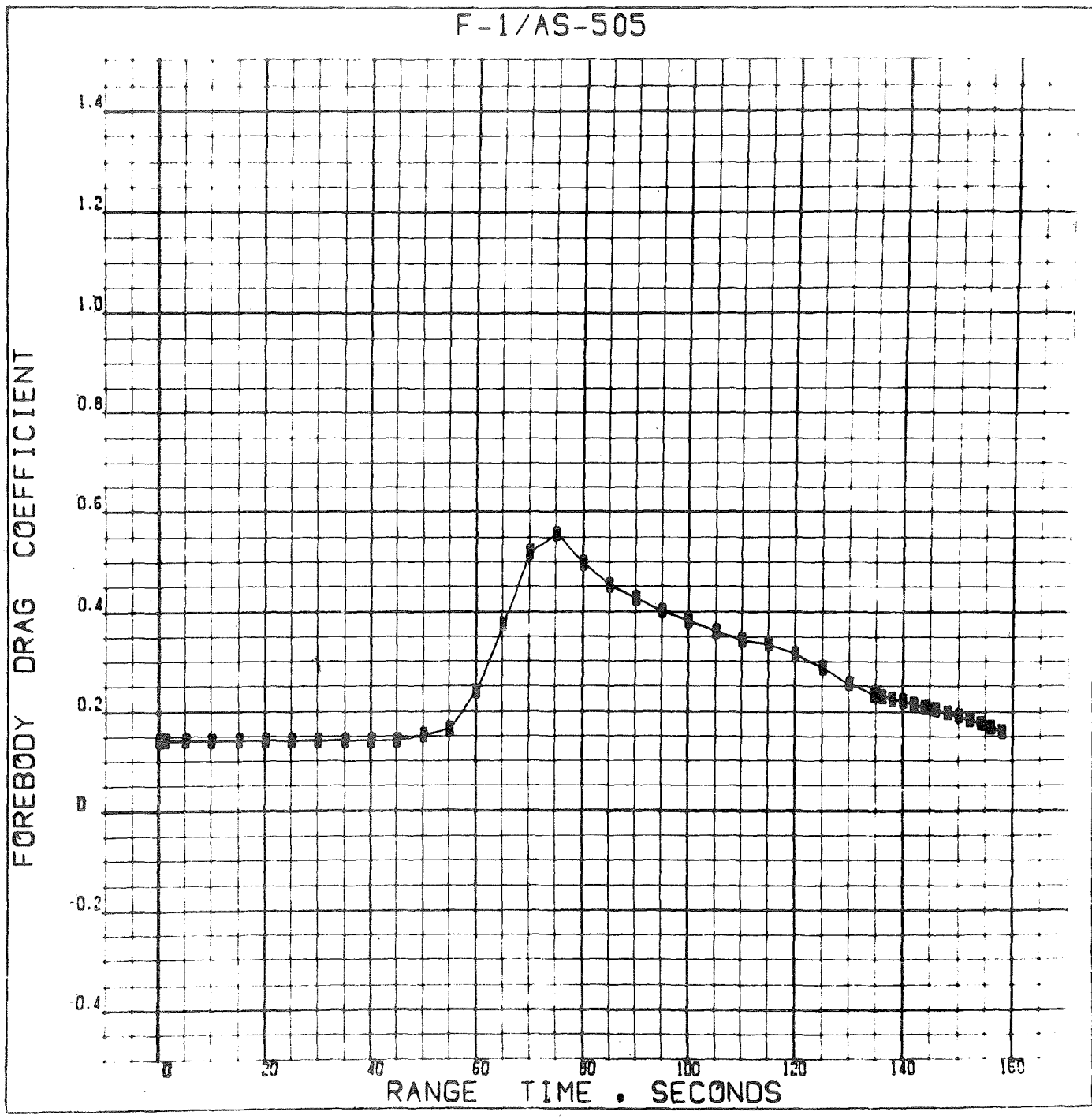

Figure 61. Vehicle Forebody Drag Coefficient

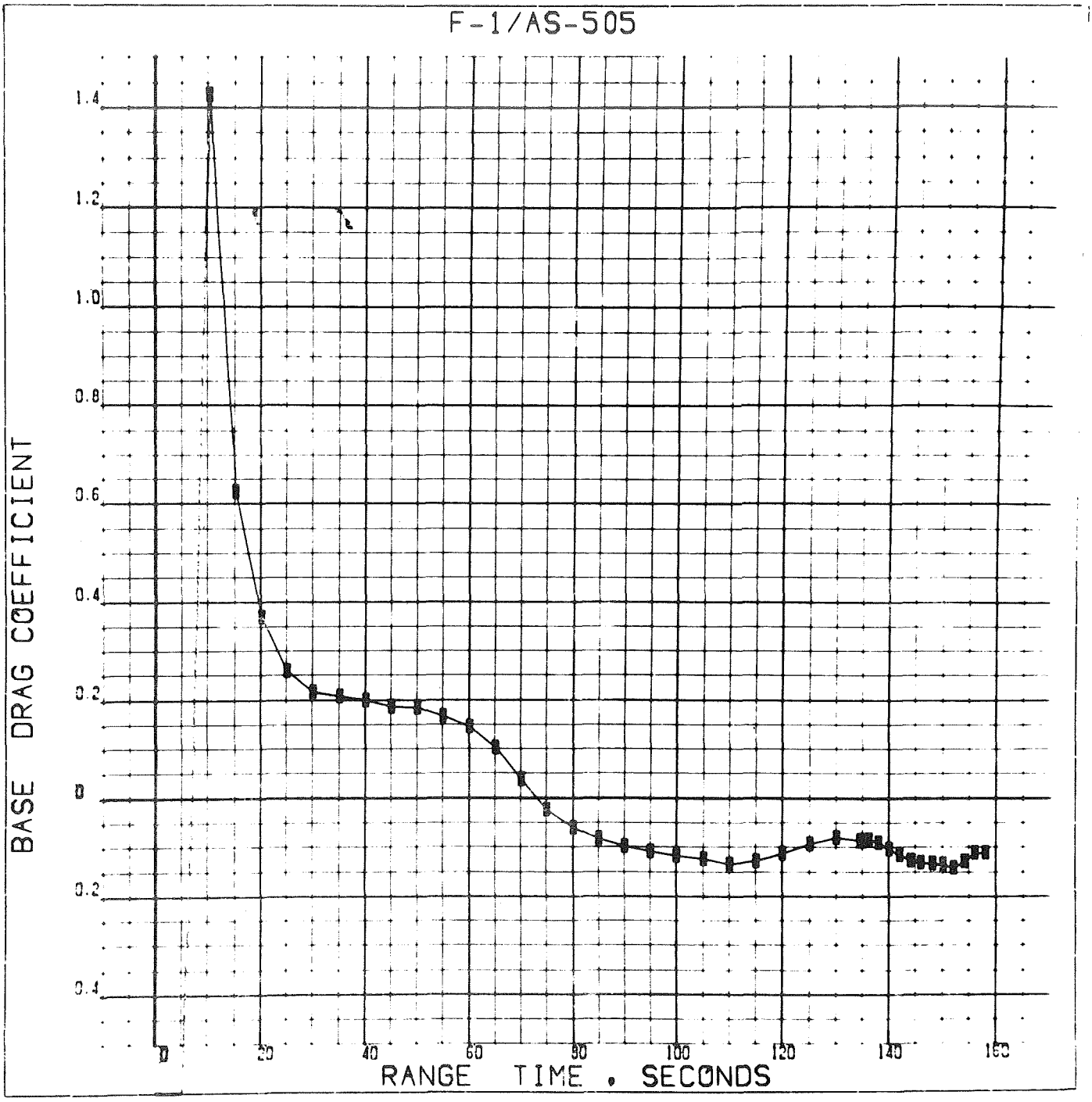

Figure 62. Vehicle Base Drag Coefficient

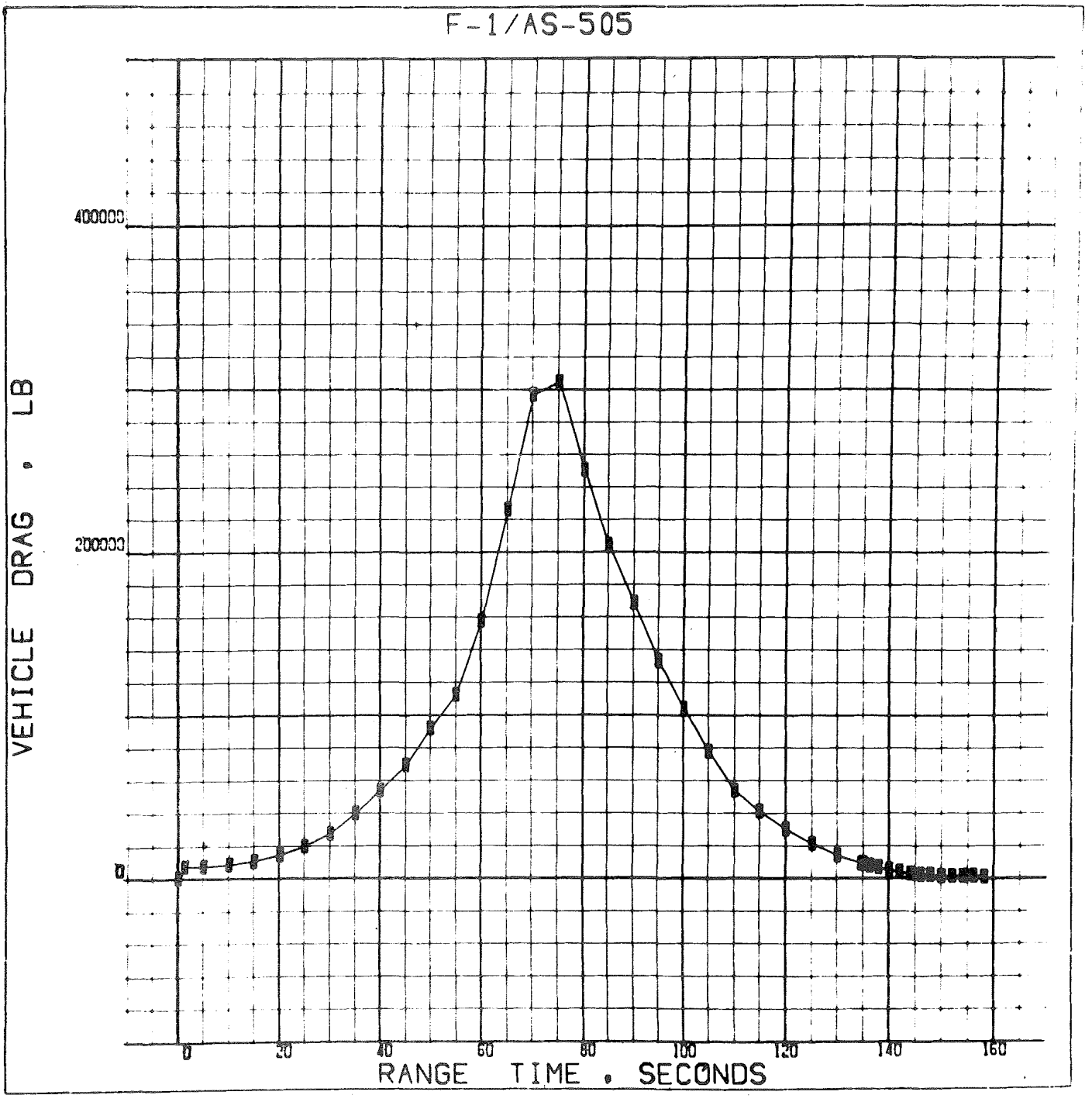

Figure 63. Vehicle Drag

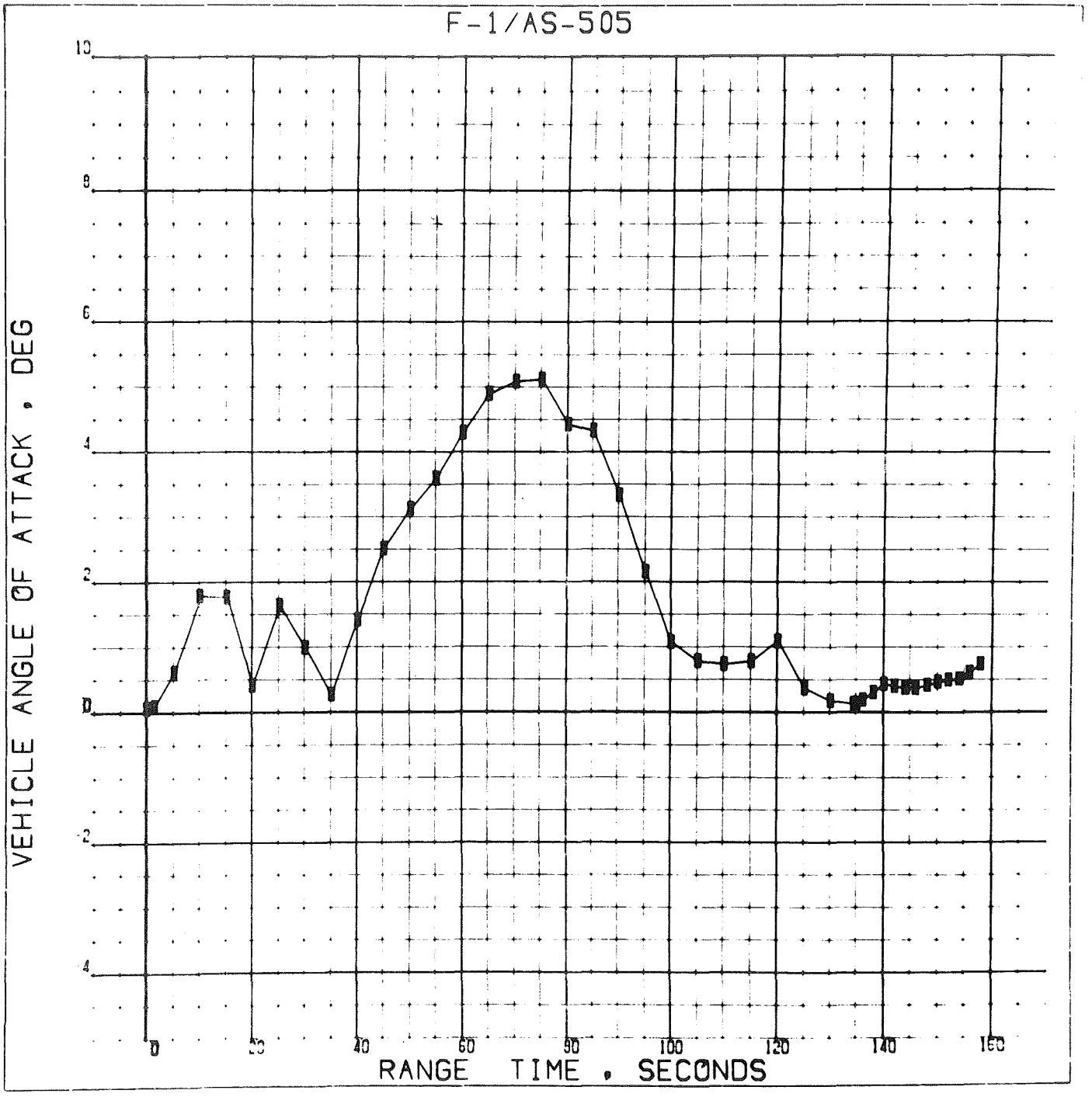

Figure 64. Vehicle Angle of Attack

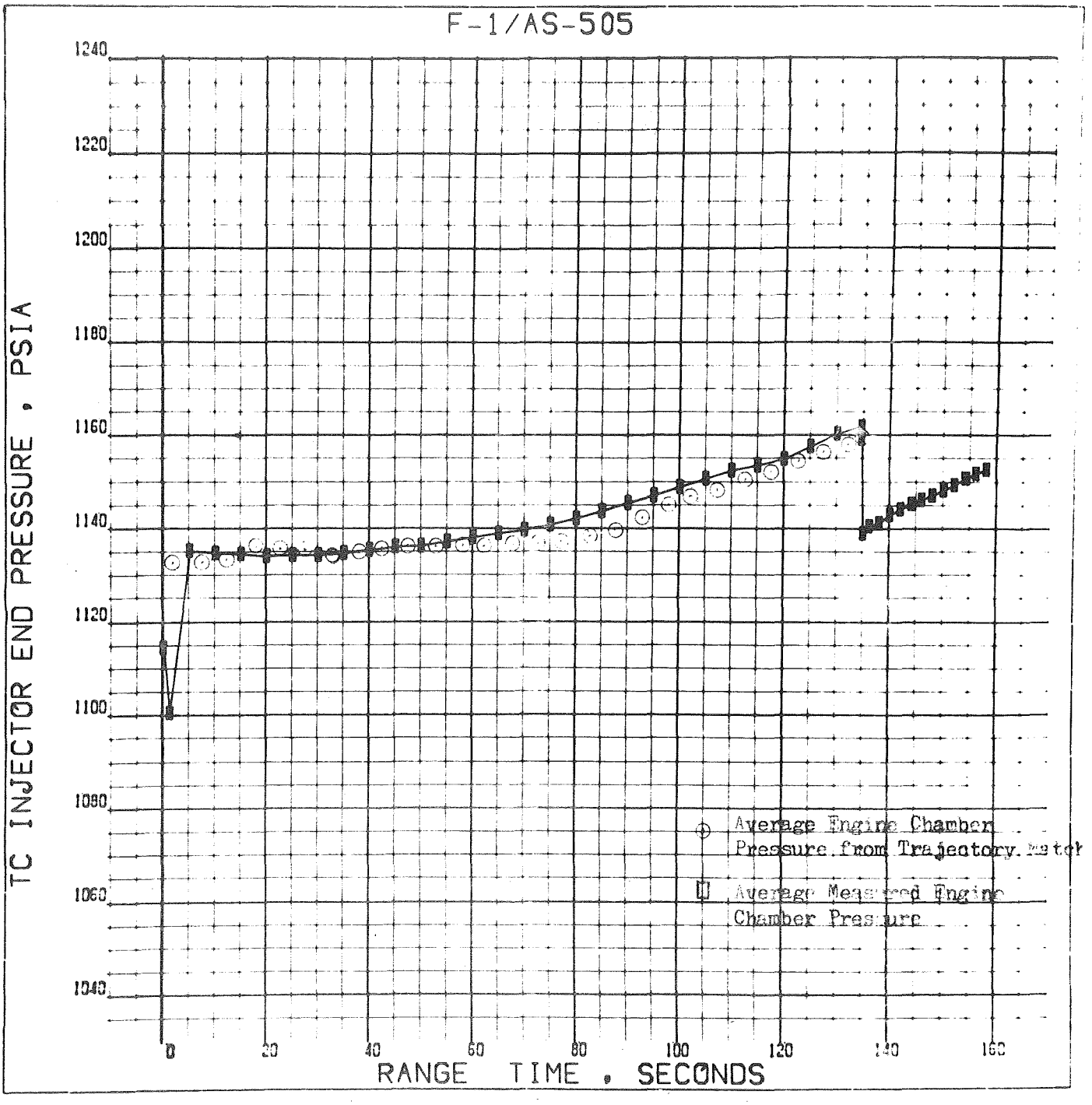

Figure 65. Average Engine Thrust Chamber Injector End Pressure

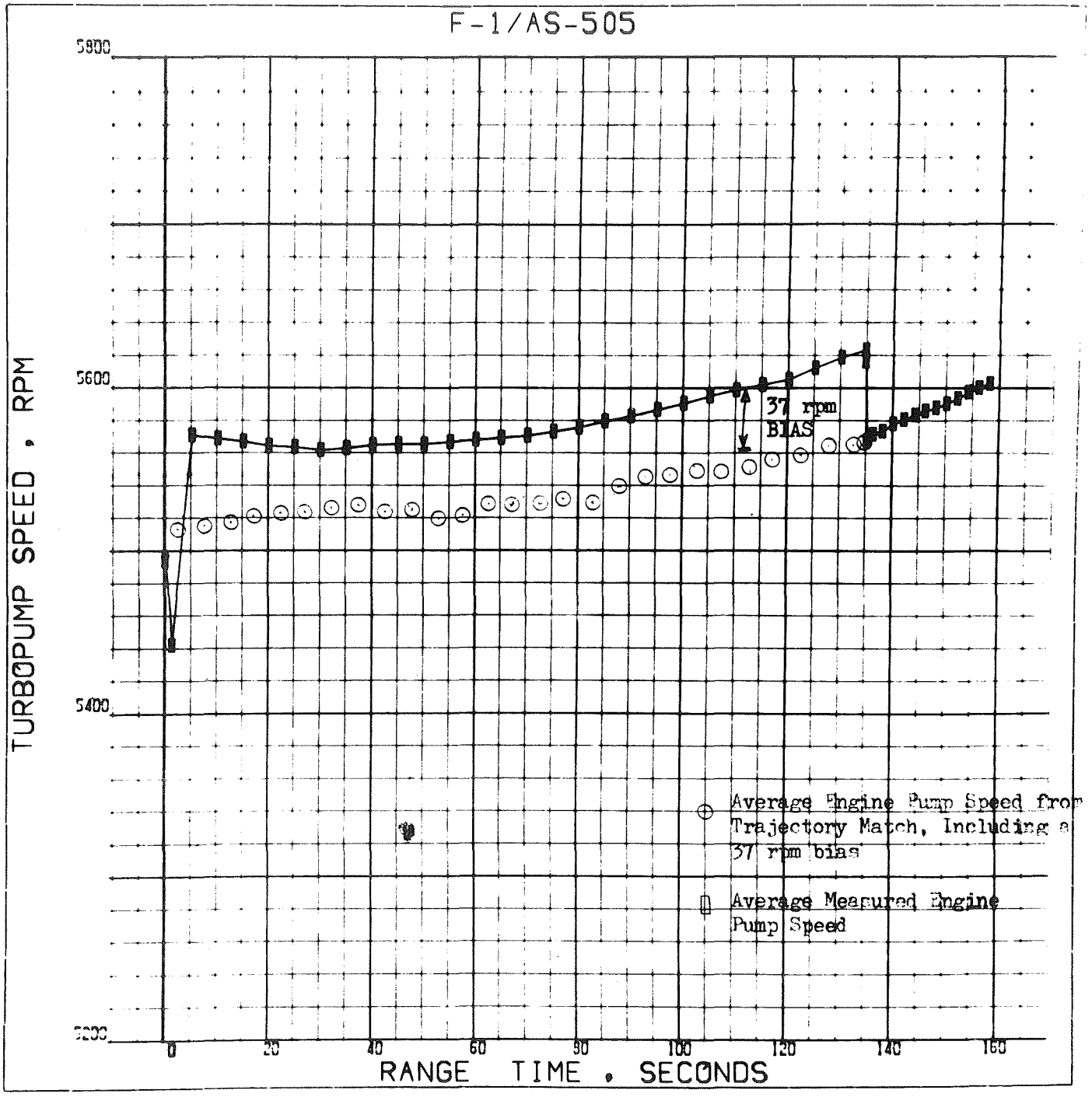

Figure 66. Average Engine Turbopump Speed

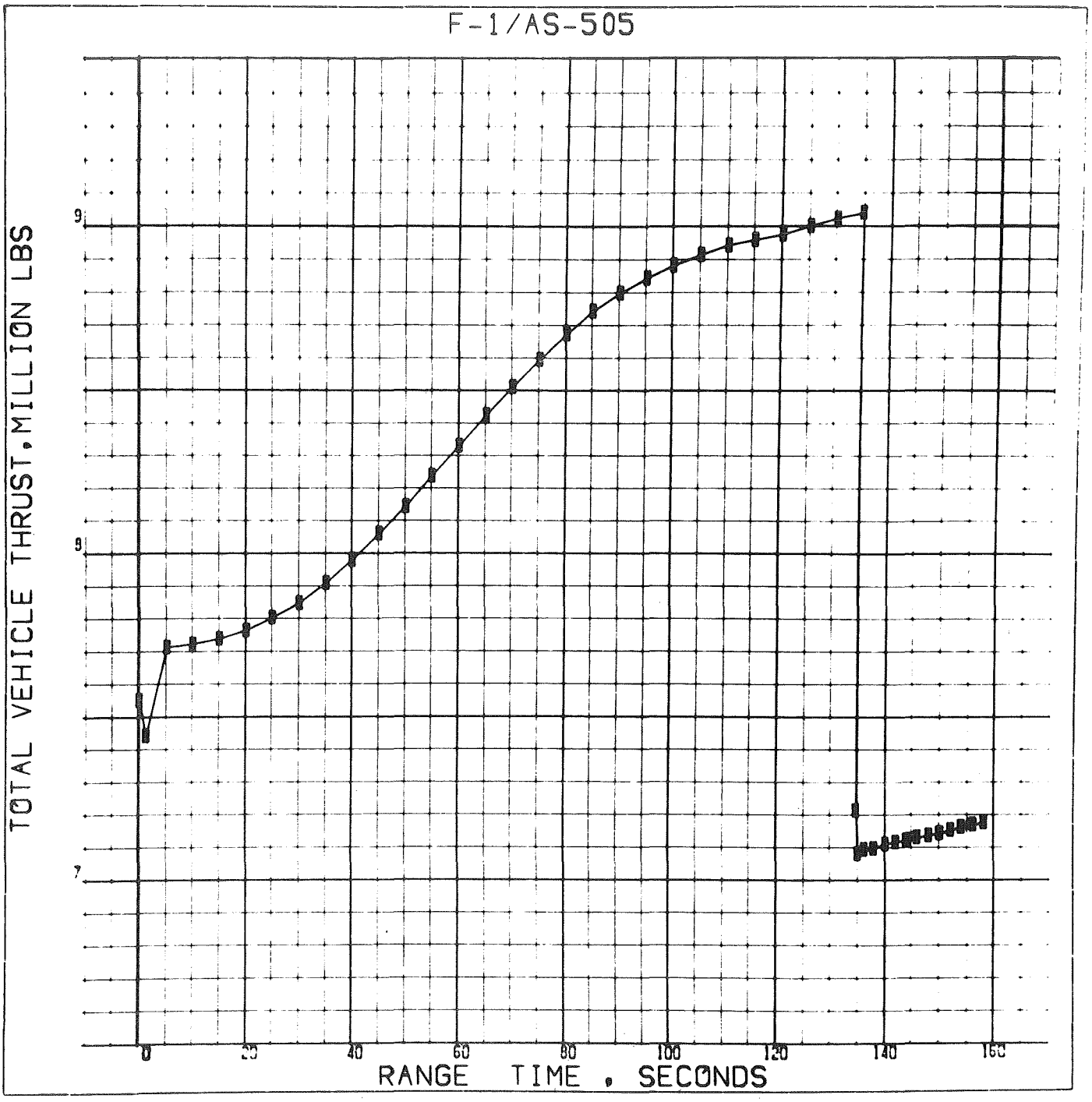

Figure 67. S-IC-5 Vehicle Total Thrust

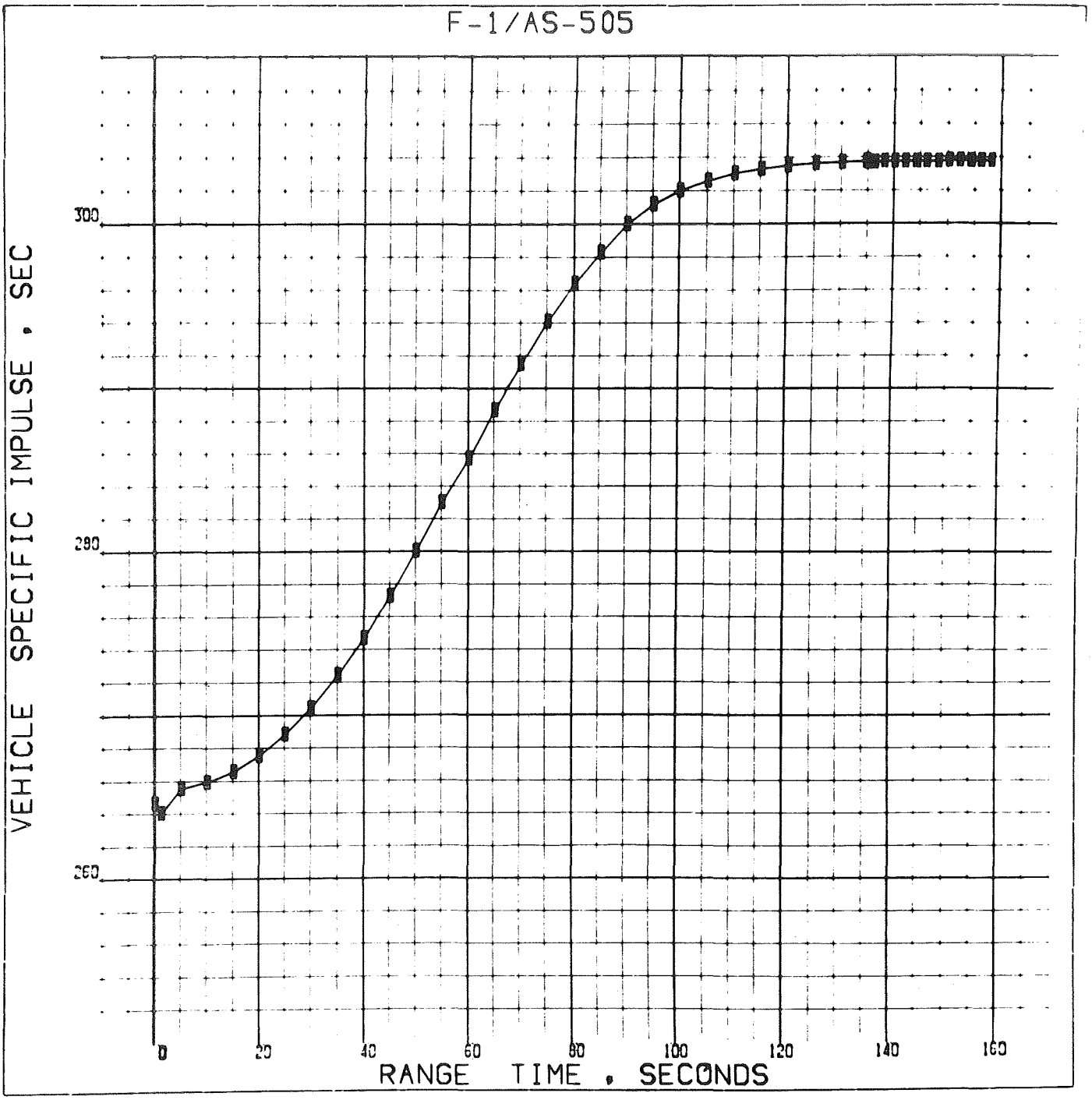

Figure 68. S-IC-5 Vehicle Average Specific Impulse

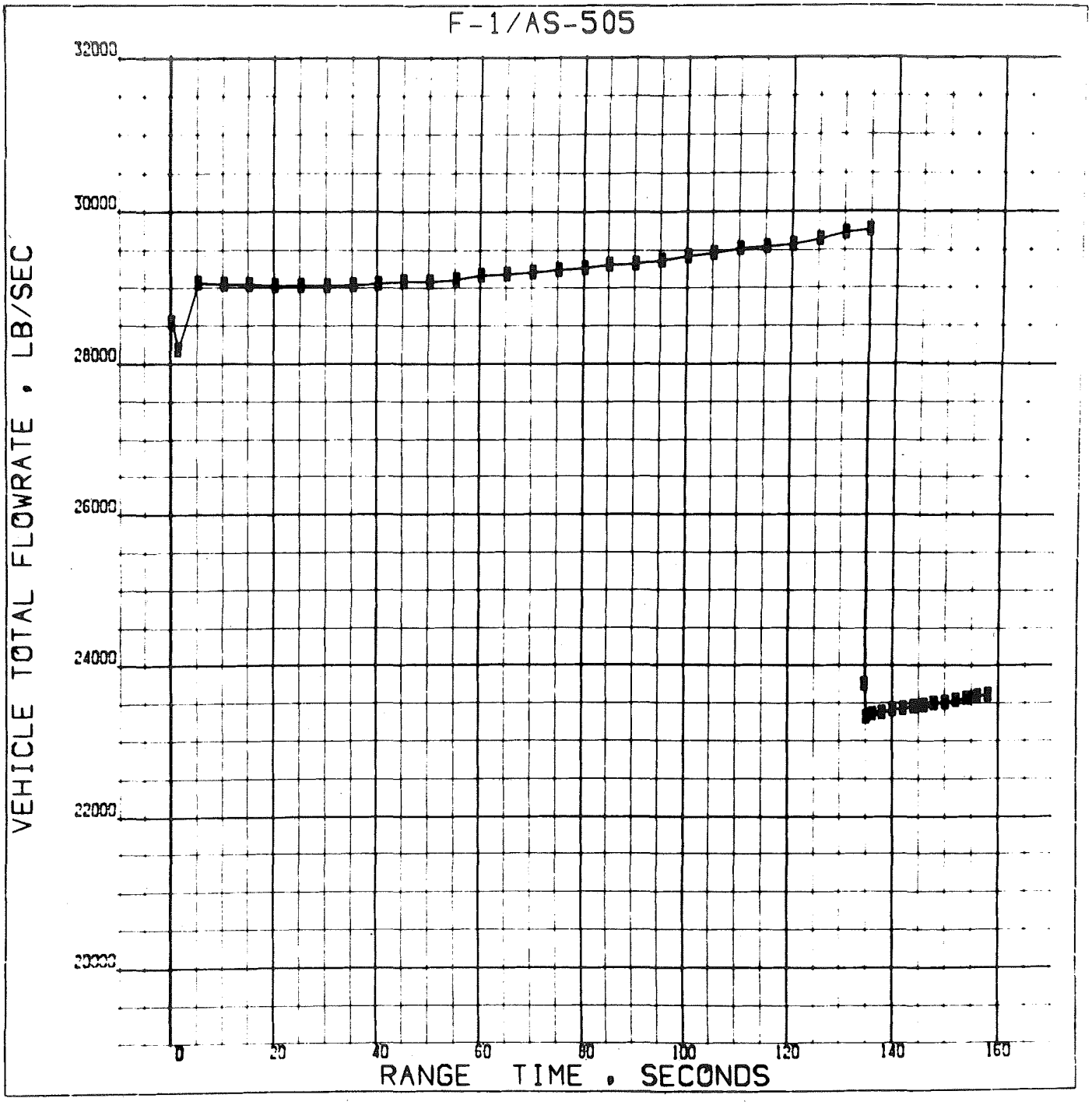

Figure 69. S-IC-5 Vehicle Total Propellant Flowrate

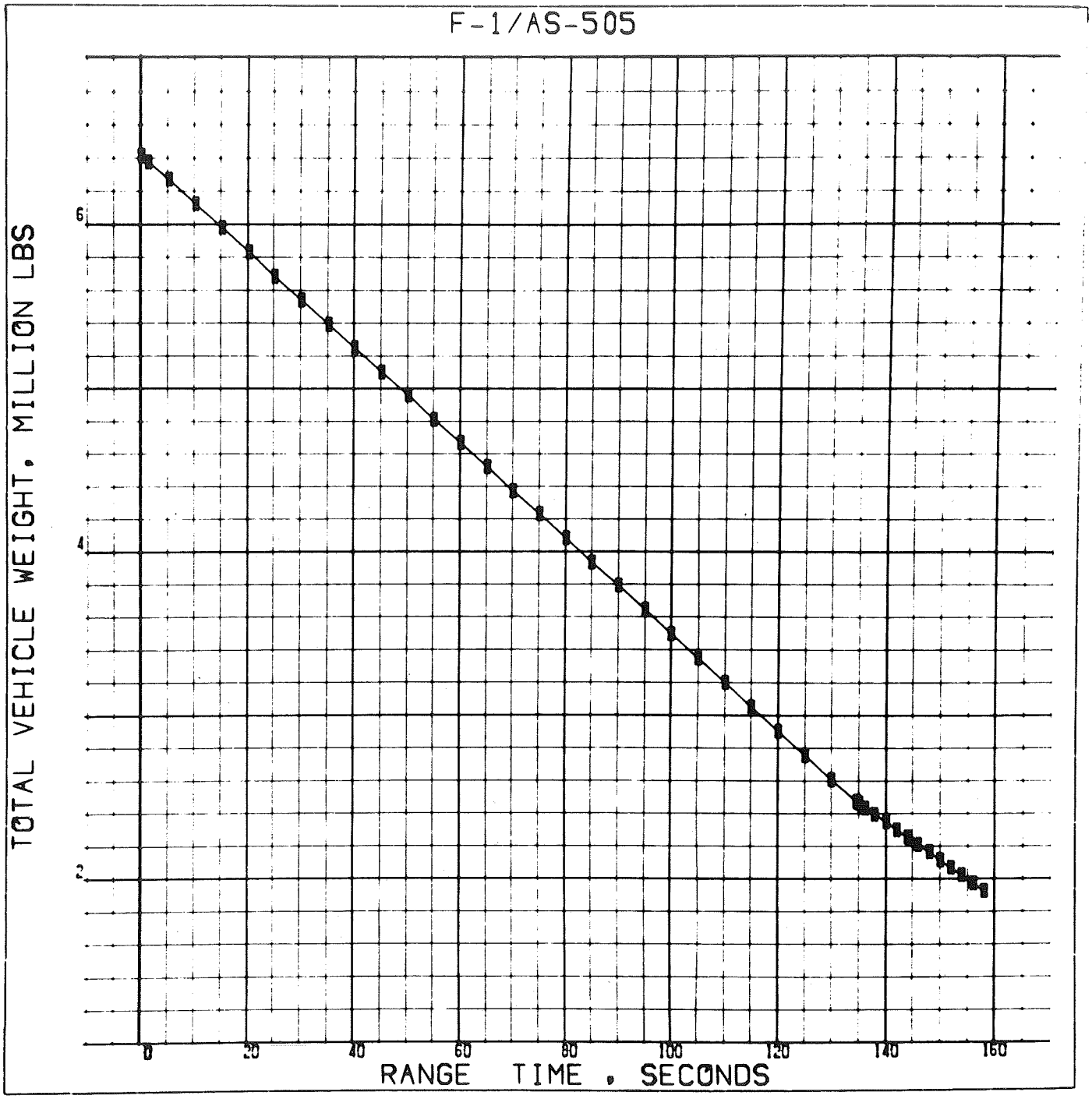

Figure 70. AS-505 Total Vehicle Weight

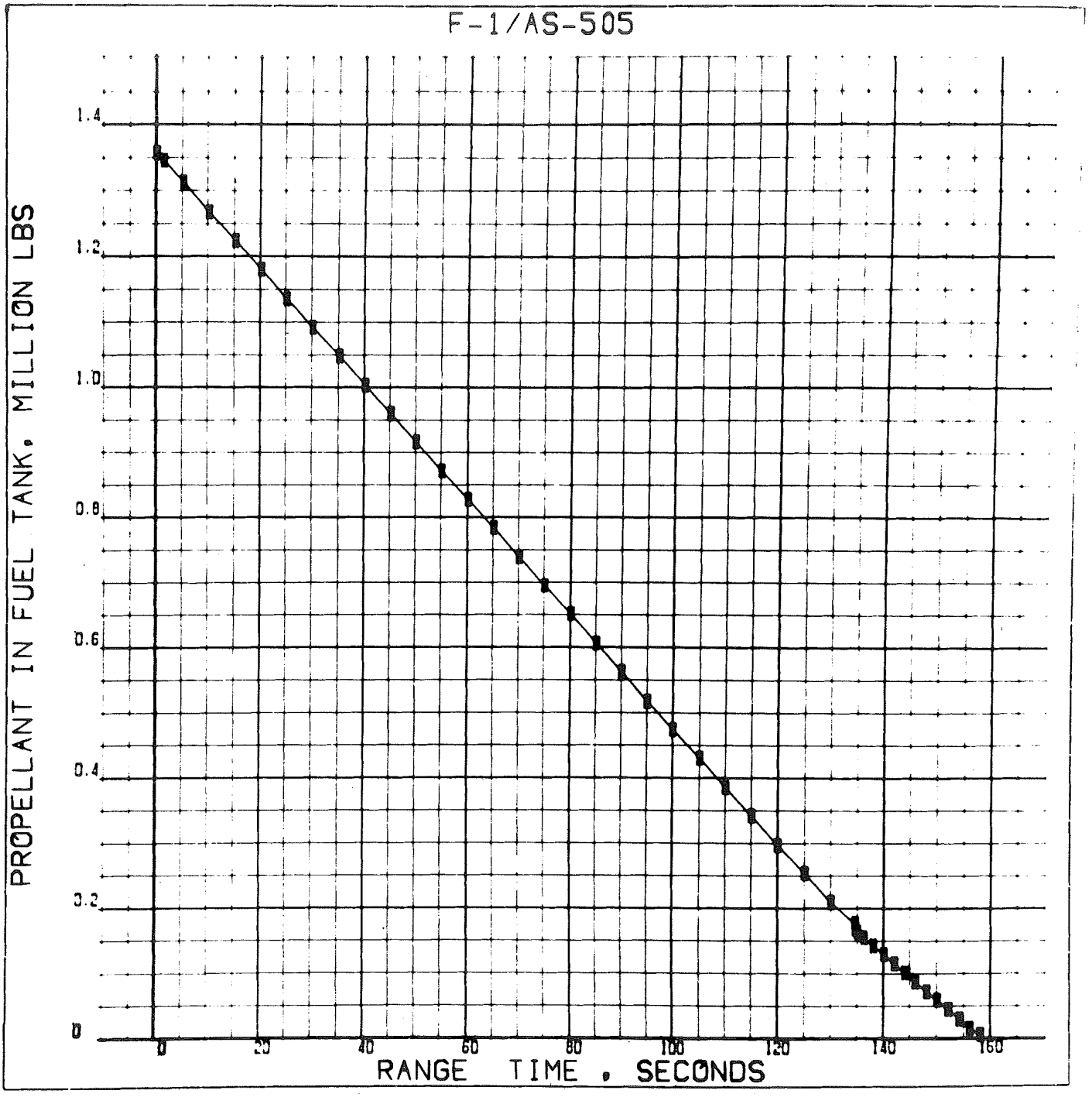

Figure 71. S-IC-5 Stage Fuel Weight

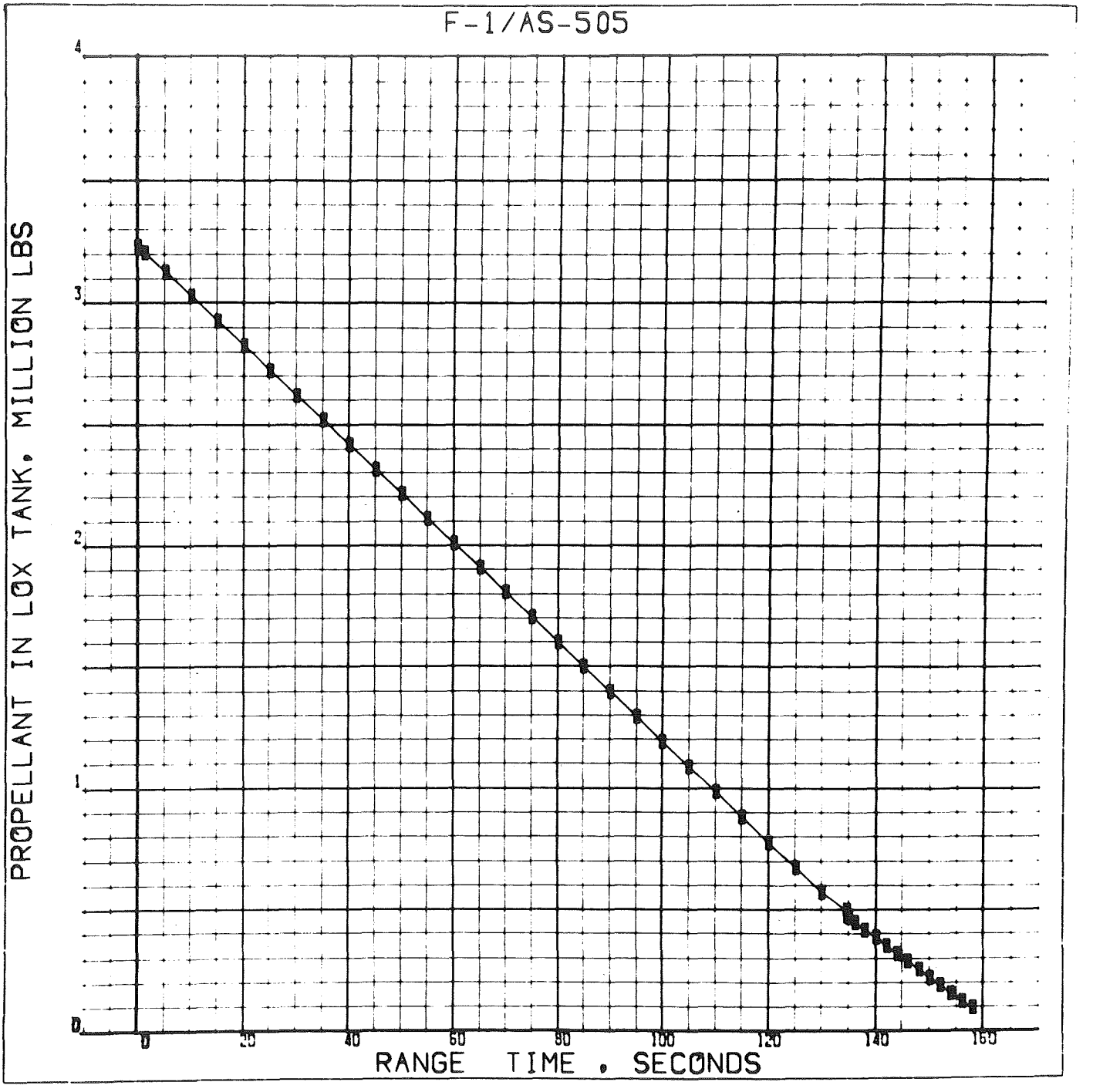

Figure 72. S-IC-5 Stage LOX Weight

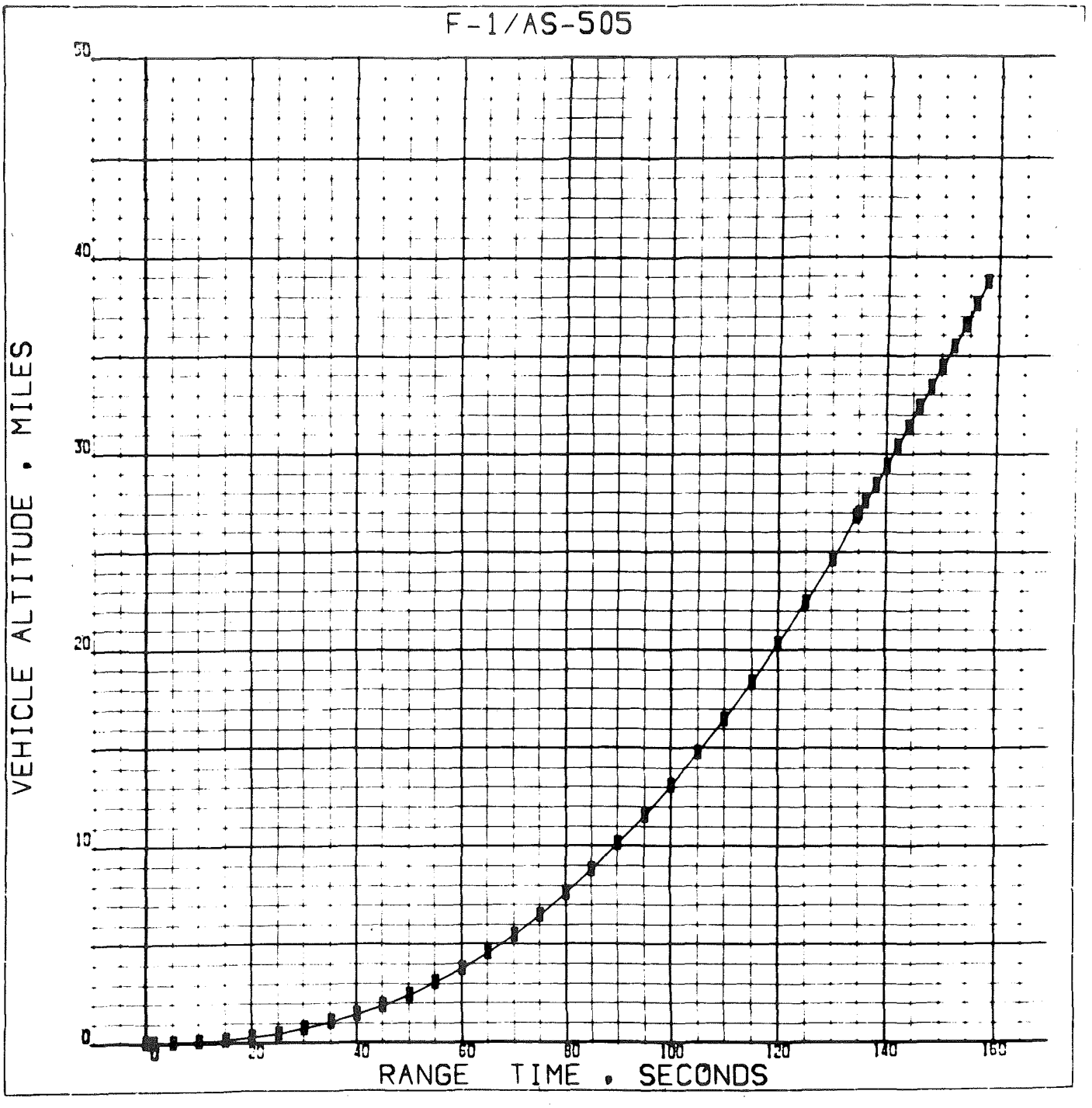

Figure 73. S-IC-5 Vehicle Altitude

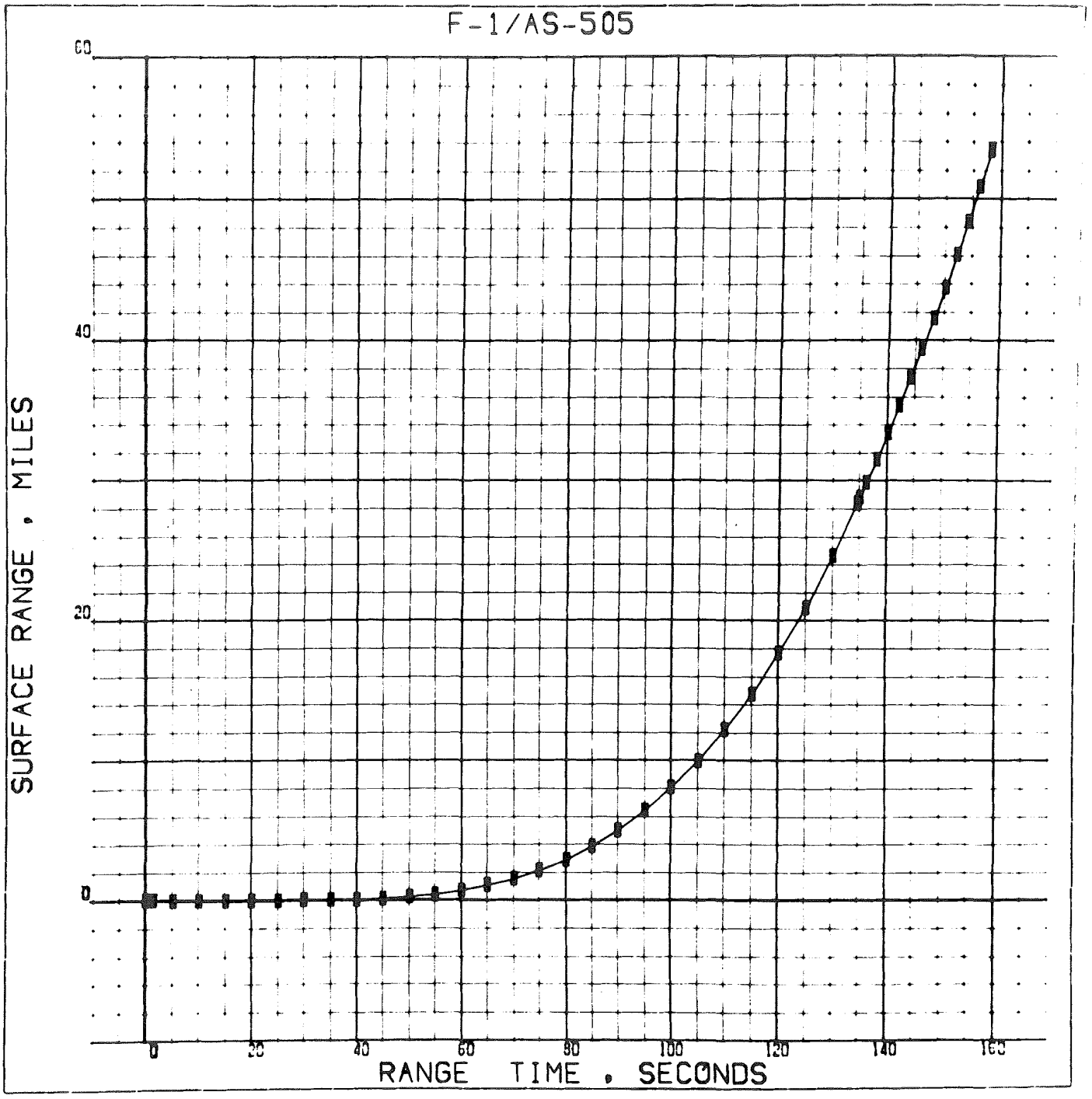

Figure 74. S-IC-5 Stage Surface Range

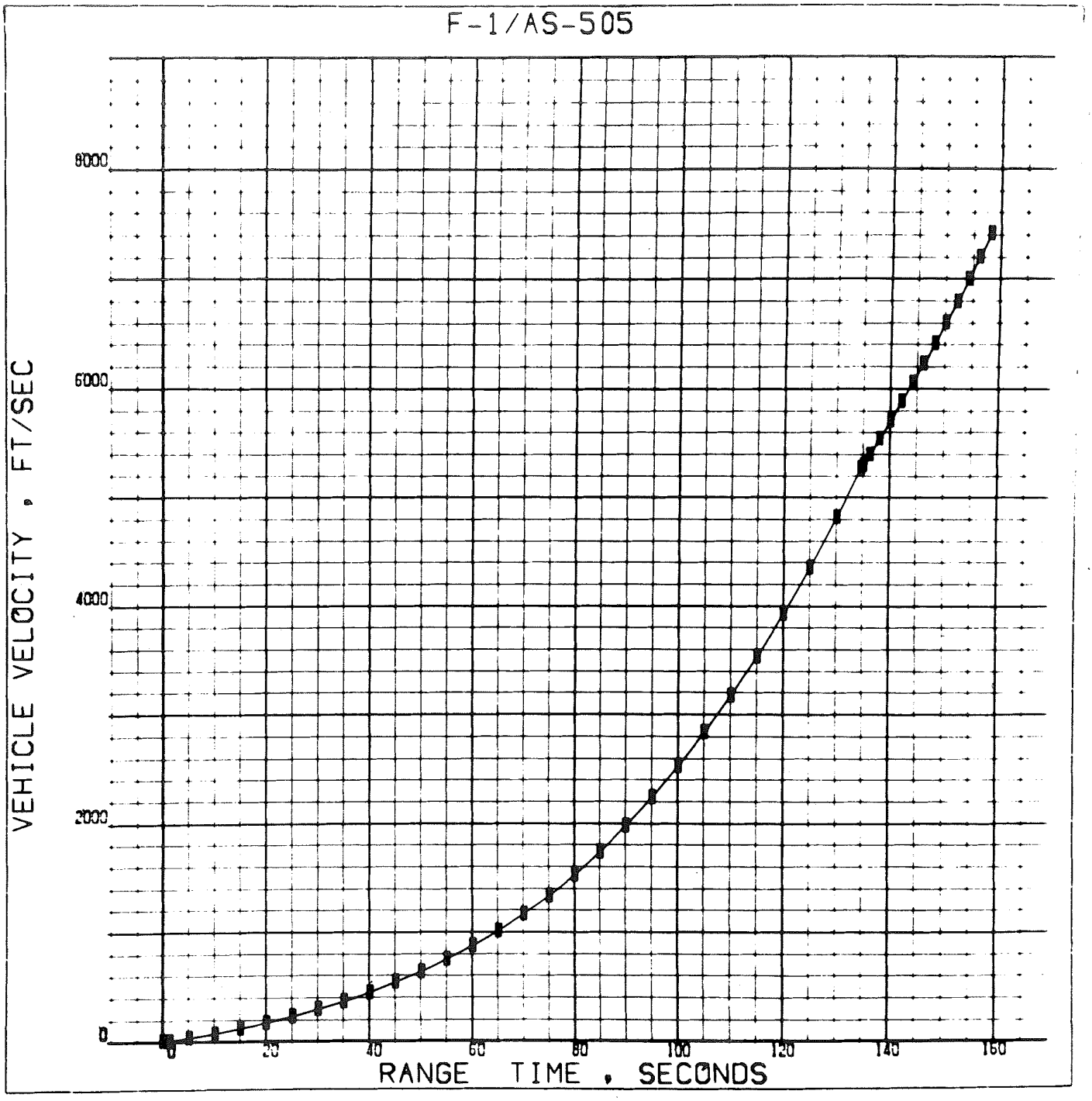

Figure 75. S-IC-5 Stage Velocity

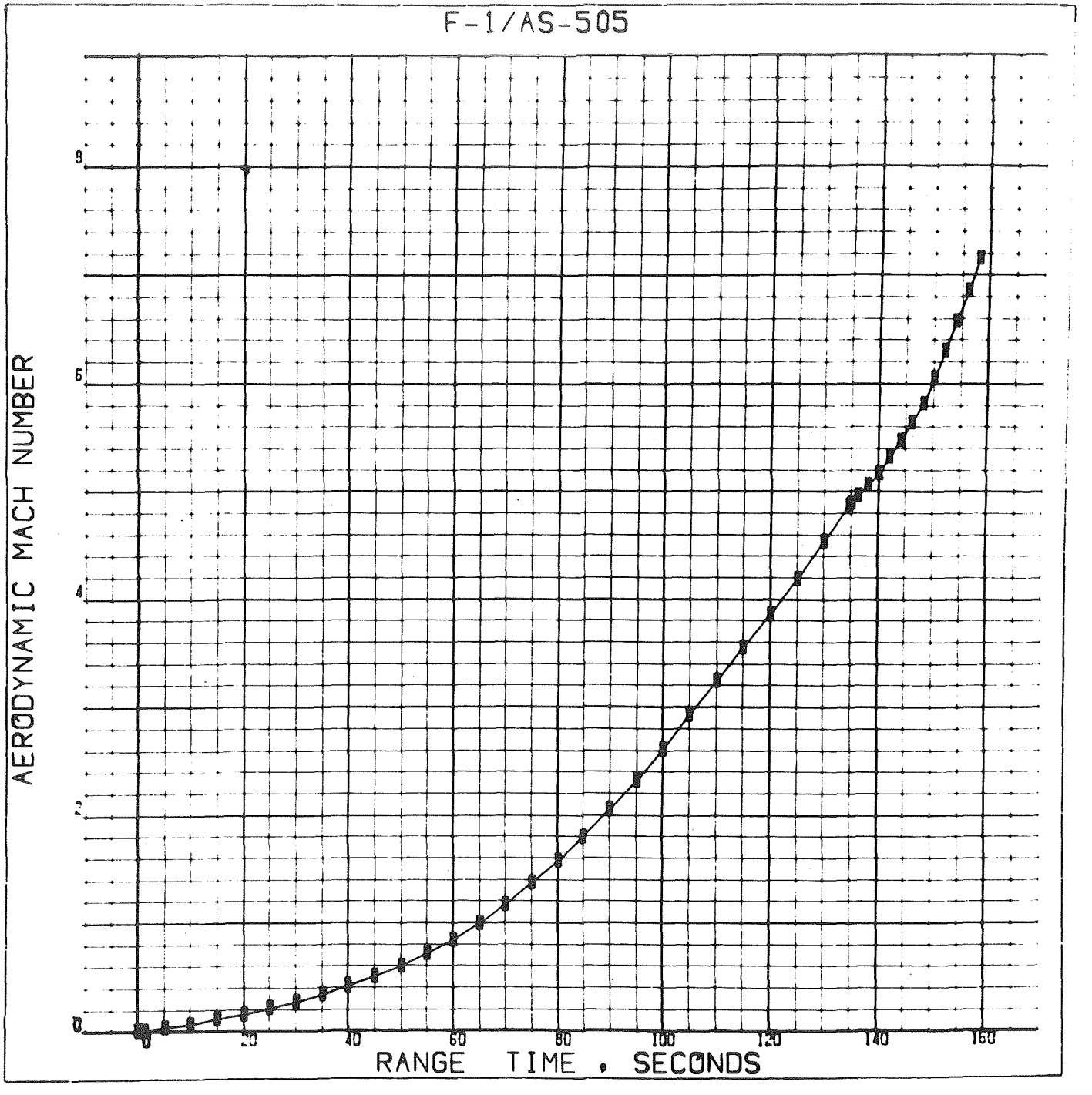

Figure 76. S-IC-5 Stage Aerodynamic Mach Number

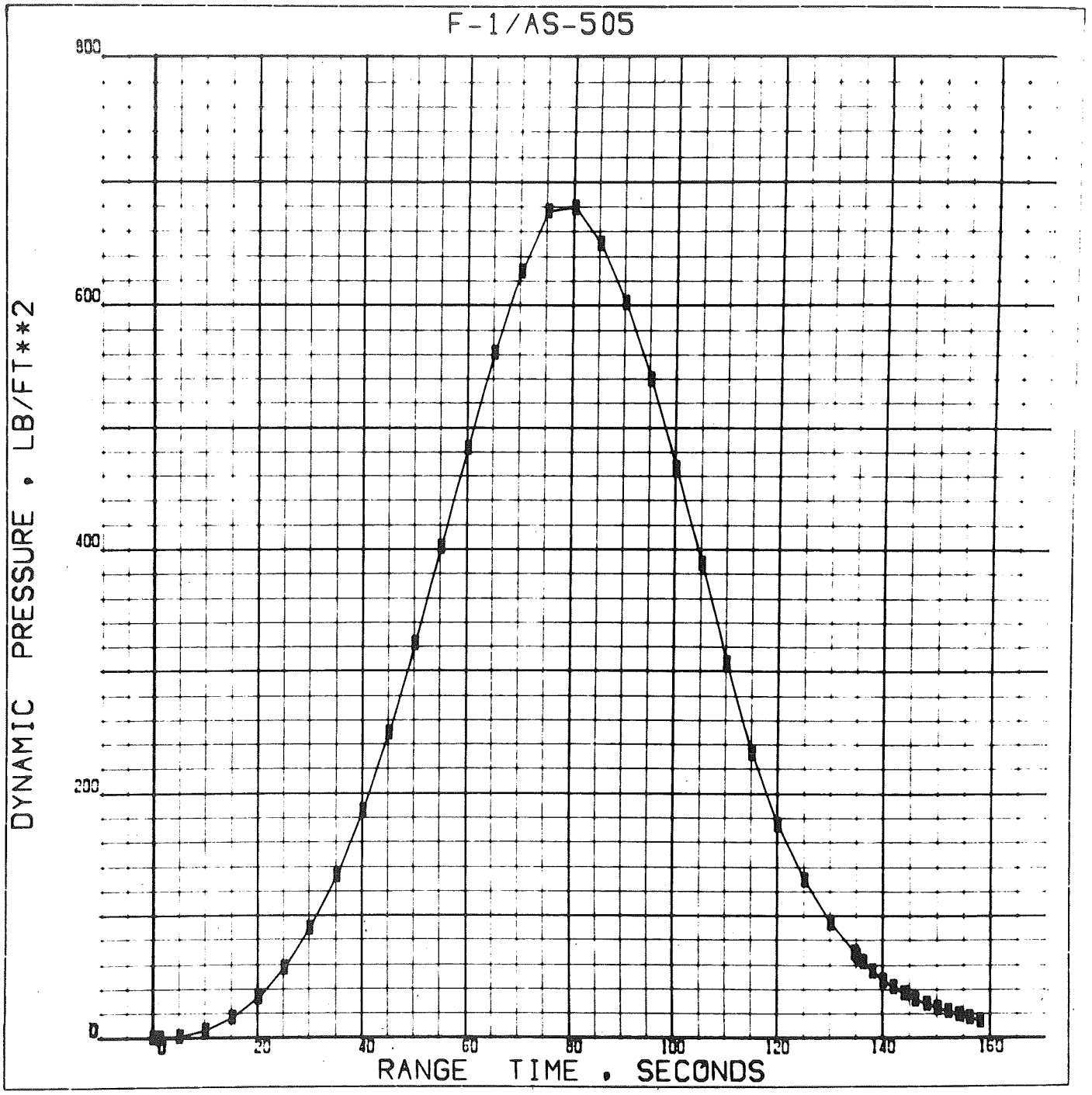

Figure 77. S-IC-5 Stage Dynamic Pressure

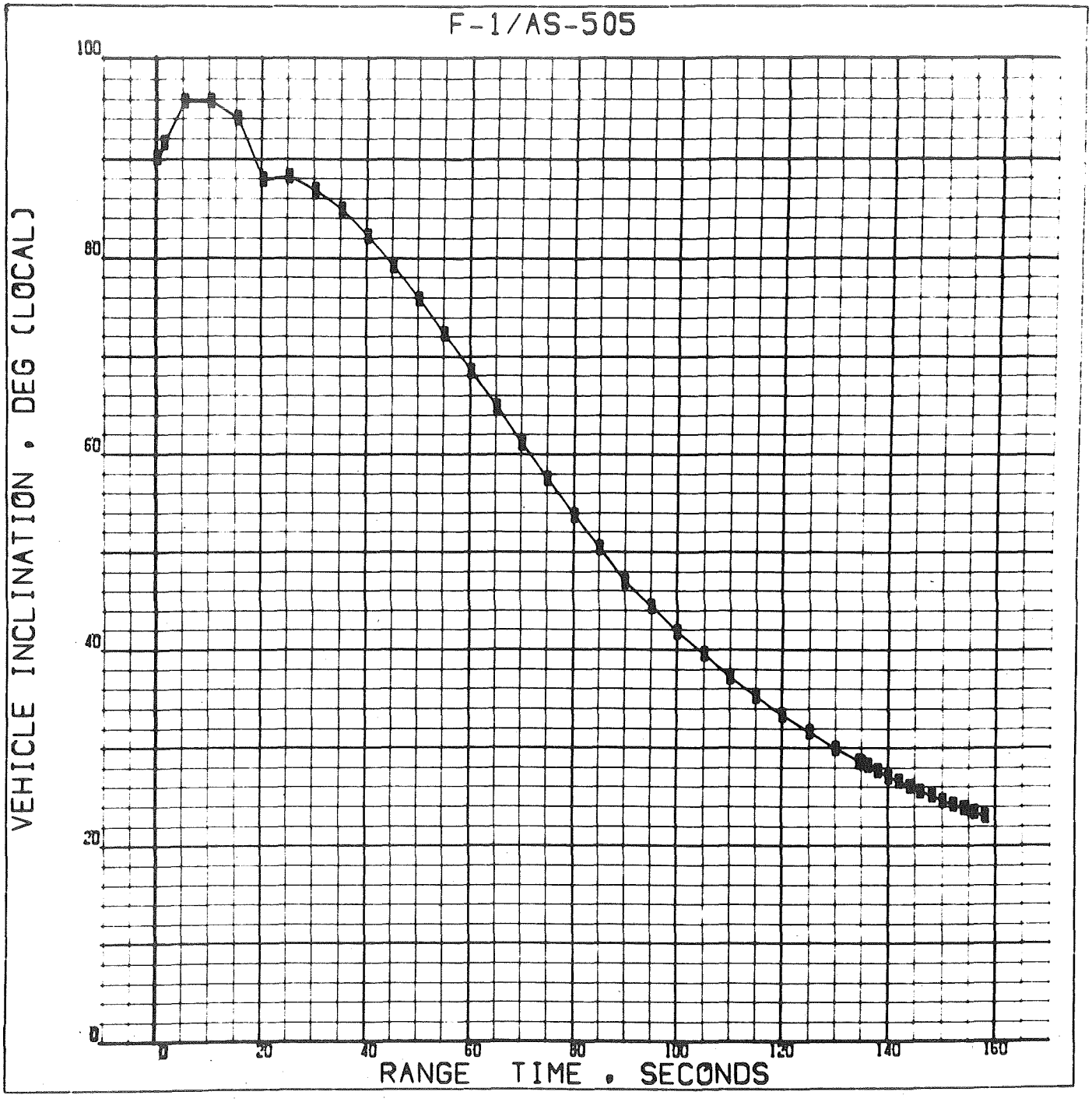

Figure 78. S-IC-5 Vehicle Inclination Referenced to Earth Horizontal Plane

TABLE 9

COMPARISON OF SIMULATED AND ACTUAL TRAJECTORY PARAMETERS
AT INBOARD ENGINE CUTOFF, 134.601 SECONDS

Parameter	Nonlinear Flight Simulation Program	Actual NASA Mass Point Trajectory
Altitude, feet	140,762	142,363
Earth Fixed Velocity, ft/sec	5245.0	5244.1
Acceleration, ft/sec^2	101.09	101.80
Inclination, degrees	28.501	28.311
Azimuth, degrees	72.268	72.173
Longitude, degrees	80.155	80.169
Latitude, degrees	28.733	28.753
Range, feet	149,505	151,956
Mach Number	4.857	4.945

ENGINE DYNAMIC DATA ANALYSIS

The analysis of engine and propellant feed system pressure oscillations and engine gimbal block vibrations was oriented toward the low-frequency range (0 to 50 Hz) because of consideration of the effect on vehicle structural frequencies. Primary vehicle structural concern is the first longitudinal vehicle mode, which, in the latter part of flight, is approximately 5 Hz.

These dynamic analyses resulted in the conclusion that POGO, or the coupling of the vehicle, propellant feed system, and engine systems did not occur.

The current analysis was obtained essentially from processed analog tape data. Brush recorded filter bandwidths of 0 to 8, 8 to 25, and 25 to 50 Hz were utilized to reveal details of the low-frequency oscillations. The parameters analyzed include the five thrust chamber pressures, LOX suction line pressures of engines 1 and 5, the No. 1 fuel pump inlet pressures of engines 1 and 5, the gimbal block accelerometers of engines 1 and 5, and the LOX pump inlet pressure of engine 1.

Power spectral density (PSD) records were processed for all parameters on analog tape in the time intervals -17 to -7, 27 to 37, 124 to 134, and 138 to 148 seconds. The time is referenced to liftoff. These plots were used to observe amplitudes at specific frequencies and to further identify the noise content in the data. Prelaunch master tape noise as well as data processing facility noise were identified with the PSD's.

CRT plots (100 SPS) in the interval of mainstage engine operation were generated for all parameters not recorded on analog tape. No dynamics anomalies were noted in these parameters, which included the following listed below.

D0004-101 through -105	Fuel Pump Inlet No. 1 Pressure, Engines 1 and 5
D0150-115	LOX Pump Inlet Pressure, Engine 1
D0151-115	LOX Pump Inlet Pressure, Engine 5
D0171-117	Fuel Tank Lower Bulkhead Pressure
D0179-115	LOX Prevalve Pressures, Engine 1
D0180-119	LOX Tank Lower Bulkhead Pressure
E0090-115	LOX PVC Support Longitudinal Vibration, Engine 1
E0091-115	LOX PVC Support Longitudinal Vibration, Engine 5

The quality of the data was good. Two transducers (measuring the LOX pump inlet pressure, engine 1, and the gimbal block accelerometer on engine 5) malfunctioned during the flight. The pressure parameter was lost at 101 seconds after liftoff. The gimbal block accelerometer on engine 5 did not function properly shortly after inboard engine shutdown.

DETAILS OF LOW-FREQUENCY OSCILLATIONS

Oscillations in the 0 to 8 Hz Range

Main chamber pressure oscillations remained random and close to the noise level, approximately 5 psi peak-to-peak, throughout most of the flight (Fig. 79).

In the intervals of approximately 116 to 128 seconds after liftoff and beginning at approximately 154 seconds after liftoff and until outboard engine cutoff, the amplitude appeared to increase to about 7 to 8 psi peak-to-peak. However, this has been identified as noise on the master tape, because it is also present during the interval after outboard engine cutoff.

Structural mode oscillations were clearly indicated by the gimbal block accelerometers which exhibited 5.5 Hz oscillations initially at 0.3 g peak-to-peak following inboard engine shutdown, decaying to the noise level approximately 12 seconds later. These oscillations are in phase

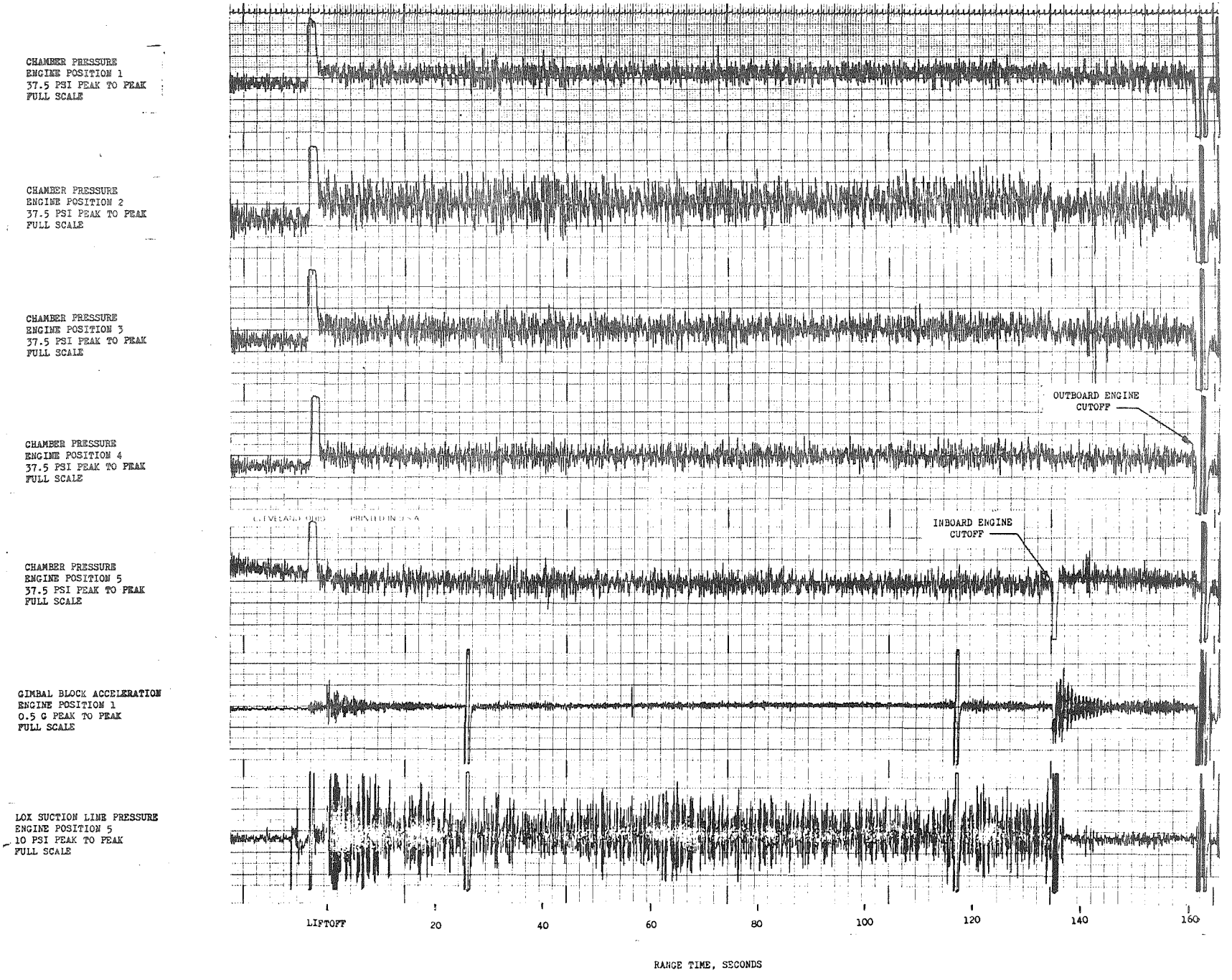

Figure 79. Vehicle AS-505, S-IC Stage, 0 to 8 Hz Low-Pass Filtered Data

with each other but not with the chamber pressures. In a 20-second interval prior to inboard engine shutdown and a 14-second interval prior to outboard engine shutdown, 2 g peak-to-peak oscillations at 5 to 6 Hz and 7 to 8 Hz appeared for the respective intervals. The gimbal block vibrations were again in phase with each other in these intervals but not in phase with thrust chamber or turbopump inlet pressure oscillations. At liftoff, 4.2 Hz gimbal block vibrations (0.125 g peak-to-peak) were excited, decaying to the noise level in approximately 20 seconds. These vibrations were in phase with each other and the fuel pump inlet pressure oscillations, but not with the thrust chamber or LOX suction line pressure oscillations (Fig. 80).

LOX suction line pressures exhibited typical nominal 2 Hz (1 to 2 psi peak-to-peak) and 6 Hz (2 to 8 psi peak-to-peak) oscillations in engines 1 and 5, respectively, throughout their respective operating intervals (Fig. 81).

Fuel pump inlet pressure oscillations were essentially random except when gimbal block vibrations occurred at which time the fuel pressures oscillated in phase and with corresponding amplitudes, not exceeding the maximum at liftoff which was 3 psi peak-to-peak.

The engine 1 LOX pump inlet pressure transducer indicated higher frequency content than the engine 1 LOX suction line pressure transducer. The LOX pump inlet transducer exhibited an intermittent 7 Hz oscillation (5 psi peak-to-peak) while it was functioning.

Oscillations in the 8 to 25 Hz Range

Thrust chamber pressure oscillations in the band of 8 to 25 Hz are random and low in amplitude, 5 to 7 psi peak-to-peak, except for the last 5 seconds of outboard engine operation, when engines 1, 2, and 4 indicate 12 Hz oscillations reaching a maximum of 8 psi peak-to-peak.

Figure 80. Vehicle AS-505, S-IC Stage, 0 to 8 Hz Low-Pass Filtered Data (Gimbal Block Accelerometers in Phase With Fuel Pump Inlet Pressure But Not Related in Phase to Chamber Pressures or LOX Suction Pressure)

The gimbal block accelerometer of engine 5 indicates 17 Hz longitudinal oscillations occurring intermittently until engine 5 shutdown. The maximum average amplitude (0.5 g peak-to-peak) occurs immediately after liftoff. Thereafter, the average amplitude remains more nearly 0.025 g peak-to-peak.

LOX suction line pressure oscillations in this range are generally random (2 to 5 psi peak-to-peak). Consistent 18 Hz oscillations (2 psi peak-to-peak) are seen only briefly for approximately 10 seconds immediately after liftoff.

Fuel pump inlet pressure oscillations are random and low amplitude (2 to 8 psi peak-to-peak), experiencing only one significant burst of 11 Hz oscillations (15 psi peak-to-peak) for a 5-second interval immediately preceding outboard engine shutdown (Fig. 82).

The LOX pump inlet pressure measurement system indicates low amplitude random oscillations (5 to 10 psi peak-to-peak) while it is operative.

Oscillations in the 25 to 50 Hz Range

Thirty Hz oscillations are strongly evident in all thrust chamber pressures. However, this frequency is also significantly present in the prelaunch period, thus indicating a high degree of noise contamination in the data. PSD plots revealed that from 30 to 100 percent of the amplitude at 30 Hz can be attributed to tape noise.

Gimbal block oscillations of engines 1 and 5 are random in this range and decrease linearly from liftoff (0.5 g peak-to-peak) to engine shutdown (0.2 g peak-to-peak).

LOX suction line pressure oscillations observed in the Brush records are highly contaminated by 30 Hz noise. PSD plots verified that this frequency is almost 100-percent noise. No other frequencies are predominant in these parameters in this range.

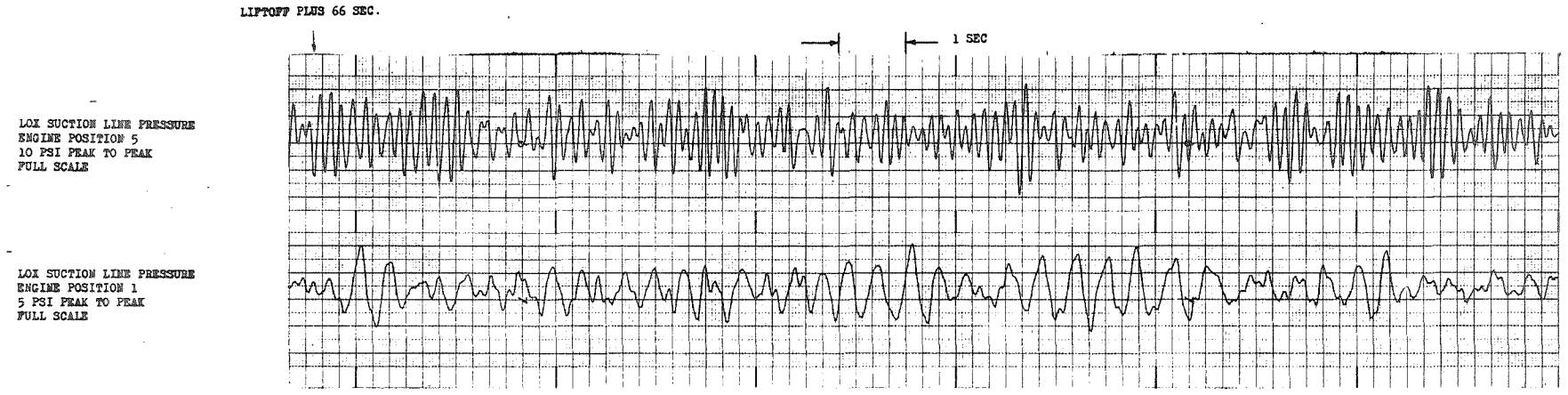

Figure 81. Typical 2 and 6 Hz Oscillations in the LOX Suction Pressures, 0 to 8 Hz Low-Pass Filtered Data

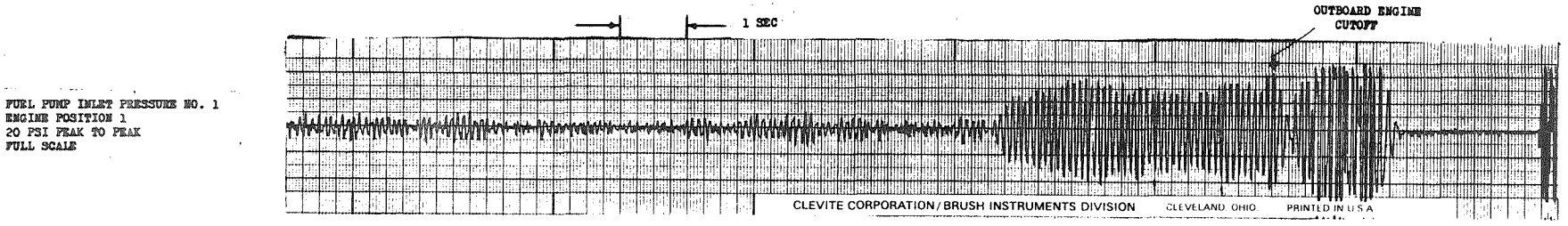

Figure 82. Fuel Pump Inlet Pressure Oscillation Burst, 8 to 25 Hz Bandpass Filtered Data

Thirty Hz oscillations in the fuel pump inlet pressures are consistently evident in the filtered Brush records, averaging from 2 to 4 psi peak-to-peak during flight. Evidence of 30 Hz noise in the preflight intervals for this parameter is less significant. PSD's identify the frequency and amplitude more accurately as 29 Hz, with an amplitude of less than 1 psi peak-to-peak.

The analysis of the dynamic data indicates that the F-1 engines on AS-505 were dynamically similar to the first stage engines of AS-503 and AS-504 with the exception of the occurrence of fuel pump inlet oscillations (11 Hz, 5 to 11 psi peak-to-peak) which persisted throughout the two earlier flights. Amplitudes of all parameters on analog tape were consistently lower than on the two previous flights, as verified by PSD plots. Table 10 is a summary of the PSD processed data.

Fifteen high-frequency (50 to 3000 Hz) vibration measurements were recorded on the F-1 engines of stage S-IC-5 during the AS-505 flight. The data recorded produced 12 measurements without significant indication of drop-outs, intermittent traces or abnormal spiking. Two measurements, E042-103 and E042-103, displayed occasional trace interruptions. Data from these two measurements were analyzed during time slices which were relatively free of the trace interruptions. One measurement, E039-101, displayed spiking throughout the flight; however, the composite g rms level and frequency spectra were similar to those observed during the previous AS-504 flight.

Engine F2035, position 1, displayed a general increase of 5 to 10 percent in composite vibration level in all measurements from a lower value at 30- to 50-seconds range time to a higher value just prior to outboard engine cutoff (OECO). Low-amplitude increases for short durations were also noted at 90- to 110-seconds range time and at inboard engine cutoff (IECO). Frequency spectra analyses indicated the 550 Hz turbopump impeller blade wake frequency component increased to a higher amplitude at approximately 140- to 150-seconds range time on five of six vibration measurements on engine position 1 (E036, E037, E038, E039, and E041). These amplitudes are within the range of previously obtained F-1 engine ground test data.

TABLE 10

PREDOMINANT OSCILLATIONS IN THE S-IC-5 FLIGHT DATA AS DETERMINED FROM POWER SPECTRAL DENSITY (PSD) DATA

(Tabulated values indicate average amplitude psi (or g) peak-to-peak)

Range Time, seconds	Engine Chamber Pressure										Fuel Pump Inlet Pressure				LOX Suction Line Pressure				Longitudinal Gimbal Block Acceleration			
	Engine 1		Engine 2		Engine 3		Engine 4		Engine 5		Engine 1		Engine 5		Engine 1		Engine 5		Engine 1		Engine 5	
	Freq Hz	Amp p-p	Freq Hz	Amp p-p	Freq Hz	Amp p-p	Freq Hz	Amp p-p	Freq Hz	Amp p-p	Freq Hz	Amp p-p	Freq Hz	Amp p-p	Freq Hz	Amp p-p	Freq Hz	Amp p-p	Freq Hz	Amp p-p	Freq Hz	Amp p-p
27 to 37	30	1.1	30	1.1	31	1.3	30	1.2	30	1.2	11.4 29	0.6 0.8	10.7 14.8 17.7	0.5 0.7 0.6	1.8	0.3	4.8	0.6	29	0.007	18.3	0.023
124 to 134	30	1.3	30	1.2	31	1.3	30	1.7	30	1.5	10.4 11.6 30	0.5 0.5 0.5	14.7 17.7	0.6 0.4	2.3	0.2	5.9	0.8	19.2	0.004	18.6	0.008
138 to 148	30	1.0	30	0.9	32	1.1	30	1.1	DNA	DNA	11.3 29	1.4 1.1	DNA	DNA	2.8	0.2	DNA	DNA	4.7	0.010	19.2 35 36	0.010 0.010 0.010

Composite vibration levels in g rms versus time are presented in Fig. 83 through 86. Tables 11 through 15 include the vibration parameter predominant frequencies and their associated rms amplitudes as obtained from power spectral density (PSD) analyses during representative time slices. The engine vibrations were primarily random with peaks associated with engine combustion processes and some superimposed sinusoidal components associated with integral multiples of turbopump speed. The observed engine flight high-frequency vibration environment is quite similar to that experienced during ground tests and previous flights.

Combustion chamber dome longitudinal accelerometers (E036) on engine positions 1 through 5 indicated typical F-1 engine vibration frequency spectra with predominant frequency components at 400 to 500 Hz and at approximately 550 Hz. The frequency component between 400 and 500 Hz is random and associated with engine combustion processes, while the 550 Hz frequency component is sinusoidal and associated with six times turbopump shaft speed. Observed composite g rms levels were highest on engine position 3 (7.3 g rms). These vibration levels are within the range of previously measured flight and ground test data.

Liquid oxygen turbopump inlet flange predominant frequencies in the longitudinal direction (E037) and radial direction (E038) displayed a random peak at 1350 to 1375 Hz. This peak was quite prominant in the radial direction (31 g rms), contributing significantly to the high composite vibration level observed during the flight. In the longitudinal direction, the 1350 to 1375 Hz random peak occurred at a lower amplitude (5.5 g rms). Other observed predominant frequencies associated with multiples of turbopump speed were present in the frequency spectra of both measurements. These frequencies and amplitudes are similar to peaks noted in previously measured ground test and flight data. With the exception of the 1350 to 1375 Hz random peak, the LOX pump inlet flange frequency spectra are similar to previously measured F-1 engine data.

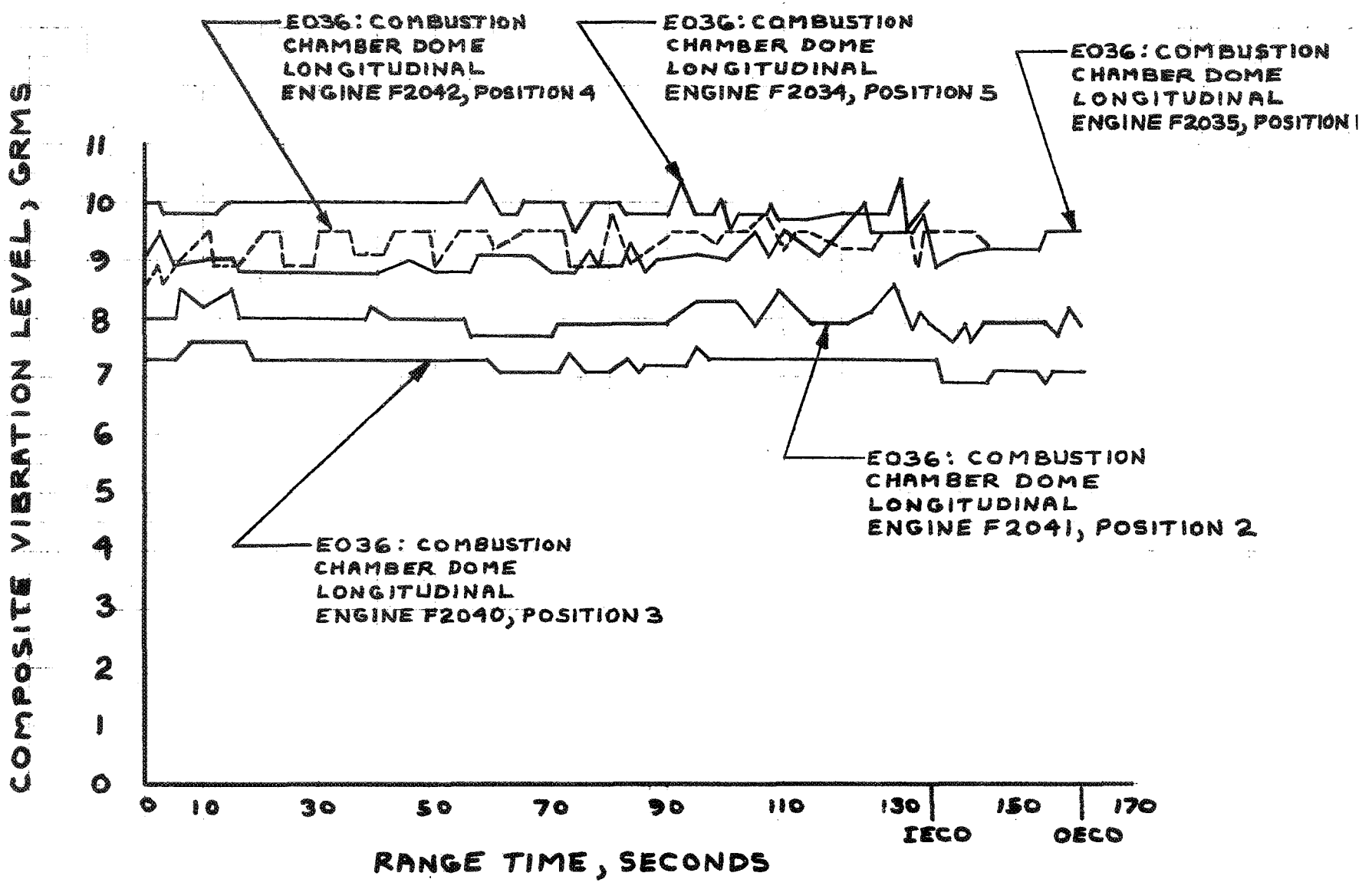

Figure 83. Engine Vibration Data: E036

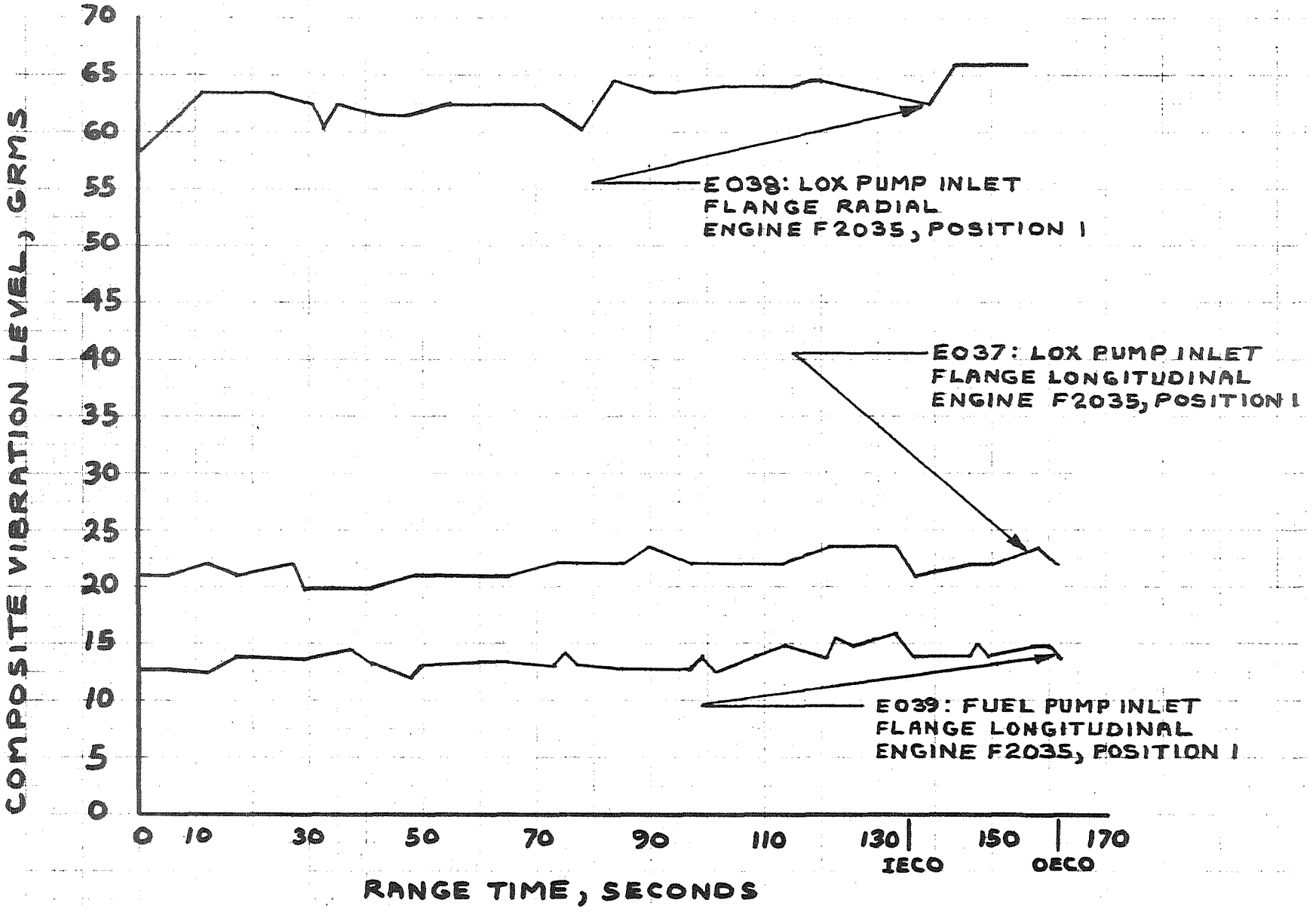

Figure 84. Engine Vibration Data: E037, E038, E039

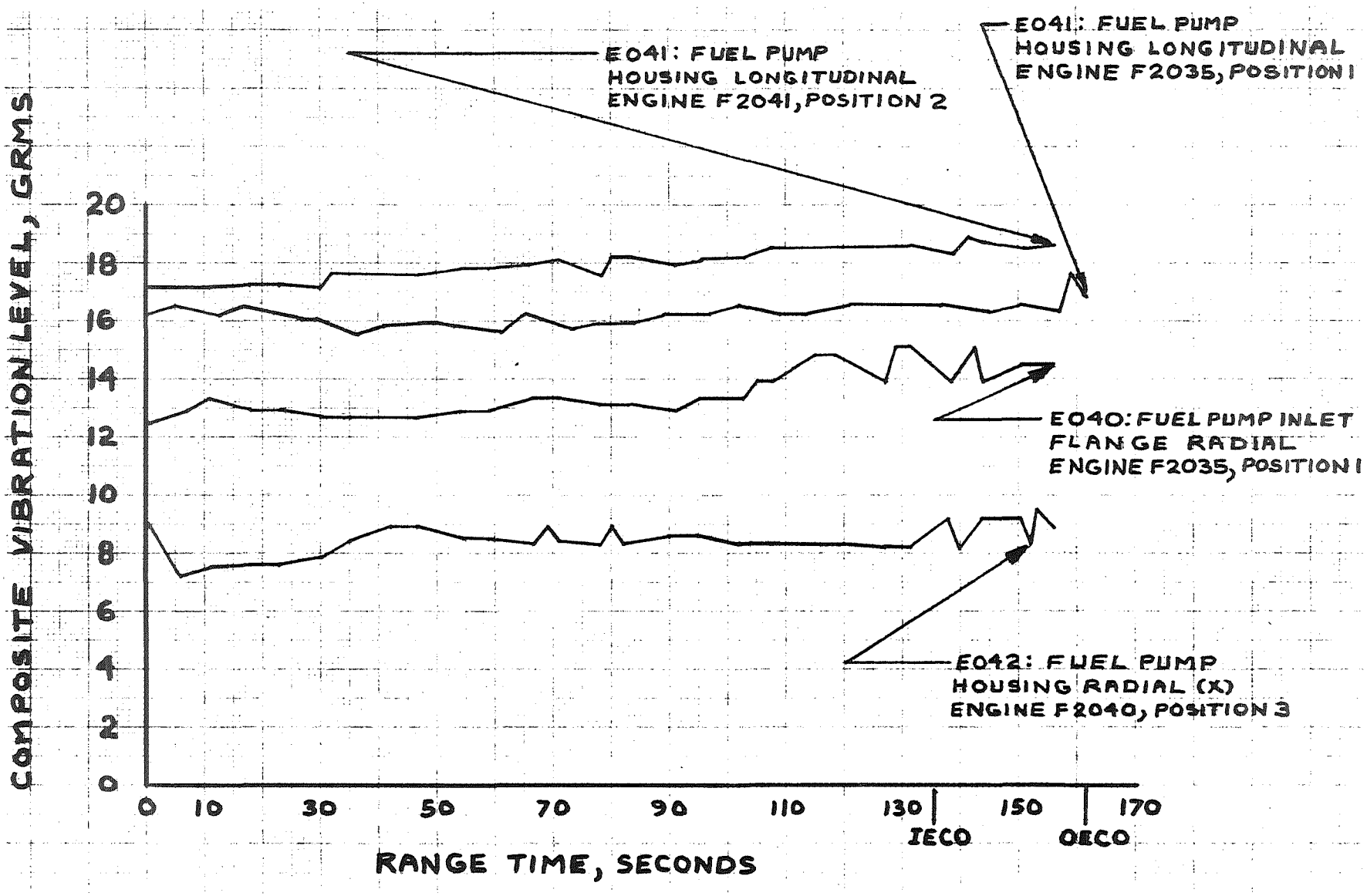

Figure 85. Engine Vibration Data: E040, E041, E042

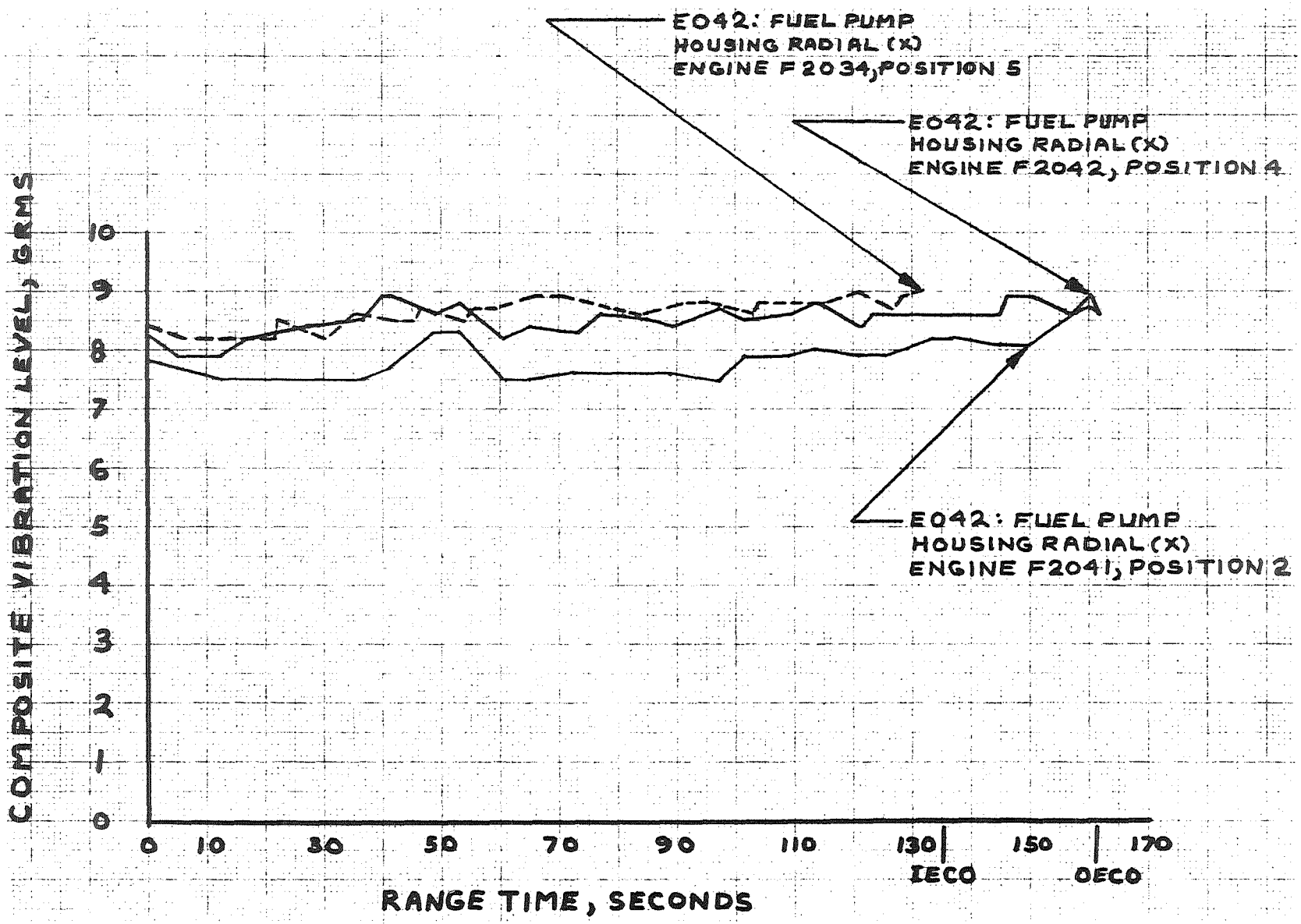

Figure 86. Engine Vibration Data: E042

Fuel turbopump inlet flange longitudinal and radial accelerometers (E039 and E040) and housing longitudinal and radial accelerometers (E041 and E042) displayed normal frequency spectra. Predominant frequencies were those associated with multiples of turbopump shaft speed. Measured vibration levels are within the range of previously measured ground test data.

TABLE 11

AS-505 VIBRATION FREQUENCY SPECTRA S-IC STAGE F-1 ENGINE F2035, POSITION 1, PREDOMINANT FREQUENCIES AND ASSOCIATED AMPLITUDES

E036: Combustion Chamber Dome Longitudinal			
Frequency, Hz	Amplitude in g rms		
	Range Time, 38 to 41 seconds	Range Time, 97 to 100 seconds	Range Time, 146 to 149 seconds
440	2.3	2.0	3.0
550	3.2	3.1	3.5
675	1.1	1.2	1.2
925	1.1	1.0	1.1
1000	1.1	1.1	1.1
1100	1.9	1.9	1.7
1700	1.5	1.4	1.3
1825	1.2	1.1	1.1
1950 to 1975	1.3	1.3	1.3

E037: LOX Pump Inlet Flange Longitudinal			
Frequency, Hz	Amplitude in g rms		
	Range Time, 38 to 41 seconds	Range Time, 97 to 100 seconds	Range Time, 146 to 149 seconds
425	1.3	1.3	1.4
550	2.7	4.8	5.9
750	- -	2.0	2.1
825 to 850	2.7	2.6	2.7
925	2.8	2.4	2.5
1100	4.7	3.3	3.4
1375	5.7	5.0	5.6
1650	2.1	2.2	2.3
1825 to 1850	1.9	2.2	2.3
2025 to 2075	3.6	4.1	3.9
2200	3.7	3.7	3.9

TABLE 11

(Continued)

E038: LOX Pump Inlet Flange Radial			
Frequency, HZ	Amplitude in g rms		
	Range Time, 31 to 34 seconds	Range Time, 104 to 107 seconds	Range Time, 140 to 143 seconds
550	4.7	5.2	5.5
725 to 750	7.7	8.2	7.0
800 to 825	7.0	7.0	5.9
900 to 925	6.6	6.6	5.5
1100	11.2	12.8	9.8
1350 to 1375*	31.5	31.8	31.3
1600 to 1650	6.3	6.6	6.3

E039: Fuel Pump Inlet Flange Longitudinal			
Frequency, Hz	Amplitude in g rms		
	Range Time, 38 to 41 seconds	Range Time, 97 to 100 seconds	Range Time, 146 to 149 seconds
375	1.6	1.9	1.7
550	3.4	3.3	3.8
725	3.2	2.9	2.5
800	1.7	1.7	- -
925 to 975	1.7	1.8	1.7
1100	2.8	3.2	3.8
1300	2.5	2.6	2.6
1400 to 1450	2.9	2.8	2.7
1650	1.8	2.5	3.2
1825 to 1950	1.3	1.5	1.7

*High amplitude random peak

TABLE 11

(Concluded)

E040: Fuel Pump Inlet Flange Radial			
Frequency, Hz	Amplitude in g rms		
	Range Time, 31 to 34 seconds	Range Time, 104 to 107 seconds	Range Time, 140 to 143 seconds
440	1.6	1.8	1.8
550	1.6	1.5	1.4
625	1.6	1.5	1.6
725 to 750	1.2	1.3	1.1
825	1.5	1.7	1.4
925	1.4	1.2	- -
1000	1.3	1.6	1.6
1100	3.6	2.6	2.4
1250 to 1275	2.1	1.8	1.6
1400	1.8	2.2	2.2
1650	4.4	7.0	7.5
2200	2.5	2.5	2.5

E041: Fuel Pump Housing Longitudinal			
Frequency, Hz	Amplitude in g rms		
	Range Time, 38 to 41 seconds	Range Time, 97 to 100 seconds	Range Time, 146 to 149 seconds
550	3.5	3.5	3.9
725 to 750	1.6	1.9	1.9
925	1.3	1.5	1.6
1100	3.6	3.1	2.9
1350 to 1400	1.7	2.2	2.3
1450 to 1475	2.3	2.2	2.2
1650	3.8	5.5	5.6
1750	2.1	2.4	2.4
1825 to 1850	2.3	2.4	2.3
1925 to 1950	2.2	2.8	2.8
2200	3.7	3.7	3.8

TABLE 12

AS-505 VIBRATION FREQUENCY SPECTRA S-IC STAGE F-1 ENGINE F2041, POSITION 2, PREDOMINANT FREQUENCIES AND ASSOCIATED AMPLITUDES

E036: Combustion Chamber Dome Longitudinal			
Frequency, Hz	Amplitude in g rms		
	Range Time, 38 to 41 seconds	Range Time, 97 to 100 seconds	Range Time, 146 to 149 seconds
440	2.2	2.1	2.3
550	3.9	3.9	4.0
675	1.1	1.2	1.1
1100	1.9	1.5	1.6
1200	1.5	1.6	1.6
1725 to 1750	1.4	1.4	1.4
1925 to 2000	1.0	1.2	1.4

E041: Fuel Pump Housing Longitudinal			
Frequency, Hz	Amplitude in g rms		
	Range Time, 31 to 34 seconds	Range Time, 104 to 107 seconds	Range Time, 140 to 143 seconds
550	3.7	3.2	3.6
725	1.4	1.5	1.9
825	1.3	1.2	1.3
925	1.3	1.7	1.9
1100	4.4	4.1	4.3
1300	1.8	1.9	2.0
1400 to 1450	2.2	2.2	2.2
1650	5.2	4.6	4.5
1750	2.2	2.2	2.4
1850	2.2	2.2	2.5
1925 to 2050	2.6	2.9	3.1
2200	3.3	4.2	4.4

TABLE 12

(Concluded)

E042: Fuel Pump Housing Radial (X)			
Frequency, Hz	Amplitude in g rms		
	Range Time, 38 to 41 seconds	Range Time, 97 to 100 seconds	Range Time, 146 to 149 seconds
550	1.4	1.0	1.1
725 to 750	1.3	1.2	1.3
825 to 850	0.8	0.8	0.8
950	0.7	0.8	0.8
1100	0.7	0.7	0.7
1250	1.1	1.1	1.1
1375	1.0	0.9	1.0
1550	1.0	0.8	0.9
1650	1.3	2.1	2.3
1800	0.9	0.8	- -
1950 to 1975	1.0	0.8	0.8
2200	0.9	1.1	1.1

TABLE 13

AS-505 VIBRATION FREQUENCY SPECTRA S-IC STAGE F-1 ENGINE F2040, POSITION 3, PREDOMINANT FREQUENCIES AND ASSOCIATED AMPLITUDES

E036: Combustion Chamber Dome Longitudinal			
Frequency, Hz	Amplitude in g rms		
	Range Time, 38 to 41 seconds	Range Time, 97 to 100 seconds	Range Time, 146 to 149 seconds
450	2.0	2.2	2.1
550	2.4	1.7	1.7
675	1.0	1.0	0.8
925	1.0	1.0	1.0
1100	1.8	2.1	2.3
1650 to 1675	1.3	1.2	1.2
1775 to 1800	1.1	1.1	1.1
1975	1.0	1.1	1.1

E042: Fuel Pump Housing Radial (X)			
Frequency, Hz	Amplitude in g rms		
	Range Time, 31 to 34 seconds	Range Time, 104 to 107 seconds	Range Time, 140 to 143 seconds
275	- -	0.7	1.0
425	0.7	0.6	0.8
550	1.0	1.1	1.1
725 to 750	1.2	1.2	1.2
825 to 850	0.7	0.8	0.9
950	0.6	0.7	0.8
1100	1.0	1.2	1.1
1275 to 1300	1.4	1.4	1.5
1375 to 1400	1.0	1.0	1.0
1650	2.0	2.1	2.4
2200	1.1	1.4	1.4

TABLE 14

AS-505 VIBRATION FREQUENCY SPECTRA S-IC STAGE F-1 ENGINE F2042, POSITION 4, PREDOMINANT FREQUENCIES AND ASSOCIATED AMPLITUDES

E036: Combustion Chamber Dome Longitudinal			
Frequency, Hz	Amplitude in g rms		
	Range Time, 38 to 41 seconds	Range Time, 97 to 100 seconds	Range Time, 146 to 149 seconds
450	2.4	2.3	2.4
550	4.5	4.6	4.4
700	1.2	1.2	1.3
1000	1.0	1.0	1.1
1100	1.7	1.9	2.0
1700	1.5	1.3	1.4
1975	1.5	1.5	1.4

E042: Fuel Pump Housing Radial (X)			
Frequency, Hz	Amplitude in g rms		
	Range Time, 38 to 41 seconds	Range Time, 97 to 100 seconds	Range Time, 146 to 149 seconds
275	0.8	0.8	1.0
450	0.9	0.8	0.9
550	1.5	0.6	1.4
725 to 750	1.9	2.2	2.1
825 to 850	1.0	1.0	1.0
975 to 1000	0.9	0.9	0.9
1100	1.1	1.3	1.1
1275	1.1	1.1	1.1
1400	1.1	1.0	1.0
1650	3.5	3.8	3.7
1825 to 1850	1.0	1.0	1.0
2200	1.4	1.5	1.7

TABLE 15

AS-505 VIBRATION FREQUENCY SPECTRA S-IC STAGE F-1 ENGINE F2034, POSITION 5, PREDOMINANT FREQUENCIES AND ASSOCIATED AMPLITUDES

E036: Combustion Chamber Dome Longitudinal		
Frequency, Hz	Amplitude in g rms	
	Range Time, 38 to 41 seconds	Range Time, 97 to 100 seconds
440	2.6	3.0
550	4.9	4.7
650	1.1	1.3
925 to 950	1.3	1.3
1100	2.7	2.6
1600 to 1675	1.3	1.3
1750 to 1775	1.5	1.6
1950	1.3	1.4

E042: Fuel Pump Housing Radial (X)		
Frequency, Hz	Amplitude in g rms	
	Range Time, 31 to 34 seconds	Range Time, 104 to 107 seconds
275	0.7	0.9
550	2.6	2.6
750	2.1	2.2
925 to 950	0.9	1.0
1100	0.9	1.0
1250 to 1275	1.0	1.0
1350 to 1375	0.9	1.0
1500	1.0	0.9
1650	3.0	3.3
1825 to 1850	1.0	1.0
2200	1.4	1.7

FLIGHT INSTRUMENTATION OPERATION

Rocketdyne supplies 35 flight instrumentation parameters per engine, for a total of 175 engine parameters per S-IC stage. During the AS-505 flight, 159 of the noted parameters were active. These parameters include 79 pressures, 30 temperatures, 5 speed, 5 flow, 15 pressure switches, and 25 valve positions. Valid data were received from all recorded parameters; however, partial loss of data was experienced on one parameter, and two parameters yielded questionable data.

Heat exchanger helium outlet pressure (D0020-101) on engine position 1 dropped to zero at approximately T + 50 seconds. Helium inlet pressure and outlet temperature data from engine position 1 indicated normal heat exchanger operation. The noted loss of pressure data is attributed to the instrumentation system, most probably a transducer failure.

At approximately T + 115 seconds, turbine manifold temperature (C0003-102) on engine position 2 decreased 85 F from the expected value of 1572 F, to 1497 F over a 10-second interval. The temperature then stabilized, followed the normal trend, at the lower value, through engine shutdown. Analysis of other performance parameters (i.e., turbopump speed, thrust chamber pressure, gas generator chamber pressure, and turbopump discharge pressures) discloses no correlation with the indicated change in turbine manifold temperature. The noted lack of correlation results in the conclusion that the temperature level change is not valid data, and is attributed to the instrumentation system.

A gradual rise from the expected value of approximately 50 psia in engine hydraulic control closing pressure (D0011-101) started at approximately T + 70 seconds, and the indicated pressure stabilized at approximately 220 psia at T + 115 seconds. Subsequent to engine shutdown, D0011-101 indicated approximately 90 psia rather than the nominal common value of approximately 30 psia indicated on the other fuel system parameters. Failure analyses of the hydraulic system have resulted in the conclusion that the most probable

cause of the indicated pressure increase is a change in sensitivity in the pressure transducer or the instrumentation system, and is not indicative of a hydraulic system problem.

Flight data indicate an intermittent voltage on the contact monitors on 2 of the 15 "Thrust OK" pressure switches (engine position 4, switches 1 and 3). Intermittent fluctuation in switch output voltage has occurred on all previous Saturn V flights. Rocketdyne engine test experience has shown that intermittent fluctuations in switch output voltage resulting from contact wiping during engine operation is not uncommon, this being the reason for the incorporation of a 44-millisecond timer into the stage shutdown circuit.

It is concluded that the noted pressure switch data are not indicative of a pressure switch anomaly and similar indications will continue to be observed on subsequent flights.

HEAT EXCHANGER PERFORMANCE ANALYSIS

Heat exchanger LOX coil operation was normal and generally similar to AS-501 through AS-504 flight operation. Heat exchanger performance data are presented in Fig. 87 through 90, and Table 16 and 17. The data reduction to standard conditions was accomplished with the analytical model for the F-1 engine heat exchanger.

The AS-505 five engine average LOX coil flowrate is presented in Fig. 87 in comparison with the same parameter for the AS-501 through 504 flights. The average flowrate during the flight lies within or close to the average flowrate data envelope obtained during the previous flights, and corresponds with the inverse relationship of flowrate to outlet temperature. The heat exchanger LOX flowrtates were all within the model specification flowrate limits of 3 to 15 lb/sec established by ECP F1-601. The maximum recorded LOX flowrate was 13.0 lb/sec on engine 2035.

The average heat exchanger GOX outlet temperatures experienced during the AS-501 through AS-504, and the AS-505 flight are compared in Fig. 88. The average GOX outlet temperature correlates well with the temperature range recorded during the previous flights.

Gaseous oxygen heat exchanger performance is presented in Table 16. The recorded GOX outlet temperature data are corrected to the model specification standard conditions of 4 lb/sec flowrate and -288 F LOX inlet temperature. The GOX heat exchanger outlet temperature at standard conditions on all five engines was within the model specification limits of 400 to 500 F at the standard data slice of 35 seconds but differed slightly from the preflight predictions. The predicted GOX outlet temperature averaged 18 F lower than the actual temperatures reduced to standard conditions at 35 seconds into flight.

The average heat exchanger helium flowrate is presented in Fig. 89. Helium flowrate is measured in the common hot riser duct which includes the flow of all five engines. Individual engine standard temperature predictions and flight reductions to standard conditions were obtained by

assuming the same flow split as that experienced during stage static test. Heat exchanger helium flowrates were within the model specification flowrate of 0.4 to 1.0 lb/sec established by ECP F1-601.

The average heat exchanger helium outlet temperature experienced during the flight is shown in Fig. 90. The helium heat exchanger outlet temperatures corrected to standard conditions of 0.6 lb/sec and -345 F are included in Table 17 with the preflight predictions. The helium heat exchanger performance at standard conditions on all five engines was within the model specification limits at the reduced data points.

The helium inlet temperature was not measured during flight, therefore an estimate of this parameter was obtained by utilizing the helium control valve inlet temperature and correcting it for the temperature change between the valve inlet and heat exchanger inlet points as measured during the AS-501 flight.

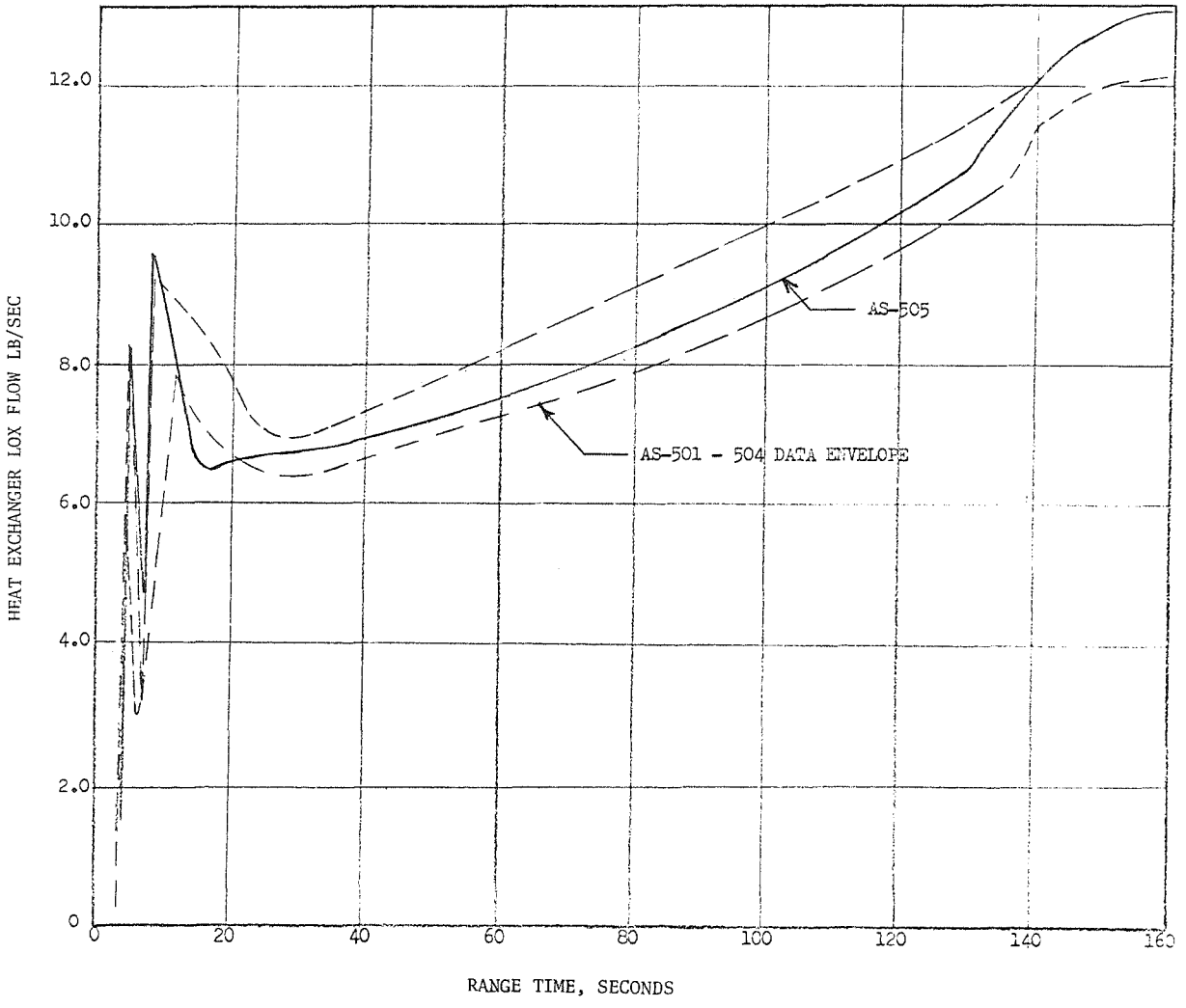

Figure 87. Average Heat Exchanger LOX Flowrate

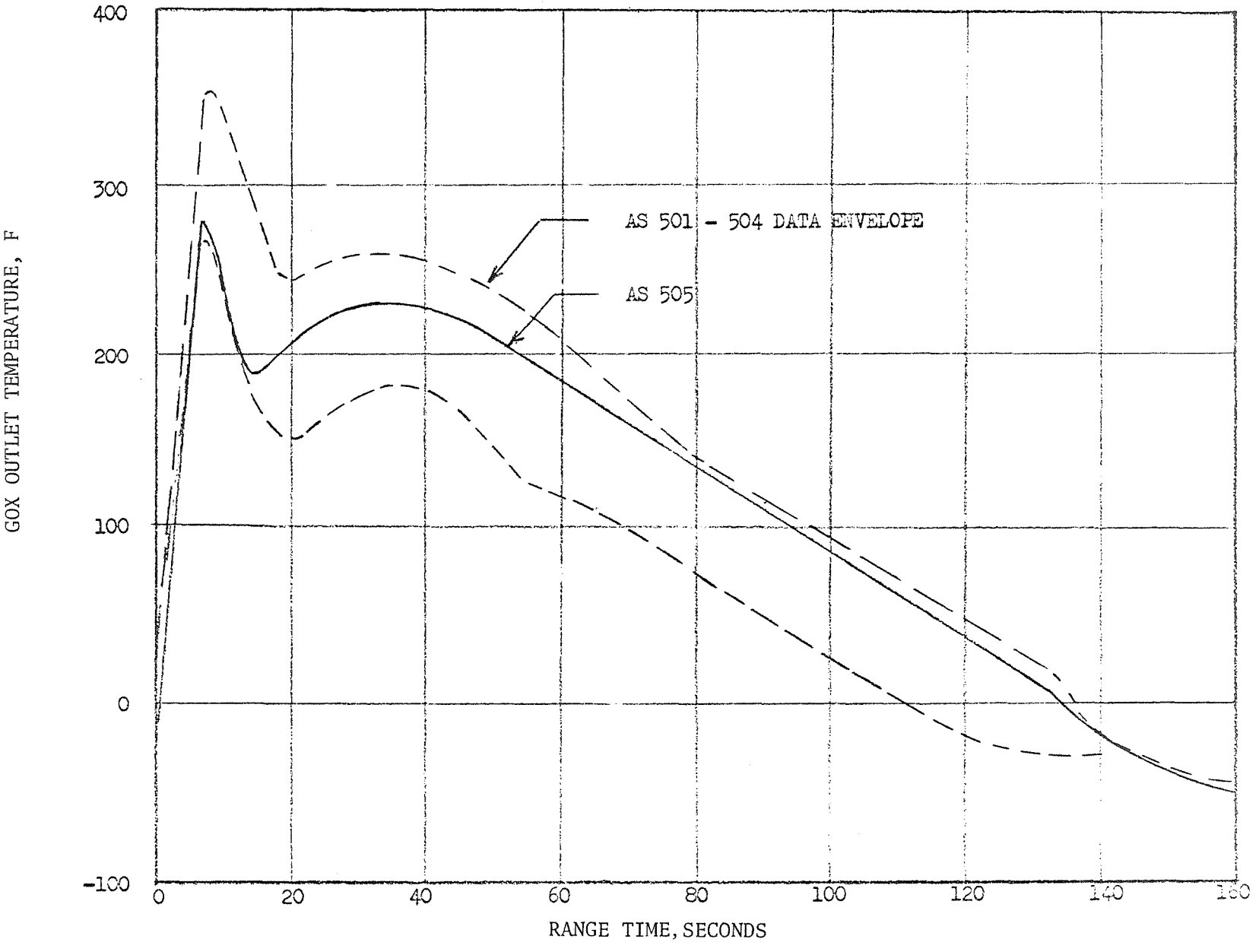

Figure 88. Average Heat Exchanger GOX Outlet Temperature

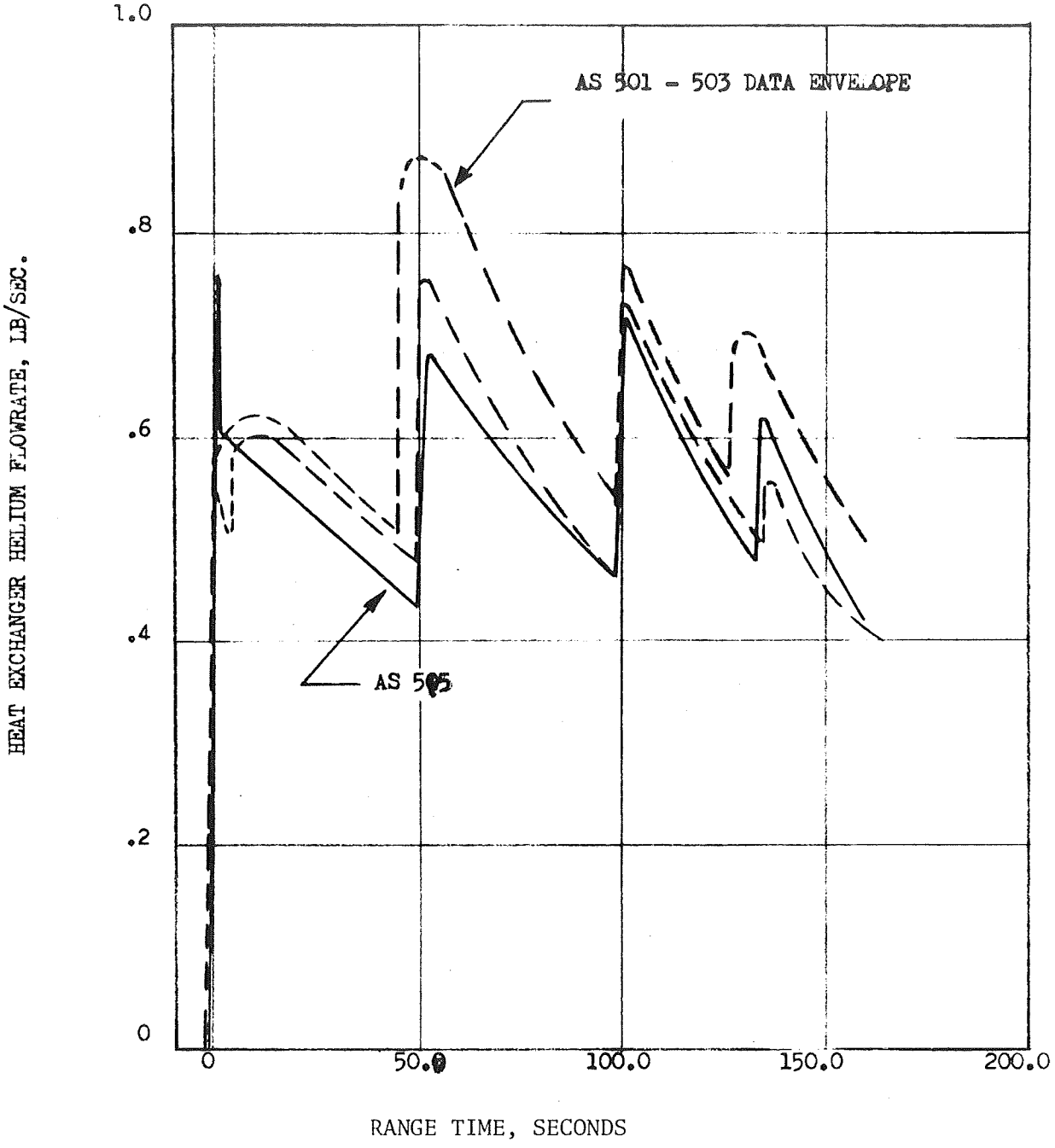

Figure 89. Average Heat Exchanger Helium Flowrate

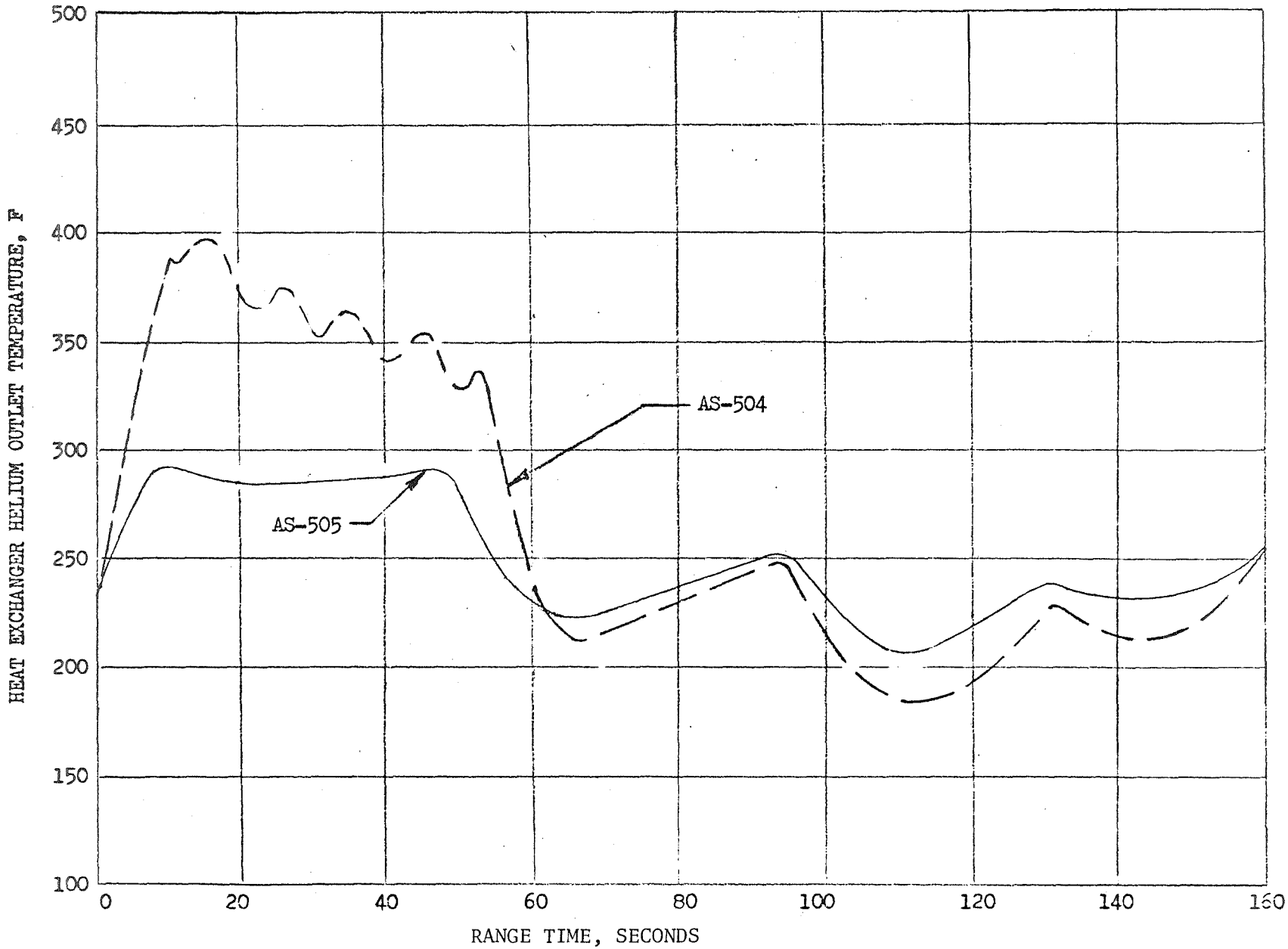

Figure 90. Average Heat Exchanger Helium Outlet Temperature, AS 505

TABLE 16

AS-505, S-IC5 STAGE F-1 ENGINES

OXIDIZER HEAT EXCHANGER PERFORMANCE AT STANDARD CONDITIONS

Engine Position	Engine Serial No.	Oxidizer Outlet Temperature, F		
		35 Seconds Range Time	105 Seconds Range Time	Predicted At 35 Seconds
1	F2035	458	422	431
2	F2041	464	435	448
3	F2040	422	393	436
4	F2042	446	414	413
5	F2034	481	451	454
Average Engine		454	423	436

NOTE: Data Reduced To Standard Conditions:

Oxidizer Coil Inlet Temperature = -288 F

Oxidizer Flowrate = 4 lb/sec

Outlet temperature at 105 seconds is on the average 31 F lower than for 35 seconds because of carbon deposition on the heat exchanger coils.

TABLE 17

AS-505, S-IC-5 STAGE F-1 ENGINES

HELIUM HEAT EXCHANGER PERFORMANCE AT STANDARD CONDITIONS

Position	Engine Serial No.	Helium Outlet Temperature, F		
		35 Seconds Range Time	105 Seconds Range Time	Predicted At 35 Seconds
1	F2035	237	201	229
2	F2041	204	193	223
3	F2040	215	194	215
4	F2042	218	195	208
5	F2034	216	197	235
Average Engine		218	196	222

NOTE: Data Reduced To Standard Conditions:

Helium Coil Inlet Temperature = -345 F

Helium Flowrate = 0.6 lb/sec

Outlet temperatures at 105 seconds are on the average 22 F lower than for 35 seconds because of carbon deposition on the heat exchanger coils.

THERMAL ANALYSIS

During the flight of the AS-505 vehicle, the F-1 engine thermal insulation satisfactorily protected the mechanical, structural, and electrical components. The thermal environment for both the AS-505 and AS-504 flights was approximately the same during most of the flight.

The AS-505 in-flight measured engine component skin temperatures under the thermal insulation on engine position 1 (except solenoid valve on engine position 5) are presented in Table 18 along with the predicted values, allowable values, and range of values for flights AS-501 through AS-504. All measured component temperatures were below the allowable limits. Assuming that the measured component temperatures are representative of the other engines, it is concluded that no component temperatures exceeded allowable values and that the thermal insulation provided adequate engine component protection.

Total heat flux measurements were taken on the thermal insulation surfaces of engine positions 1, 3, and 5. The peak heat flux at each measurement location for flights AS-501 through AS-505 is presented in Table 19. The peak values for the AS-505 flight are similar to those for the other flights.

Thermal insulation surface temperatures were calculated from the measured heat fluxes for three representative locations. They are presented with the predicted and AS-504 temperature-time histories in Fig. 91 to 93. Generally, the AS-505 and AS-504 profiles agree well. However, the maximum temperatures on the AS-505 flight were slightly higher than on the AS-504 flight. The reconstructed temperatures would be approximately 100 to 200 F lower if the radiant heat fluxes were corrected for the emissivity (estimated at 0.8) of the insulation. Because there is no accurate way to determine the amount of radiant flux from the total heat flux measurements, no corrections were made to the measured heat fluxes.

The engine environmental temperatures (C242) within the thermal insulation cocoon fell within the range of the temperature envelope experienced during AS-501 through AS-504 flights, indicating good correlation with previous flight data and verifying the low temperatures recorded during the earlier flights (Fig. 94).

TABLE 18

S-IC STAGE F-1 ENGINE COMPONENT
TEMPERATURES DURING FLIGHT

Component	Allowable Temperature, F	Predicted Temperature, F	AS-501 to 504 Flight Temperature Range, F	AS-505 Flight Temperature Range, F
Heat Exchanger Bellows	1500	1300	40 to 1150	70 to 1200
Temperature Outboard Gimbal Actuator (Boeing Component)	165	--	65 to 115	65 to 110
Temperature, Gas Generator Position Switch	165	--	0 to 35	0 to 30
Temperature, Fuel Valve Housing	250	70 (RP-1 Temperature)	62 to 82	65 to 80
Temperature, Exhaust Manifold	1750	1300	50 to 1180	70 to 1200
Temperature, Aft Nozzle External	1500	1325	50 to 1350	80 to 520
Temperature, Fuel Discharge Line	250	70 (RP-1 Temperature)	30 to 150	50 to 140
Solenoid Valve (Under Insulation)	165	70 (RP-1 Temperature)	12 to 80	35 to 50

TABLE 19

SI-C STAGE F-1 ENGINE THERMAL INSULATION

PEAK HEAT FLUXES DURING FLIGHT

Coloriometer	Peak Heat Flux, BTU/$_{ft}^{2}$/$_{sec}$				
	AS-501	AS-502	AS-503	AS-504	AS-505
C0014-101	26	28	--	32	32
C0015-101	25	12	18	28	28
C0016-105	29	34	30	32	32
C0017-101	24	32	29	31	33
C0018-101	6	14	6	9	7
C0019-101	12	29	24	25	34
C0020-105	12	21	8	19	20
C0021-101	12	24	21	23	27
C0022-101	11	20	20	22	24
C0023-101	4	6	4	6	5
C00123-103	26	36	31	33	34
C142-103	19	32	30	24	31

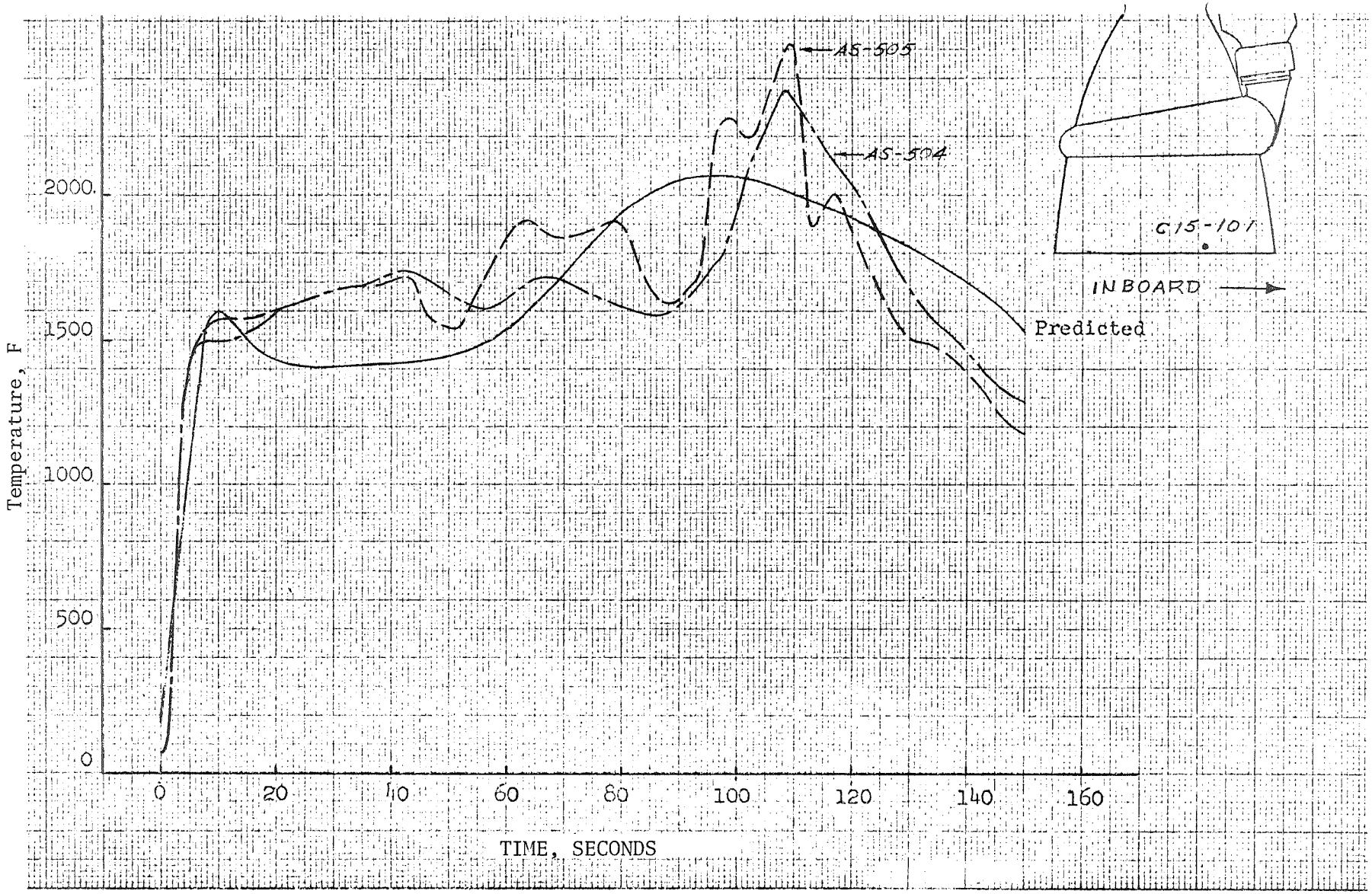

Figure 91. S-IC Stage Insulation Surface Temperature (C0015-101)

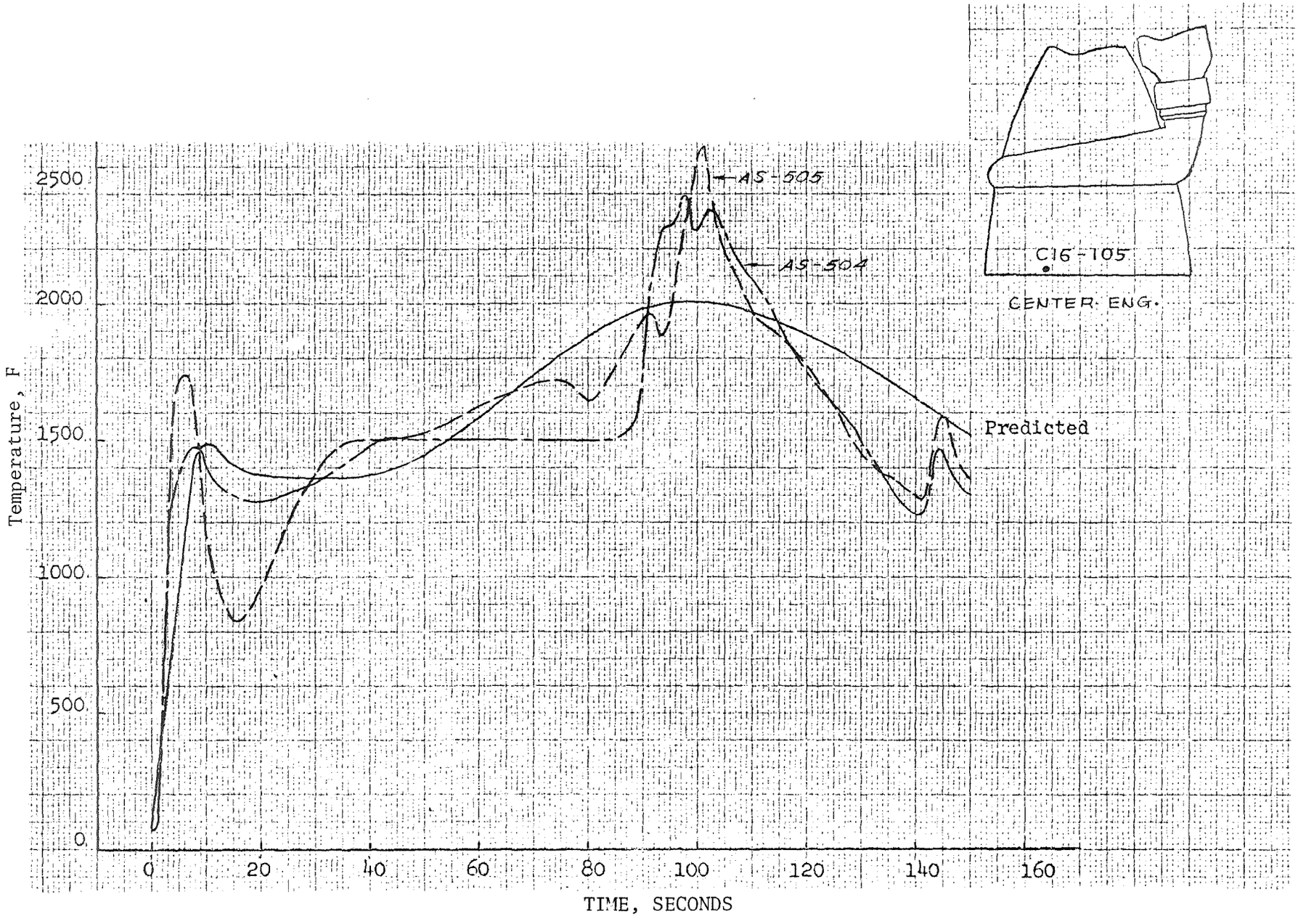

Figure 92. S-IC Stage Insulation Surface Temperature (C0016-105)

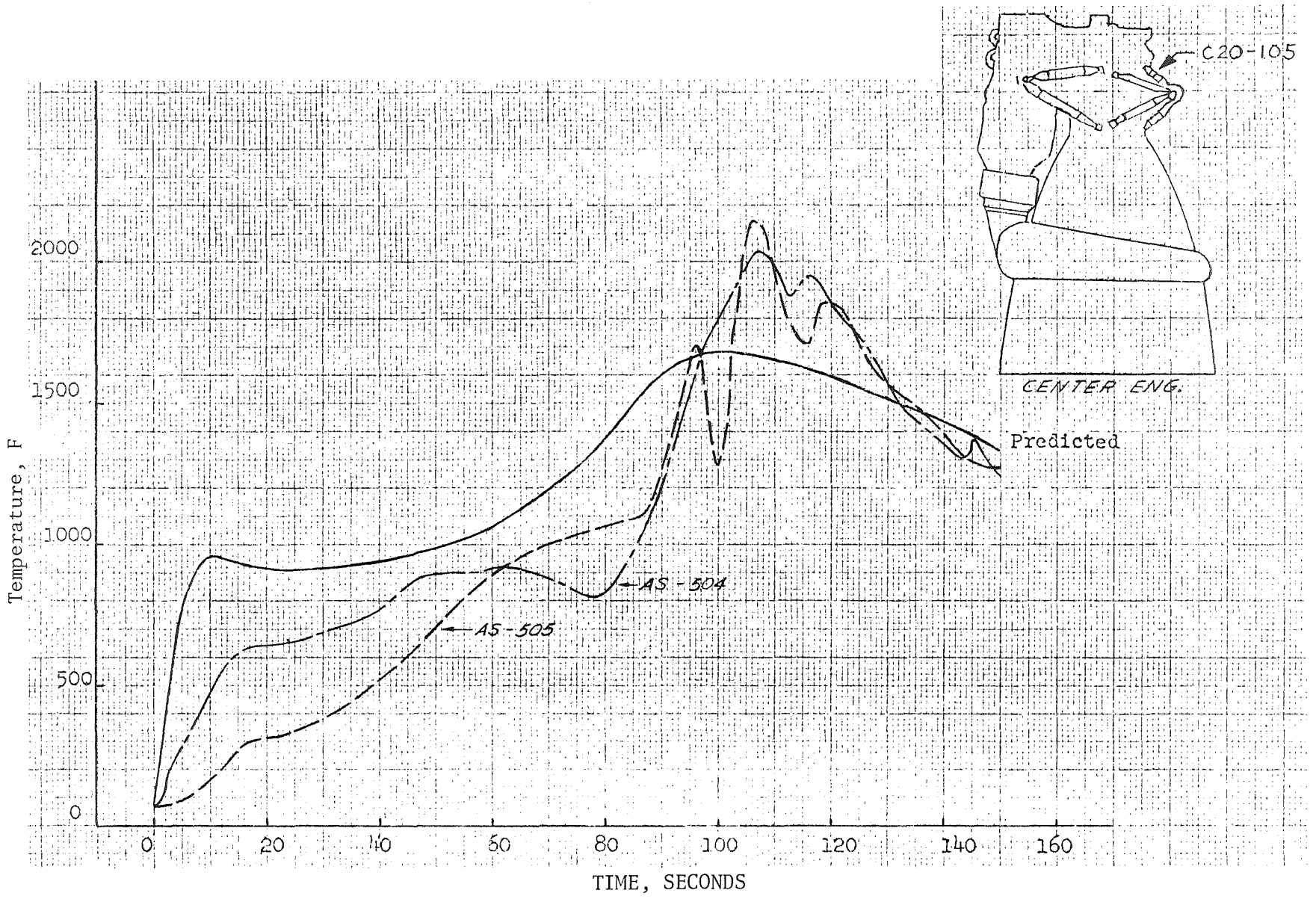

Figure 93. S-IC Stage Insulation Surface Temperature (C0020-105)

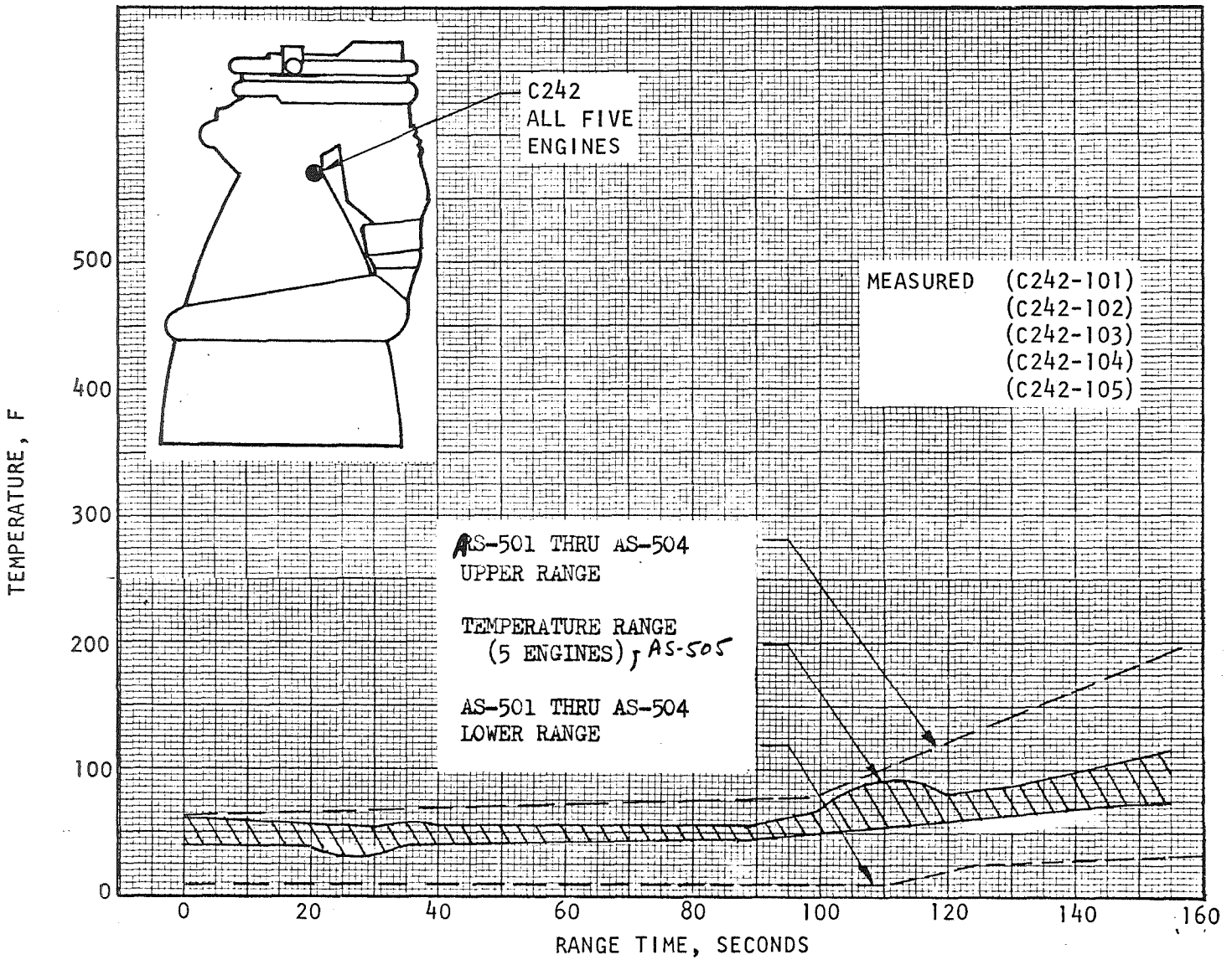

Figure 94. S-IC Stage Engine Environmental Gas Temperature Within Cocoon

APPENDIX A

ENGINE AND THERMAL INSULATION CONFIGURATION

Qualification II F-1 engines were used for the AS-505 flight. The configuration of engines F2035, F2041, F2040, F2042, and F2034 as launched were:

1x7 11x13 14x16x18x20 22x24x26x29x31 33x35x37 39x42 43x46 47x49 51x54 55x57x59x61x63 73x75 79x84x87 90x92x94 97x99 102x104 107x109 110x112x114 115x117 122x124 127x130x134 135x138 139x144x149x154x156x158 160x163x168 169

MD 99 does not apply to F2035 (Pos 101) and engine F2034 (Pos 105)

Thermal insulation (Part No. 145001) sets 13-4, 12-6, 12-7, 14-4, and 15-1 were installed on engines F2035, F2041, F2040, F2042, and F2034 respectively. These sets incroproated ECP's, F1-265R2, F1-266R1, F1-349R1, F1-397, F1-466, F1-479R2, F1-481R1, F10488R1, F1-489R1 (excluding engine F2034), F1-516R1, F1-565R1, F1-573R2, F1-575R3, and F1-588 (engine F2042 only).

APPENDIX B

ENGINE TEST HISTORY

Information concerning engine test history is presented in R-6852-4 F-1 Flight Readiness Report, Saturn S-IC-5 Stage, Vehicle AS-505.

A summary of the test history of each engine is presented below:

Engine F2035	Total Tests	Mainstage Times, seconds
Acceptance Tests	3	249.3
Stage Tests	1	126.9
Total Prior to Launch	4	376.2
Engine F2041		
Acceptance Tests	3	249.2
Stage Tests	1	126.9
Total Prior to Launch	4	376.1
Engine F2040		
Acceptance Tests	3	249.1
Stage Tests	1	126.9
Total Prior to Launch	4	376.0
Engine F2042		
Acceptance Tests	4	415.3
Stage Tests	1	126.9
Total Prior to Launch	5	542.2
Engine F2034		
Acceptance Tests	4	415.3
Stage Tests	1	126.9
Total Prior to Launch	5	542.2

APPENDIX C

PRELAUNCH OPERATIONS

The S-IC-5 stage arrived at Kennedy Space Center by barge on 27 November 1968. The stage was erected on Launch Umbilical Tower (LUT) No. 3 in the Vertical Assembly (VAB) 3 December 1968 and was subsequently mated to the upper stages of the AS-505 vehicle.

On 12 March 1969, Saturn V Launch Vehicle AS-505 was transferred from the VAB to pad B of launch complex 39.

The following propulsion system verification tests were accomplished at the launch pad as the final tests of engine system integrity prior to launch.

1. F-1 Engine Sequence Test Procedure V-24024: Performed to verify correct operational sequence and engine valve timing during a nominal engine start and stop sequence. Accomplished 19 March 1969.
2. F-1 engine post flush leak check and injector inspection, procedure V-24342. Accomplished 12 April 1969.
3. Thrust OK pressure switch functional test, procedure V-24040. Accomplished 23 April 1969.
4. Main fuel valve leak check: Performed as part of procedure V-34012, launch system preparations. Accomplished 6 through 9 May 1969.

Servicing operations accomplished on the launch pad to ensure removal of any contaminants introduced during the course of verification testing were:

1. F-1 engine thrust chamber fuel jacket flush and purge, procedure V-24275. Accomplished 4 April 1969. The fuel jacket flush and purge was reaccomplished on engines F2035, F2040, F2042, and

F2034 on 29 May 1969 resulting from an improper residual fuel drain which allowed fuel to back up the drain lines on the fuel inlet manifolds of the subject engines.

2. F-1 engine LOX dome flush and purge, procedure V-24028. Accomplished 13 April 1969.

3. S-IC residual fuel drain; performed as part of procedure V-34008, F-1 engine valves and feed system fuel leak check. Accomplished 29 April 1969. The residual fuel drain was accomplished again 2 May 1969 per procedure V-34012, S-IC Stage Propulsion Systems CDDT and Launch Preparations. A final residual fuel drain was performed 10 May 1969 subsequent to the S-1C fuel hydrostatic test required as a final integrity verification of the S-IC fuel tank.

The following milestone events were completed prior to launch.

1. Transfer to Launch Pad, 12 March 1969.

2. Flight Readiness Test, 8 April 1969

3. RP-1 Loading Accomplished 26 April 1969. RP-1 loading was re-accomplished 1 May 1969 subsequent to draining the S-IC fuel tank to determine its structural integrity following the damage to the S-IC fuel tank upper bulkhead.

Wet Countdown Demonstration Test (CDDT) was begun at 0700 hours (EDT) on 29 April 1969. This represented a 12-hour slip in the beginning of CDDT (wet) resulting from damage to the S-IC fuel tank upper bulkhead incurred subsequent to fuel tanking. The count continued to T-48 hours and entered an 18-hour hold to load fuel. The count was resumed at 1300 hours (EDT) on 2 May 1969 and progressed to T-1 hour and 15 minutes and entered an unscheduled 2-hour hold to allow additional time for numerous launch vehicle functions which were behind schedule. At T-3 minutes and 8 seconds, the count was recycled to T-22 minutes resulting from problems in

the launch vehicle guidance system. The count was resumed at 0946 hours (EDT) and continued to completion at 1009 hours (EDT) on 5 May 1969.

No F-1 engine problems were encountered with the exception of the environment temperature on engine F2034, position 105 which became erratic subsequent to LOX loading. The discrepancy was isolated to a DC amplifier assembly which was replaced prior to the launch countdown.

The launch countdown began at 1500 hours (EDT) on 12 May 1969. Subsequent to LOX loading, the environmental temperature on engine F2034, position 105, became erratic for the second time. The measurement stabilized shortly prior to flight and the descrepancy was attributed to the flight instrumentation system. Liftoff of vehicle AS-505 occurred at 1249 hours (EDT) on 18 May 1969.

S-1C-5 problems encountered at the Kennedy Space Center prior to launch and Engine Field Inspection Requests (EFIR's) performed are discussed in Appendix D.

APPENDIX D

PROBLEM AND ACTION SUMMARY

ENGINEERING FIELD INSPECTION REQUESTS

EFIR F1-49, Cleaning of Gas Generator Oxidizer Ducts (Valve End) Instrumentation Ports for Possible Lubrication Contamination

The plugs from instrumentation ports G01A and G01B on the gas generator oxidizer duct (valve end) of engine F2035, position 101, were removed and the instrument ports swab checked. The plugs and swabs from the subject ports were returned to Canoga Park for analysis. No indications of improper lubrication were found.

S-IC FUEL TANK DAMAGE

Following the S-IC stage RP-1 loading, a leak was noted at the LUT tower GN_2 supply balance valve. The tower system was vented to replace the valve which resulted in the unscheduled opening of the fuel prevalves with the fuel tank vent closed and the fuel drain lines attached to the S-IC-5 engines. The negative pressure created from draining the fuel through the overboard drain lines with the tank vent closed resulted in the partial collapse of the fuel tank upper bulkhead. Subsequent inspection, including a hydrostatic test of the fuel tank, revealed no significant structural damage.

MISLOCATION OF THE HYPERGOL LOCKING-PIN HOLE ON ENGINE F2041

During the installation of hypergol ordnances, interference between the hypergol access door in the T.I.S. and the hypergol cartridge locking pin was encountered on engine F2041. Subsequent investigation revealed that the locking-pin hole was located 90-degrees counterclockwise from the

specified drawing location and would not allow the installation of the T.I.S. hypergol access door. This descrepancy had been previously cleared by Material Review action. The interference condition was corrected by replacing the hypergol locking pin with an equivalent locking pin of a shorter length.

ENGINE ENVIRONMENTAL SYSTEM

During the Countdown Demonstration Test (CDDT) the engine environmental temperature reading for engine F2034, a redline parameter from the start of the LOX loading to the start of automatic sequence, became erratic shortly after the start of LOX loading. Investigation subsequent to the completion of CDDT indicated a defective DC signal conditioning amplifier. The amplifier was replaced.

At approximately T-4 hours of the countdown, the engine environmental temperature reading for engine F2034 again became erratic. Two temperature measurements were used as alternatives on engine F2034 for the remainder of the count; C131-105, four-way solenoid, and C134-105, thrust OK pressure switch external temperature. The engine environmental temperature measurement stabilized just prior to liftoff and remained stable throughout the S-IC flight. The discrepancy was attributed to the flight instrumentation system.

MAIN FUEL ORIFICE IDENTIFICATION

During the engine orifice verification portion of procedure V-36001, Precheckout Preps, an identification discrepancy relating to the No. 2 main fuel orifice on engine F2041, position 102 was noted. The engine logbook entry for the No. 2 main fuel orifice is RD251-4100-3775. The orifice itself is identified as RD251-4100-3756 with light "x" marks etched over both the 3756 portion of the identification number and the No. 2038, indicating that the 3756 representing an orifice diameter of 3.756 inches and the 2038 representing the serial number of the engine intended are

no longer valid. Based on a review of the engine log-books and the history of spare main fuel orifices, it was concluded that the correct No. 2 main fuel orifice, RD251-4100-3775, is installed in engine F2041 and physical verification of the orifice size was not required.

APPENDIX E

DATA PROCESSING

STEADY-STATE DATA

Standard NASA format telemetry tapes supplied by the Boeing Company were the data source used to determine engine performance. Several telemetry tapes at various sampling frequencies were merged to form a single tape with a sampling rate of four samples per second. From this tape, selected parameters averaged over 3-second intervals taken every 10 seconds were generated, and input to the FLT F1 data reduction program. A least-square mathematical curve fit of data over 5-second intervals was used for input to the linear influence coefficients flight reconstruction program.

Turbopump speeds at 35 seconds were obtained from hand counts from MAF.

Prelaunch averages were employed to determine zero shifts which were applied to specific measurements listed in Table 20. In addition, "flight" transducer to "facility" transducer biases derived from acceptance test data were applied to specific measurements. The values used for these biases are summarized in Table 21. The total parameter correction value is the algebraic sum of the zero shift and transducer biases included in Tables 20 and 21, which is subtracted from the telemetry averaged slice value. Data for inlet LOX and fuel temperatures and fuel pump inlet pressure were the average of all five engines. For the inlet LOX pressure, position 1 through 4 were averaged and data for position 5 was used independently.

Zero shifts (prelaunch values) for the mean readings were used for the following parameters: fuel pump discharge pressure No. 1 and 2 (D0006 and D0007), and LOX pump inlet pressure (DO 127 to 130), prelaunch readings for main chamber pressure (D0008), and gas generator chamber pressure (D0009) were adjusted to ambient pressure.

TABLE 20

INSTRUMENTATION ZERO SHIFTS

Parameter Identification, Number and Title	Engine Position				
	1	2	3	4	5
C0003-10X Turbine Manifold Temperature	10	-9	-14	13	-1
C00024-10X Fluel Inlet Temperature	0	0	0	0	0
C0197-0201 LOX Inlet Temperature	0	0	0	0	0
D0002-10X LOX Pump Discharge Pressure No. 1	2	35	19	-12	30
D0003-10X LOX Pump Discharge Pressure No. 2	13	6	-17	3	8
D0004-10X Fuel Pump Inlet Pressure	0	0	0	0	0
D0006-10X Fuel Pump Discharge Pressure No. 1	2	-11	-7	-14	-6
D0007-10X Fuel Pump Discharge Pressure No. 2	3	3	0	8	11
D0008-10X Thrust Chamber Pressure	4.6	0.6	3.0	2.8	-1.6
D0009-10X Gas Generator Chamber Pressure	-8	1	-6	1	-4
D0010-10X Turbine Exit Pressure	-0.2	-0.2	-0.1	0.1	-0.4
D0127-D0131 LOX Suction Line Pressure	0	0	0	0	0

TABLE 21

INSTRUMENT "FLIGHT" TO "FACILITY" TRANSDUCER BIASES

Parameter Identification, Number and Title	Engine Position				
	1	2	3	4	5
C0003-10X Turbine Manifold Temperature	-24	-24	-24	-24	-24
C0024-10X Fuel Pump Inlet Temperature	-0.2	-0.2	-0.2	-0.2	-0.2
D0003-10X LOX Pump Discharge Pressure No. 2	-8	6	-29	11	-12
D0004-10X Fuel Pump Inlet Pressure	-1.4	-1.4	-1.4	-1.4	-1.4
D0007-10X Fuel Pump Discharge Pressure No. 2	-5	7	-5	-25	-22
D0008-10X Thrust Chamber Pressure	2	2	2	2	2
D0009-10X Gas Generator Chamber Pressure	8	8	8	8	8

Prelaunch turbine inlet manifold temperatures (C0003) should have been reading 46F, as did engine environmental temperature (C0242). Estimates for prelaunch values of LOX pump discharge pressures No. 1 and 2 (D0002 and D0003) were based on LOX suction line prelaunch values corrected for head differences because of transducer locations as were fuel pump discharge pressure No. 1 and 2 (D0006 and D0007). The main chamber pressure values were recalculated based on the Rocketdyne key number method which was described in the AS-503 flight report. All biases presented for the chamber pressure were determined from the key number pressures.

Dynamic Pressure Data

Dynamic pressure data were available in analog format. The analog data tapes were supplied by NASA/MSFC. Data processing was concentrated on two basic types of output: (1) Clevite Brush composite and bandpass filtered records, and (2) power spectral density (PSD) plots. The Brush records were used to obtain a broad overall view of the data. Since POGO oscillations were a chief area of interest, low-pass filtering was accomplished to determine whether and when the POGO phenomenon occurred, together with the amplitudes and frequencies associated with it in the various parameters.

The PSD plots were generated to define oscillations from 1 to 50 Hz in 11 FM/FM parameters.

Vibration Data

Data were received from the flight in the form of dubbed telemetry tapes. Slow-speed oscillogram records were produced from these tapes. After the slow-speed oscillogram records were reviewed to determine data validity, time slices were selected for further analysis as follows:

1. Amplitude mean square (AMS) charts were obtained to present the composite vibration level in g rms as a function of time.

2. Power spectral density (PSD) plots, which provide an estimate of the average power in a selected frequency bandwidth plotted as a continuous function of frequency were then obtained from time slices selected at approximately 35-seconds range time, approximately 100-seconds range time, and at approximately 145-seconds range time (after inboard engine cutoff).

APPENDIX F

ABBREVIATIONS AND SYMBOLS

The abbreviations and symbols used within this report are as follows.

CDDT	=	countdown demonstration test
EFIR	=	Engine Field Inspection Request
KSC	=	Kennedy Space Center
LUT	=	launch umbilical tower
TIS	=	thermal insulation
VAB	=	vertical assembly building
km	=	kilometers
F	=	degrees fahrenheit
m/sec	=	meters per second
LOX	=	liquid oxygen
GOX	=	gaseous oxygen
EST	=	eastern daylight time
sec	=	second
K-lb	=	kilopounds
psig	=	pounds per square inch gage
psia	=	pounds per square inch absolute
ENG	=	engine
S/N	=	serial number
Temp	=	temperature
UCR	=	Unsatisfactory Condition Report
MAF	=	Michoud Assembly Facility

EFL	=	Edwards Field Laboratory
MSFC	=	Marshall Space Flight Center
DEE	=	digital events evaluator
K-lb-sec	=	kilopound-second
ECP	=	Engineering Change Proposal
MD	=	Model Designator
FRT	=	flight readiness test
$in.^3$	=	cubic inches
MFV	=	main fuel valve
AS	=	Apollo Saturn
rpm	=	revolutions per minute
p-p	=	peak-to-peak
cps	=	cycles per second
TAG	=	anticipated or predicted flight values at sea level and turbopump inlet standard conditions
PSD	=	power spectral density
Btu	=	British thermal units
E	=	emissivity
NPSH	=	net positive suction head

UNCLASSIFIED
Security Classification

DOCUMENT CONTROL DATA - R & D

(Security classification of title, body of abstract and indexing annotation must be entered when the overall report is classified)

1. ORIGINATING ACTIVITY (Corporate author)	2a. REPORT SECURITY CLASSIFICATION
Rocketdyne, a Division of North American Rockwell Corporation, 6633 Canoga Avenue, Canoga Park, California 91304	Unclassified
	2b. GROUP

3. REPORT TITLE

F-1 ENGINE OPERATION IN THE S-IC-5 STAGE OF THE SATURN V AS-505 FLIGHT

4. DESCRIPTIVE NOTES *(Type of report and inclusive dates)*

5. AUTHOR(S) *(First name, middle initial, last name)*

Rocketdyne Engineering

6. REPORT DATE	7a. TOTAL NO. OF PAGES	7b. NO. OF REFS
18 July 1969	188 & xiv	-

8a. CONTRACT OR GRANT NO.	9a. ORIGINATOR'S REPORT NUMBER(S)
NASA-18734	R-7313-4
b. PROJECT NO.	
c.	9b. OTHER REPORT NO(S) *(Any other numbers that may be assigned this report)*
d.	

10. DISTRIBUTION STATEMENT

11. SUPPLEMENTARY NOTES	12. SPONSORING MILITARY ACTIVITY

13. ABSTRACT

This report presents the flight performance analysis of the five F-1 engines used in the S-IC-5 stage of Apollo/Saturn, Vehicle 505.

DD FORM 1 NOV 65 1473

UNCLASSIFIED
Security Classification

14. KEY WORDS	LINK A		LINK B		LINK C	
	ROLE	WT	ROLE	WT	ROLE	WT
Engine Transient Analysis						
Turbopump Functional Parameter Analysis						
Engine Steady-State Performance Analysis						
Trajectory Reconstruction Analysis						
Engine Dynamic Data Analysis						
Flight Instrumentation Operation						
Heat Exchanger Performance Analysis						
Thermal Analysis						
Engine Configuration						
Engine Test History						
Prelaunch Operations						
Data Processing						